The co-administration of anticancer and pro-apoptotic agents as a novel approach in liver cancer therapy

By

Wejdan AL-Shakarchi

A thesis submitted in partial fulfilment of the requirements of Keele University for the degree of Doctor of Philosophy at the School of Pharmacy

July 2018

Abstract

Hepatocellular carcinoma accounts for 85% of primary liver cancer that are usually characterised by defective or ineffective apoptosis which is considered to be the main cause of cancer progression. In this study, Cytochrome-C which is a pro-apoptotic protein is combined with hybrid (iron oxide-gold) nanoparticles and triggers mitochondrial downstream apoptosis pathway in the tumour cells. The nanoparticle complex enables delivery of this difficult protein through the cell membrane. In this research, five different anticancer drugs (doxorubicin, oxaliplatin, paclitaxel, vincristine and vinblastine) were used against liver cancer and U937 cell lines to assess their IC_{50} values alone and to check their toxicity after their co-administration with cytochrome C hybrid formulation. These combinations resulted in an increase in the cytotoxicity of the used chemotherapeutic drugs and remarkable decrease in the amount needed to kill hepatic cancer cells. For that reason, Iron-gold hybrid nanoparticles offer a promising tool for cytochrome-c delivery into tumour cells and enhance the specific targeting of therapeutic particles to their site of action.

The preliminary results reflected the increasing killing abilities of chemotherapeutic therapies when co-administered with cytochrome C hybrid formulation by targeting the natural killing mechanism inside the cells and activating its pathways. Subsequent to these results, further work was done in formulation of one platform therapeutic device with Polymeric amphiphiles hydrophilic poly(allylamine) polymer (PAA) grafting with 5-(4-chlorophenyl)-1,3,4-oxadiazole-2-thiol(oxadiazole, Ox). Paclitaxel (PTX) was selected as a hydrophobic drug model to check its water solubility behaviour after loading into PAA-HNP-C platform. These new devices showed a significant increase in drug uptake level and increase in PTX cytotoxicity against liver cancer cell lines. The data from this work showed a significant increase in the apoptosis activities of combining treatment anticancer agents (doxorubicin, paclitaxel, oxaliplatin, vinblastine and vincristine) and the hybrid

formulation of the cytochrome-C within the liver cell lines, which leads to cellular death. Therefore, this combined method may give promise step for the future of liver cancer treatment regimes. In addition to, formulating the HNP-CYT-C and PTX into as active single platform for increasing the PTX cytotoxicity. More laboratory investigation is needed to check the activity of this formulation as a preparing step to further *in vivo* studies.

Acknowledgements

I would like to express my deepest thanks to my two amazing supervisors, Dr Clare Hoskins, and Dr Anthony D.M. Curtis for their continuous support and help in my project.

I also would like to express my thanks to the Iraqi Ministry of Higher Education and Scientific Research for giving me the chance to fund this research project and for the continued support.

My special Thanks will go to my husband and to my children (Khalid and Areej) for their support and for being patient with all my complaining and frustration. Special thanks to my family (parents and brother) for showing loving help and encouragement.

I would like to gratefully acknowledge my amazing colleagues, in Keele Nanopharmaceutics Research Group especially Mohanad Alfahad, Maryam Malekigorji, Adeolu Oluwasanmi, Ali Alsuraifi and Vaibhav Khare for their advices and supports, and for all amazing times in the working lab.

Wejdan

Table of contents

Contents

List of Figures

List of Tables

List of Abbreviations

DOX doxorubicin

PTX paclitaxel

OXA Oxaliplatin

vinb Vinblastine

vinc Vincrisine

AFM Atomic force microscopy

DMSO Dimethyl sulfoxide

EPR Enhanced permeability and retention

FTIR Fourier Transform Infrared spectroscopy

HNPs Hybrid nanoparticles xv

HPLC High performance liquid chromatography

IVIVC In vitro in vivo correlations

MNPs Magnetic nanoparticles

MPS Mononuclear phagocyte system

MRI Magnetic resonance imaging

MTT 3-(4,5-dimethylthiazol-2-yl)-2,5-diphenyltetrazolium bromide

NIR Near Infrared

NPs Nanoparticles

PAA Poly (allylamine)

PCS Photon correlation spectroscopy

PDI Polydispersity index

PEG Polyethylene glycol

PEI Polyethyleneimine

RME Receptor mediated endocytosis

SPIONs Super paramagnetic iron oxide nanoparticles

SPR Surface plasmon resonance

HCC Hepatocellular carcinoma

Chapter One

Introduction

1.1. Cancer

Cancer is defined as a malignant neoplasm disease which is produced by abnormal and uncontrolled cell growth and is considered as the second cause of death after heart disease worldwide. The nature of this disease is categorised as the most dangerous type of cell proliferation, with heterogeneous abnormal growth of cells that may localize within an affected organ (or invading to other body parts with process called metastasis) (World Health Organization, 2014). However, not all types of tumours are defined as cancerous; benign tumours also exist which are not capable of transferring into other parts of the body. Malignant tumours, develop and when they undergo metastasis they begin to other regions of the body. Mortality caused by malignant evolution of cancer increases every year due to several factors (Figure 1.1.) such as chemo-resistance, improper delivery of the drug at the required dose inside the specific cells, gene alteration of the tumour cells and other factors that affect the normal cell cycle (de Miguel *et al.* 2016).

The lungs, liver, brain, and bones are the usual metastasis locations arising from original tumour cells (National Cancer Institute, 2008). The tumour initiates once cells grow in an uncontrollable manner, dividing and developing into a bulge or cancer. In this study, the retardation of liver cancer progression was investigated by developing new delivery technique of bio-therapeutic molecules. The majority of liver cancers are either hepatocellular carcinoma, or hepatoma, accounting for 85% of all cases. These occur in the liver cells (hepatocytes) particularly in patients suffering from liver cirrhosis. The other types represented in a lower

percentage include (Cholangiocarcinoma, Angiosarcoma and Hepatoblastoma) (Khan, SA. *et al*. 2012).

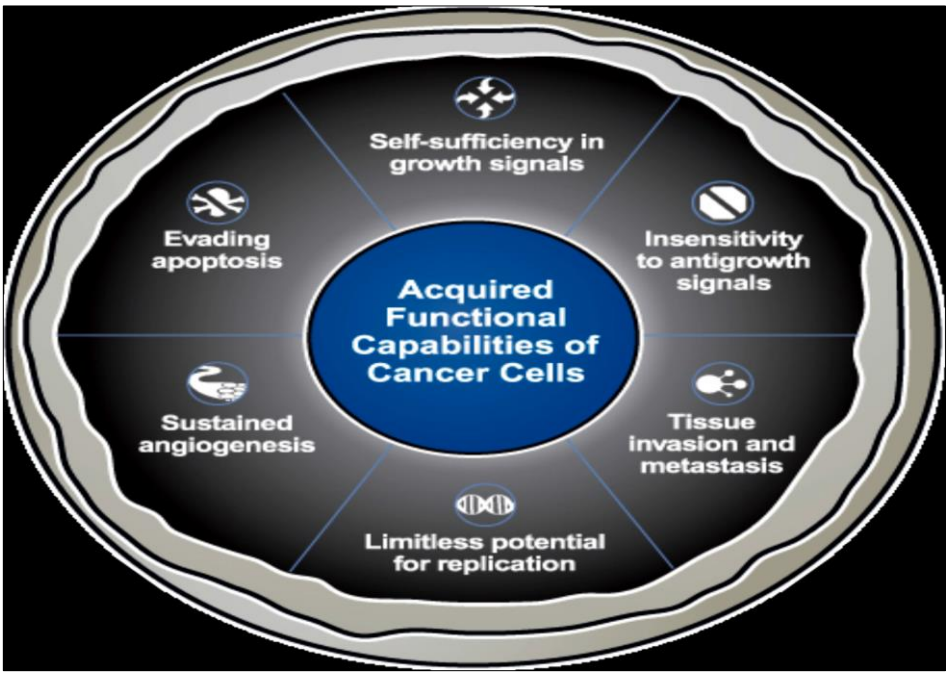

Figure 1.1. Critical elements of cancer development (Hanahan and Weinberg, 2000).

1.1.1. Liver cancer

The liver (the second biggest organ of the body) is one of the most important organs in the body, it controls 500 processes or more inside the human body, for instance fat digestion, eliminating toxins and poisons, controlling blood pressure by monitoring the blood clotting factors and various types of hormones. Therefore, liver cancer is the most dangerous malignant type of growth which results in the disturbance or stoppage of many of the normal functions of this vital organ. In the UK, 2014, there were 5,550 new cases of liver cancer discovered. Affecting about

3,652 (66%) of men and 1,898 (34%) of women with nearly 70% of cases include 65 years of age or older people. During recent years, the prevalence of the liver cancer in the UK has grown abruptly with increase the cases of alcohol abuse and obesity (Figure 1.2.). Liver cancer is the fifth main continually diagnosed cancer and the third biggest cause of cancer related death in the world after the lung and stomach cancer (Lozano, R ,2012).

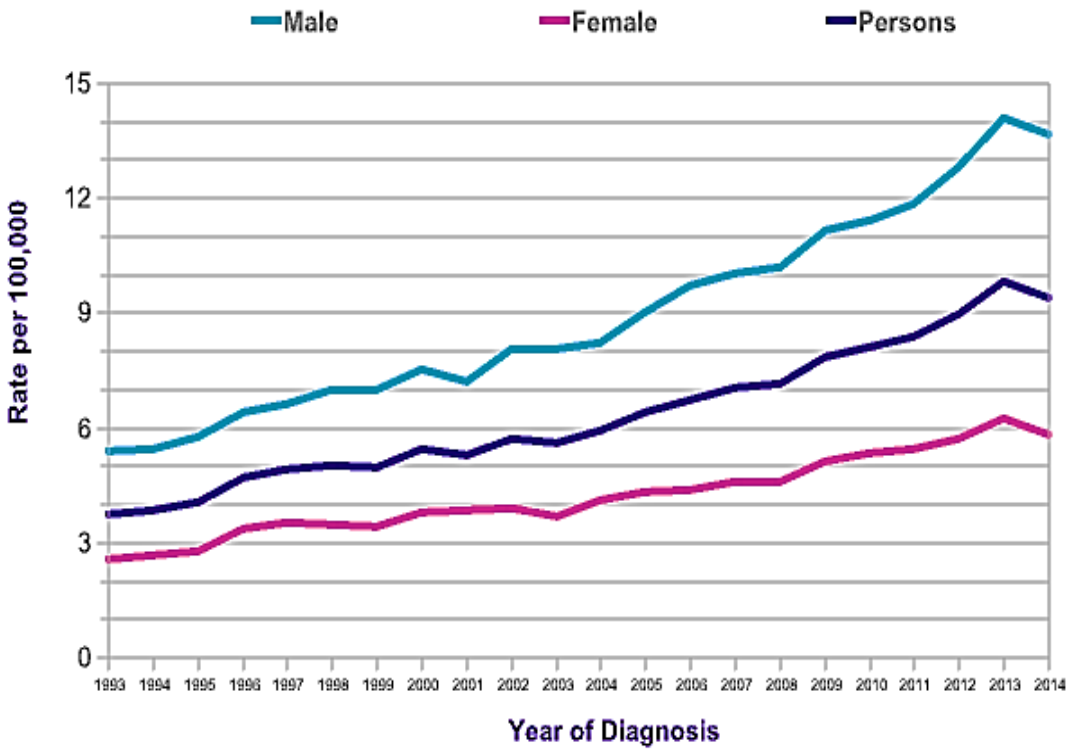

Figure 1.2. Average Number of New Cases of liver cancer Per Year, UK Liver Cancer (2014).

1.1.2. Causes of liver cancer

There are several sources of the liver cancer including: Viral infection, Hepatitis C virus (HCV) and Hepatitis B virus (HBV) (Figure 1.3.) which are responsible for 80% of all types of liver cancer especially hepatocellular carcinoma (HCC) (Jeong *et al.* 2012; Ralphs *et al.* 2013; Kew and MC,2013; Sharma *et al*. 2016).

The main reason of developing the hepatocellular carcinoma with hepatitis C or B virus infection is the countless abnormal cells fibrosis that lead to cirrhosis effect inside the liver and caused by the virus infection with yearly occurrence of 1.7% in HCV-diseased patients (Fattovich, 2004)**.** About 5-10% of HBV patients are registered as chronic stage and around 30% of these cases are developed to HCC (Jeong *et al*. 2012). Moreover, viruses may affect the liver cells resulting in a significant genetic alteration in the normal growth pathways of liver cells by targeting viral duplication or persistence and/or inhibiting the normal signaling mechanism of apoptosis. (Fattovich, 2004). The second source of liver cancer is cirrhosis, which is mainly related with alcohol abuse. This accounts for 37% of all the cases of liver cancer related death. Irresponsible consumption of alcohol links with development of liver cancer affecting two points, the oxidative stress levels within cells and the process of alcohol metabolism inside the liver may produce chemicals groups which cause chronic inflammation and fibrosis. Besides, the damaging effect of excessive alcohol intake on the liver, the intestine may also be infected due to the bacteria toxins inside the intestine permeating into the scarring and fibrosis (Di Tommaso *et al.* 2013). Food contamination with *Aspergillus flavus*

and *Aspergillus parasiticus* (Alfatoxin) can also be considered as a harmful and toxic cause of hepatocellular carcinoma. The most common food types with this kind of contamination include: peanuts, cereals and other types of vegetables.

These categories of toxic fungi contamination are presented in large proportion in Africa, China and South-East Asia, in the prevalence of three times more dangerous than HBV infection (Razumilava *et al.* 2013; DeBaun *et al*. 1998)**.** More causes are concerned with obesity and the development of steatohepatitis, diabetes.**,** smoking and cholangiocarcinoma (5-10%) of the human with primary sclerosing cholangitits (Chuang *et al*. 2009) as the additional causes of HCC.

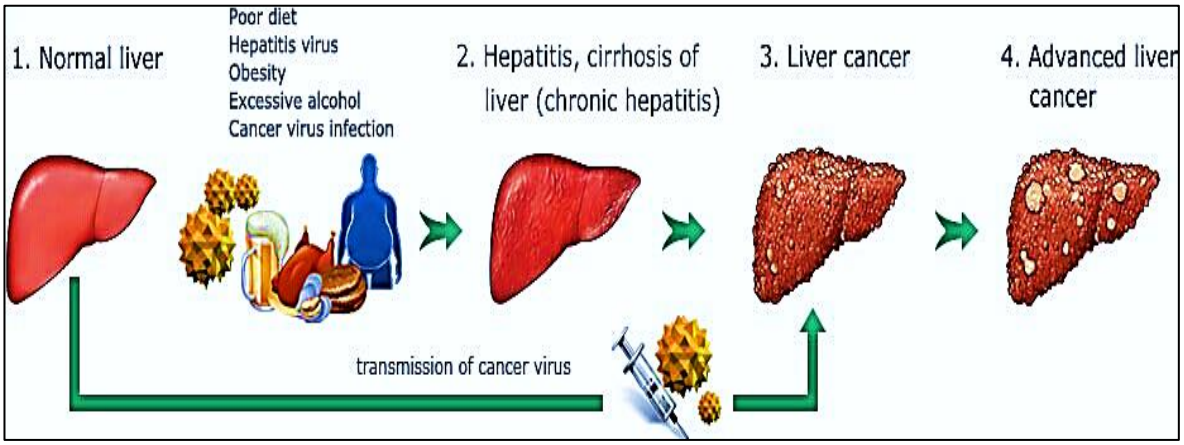

Figure 1.3. The main causes of liver cancer. (Modern Cancer Hospital Guangzhou, 2012)

1.1.3. Types of liver cancer

There are many types of liver cancer that classified according to the affecting liver parts and the most common one is the Hepatocellular carcinoma (HCC) that originates primarily on the liver cells. In addition to other malignant types of liver cancer as illustrated in Table 1-1.

Table 1-1.Types of liver cancer.

Types	Origin	Percentage
Hepatoma ,Hepatocellular carcinoma(HCC)	liver cell	75% of liver cancer cases, (Razumilava *et al.* 2013)
(Cholangiocarcinoma (Cystadenocarcinoma)	bile duct cancer	Approximately 6% of liver cancer cases.(Di Tommaso *et al.* 2013)
Hepatoblastoma	the right lobe of the live , blood vessel and immune system	1% of children and 79% of liver tumour lower than age 15, (Chuang *et al*. 2009)
Angiosarcoma	Blood vessel cancer	1% of adult primary liver cancer
Fibrosarcoma	mesenchymal connective tissue	< 10% *(*Bruix and J; Sherman,2011)
Rhabdomyosarcoma	liver muscle cancer	65% of cases in children 10 to 18-year-old age group. (Bruix and J; Sherman,2011)

The cancer can originate from another part in the body and then spread to the liver through metastasis, the most common point of origin for this is in the gastrointestinal tract or due to ovarian renal or prostate cancer (Emre, S *et al*. 2004; Khan *et al*. 2012).

The cancer cells are diagnosed either by routine screening or observed symptoms depending on the origin and the size of the cancer. Liver cancer may appear as a locally affected region or as a diffuse abnormal growth, which cannot be easily distinguished from the neighboring liver cirrhosis. The lesion may effects the biliary system that can develop to vascular obstruction and accompanied with improper surgical liver amputation or chemoresistance therapy which leads to liver failure and death (Seeff, 2004; Bosch, *et al*. 2004).The proper diagnosis of hepatic cancer is very difficult since the diagnosed symptoms do not present themselves until the final stages of cancer progression. They involve mainly: nausea, unclear loss of weight, vomiting, jaundice yellowing color of the skin and eye and others depending on the type and the stage of liver cancers primary or secondary origin (Lake , 1993).

Systemic or local chemotherapy have been used as one of hepatocellular carcinoma therapeutic pathways, but this method is faced with slightly and temporary responding effects as reported previously with various treated cases. Doxorubicin is reported with negligible positive results in 20-30% HCC treated patients that effect on the survival rate. There is also specific limitation with single treatment types such as with radiofrequency ablation (RFA) treatment(Liu *et al.* 2014) In an effort to provide alternative pathways to improve the action of

chemotherapy, most of the new studies are focused on discovering of the new bio-therapeutic technique to overcome these therapeutic resistances. (Mathurin P *et al*. 2003; Sharma *et al*. 2016).

1.1.4. Types of Hepatocellular carcinoma treatment

Surgical resection is considered as a main choice for non-cirrhotic liver cancer, while the chance with the cirrhotic type it is less useful because of the possibility of liver failure after resection (Bruix *et al*. 2011)**.** Liver transplantation is other applied therapeutic method with less than 30-40% of patients responding to this option accompanied with late diagnosed problem of liver. Radiofrequency ablation (RFA) may be suggested as an alternative way of surgery in the treatment of liver cancer and favored in early stages of cancer, preferably when the tumour smaller than 5cm (2 inches) in diameter. This treatment option may be applied with larger cancer cell size (more than 5cm) but it may be repeated with additional substances such as acetic acid or ethanol. Directed heat /radiation into the liver by the process called percutaneous ablation is also considered as another way of HCC treatment using needle through different ways (percutaneous needle applied through abdomen) but with precaution in applying of heat or radiation that may spread to the normal neighbor cells or blood vessels near liver (Wang *et al*. 2013). Systemic use of antineoplastic drugs is not very effective in HCC treatment, in spite of using local trans-arterial chemoembolization of specific drugs such as

doxorubicin or oxaliplatin. Many problems are faced with this procedure such as blockages of the liver artery by gelatin or small drug particles. A new drug called sorafenib is considered as a main hope in the treatment of HCC that targets the abnormal liver cancerous cells and excessive blood vessel proliferation (de Lope *et al*. 2012). A main aim in the treatment of cancer cells is to initiate the apoptosis in the abnormal cells. However, many cancer types are possess a highly resistance response to the action of anticancer drugs, so novel therapeutic ways to overcome this resistance and to initiate programed cell death is the aim of the most recent studies in this field. Combination therapies of cancer treatment are represented as an ideal way in which cancer cell regression occurs by targeting apoptosis signalling pathways and leaving normal cells without any additional harmful effects (Ray S and Almasan, 2003).

1.1.4.1. Chemotherapy Treatment

Chemotherapy uses chemical substances to destroy cells that are rapidly separating in the body by targeting cell cycle and interfere with cell division process, particularly at the level of DNA to initiate apoptosis. They are classified according to the mechanism of action, anthracycline group such as Doxorubicin affect the synthesis of the DNA and inhibiting topoisomerases prevent the replication of the DNA, Platinum group such as oxaliplatin directly interfere with DNA synthesize and transcription leading to the initiation of apoptosis and death of tumour cells, Taxan mitotic inhibitor group for example Paclitaxel and Vinca

alkaloid group Vincristine and Vinblastine inhibit microtubule formation that prevent DNA synthesis and promotes cell death(Waterman-Storer CM, *et al*. 1997).

Chemotherapy studies have shown the cytotoxic effects of antineoplastic drugs such as Doxorubicin, oxaliplatin, paclitaxel and vincristine that works in different targeting pathways to treat many types of the tumour cells, but the biggest difficulties in applying these therapies are the indistinguishable drug targeting that produced harmful effect on the normal body tissues and unbalanced relation between the sensitivity of these drugs and the resistance response of the tumour cells to chemotherapy effect(Nakamura *et al.,*2000). For that reason, studies on drug metabolism, drug transport and clearance rate are considered as vital ways to determine the pharmacokinetic and pharmacodynamics properties of the drug inside the body. Many of the anticancer drugs show a sharp dose-response curve and low therapeutic index with high systemic toxicity that can be life threatening. Therefore, the use of combination technique by treating with more than one type of anticancer drugs can be the way in opening new clinical approach and interaction of the multiple drugs pharmacokinetic that achieved remarkable modification in host toxicity and drugs therapeutic response. The interaction between different pharmacokinetic properties of the individual chemotherapeutic drugs may lead to multiple toxicity effect causing the chemoresistance (Kivisto *et al*. 1995).

1.1.4.1.1. DNA damage drugs

Anthracycline antibiotic such as Doxorubicin has been generally used as anticancer drug to cure several types of the tumour cells (Singal, P. K., and Iliskovic, N,1998; Buzdar *et al*.,1985) recent researches have been concentrated on doxorubicin induced apoptosis pathway (Nakamura *et al.,*2000; Wang *et al*.,1998).The p53 factor is considered as a major protein to start programed cell death by tumour suppressing effect and protecting cells against carcinogenic activation (Agarwal *et al*.,1998; Ko, *et al.,*1996). The principle pathway of apoptosis is by targeting p53 protein, for most anticancer drugs including doxorubicin (Lowe *et al*.,1994; Lotem *et al*.,1996). Any alteration or mutation in p53 results in major resistance to the effect of doxorubicin (Magnelli *et al.,* 1995). The mechanism by which doxorubicin acts is either binding to the DNA and interrupting the topoisomerase-ll-mediated DNA repair or *via* the formation of free radicals that affect the integrity of DNA, protein and cell membrane.(Gewirtz DA,1999) The way by which doxorubicin forms free oxygen radical is by oxidizing doxorubicin to semiquinone (unstable metabolite), that is converted back to doxorubicin after releasing oxygen radical. These free radical can be consider as one of many stimuli in initiating apoptosis by means of lipid peroxidation, DNA destruction and oxidative stress (Doroshow JH, 1986) The over activity of antioxidant enzymes are attenuated doxorubicin ability to procedure free radicals and inhibited apoptosis (Gouaze *et al.,*2001; Suresh *et al*.,2003). On the other hand, doxorubicin is directed to the nucleus and causes its lethal effect on the topoisomerase-II, leading to DNA damage and death of the cells (TeweyKMetal,

1984). Another DNA damage drug used in this study is oxaliplatin, which is classified as a member of the platinum-cytotoxic group and is responsible for damaging the DNA through the formation of intra and inter-strand cross linking in the structure of the DNA and also between the building protein units of the DNA. The most common cytotoxic site of oxaliplatin is focused on the binding ability with nitrogen atom of guanine to form the mono and di adducts affecting the genomic levels of DNA and also nucleosomes (Faivre S, *et al.* 2003). The significant cytotoxic effects of oxaliplatin are mainly observed with lethal biadduct effect on the DNA synthesis which inhibits the proper processes of DNA replication and transcription, leading to activate the apoptosis pathways subsequent to arrest of the cell cycle (Di Francesco A, *et al*. 2002). Colon cancer cells treated with oxaliplatin have been reported in the activation of caspase-3 and releasing of pro-apoptotic proteins (cytochrome C) as a normal step in apoptosis pathway activation (Arango D, *et al.* 2004). More recent studies are performed with the development of platinum (IV) prodrugs derivatives of oxaliplatin and studied their apoptotic effects *in vitro* and *in vivo*. The cytotoxicity test are performed with colon carcinoma cell line under two different conditions of incubation (normoxic and hypoxic), the modification in the axial ligand are recorded to improve the cytotoxic effects of oxaliplatin by interfering with plasmid DNA and inducing apoptosis (Simone Göschl, *et al*. 2017).

1.1.4.1.2. Anti-microtubule targeting drugs

The targeting of microtubule and disturbing the normal spindle function during the cell cycle have recognised as a new directing site of cytotoxic drugs in treating different types of cancer (Figure 1.4.), by disturbing the normal dynamic of microtubule assembly and affecting the normal cell cycle mitosis and consequently leading to cell death (Eiman Mukhtar, *et al*. 2014). The microtubule are played a major biological role in the cell cycle processes by polymerisation (Waterman-Storer CM, *et al*. 1997),the main two activated mechanisms are participated in polymerization of microtubule concerned with reversible nucleation and elongation processes and the addition of α and β dimers at microtubule ends(Jordan Ma and Wilson L. ,2004). Mitosis phase aids in the proper separation of chromosome into two identical sets. The successful separating processes are required with presence of proper dynamic microtubule (Mitchison TJ.1988; Rusan NM. *et al*. 2001). The critical point in the dynamic of microtubule is timely dependent with proper attachments of chromosomes at kinetochores with spindle after the breakdown of nuclear envelope and is called pro-metaphase, during this phase proper aligned of chromosome are placed preparing to anaphase and telophase stages (Jordan MA and Wilson L. 2004), pro-metaphase is characterized with microtubule originate from each poles of spindle to reach 5-10 μm, and shorten again to re-grow successfully till to close chromosome kinetochores (Hayden JH, *et al*. 1990). It is important that each chromosome is attached to microtubule bipolar spindle; unsuccessful attachment processes are enough to halt cell cycle

transition to next anaphase steps and to initiate signaling pathway of apoptosis (Yvon AM, *et al*. 1999; Jordan MA. 2002; Gabrielli *et al*. 2012).

In conclusion, the proper assembly and disassembly of microtubule is considered the critical points for proper cell division and growth which adapted to different growth environment to progress with suitable shapes (Mitchison TJ. 1988). For that reason, great success are reported with anti-microtubule cytotoxic drug as effective chemotherapeutic agents against different types of cancer and for further developments in the therapeutic regime to halt tumour progression (Giannakakou P. *et al*. 2000).

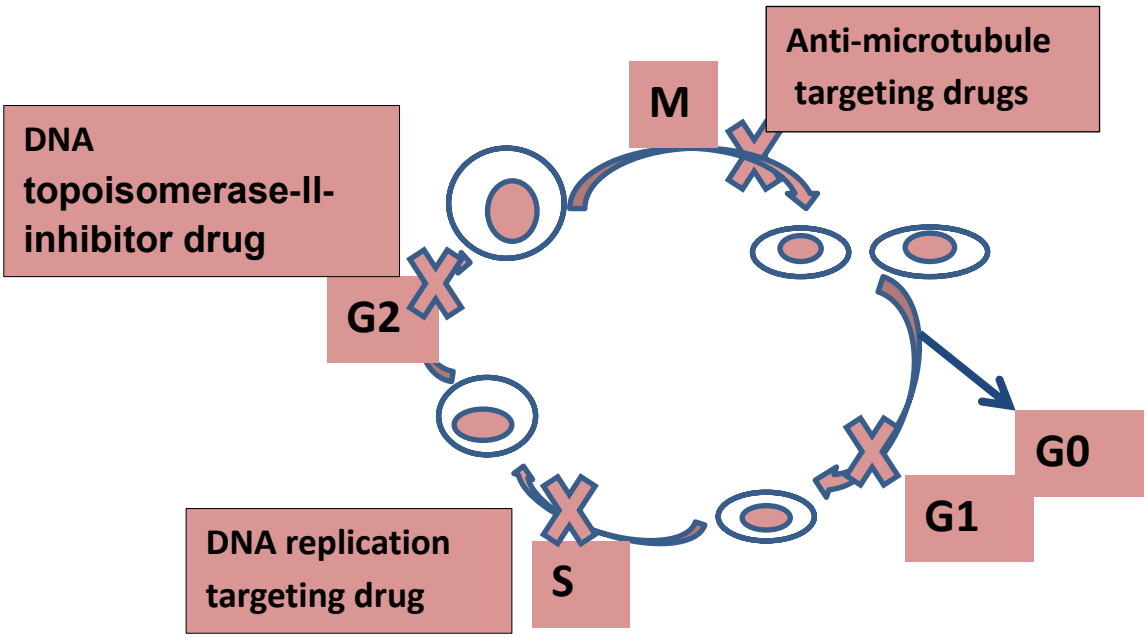

Figure 1.4.Defective cell cycle as targets for anti-cancer therapies.

Paclitaxel is member of taxan anti-microtubule drugs that has essential effect in cancer treatment by targeting the β-tubulin subunit of microtubule, binding the tubulin alongside to the microtubule and increase the polymerization processes. Consequently, remarkable conformational changes are observed with M-loop part of β-tubulin and stable interaction between proto-filament in lateral level. In other hand, small amount of paclitaxel are reported to stabilize the microtubule dynamic without affecting the rate of polymerization (Nogales E. *et al*. 1995; Yvon AM. *et al*. 1999). Jordan group researchers illustrate that mitosis processes are blocked at 8 nM dose treatment of paclitaxel in hella cultured cells, while no growth in the polymer mass was recorded at 10 nM dose of paclitaxel till the dose was increased to 80 nM (Jordan MA. *et al*. 2002). The cytotoxic effect of paclitaxel are noted with suppression of the proper microtubule –spindle separation steps and

stops the cancer cells to move from metaphase to the next anaphase cell cycle that prevent cell progression and kill the cells by apoptosis (Jordan MA. *et al*. 2002; Yvon AM. *et al*. 1999; Kelling J. *et al*. 2003). Additional microtubule targeting drugs are vinca alkaloids (vinblastine and vincristine) which tested to destroy mitotic spindle at dose (10-100 nM) in cultured HeLa cells and showed irregular depolymerizing processes, therefore halting the cancer cells with blocked mitosis and abnormal chromosome condensation. For example, vinblastine is powerfully blocked mitosis in HeLa cells and indicated IC_{50} at (0.8 nM) , apoptosis markers were also tested as cell suicide pathway (Jordan MA and Wilson L. 2004),illustrating the apoptotic effect of vinblastine is concentrated with blocking of normal dynamic of microtubule rather than the depolymerisation effects in microtubule (Jordan MA. *et al*. 2002). The main mechanism of action of vinblastine is binding to the tubulin dimers at the β-subunit with specific targeting region called Vinca-binding domain (Bai RL. *et al*.1990). This type of binding is rapid and reversible and produces remarkable changes in the self-association of the tubulin. This specific domain is considered as vital targeting site of the other various novels chemotherapeutic (Jordan MA. 2002; Lobert S and Correia JJ. 2000). *In vitro* studies have shown that vinblastine binds to other targeting sites at the end of microtubule and suppresses the building frame of the tubulin (Jordan MA. 2002; Singer WD. *et al.*1989). The binding of one or more of vinblastine molecules is enough to reduce tread milling and produce dynamic instability by 50% without remarkable changes in microtubule depolymerisation. This mechanism is responsible to affect the normal assembly of the mitotic spindle at the kinetochores of each chromosome and to block the cell cycle to move from the

metaphase into anaphase and the cells are exposed to apoptosis signaling pathways and die (Jordan MA. 2002; Singer WD. *et al.*1989).

1.1.5. Mitochondria and liver cell

The greatest number of mitochondria which acts as the main power home of energy for all metabolic process inside the body are founded in the liver cells (1000-2000 of mitochondria per cell) and to get the maximum levels of their energy that served the requirements of the numerous functions of the liver. Recently, most of the cancer researchers are focused on the role of chemotherapy on the mitochondria by affecting different parts or chemical reactions of the cells. Mitochondria are represented the goal of many drugs either by direct way through affecting its function or indirectly by affecting other cellular parts. Any disturbance in the activating sequences of apoptosis offered the way to abnormal tumour progress, so the identification of mitochondrial signaling pathways improved the precise mechanism of apoptosis (Korsmeyer S.J. *et al*.,1995). There are many targeting sites for anticancer drugs inside the mitochondria relating to the electron transport chain, ATPase enzyme, outer membrane permeability, (ROS) reactive oxygen species, DNA and synthesis process of other protein, pro-apoptotic and anti-apoptotic signal and other parts in the mitochondria (Finsterer, J., and Segall, L.,2010). Cancer is commonly treated using several methods including chemotherapy, radiation therapy and surgery depending on the stage, location and the type of cancer. Within the past two decades, there has been an exponential

rise in studies exploring the use nanotechnology as therapeutic agents or carriers in cancer therapy (Lind M.J. ,2008). Cells that are exposed to cytotoxic effects of anticancer drugs are organized with apoptotic changes, including cell contraction ,chromatin collection and fragmentation of the DNA within cells, the main linking between the anticancer drugs and apoptosis has been shown by the compatibility in the genetic bases among them ,targeting the same stimulator proteins (Bcl-2 family, caspase cascade, death receptor and p53 encode gene) and other death proteins participating in the up and downstream of apoptosis (Debatin, 1999; Kaufmann *et al.* 2000; Makin *et al*. 2000). The apoptotic changes have been detected in the function of mitochondria starting with increase mitochondrial membrane permeability, releasing of apoptotic proteins such as cytochrome c, formation of reactive oxygen species (ROS), decreasing the stabilization effect of anti-apoptotic Bcl-2 on the outer mitochondrial membrane to initiate apoptosis that are considered as the main mechanism of action of most anticancer drugs (Costantini *et al*. 2000). .

Cytochrome C plays a main role in cellular respiration and in apoptosis pathway after being released into cytosol by the action of Bcl-2 family group Bax and activating series of caspase cascade. However, in some types of the cancer, cytochrome c release are stopped even in the presence of DNA division abnormalities by disturbing the normal activation of Bcl-2 family on the outer mitochondrial membrane, so the tumour cell with abnormal divided and proliferation rates are presented with genetic alteration of apoptotic signaling pathways(Dubrez-Daloz L *et al*. 2008). For that reason, it is very important to

target the anticancer drug directly towards cancerous cells and activated apoptosis mechanism. New delivery techniques with nanoparticles are offering new hope in cytochrome c delivery technique to specific sites in the cancer cells (Pilkington GJ *et al*., 2008).

1.1.6. Chemotherapy resistance

Chemotherapy is the main therapeutic technique that is used in the treatment of many types of primary or metastatic cancers. In spite of the various methods of chemotherapeutic applications, Positive results (but not statistically significant) are recorded with most types of treated cancer. Resistance to chemotherapy can be contributed to several reasons related to either host factors for example partial absorption rate or quick drug metabolism and excretion, leading to unsufficient drug levels in cancer cells and reducing their therapeutic effect. Moreover, chemotherapy or genetic or epigenetic modifications factors in the tumour and non-tumour cells that disturb the normal metabolism pathway of the drug in the non-tumour cell. Unfamiliar structures of the blood vessels in the tumour cells are diagnosed with remarkable alteration levels of the drugs uptake into tumour cell and interaction levels of cancer cells with other interstitial normal cells in the body (Pluen A *et al*. 2001; Green SK *et al*. 1999) Each type of cancerous cells has its own reaction towards chemotherapy depending on the type and origin of cancer tissues and on the oncogene pattern variation resulting in mutation phenotype that leads to different response gene of chemo resistance. Apart of these resistance as shown below in(Figure 1.5.) concerning with loss of the specific receptors on the

cell surface, alteration in the pharmacokinetic and pharmacodynamics properties of anticancer drug (low drug uptake or high efflux level) due to mutation effect of cancer cells are also involved. These changes in drug properties resulting in the alteration of the normal signalling pathway to initiate programmed cell death(apoptosis) that is considered the main goal of most the chemotherapy, besides to abnormal modification in the regular cell cycle checkpoints that affects the normal targeting sites of chemotherapies(Borst P *et al*.,2000; Ambudkar SV *et al*.,1999).

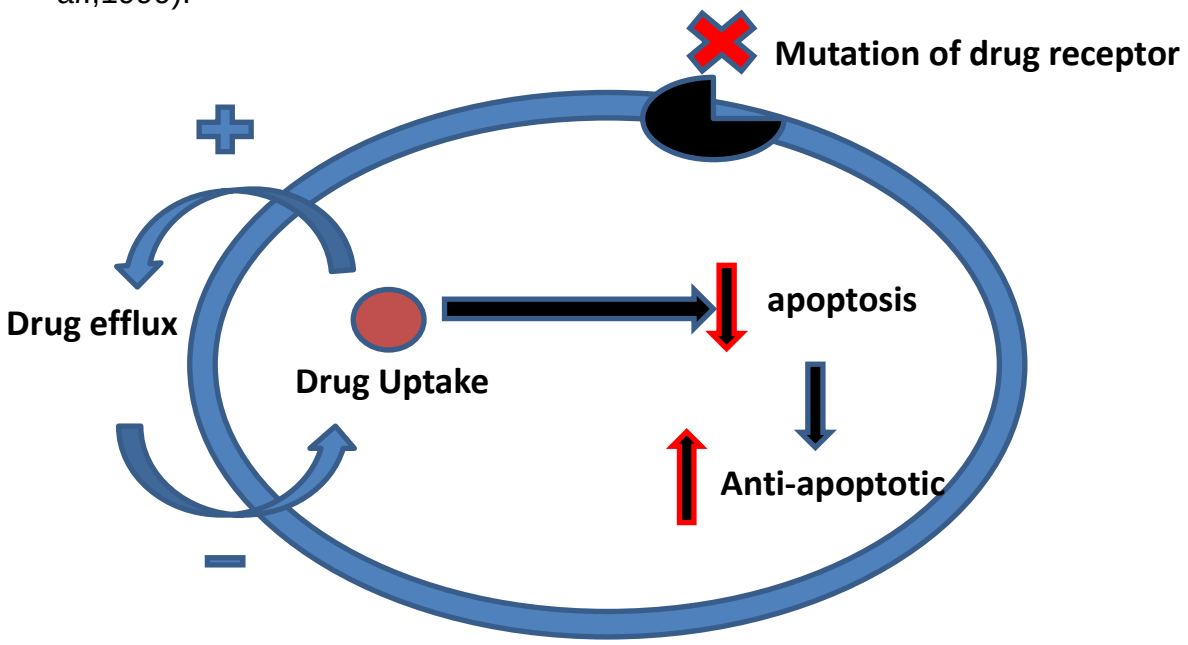

Figure1.5 Mechanisms of chemo resistance.

The main mechanisms of multidrug resistance (MDR) are mainly related to the occurrence of ATP-binding cassette (ABC) family. Overexpression of ABC family proteins is the main cause of chemo-resistance, which leads to pumping drugs out of the cancer cells. The drug efflux transporter P-glycoprotein is the ABC transporter; it is encoded by the *MDR1* gene, which decreases the response of the

cancer cells to chemotherapeutic drugs (Michael M. *et al*. 2009) . .

The P-glycoprotein efflux pump has a broad drugs resistance effect that is responsible for resistance against different types of drugs, such as anthracyclines, vinca alkaloids and taxanes, so limiting their use (Noack *et al*. 2014)

1.2. Apoptosis

1.2.1. Introduction

Apoptosis, or programmed cell death, is defined as one of the most important physiological processes inside the body. Apoptosis is responsible for the regulation, immune response, tissue development and homeostasis. This type of cell death is controlled by triggering several signaling molecules, protein-protein interaction, binding receptor and gene encoded in their pathways to stimulate specific signaling proteins and to produce the required energy for cell work. In contrast to apoptosis there is another process called necrosis which is defined as an uncontrolled cell death resulting from injury. Apoptosis requires energy to complete its process; the same stimuli for the apoptosis in the presence of energy may induce necrosis in the absence of it (Saikumar *et al*., 1999)

Apoptosis refers to the death of cells ensuing from a regular sequence of genetically programmed steps and removed the odd or aged cell that produces during abnormal cell growth with keeping the balance between cell production and cell death. Any disturbance in these steps leads to variety of diseases including cancer. (Kasibhatla and Tseng, 2003). Apoptosis has been considered a key role

in human disease and repeatedly reviewed in many research papers. (Thompson, 1995).

1.2.2. Morphological changes during apoptosis

During apoptosis, the cell follows a number of genetic controlled steps to initiate programmed cell death. As shown in (Figure 1.6.), in this process, the cell first will be diagnosed with a drop in size as its cellular components collapse, followed by bubble balls called blebs indicated on the outer membrane of the cell before dividing into smaller portions called (apoptotic bodies). Since these pieces are either enveloped in membranes they will not affect the neighbor cells or engulfed by phagocytic cells and break the apoptotic bodies with no inflammatory effect. The main reason in discarding and replacing the abnormal cells is to get proper function of the cell and to avoid any undesirable abnormal growth of cells that considered as main cause of cancer (Sasi *et al*., 2009; Marino *et al*., 2014).

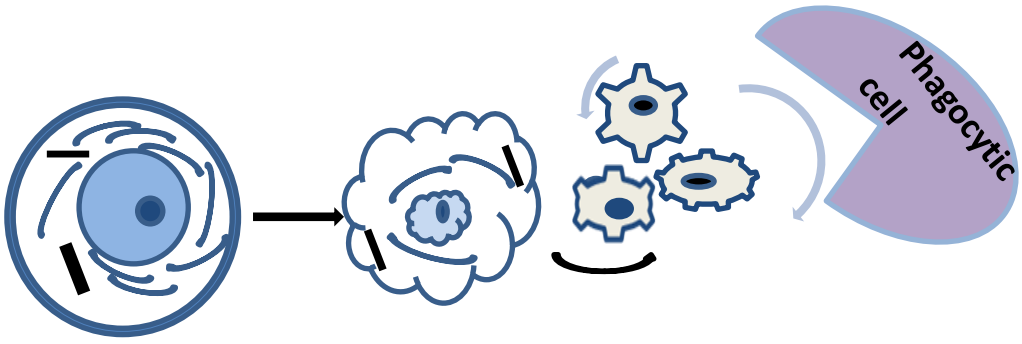

Figure 1.6..Morphological changes during apoptosis.

1.2.3 Role of apoptosis inside the body

Apoptosis processes are controlled by many physiological conditions, such as the formation of new tissue in the embryonic stage, physiological transformations of the endometrium, and the deterioration of lactating breast and changes of the epithelium in the gut. In addition to, monitoring many pathological processes such as uncontrolled cell growth (tumour), death of the effective cells in Alzheimer's disease and Parkinson's disease (degenerative diseases), unnatural cell production after exposure to radiation, low oxygen level (hypoxia) or moderate thermal injury of the cell and in the myocardial infarction affecting the heart cells (Morhan H, 2010 , Merkle CJ, 2009)

1.2.4. Pathways of apoptosis

There are many stimuli for initiating programmed cell death which is divided into two main signaling pathways: 1) extrinsic pathway and 2) intrinsic pathway.

1.2.4.1. Extrinsic pathway

The extrinsic pathway is initiated by triggering specific ligands of the cell death receptor: TNF/FAS (CD95) family followed by stimulating of adaptor proteins (FADD, TRADD and RAIDD) to produce death-inducing signal complex (DISC). Morphological changes in the mitochondria and specific proteolytic enzymes called caspases (family of cysteine proteases) are detected with activating death complex (Jourdain *et al*., 2009).

1.2.4.2. Intrinsic pathway

The mitochondria play a major role in the intrinsic apoptosis pathway which is known also as mitochondrial apoptotic pathway. These pathways are followed genetically controlled stimuli inside the mitochondria. Many apoptosis signals are started once the nuclear receptors are joined with one or more of the following stimuli (Figure 1.7.) such as Corticosteroids, external sources of heat or radiation, low oxygen level, viral infection and DNA cleavage or any other factors that affect the permeability of the mitochondrial cell membrane or elevating intracellular Ca^{2+} concentration all these previous factors are considered as a key step in starting apoptotic pathways (Chiarugi A and Moskowitz MA, 2002).The first step in the apoptotic process is the release of the pro apoptotic proteins located in the intermembrane space by altering the permeability features of mitochondrial outer membrane controlled by the BCL-2 family that is responsible to release special proteins such as (cytochrome-c, Smac/DIABLO) to the cytosol and activate caspase-9, which is played main role in activating effector caspases-3, -6 and -7 and their special cellular substrate release to the cytosol for initiating the morphological changes of apoptosis (Zou H *et al*.,1999; Kuida K *et al*.,1998).The p53 tumour suppressor protein is considered as another way to initiate the intrinsic and extrinsic apoptotic pathways by activation of many pro-apoptotic gene that have p53 binding sites, pro-apoptotic BCL-2 can also be activated by p53 transcriptional and transcription-independent initiation of Bax.(Vousden KH and Lu X 2002).

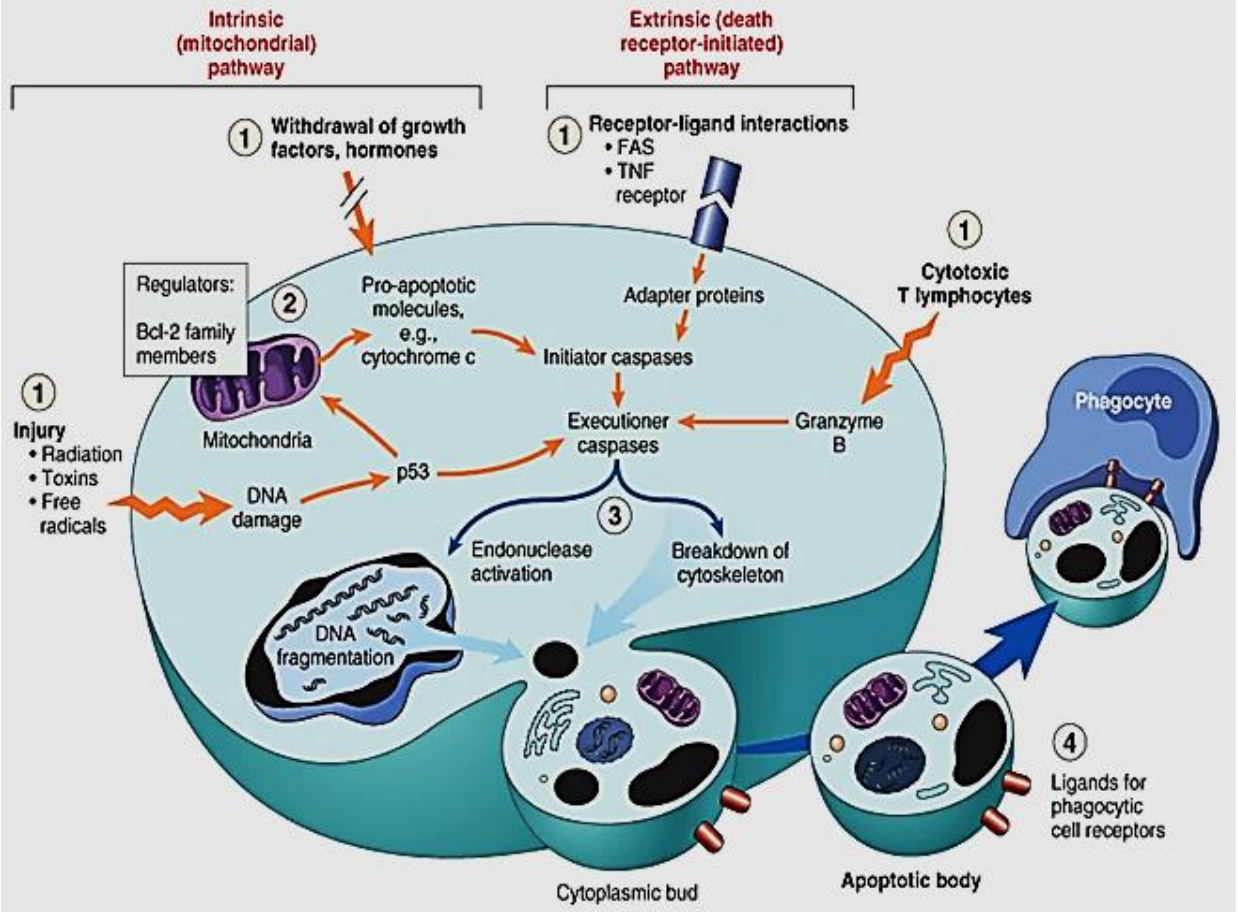

Figure 1.7. Mechanism of apoptosis (from Kumar Robbins Pathology 7th edition 2005).

1.2.5. Inter Mitochondrial Membrane Space Proteins (IMMS) Proteins

The energy metabolism in the mitochondria, plays a major role in apoptosis by releasing of many types of proteins that are located in inter mitochondrial membrane space. Upon increase in the outer mitochondrial membrane permeability controlling by Bcl-2 family, a group of proteins are released, and these initiate to apoptosis in a caspase-dependent or -independent way.

- Cytochrome c is the first mitochondrial protein to be released and directly stimulates caspase cascade by contributing to the apoptosome formation on condition that apoptotic protease-activating factor-1 (Apaf-1) is expressed.(Figure 1.8.) (Cory and Adams, 2002)
- The Endonuclease G and apoptosis-inducing factor (AIF) proteins are mediated in degradation of nuclear DNA, chromatin condensation and cleavage of DNA into fragments and initiate apoptosis.(Susin *et al*.,1999).
- Smac/DIABLO (second mitochondria-derived activator of caspase/direct IAP-binding protein with low PI) are released, which initiate cell death by indirect activation of caspases and abolishing the activity of inhibitor of apoptosis proteins (IAPs) a family of caspase inhibitor. (Shi, Y. 2002)
- HtrA2/OMI (high-temperature requirement protein A2), stimulate caspase activation and initiate caspase-independent cytotoxicity and released in response to thermal and oxidative stress affecting cells. (Suzuki, Y. *et al.* 2001)

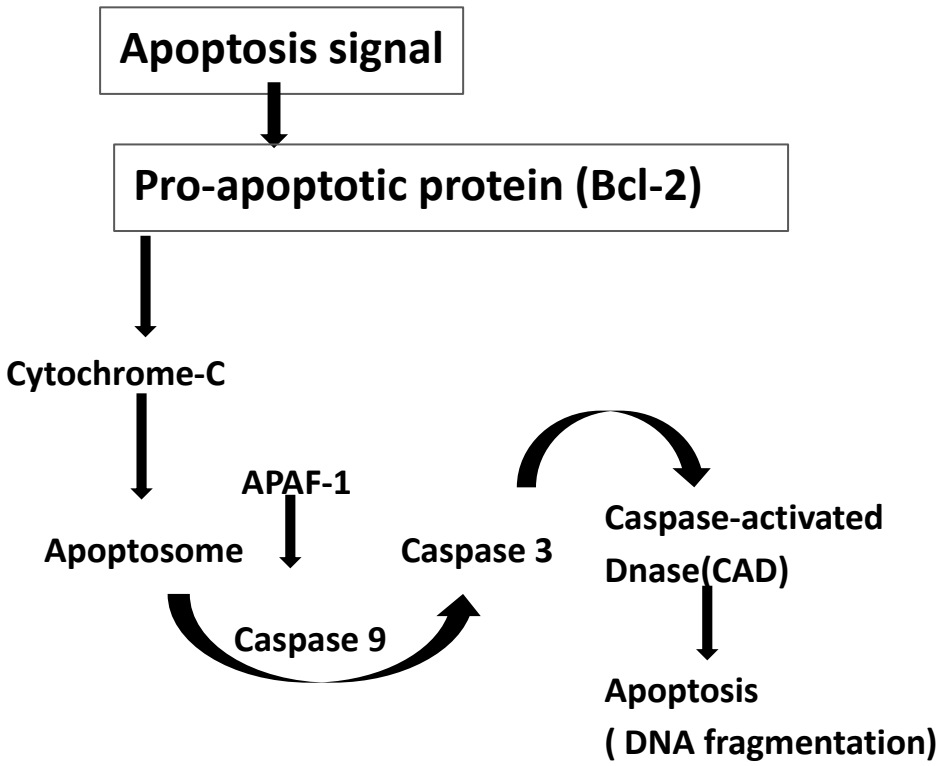

Figure 1.8. Function of Cytochrome –C in apoptosis.

1.2.6. Members of BCL-2 family

The apoptotic way in mitochondria is basically depended on Bcl-2 family proteins involving:

1. Pro-apoptotic members including three BH domain proteins Bax and Bak or the single, BH3 domain proteins (e.g. Bid, Bad, Bim, Noxa and Puma) are responsible proteins in altering mitochondrial permeability and participate in the release of

cytochrome c to the cytoplasm and stimulate the pro-apoptotic caspase cascade series starting apoptosis (Adams and Cory, 1998; Kroemer *et al*. 2007).

2. Anti-apoptotic members including the four Bcl-2 homology (BH) domain proteins (e.g. Bcl-2, Bcl-xL, Bcl-W and Mcl-1) that inhibit mitochondrial permeability, or inhibit the mitochondrial release of cyt c. (Youle and Strasser, 2008).

Bax represents a good example in illustration the mechanism by which the Bcl-2 family form voltage ion channel in mitochondrial membrane. In normal condition, Bax is located in the cytosol with a negligible amount attached to mitochondria (Hsu *et al.* 1997). After specific apoptotic stimuli, BH3-only proteins involving Bid and Bim can cause many changes in the structure of Bax first including its hydrophobic C-terminal part that was hidden within the hydrophobic part to become uncovered and transport Bax to the mitochondrial outer membrane, then the second conformational changes that permit its helices number 5 and 6 to insert in the Mitochondrial outer membrane resulting in Bax oligomerisation inside the mitochondrial membrane and changing the permeability to release the cytochrome c and Smac/DIABLO into cell cytosol (Antonsson *et al*. 2000; Eskeet *et al*. 2000 Ramon Roset. *et al*.2007);.

Cytochrome c is encoded by the nuclear DNA and it is found as apo-cytochrome c in the cytoplasm ribosomes that can insert into the outer membrane of the mitochondria by a special procedure. After it's activated with a specific enzyme called cytochrome c heme lyase, heme is merged and the protein released into the

intermembrane space of the mitochondria under the controlling of Bcl-2 family proteins (Gonzales *et al*., 1990; Stuart *et al*., 1990)

The cytochrome c is a small protein that is found in the inner mitochondrial membrane as a main part of electron transport chain and have two main action in cell energy metabolism and apoptosis, after being released into the cytoplasm and binding to apoptotic protease activating factor-1 (Apaf-1) which considered as a key molecule of apoptosis and activating procaspase-9 causing series of complicated steps to start programmed cell death (Green and D. R., 2005; D. Nijhawan *et al*. 1997).

1.2.7. Mitochondrial outer membrane

The modification of the mitochondrial outer membrane is a key point in apoptosis, in normal state the limited size for molecule to pass through mitochondrial membrane is less than (5 KDa) resulting from the presence of specific channel in mitochondrial membrane known as VDAC (voltage-dependent anion channel) (Colombini, 1979; Dolder *et al*. 1999)

VDAC channels are only permitted to 2–3 nm molecule size to pass and preventing the larger ones especially Cytochrome c apoptotic factors to pass into cytosol which is considered as a first step in starting apoptosis and activating caspase enzymes. For that reason, the cell requests urgent alteration in the mitochondrial permeability and forming larger pores (up to 100 nm in diameter) by

stimulating Bcl2 family that act together to alter mitochondrial membrane permeability and initiate apoptosis. (Schafer *et al*. 2009; Bleicken *et al*. 2010) The capability of Bcl-2 family to initiate pores in the mitochondrial membrane starts when Bcl-xL, Bax and Bak works together on voltage-dependent anion channel (VDAC) in the outer membrane of mitochondria and forming large pores that are suitable to release cytochrome c into the cytosol and start apoptosis process. (Saito M *et al*., 2000)

Many groups of Bcl-2 family (Bcl-xL, Bax and Bak) (Schlesinger *et al*. 1997) have been examined in artificial types of membranes and showed greater abilities to form ion channel in the surface membrane (Minn *et al*. 1997;. Schendel *et al*. 1999). The Bcl-2 family proteins are also discovered in the nuclear envelope and in other parts of body cells .The ability of these proteins in forming pore through ion selectivity feature inside the artificial membrane has been recognised in many researches but still the physiological significance of these ability is not clear (Antonsson *et al*. 1997)

By activation of BAX through apoptotic stimuli, BAX translocate to the outer mitochondrial membrane and helps in the releasing of pro-apoptotic proteins from the intermembranes space of mitochondria (Figure 1.9.). There are two methods for releasing the intra mitochondrial membrane constituent, the first one by binding of the BAX, a member of BCL-2 family, to the mitochondrial membrane and the second by stimulating the mitochondrial permeability transition (PT),happening mostly due to the release of Ca^{2+} ions from endoplasmic reticulum (ER) , elevated

Ca^{2+} levels inside the mitochondria and swelling of the matrix of mitochondrial membrane and burst to release of inter-membrane space content to the cytoplasm which is mainly controlled by localizing of Bcl-2-family proteins at the (ER).(Scorrano L *et al*. 2002; Hsu *et al*. 1997; Gross *et al*. 1998)

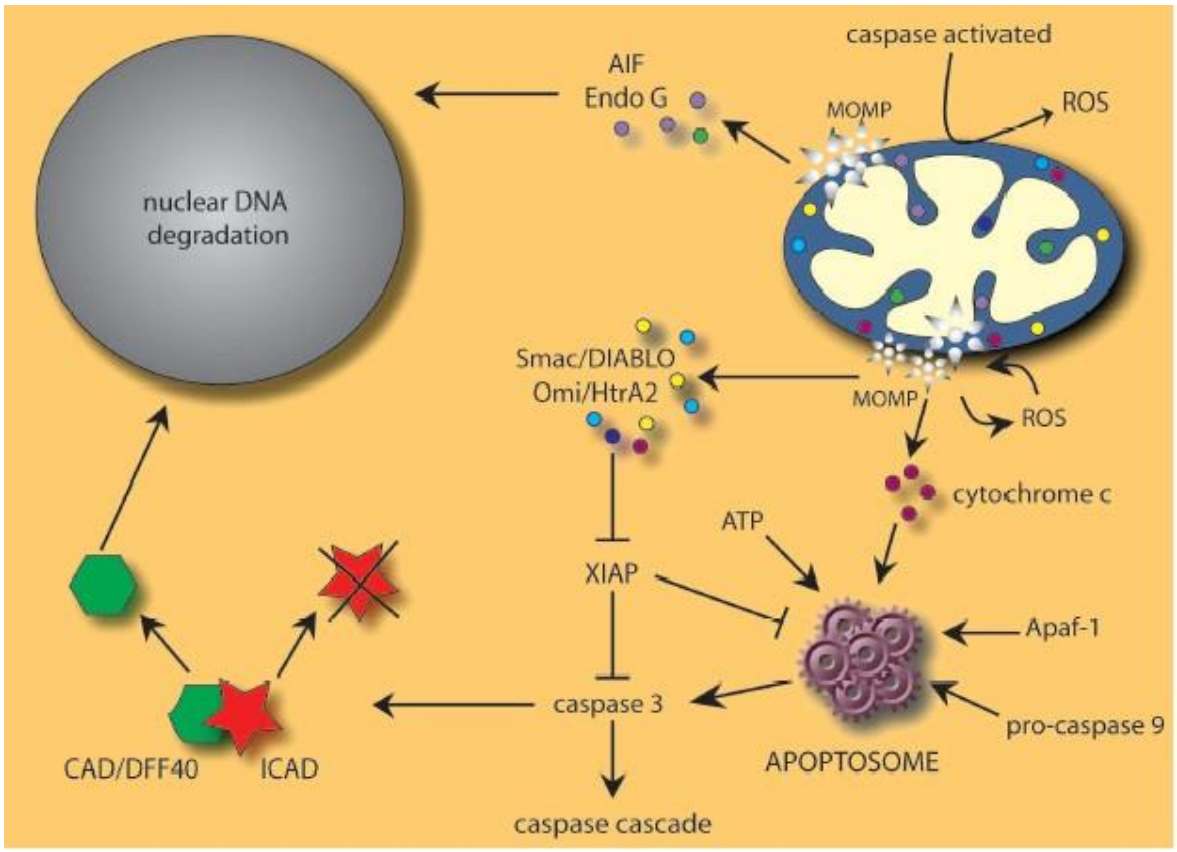

Figure 1.9. The mechanisms responsible for mitochondrial outer membrane permeability (Bras M. *et al*. 2004).

Tsujimoto's group are discovered the interactions between BAX and 14-3-3 proteins (molecules found in the eukaryotic cell that have the capacity to bind to specific site of functional specialization signaling proteins such as phosphatase and transmembrane receptor) in the cytoplasm of living cells and BAX dissociate

from this interaction by two principle ways including: caspase -dependent and caspase- independent mechanisms (Tsujimoto, 2003).

There are two types of modules by which the BH3-only domain activate the outer membrane permeability, the direct binding of BH3-only domain to Bax or Bak domain and move them in the direction of outer membrane.(Cartron *et al*. 2004; Marani *et al*. 2002) .The other module is called indirect activation, in which BH3-only proteins need to attach and inhibit anti-apoptotic members including Bcl-xL or Bcl-2. By inhibiting the activity of these groups this will open the way for Bax and Bak to be free from the anti-apoptotic group's inhibitory effect and move to the outer membrane allowing their release towards the cell cytosol (Adams and Cory, 2007).

1.2.8. P53 and cancer

PUMA (p53 up regulated modulator of apoptosis) also called as Bcl-2-binding component 3 (BBC3) have been shown to interact with anti-apoptotic Bcl-2 family members such as Bcl-2, Bcl-xL, Bcl-W and Mcl-1, inhibiting their binding with the pro-apoptotic proteins, Bax and Bak, that is lead to translocation of Bax and increasing of mitochondrial membrane permeability which consider the first step in releasing of IMMS proteins cytochrome c, SMAC, and apoptosis-inducing factor (AIF) starting in caspase activation and apoptosis.(Nakano K and Vousden KH , 2004). Additionally, numerous types of cancers hold p53 mutation (Vogelstein B and Kinzler KW 2004), that is responsible to block PUMA activity, in spite of the presence of DNA damage stimulated by radiotherapy or chemotherapeutic use.

(Yu J and Zhang L, 2005) Some types of cancers that show over activity of anti-apoptotic proteins of Bcl-2 family suppress the apoptosis induced action of PUMA. (Adams JM and Cory S, 2007)

Although PUMA function is banded in many types of the cancer cells, it does not mean that alteration in the genetic sequence of PUMA is a main area of cancer research (Hoque MO *et al.* 2003; Kim MR *et al*. 2007; Yoo NJ *et al*. 2007). Anticancer drugs that stimulate apoptosis in cancer cells can also cause the same effects in the normal cells, so the inhibition of apoptosis stimulated by PUMA mutation can be considered as a new target to decrease the adverse effects of chemotherapy in cancer treatment and a new way to detect many types of cancer because many tumour cells show p53 mutation effect.(Yu J and Zhang L, 2008)

All the cancer researchers are focused in developing the suitable therapeutic ways to stimulate apoptotic pathways in the chemotherapeutic treatments, so the tumour suppressor p53 has been considered as a main controller of apoptosis pathway.

There are many stimuli that are caused the translocation of p53 towards mitochondria including damage of the DNA, UV irradiation, low oxygen level and others which lead to increase permeability properties of the outer membrane which can in direct or indirect way stimulate Bax (BCL-2 associated X protein) and Bak (Bcl-2-antagonist/killer) which stimulate the outer membrane of the mitochondria to release different types of apoptotic proteins such as cytochrome c, Smac/DIABLO to initiate apoptosis. (Erster and Moll, 2005; Schuler and Green, 2005)

1.2.9. Evasion from apoptosis

There are many factors that affect the normal pathways of apoptosis leading to cancer progression which includes: The imbalance between pro-apoptotic and anti-apoptotic proteins, disturbance in the caspase function, reduced normal signaling of the death receptor and other abnormal resistance to the function of many apoptotic proteins such as (SMAC/DIABLO), cytochrome C, BCL-2 family proteins and other activators of apoptosis. The over expression of Bcl-2 family has been formerly described to keep cells away from necrosis and defending the cancer cell against apoptosis, showing the importance of the membrane stability for the function of this protein.

Many energies are used in cancer researches to make cancer cells more sensitive to the action of chemotherapeutic drugs or other formulation compounds These have been focused on the several signaling steps to decrease the expression of Bcl-2 family proteins or stabilize their action as the pro-apoptotic groups are concerned to exert many morphological changes of the apoptosis such as blebbing and destruction of the cell membrane, in contrast to anti-apoptotic proteins action that keeps the integrity of the cell structure (Vaux D.L 1993).Any type of cells that follows uncontrolled growth mechanism and abnormal increase in the mass of tumour is considered as main cause of cancer and reveled the improper balance between anti-apoptotic proteins and pro-apoptotic protein inside apoptotic cells.

The first step in treatment regime is to understand cancer mechanism in evading apoptosis and to discover new approach that helps in blocking tumour growth (Gyrd-Hansen M and Meier P., 2010). In most cases, chemotherapy resistance is caused by the same mutation mechanisms that suppress apoptosis and reduce chemotherapeutic response against cancer cell even after DNA mutation. (Korsmeyer SJ *et al*. 1995) All these series of disturbances are responsible in abnormal genetic alteration and converts normal cells to malignant type of cell growth (Hanahan D and Weinberg RA, 2000). In addition to the previous local disturbance, the metastasis stage of cancer can also be distributed to other parts of the body *via* blood stream, lymphatic system and other ways that place a new challenge in cancer therapy (Racila *et al*. 1998).

1.3. Intracellular delivery technique using nanoparticles

Intracellular-acting proteins have been applied as an alternative way to extracellular–acting molecule, but there are multiple restriction factors in their efficiency and presence of many challenges in the cell membrane restricted permeability. Cancer resulted from the absence or faulty function in proteins concerning in cellular programmed death. Recent techniques have been performed by affecting abnormal cancer cell signaling using intracellular apoptotic proteins as tumour inhibitors.

Intracellular healing proteins (pro-apoptotic proteins -cytochrome c) have faced a lot of difficulties to be applied for therapeutic purposes because the nature of their

physical and chemical instabilities inside the human body such as proteolysis, denaturation and aggregation which restricted their therapeutic effects inside living body. For that reason, many efforts have been focused to use a new nanotechnology as active therapeutic delivering vehicle (Tabata Yand Ikada Y, 1998; Manning M *et al*. 2010)

Nanoparticles have been known to control the release of the binding proteins and drugs depending on the surface degradation manner of the nanoparticle. The accumulation of the nanoparticles at higher concentration in the cancer tissues than normal drugs enhances the bioavailability of the conjugated NP drugs and reduces the systemic toxicity. Nano-system properties have been used to deliver drugs to the most challenging sites in the body, for example the brain tissue and the presence of the blood brain barrier (Sahoo and Labhasetwar, 2003; Rawat *et al*. 2006). Other properties of the nanoparticle are noted with large surface area to the mass ratio enabling NP to be activated as functional platform with several groups and offered as easily directed particles to specific sites in the cells. Adding to the smaller size of the NP (1 to 100 nanometers) that helped in favorable aggregation at tumour sites (as the tumour do not have lymphatic drainage system)(Nie *et al*. 2007).

1.3.1. Nanoparticles behavior *in vivo*

In biological environment the behavior of nanoparticles is largely affected with their type of interaction with bio-molecules such as peptides, lipids and nucleic acids. The nanoparticles properties of the large surface to mass ratio serves as an

effective adsorption platform for different bio-environment molecules, this type of binding forms a specific complex which is known as nanoparticles corona. Proteins are defined as polypeptide with net surface charged according to the pH of surrounding environment. The binding protein to the surfaces of nanoparticles is done by different types of forces such as H-bond, Van der Waals interactions and others. This type of binding is not only related to the characteristic features of nanoparticles but also on the association and dissociation features of binding protein. As a result two types of protein corona can be formed either (hard corona) with long term binding abilities to the nanoparticles or (soft corona) with easily exchange protein rates (Cedervall *et al*. 2007; Karajanagi *et al*. 2004)

Cellular proteins are represented as complex biological system and the complex of NPs with these bio-molecules can formed in several systems *in vivo*. For example the inhaled NPs must first pass the mucosal layer and then to lung epithelial cells to entered finally to the blood stream.by the same way the NPs which entered the cellular levels by monocyte phagocytosis, and then taken into endosome with different types of protein that each type of them represent unique environment to changing NP complex processes according to adsorption and desorption of environmental proteins. Nanoparticles that have introduced inside the body have to be measured according to different shaped acquired by protein binding in surrounding medium (Cedervall *et al*. 2007). The amount of protein binding is ruled by the concentration of surrounding protein, as approved by Monopoli and his researchers by applying different protein concentration ranging from 3% to 80%, while other methods are approved that the silica and polystyrene types of

nanoparticles are affected with plasma concentration on their range of protein binding (Monopoli *et al.*2011). The travelling of nanoparticles through various rich protein environments may form pre-coated layer of specific protein that behave as pre-coating sheet for further protein binding with new biological fluid incubation (Gasser *et al*. 2010; Lundqvist *et al*. 2011)

When nanoparticles are hosted inside human plasma, they conjugated with different serum protein such as albumin, fibrinogen, apolipoprotein etc. A recent research of Hellstrand groups approved the binding of protein corona of high density lipoprotein on polystyrene types of nanoparticles (Hellstrand *et al*. 2009)

The protein adsorption pattern on the surfaces of foreign inorganic particles follows dynamic control way by concerning with albumin and fibrinogen as the first two binding protein to the nanoparticles surfaces and consequently replaced with other highly affinity proteins as approved by Vroman theory in sequential protein binding with walled carbon nanotubes. In contrast to ultra-small super paramagnetic iron oxide (SPION) binding to plasma protein did not follow the Vorman theory when introduced to new types of plasma proteins. So, this theory cannot be granted to all types of universal nanoparticles (Vroman ,1962).

The other factor that effect the protein adsorption to the nanoparticle, it is the protein properties itself and these types of binding may affect the type of the bio particles effect inside the biological medium. Some researchers are observed special adsorption pattern on the surfaces of nanoparticles as shown with human serum albumin were adsorbed on the surfaces of iron –platinum NP as a

monolayer pattern, while Rezwan and co-workers noticed the adsorption of bovine serum albumin (BSA) as a monolayer by applying 36% of its negative charge on the aluminium oxide NP. Additionally, the further bovine serum albumin was introduced as dimers pattern on the NP surfaces with additional amount of BSA founded in the surrounding medium (Rezwan *et al*. 2004).

1.3.2. Mechanism of nanoparticles cellular uptake

The penetration of the nanoparticles across the membrane barrier is largely dependent on the particles size. The acceptable particle size to enter cells is below 100nm, while the particle size with less than 40nm and 35nm is suitable one to enter cell nucleus and blood- brain barrier, respectively. The cellular uptake follows different uptake mechanisms such as (phagocytosis, endocytosis and macropinocytosis) as shown in (Figure 1.10.).The fate of uptake NPs is varied between the formation of lysosome particles accumulation and/or intracellular vacuoles in the cellular cytoplasm, this point is very critical to researchers for evaluation of bio-nanoparticles activity after dissolve with acidic lysosome and exerts the cytotoxicity effect of targeting particles (Dos Santos *et al.*2011; Albanese *et al*. 2011)

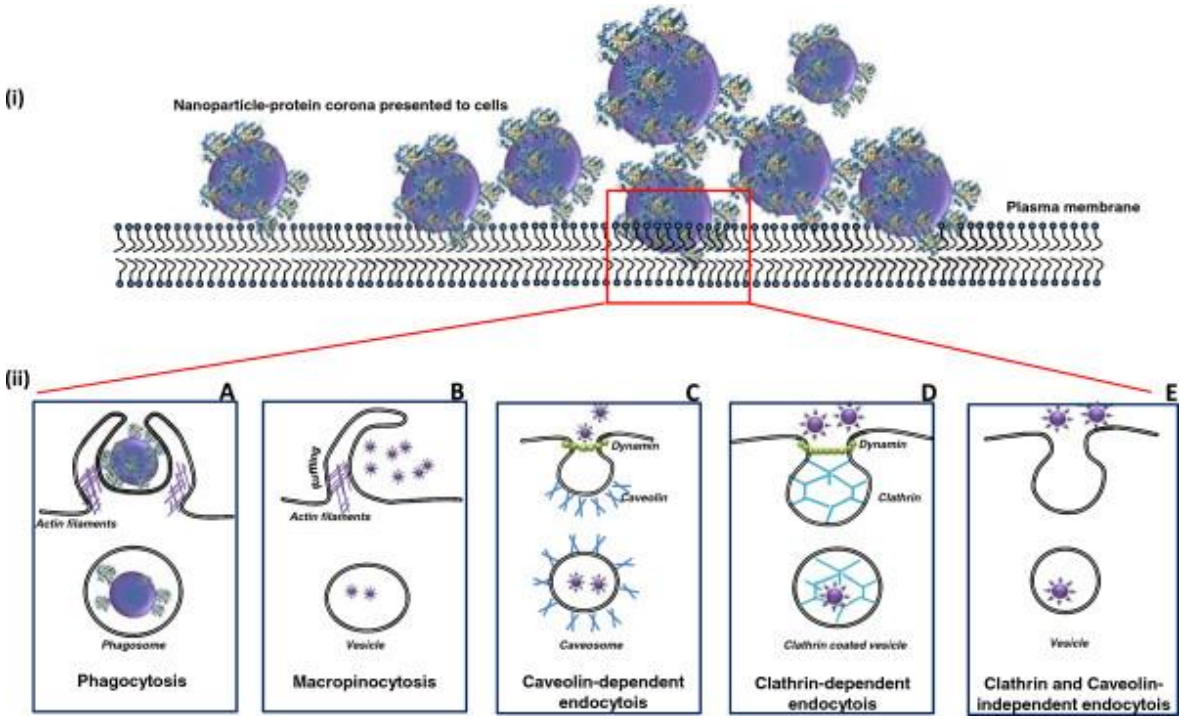

Figure 1.10. Interactions of nanoparticles with the cellular interface (Shruti *et al*. 2013).

The cellular uptake of nanoparticles is tracked by two types of pattern either specific one with specialized NPs ingestion by phagocytosis cells (macrophage and neutrophils) which forms special structure of folding plasma membrane around NPs called phagosome or non-specific uptake methods may also happen *via* extracellular fluid aggregation of NP. These methods are hosted with macropinocytosis by forming plasma membrane vesicle to engulf NPs. Additionally; endocytosis of NPs is also reflected by different plasma membrane receptors known as caveolins and clathrin-coated vesicles (Ruge *et al.* 2011; Wang *et al.* 2009).

1.3.3. Nanoparticle technologies for cancer therapy

Nanotechnologies are used as one of the most activated search tools in clinical therapy during the last two decades. The liposomes and polymeric nanoparticles have been approved as additional advance delivery technique for many therapeutic drugs.

In recent years, scientist are concentrated their efforts to find a vital solution against chemoresistance, which is responsible for unsuccessful treatment of the most cases of cancer. Nanoparticles are presented as the alternative ways to overwhelm most of these difficulties and to develop cancer treatment in the future (Davis ME *et al*. 2008).

The cancer cells have different physiological properties compared to normal cells including high percentage of proliferated endothelial cells, extremely spreading of cancer vessels leading to create free spaces between endothelium lines, these free pores enable macromolecular particles to penetrate through cancer vessels and highly interstitial pressure of tumour cells that helped in external conduction of fluid from tumour interstitial. Therefore, this can be considered as one of the transport route for anticancer drugs controlled by physiological, physicochemical features of interstitial (pressure, structure and composition) and physicochemical properties of the used therapeutic molecules (charge, hydrophobicity and other features) (Maeda H. 2001). The permeable abilities of nanoparticles through abnormal endothelial proliferation spaces of cancer cells are offered a chance to

increase the selectivity of nano- binding therapeutic drugs toward tumour cells and to avoid undesirable toxic effects of anti-cancer drugs in healthy cells (Brigger *et al*., 2002).

There are several reasons for using nanotechnology as drug delivery system. One of them is that, most of therapeutic drugs are available as oral or injection dose but this form is not optimal formulation for nucleic acid or protein formulation. For these therapeutic molecules more innovative design should be used to keep protein and nucleic acid efficacy and protect its structure from undesirable degradation (Slowing II, *et al*. 2007).

The best method to increase the potency and decrease the toxicity of chemotherapy is to direct the active therapeutic parts to its goal and keep it there with sufficient concentration and enough time to get the required therapeutic effect. The restricted factor that affects drug deliver to various parts of the body is drug particle size. Nanotechnology has the ability to increase drug bioavailability, control the time of drug molecules release, and support drug targeting .Many applications were performed for nanotechnology in drug and gene delivery. .Additional uses of Nano scale as drug carriers served as active vehicle to decrease drug toxicity and increase drug distribution (Cai and Chen, 2007).

Advantages of nano-formulated drug technique include the direct delivery capacity of drug into cells and the ability to target cancer cells inside healthy tissue (Drummond *et al*.,1999).

The leaky nature of the tumor microvascular is offered natural architectures strategy for passive or diffusion of nanoparticles into tumor cells. The range of

these pores are between 100-1000nm in diameter, while the healthy cells microvascular pores are less than 10nm.Therefore,the formulated nanodrug design into tumor cells within healthy cells should be greater than 10nm but at the same time less than tumor pores diameter range to confirm the proper delivery of directed drug inside tumor cells(Moselhy *et al*.,2000).

The penetrations of drug barriers with negligible loss of their activity in the blood are offered a maximum benefit of anticancer drugs that can largely controlled by the size of the injected NP. They should be large enough to avoid their rapid escape into blood capillaries, but at the same time they should be small enough to penetrate the reticulo-endothelial system, for instance the liver and spleen. The suitable size for the NP to avoid these two problems are ranged between (30-100 nm) to penetrate tumour tissues (Yuan F *et al.* 1995). Additionally, the pharmacological and pharmaceutical properties of drugs can be controlled with new nano-technique of drug delivery systems (pharmacokinetic and bio distribution) to exhaust the possibilities of drug toxicity and to increase therapeutic effects against specific part of infected cells (Walsh MD *et al*. 2012; Chu KS *et al*. 2013).

1.3.4. Nanoparticle application

The theory of nanoparticle was first discovered by Richard Feynman in 1959, by expressing the ability to create smaller machine of atoms by using larger machine (Feynman, 1959).

Nanotechnology is Greek word that referred to one billionth or dwarf. This technology is the fastest developing technologies in the recent years for chemical, biological, engineering and medical applications. Furthermore, it is considered as a promising tool for developing a novel platform in cancer therapy. The particular smaller size of nanoparticles which is usually less than (100nm) is enhanced their interaction with many biological system and targeted the cell surfaces and/or the cellular contents. This technology is used in developing smart methods for targeting therapeutic particles towards cancer cells, in addition to many medical purposes in diagnosis, detection and treatment (Cai and Chen, 2007).

Gregoria *et al.* are the first group that prepared liposomes as a device for drug delivery (Gregoria et al., 1974). The variety features of nanoparticles concerning with their size, shape and chemical features of prepared nanoparticles opens new avenues in medical and technical applications.

The variety types of nanoparticles are used for different application such as quantum dot in biological labelling and detection relating to their fluorescence size dependent features (Chan and Nie, 1998; Lee *et al*. 2012). Magnetic nanoparticles are used in drug delivery and as magnetic device in hyperthermia treatment (Joubert, 1997; Koppolu *et al.* 2012).Polymeric nanoparticles have been examined in drug delivery towards specific goals by encapsulation of therapeutic agents and the enhanced permeability and retention(EPR) ability of cancerous cells in delivering processes(Farokhzad and Langer 2006; Moses *et al.* 2003). Photothermal therapy is concerned with carbon-based type of NPs which is also applied in drug delivery (Bekyarova *et al*. 2005; Bianco *et al.* 2005).

1.3.5. Metallic nanoparticles

Metallic NPs have been used extensively in many biomedical applications (Conde *et al.* 2012; Lin *et al*. 2014). These types of NPs have presented unusual physical and chemical properties due to their smaller size and controller ability in their synthesis and composition processes (Kogan *et al*.2007; Kawamura *et al*. 2013).

The most appropriate methods in fabricated metal NPs are bottom-up and top-down methods. The top-down method is dependent on the creation of the bulk piece of ingredient, which is followed by gradual removed object to form nano scale particles (Feynman, 1959). The bottom-up method have been considered as more controlling way in producing one atom nanostructure particles at a time (Pattekari *et al.* 2011).

The nickel and cobalt type of metal are characterised by magnetic properties but they have highly toxic effect that restricted their biological application (Denkhaus and Salnikow, 2002). Iron oxide and gold NPs have been applied in many biological and clinical fields with specific surface decoration to increase their stability inside biological system (Auffan *et al.* 2009).

1.3.5.1. Iron oxide nanoparticles

Metallic nanoparticles have been involved in much reported research concerning with drug delivery, hyperthermia treatment and imaging technique due to their multiple advantages in utilising the EPR effect in their passive delivery to

cancerous cells or using external guide(bio-recognising particles) which served as active targeting way in NPs delivery (Comoucka *et al*. 2010; Arruebo *et al.* 2007).

The magnetic separation features of iron oxide NPs are served as vital role in their preparation which offered the cheapest and easiest way in NPs synthesis. Moreover, these magnetic properties facilitate the biological interaction between the NPs and cells. In addition to the large surface to volume ratio, surface decorating and controlled pH surfaces at physiological environment. However, one exceptional problem are experienced with magnetic types of NPs which leads to undesirable aggregation of these magnetic NPs inside the biological system as a feature of inherent magnetic property that affect the stability and the particles size inside the biological environment (Chan, 2007). In addition to degradation nature of iron oxide that produces harmful free ions when entered the biological environment and negatively affects the cells integrity and cell contents (Stroh *et al*. 2004; Hoskins *et al.*2012a; Hoskins *et al*. 2012c). To overcome the degradation problem most of the researches are concerned with fabrication of magnetic NPs and coated their surfaces with more biocompatible material that give additional properties in the NPs synthesis processes. Some of these coated materials are polyethyleneimine (PEI) (Wang *et al*. 2009), poly acrylic acid (PAA) (Mak and Chen, 2005) or Dextran (Ciobanu *et al*. 2012). Additional features of coated processes are offered more biocompatible NPs, more biological stability and proper voiding from reticuloendothelial uptake problem by managing their size.

1.3.5.2. Gold Nanoparticles

Gold nanoparticles are one of the most popular types of metallic nanoparticles that are used in various branches of science for their biocompatible applications, non-toxic and simple preparation methods. Recently, remarkable increase in the biological applications of gold nanoparticles either alone or in formulation with other types of nanoparticles are noticed in drug delivery, photo thermal or as diagnosis tools in different medical application (Mikami *et al*. 2013).

The types of gold nanoparticles are classified according to their shape, size and other chemical and physical properties which recorded as nanosphere, nanocages or nanorods with different physical and chemical properties for each unique type (Kawamura *et al*. 2013)

Generally, the gold nanoparticles diameters between (2 nm to 100nm) are controlled by the wet chemical method in their synthesis. This method is concerned with reduction of chloroauric acid ($HAuCl_4$) as a principle step in gold nanoparticles synthesis (Cai et al. 2008). Gold nanoparticles with 2nm in diameter are demonstrated as active vehicles in many biological applications and imaging processes (Qian *et al*. 2008; Jain *et al*. 2012).

Recently, gold nanoparticles are used as an active platform for the delivery of therapeutic and imaging vehicles that experienced with low pharmacokinetics behaviour inside biological environments (Zhang *et al*. 2011; Pylaev *et al.*2011). These types of metal nanoparticles have the abilities to deliver biological compound that have unstable physical and chemical properties when introduced

into biological environments such as proteins and enhance their intracellular level penetration levels such as si RNA (Lee *et al*.2011; Lu *et al*.2010). The large surface to mass ratio of gold nanoparticles are offered the chance to optimise the gold surface binding ability with different ligands and functional targeting particles for specific disease types and sites (Torchilin *et al.* 2001;Jiang *et al.* 2008).

The main mechanism of gold nanoparticles to penetrate cellular membrane is named receptor mediated endocytosis (RME) (Shukla *et al*. 2005). The penetration abilities of gold nanoparticles are greatly dependent on the particles size which is ranged from (1nm) for interaction with nucleus and binding with DNA to other size scales between (20-50nm) that show perfect cell membrane penetration with no cytotoxic effect (Gao *et al*. 2011). The surfaces of gold nanoparticles can be functionalised with other particles such as protein, carboxylic and disulfides (Aubin-Tam,2013;Delong *et al.*2010) by either electrostatic or covalent interaction especially those with thiol groups(Lee *et al*. 2010).

1.3.5.3..Gold-Iron oxide hybrid nanoparticles

Iron oxide nanoparticles have multiple properties that are employed in many areas of biological researches such as high surface area to volume ratio, surface charge and their magnetic features to ensure easy aggregation inside the target cells. In some cases adverse aggregation may affect the stability of this type and cluster formation which leads to unwanted effects in therapeutic application. For that reason, special treatment has been applied to the surface of magnetic

nanoparticles by coating the surface with gold, silica or other polymeric substances (Arruebo *et al*. 2007; Bulte *et al*. 2007; McCarthy and Weissleder, 2008).

The most practical type of magnetic nanoparticles is iron oxide surrounded by biocompatible surface material which offers equilibrium state in biological environment and applying highly affinity ligands to the iron surface which serves as good binding features to therapeutic particles such as drugs, proteins and others. Additionally, protect the physiological space from the harmful effects of free iron oxide radical which could damage the cells *in vivo* (Tartaj *et al*. 2003; Gupta and Gupta, 2005).

Hybrid nanoparticles are defined as a collection of more than one type of effective particles to be employed in scientific application by combining the multiple physical and chemical properties of complex nanoparticles constituents. Iron oxide –gold nanoparticles use the physicochemical features of the gold and magnetic property of iron oxide (Hoskins *et al*. 2012a; Hoskins *et al.* 2012c).

This combination gives additional features of a rigid structure of iron and protecting the biological system from harmful iron oxide free radical generation (Goon *et al*, 2009; Smolensky *et al*. 2011; Zhang *et al*. 2010).

1.3.6. Importance of gold Nanoparticles application

Recently, cancer researchers are focused on nanotechnology as vital technique in targeting and destroying cancer cells. There are a lot of attractive properties such as large surface to mass ratio, small size, unique physical and chemical

properties, and existence of surface plasmon resonance (SPR) with great biocompatibility and ease of surface binding to different functional groups. Gold nanoparticles have been operated in medical field during the history of research progress for several aspects counting with uncomplicated synthesis technique, cheap, inert, highly sized range 2-500 nm using different reaction parameter, the existence of surface negative charge enhance the binding with thiol and amine group. These features provide additional ability to target specific site within the body, reduce the required dose of chemotherapy, improving its efficacy and reducing therapeutic toxicity. Gold nanoparticles have the chance to deliver loaded particles through smallest arterioles, endothelial fenestration and cell membrane by enhanced permeability and retention ability (EPR) enabling the cumulative prosperities of nanoparticles into target cells but the main challenges that face circulating nanoparticles are the entrapment of gold nanoparticles in the system of phagocytosis (Danhier, F. *et al*. 2010).

However, these features may possibly use as a feature point in liver cancer treatment by penetrating cancer cells and releasing loaded particles. The special surface modification of gold nanoparticles with polyethylene glycol (PEG) increased the presence of gold nanoparticles in the circulation and escape from phagocytic system (Huang, X. *et al*. 2007).

The possibility to utilise protein delivery in the treatment of cancer has a major challenge by keeping efficient intracellular delivery of therapeutic proteins without

significantly damaging its biological function. In order to achieve these aims, a novel method of nanotechnology to deliver drugs and proteins in cancer therapy is required. The release of cytochrome-c attached to nanoparticles through the targeting cell is responsible to activate the intrinsic apoptotic pathway (Kim, S. K.*et al.* 2012). The metal structure type of NP is a thin layer of metal material such as: gold, platinum, silver and palladium encapsulating a central material for example a silica nanoparticle. These metal layers can be activated by using irradiation or magnetic field to be used as thermal release drug delivery system the method of conjugation with drug involves: electrostatic magnetism, nanobead connection or lipophilic interaction (Gareth A. Hughes., 2005) Chrysotherapy, the application of the gold in therapy has been recognized since olden times in Egypt, India, China and other culture. They have used these techniques to cure a lot of diseases such as skin diseases, measles and syphilis. (Huaizhi and Yuantao 2001; Richards *et al*.2002; Gielen and Tiekink 2005).

The important points that restricted the proteins delivery within a living system are present with permeability of the proteins through the membrane of the cells and the second challenge is the breakdown of the proteins by enzymes in the body. Actually, the gold nanoparticles (Au NPs) gives the property of Au- thiol binding feature to the surfaces of protein *via* dative covalent bond and facilitate the proper protein delivery to the targeting affecting cells to exert their therapeutic goal (Malekigorji *et al*. 2014).The new covalent and non-covalent approaches have been used for binding proteins or drugs onto the surfaces of gold nanoparticles. Each type of binding has its own properties; covalent bond gives stable delivery

way, but needs intracellular pro drug handling while the non-covalent type of binding permit the release of active type of drugs directly (Morgan MT *et al*. 2006). As shown in (Figure 1.11.) the mainly vital points to apply drug delivery system is depended on proper coated processes of active drug by nanoparticle, targeted specific area with successful manner and productive release of active drug there.

West *et al.* have applied a 120nm diameter nanoshell surrounded by gold using it in cancer therapy research. These types of nanoshells allow the nanoparticle loaded drug to successfully bind to the targeted cancer cell either by connecting with antibodies or peptides to the surface of the nanoshell. By using irradiation in the direction of specific area of the tumour, the gold part is heated with passing the shell and cause death to the tumour specific cell. (Loo C *et al*., 2004)

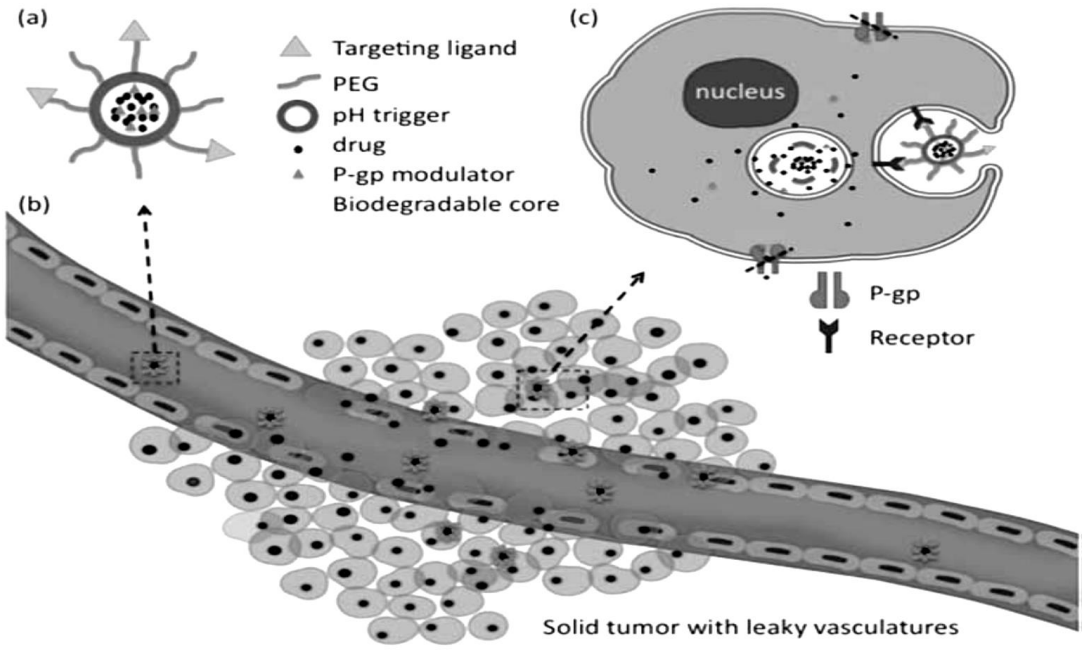

Figure 1.11. Nanoparticle drug delivery to cancer (Hu *et al*. 2009).

The biological application of nanoparticles have special restricted points including the surface properties of the nanoparticles that prefer to be polar in nature to prevent aggregation of particles inside the body by giving aqueous solubility feature and binding of nanoparticles to biological units such as peptides that can represent as address labels to move the nanoparticles towards certain sites inside the body. (Akerman ME. *et al*. 2002). The properties of the nanoparticle concerning large surface to mass ratio, particles size and magnetic ability are extremely changed from there bulk original substances and have different methodology application in clinical research (Kim, 2007; Heath and Davis, 2008).

Industrial progress and functional modification in the synthesis of the nanoparticles gives a new line in the modification of molecular properties such as particles targeting, drug loading and the ability to cure diseases by using new imaging technique. New devices of multifunctional ability have been used to overcome specific barrier and to drop into specific diseased tissues with appropriate dosage of therapeutic agent ,these types of advance regulatory devices are offered additional time and money saving in chemotherapeutic course treatment (Baptista, 2009; Minelli *et al*. 2010; Ma *et al*. 2011; Conde *et al.* 2012).

Several problems are related to chemotherapy clinical application concerning with the absence of specificity of anticancer drugs and rapid bio-distribution inside the body affecting both cancer and normal cells. Additionally, tumour cells may not be able to receive required therapeutic dose of these drugs that are responsible to produce most of the cancer resistance types and metastasis (Panyam J and Labhasetwar V.,2004; Suh H,*et al*. 1998).For that reason, alternative modification

in the drug delivery system are required by applying heat therapy “hyperthermia” and photodynamic may facilitate cancer regression through necrotic pathway activation with precaution of releasing cellular contents to the extracellular spaces and affects neighbour healthy cells during necrosis (McCarthy JR, *et al.* 2008; Park JH, *et al.* 2010).Opposing to necrosis ,programmed cell death is the aim of the most recent cancer research to be activated inside tumour cells and break down cells constituent without affecting normal cells by normal clearance through lymphocyte and macrophages, cytochrome c is considered as a key point in activating apoptosis in cancer cells with proper encapsulation of pro-apoptotic protein inside nanoparticles gives a new regime in cancer treatment with high therapeutic efficacy and low side effects (Slowing II, *et al*. 2007).

Active protein targeting research give great hope for treating tumour cells, but great difficulties have been faced with this process ,such as low protein stability through blood circulation and low permeability through cell membrane (Michaelis, K., *et al.* 2006). Despite, the successful of some proteins in penetrating cell membrane may come to be captured and degraded inside endosomes inhibiting their binding to specific cellular parts (Dutta, D., *et al.* 2007). Membrane permeable sequences (MPS) can direct protein therapy to specific cell sites by using unique surface modification properties of nanoparticles controlling their size, structure and general shape which are totally controlled by the type of loading drugs or therapeutic protein. The NPs have high solubility rate *in vitro* and *in vivo*, enhancing the effective targeting of cytochrome C pro-apoptotic protein without aggregation problem that normally occurs into protein binding *in vivo* and this is

achieved by proper functionalised processes of nanoparticles with external ligands to get successful targeting process and to keep the physical and chemical properties of binding protein or drugs inside body. In addition to, proper Activation of the signalling pathways of apoptosis in the cancer cells retarding their growth. Therefore, nanotechnology reflected the future hopes in developing the drugs delivery system with high efficacy and lower prices (Baptista *et al*., 2008; Lammers *et al*., 2011).

1.4. Aims

The aim of the project is to determine whether nanoparticles can act as vehicles for cytochrome c transfection into cells. This will be achieved via the following objectives:

-Synthesis and characterisation of nanoparticles,

-Conjugation of cytochrome c onto nanoparticle surface.

-Intracellular concentration quantification of cytochrome c after cellular exposure

This research is based on the synthesis and characterisation of hybrid iron oxide-gold nanoparticles; The ICP-OES, UV/Visible spectroscopy and photon correlation spectroscopy are used to describe the physical and chemical properties of the nanoparticles to confirm the proper coating steps in each adding process. Additional, techniques AFM and TEM will be used to determine the size and the shape of the particles. Here, the cytochrome C protein loading is achieved via Au-

thiol bond between the positively charged protein and negatively charged gold of HNPs.

Graphpad prism was used throughout the thesis to detect IC_{50} and t-test to compare between two independent groups by Microsoft Excel software package.

Biological investigations were used in chapter 3 (MTT assay, trypan blue) for the cell viability assays and more to evaluate the apoptosis markers (caspase 3, western blot, TUNNEL assay, fluorescent microscope and AFM). These techniques were used in evaluation of the five different chemotherapeutic drugs (doxorubicin, oxaliplatin, paclitaxel, vincristine and vinblastine) cytotoxicity against (HepG2, Huh-7D, SK-hep-1 and U937) cell lines at specific concentrations to assess their IC_{50} values, and then novel combination of HNP-Cytochrome C was co-administered with previous cancer drugs in 10% growth inhibition concentration (0.012 $mgmL^{-1}$) of CYT-C in nano-formulation against liver cancer cell lines. This combination will test with several cell viability assays and imaging studies to evaluate the potency of each anti-cancer drug. Furthermore, the levels of apoptosis were also evaluated in treated cancer cells after triggering with CYT-C protein to enhance the mitochondrial apoptotic pathways.

Chapter Two

Synthesis and characterisation of hybrid iron oxide-gold Nanoparticles & conjugation of protein

2.1. Introduction

Hybrid iron oxide-gold nanoparticles have been the focus of recent cancer research dealing with biomedical, drug targeting and gene therapy.(Hoskins *et al.*2012a; Seied Sajadi *et al*. 2014;Starha *et al*. 2015). By combining the magnetic property of the iron oxide core and large surface to volume ratio with gold and PEG surface fabrication in (HNP), this platform results in biocompatible nanoparticles to be used in cancer treatment (Hoskins *et al.*2012b). Additionally, the gold surface fabrication of the (HNP) facilitates the binding of the active thiolated (-SH) molecules to the gold according to Au-S chemistry (Robinson *et al*.2010).

The chemo physical stability of the gold surface of the HNP results in more biocompatible and simply functionalised group to therapeutic proteins and drugs. These properties give rise to more accurate targeting delivery of the therapeutic particles in the cancer research. In the recent years, some research has focused on polymer as the intermediate layer between iron oxide core and gold shell in HNP which work as protective cover to the gold migration toward the core and to get highly saturated and stabilized particles (Goon *et al.*2009).

There are a number of protocols described for hybrid iron oxide-gold NPs synthesis such as iterative reduction and precipitation methods (Cho *et al.*2005; Lyon *et al.*2004), all strategies are concerned with the importance of sequential creation of magnetic iron core and gold shell as a bottom –up processing, which was followed with the iron oxide-gold HNP synthesis to produce mono-disperse

particles (Goon *et al.*2009). This method can create hybrid NPs with the shell size range of 0.5-2.0 nm and core size between 5-15 nm. Thermally activated method can be used as alternative way to process mixed solution of iron oxide and gold NPs precursors. This technique increases the thermal induced method in producing metal NPs combination (Schadt *et al.*2006).

The electrostatic binding between the polymer coated magnetic NPs and the gold seed (followed by the subsequent reduction of the gold on this coated surface) can result in the whole covering of NPs with gold (Goon *et al.* 2009; Zhang *et al.* 2011).

By using gold seeding technique we can get the highly controlled gold shell thickness with 10 nm range. The direct relation between the gold shell thickness and the SPR make this process very important to get highly SPR properties with thinner shell (Goon *et al.* 2009; Zhang *et al.* 2011).

Barnett and co-workers synthesised magnetic gold NPs with 70 nm core and PEI as an intermediate polymer. The produced particles were coated with PEG polymer through dative covalent bonding between polymer thiol groups (-SH) and Au shell of the particles (Barnett *et a*l. 2013). HNPs were synthesised following the Goon and co-workers method by several steps starting with wet chemical precipitation method in iron oxide NP synthesis followed by the iron core coating with polyethylenimine (MW 750,000) as an intermediate layer between the magnetic core and the gold shell (Goon *et al.* 2009). Reduction of the $HAuCl_4$ is used in the gold seeds production with (2 nm) nano-size that is binding electrostatically to the polymer surrounding the iron core. While the iterative

reduction of the $HAuCl_4$ producing the complete covering of the particles with gold. Finally, to enhance the bioavailability of the particles, they covered with PEG polymer to increase the particles circulation time and hiding the particles from the engulfing immune cells. The HNP synthesise steps were characterised by several techniques to recognize the size, charge and shape of the particles including (photon correlation spectroscopy, UV/Visible spectroscopy, ICP-OES, TEM and AFM for morphological characteristic of NPs.

Hybrid iron oxide-gold nanoparticles with magnetic core and biocompatible gold shell are offered a good functional platform for precise therapeutic delivery system into targeting cells resulting in remarkable decrease of therapeutic side effects. Hybrid NPs have presented in previous researches as effective delivery vehicles of 6-thioguanin in pancreatic cancer treatment, as shown highly drug uptake to the cells binding to NPs comparing to free drug (Barnett *et al*., 2013).

The promising steps in cancer treatment have been applied with application of nanotechnology in biological field, one of these steps is the targeting of therapeutic protein towards cancerous cell by binding with HNPs to enhance the potency of co-administer chemotherapeutic drugs in treatment course. Cytochrome C which is served as pro-apoptotic signalling protein in intrinsic pathway of apoptosis was conjugated with HNPs in liver cancer treatment accompanying with DNA damage drug (doxorubicin). This formulation was recorded a significant decrease in doxorubicin IC_{50} co-administered with signalling protein (CYT c) comparing to IC_{50} noted with free drug (Malekigorji *et al*. 2014).

Pro-apoptotic protein (cytochrome c) with 12KD molecular weight is categorized as a model bio-therapeutic protein for molecular cancer therapeutic evolution. It consists from 104 amino acid peptide covalently binding with heme C (Figure 2.1.) group at Cys [14] and Cys [17.] Also, it is one of the most important proteins in shuttling the electrons from complex III to complex IV in oxidative phosphorylation process after its release from intra- mitochondrial membrane space, in addition to form of apoptosome complex by binding of (Apaf-1, pro-caspase9 and dATP) that is responsible to activate the caspase cascade series to initiate apoptosis (Hill *et al*. 2004; Saelens *et al*. 2004).

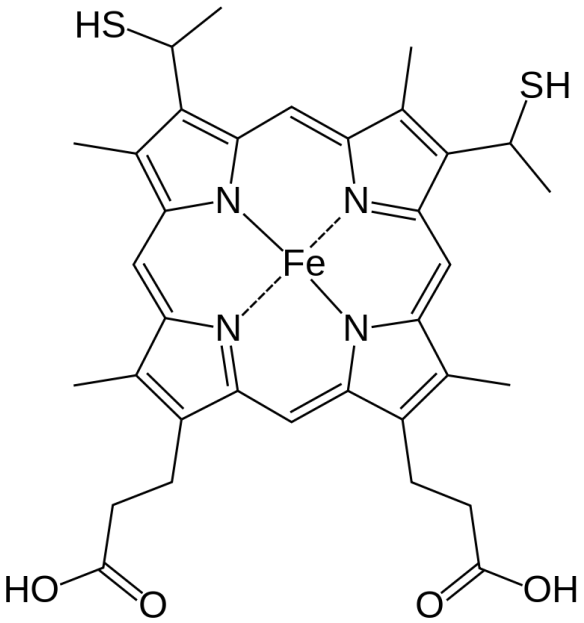

Figure 2.1. Structure of heme C (Mavridou *et al*. 2013).

Nanoparticle characterisation is an important factor in the design and fabrication of new nano-sized formulations. Below the major techniques which will be used in this work have been outlined.

2.1.1. Photon correlation spectroscopy (PCS)

Photon correlation spectroscopy (PCS) or also known as dynamic light scattering (DLS) is vital instrument for detecting the size and charge of nanomaterials (Berne, 2000). The main principle of PCS working is depended on the light scattering direction by the suspension particles which follow the Brownian motion principle and resulted from the random motion of the small particles in the suspension and the collisions with fast particles movement in different direction. PCS is used to measure the particle size of different materials such as carbohydrate, protein and nanoparticles. Moreover, polydispersity index (PDI) is the term applied in the PCS software and reflected the types of particles population within the solution. The measured solution with one type of particles size is measured as zero value of PDI in contrast with different population size of particles which shows PDI values range between (0-1). This values is represented the degree of solution stability and the rate of aggregation and hydrodynamic diameter changes over time. This analysis is used to measure the nanoparticle size of our formulation during each steps of hybrid formulation (Berne, 2000).

2.1.2. Zeta potential

The measurement of the zeta potential is considered as one of characteristic features of nanoparticle stability by measuring the electric potential energy of nanoparticles and their voltage at their surface and the parallel relation between their charge and the surrounded solution (Montes Ruiz-Cabello et al. 2014). The size of nanoparticles is controlled the value of zeta potential and its noticeable with smaller size that exerts remarkable electrostatic repulsion and highly stable zeta potential with range >30 mV. Zeta potential values lower than < 20 mV is revealed aggregated particles with poorly dispersed solution. The biological activity of nanoparticle size is directly related to acceptable zeta potential value and proper pharmaceutical designing (Patel & Agrawal 2011; Bhattacharjee 2016).

2.1.3. Transmission electron microscopy

The transmission electron microscopy (TEM) is a very helpful tool to detect the size, shape and the behaviour of nanomaterial at high resolution levels. A resolution ability of light microscope is restricted only by the visible light wave length while the electron microscopy is dependent in fast moving electron with wave length less than 1A (1A= 10-10 m),by this technique highly improvement in image resolution can be done. A series of lenses are used to focus the electron onto the specimen and to magnify the image. The magnification ability of TEM is nearly to one million times, so the fundamental features of nano-size can be

visualised easily, recent types of TEM are provided images with more than 50 million times, making the nanoscale imaging even easier (David J. Smith, 2015). The formation of TEM imaging is more complicated than the optical microscope by focusing the electron beam through the lens and the restricted performance with possible deviation of electron lenses (David J. Smith, 2015). The standard imaging method of TEM microscope is focused on amplitude or diffraction contrast, by passing a small part of electron through the specimen to magnify the final image. Greatest number of scattered electron are blocked to reach the image plane by placing small objective of aperture at the back face of the lens at focal plane which serves as helpful tool for the image contrast(David J. Smith, 2015).

2.1.4. Inductively coupled plasma –optical emission spectroscopy

Inductively coupled plasma –optical emission spectroscopy (ICP-OES) is one of the metal analytical techniques by detection and analysing of photon emission from the excited ions and metal atoms (Mermet 2005).Different sample state can be used to detection by (ICP-OES) by direct injection of the sample straight into the instrument with exceptional solid state which needs to be digested by acid first to ionise the sample (Mermet 2005). Argon gas is used to form plasma which is crucial to emit electromagnetic waves from the atom and excited electrons are detected by emission of specific wave length after return back to their ground state. The sample solution is injected first with a stream of argon to work as a nebulizer and passed through plasma at 7000°C to get excitation electron levels of

the samples. In our formulation, (ICP-OES) is used to detect iron and gold concentration in in hybrid nanoparticles formulation (Hou and Jones, 2000).

2.1.5. UV/Visible spectroscopy

UV/Visible spectroscopy is one of vital analytical instrument in chemistry which used to measure the absorbance of the material at ultraviolet-visible region. Once the material is adsorbed light, the outer surface electrons are excited to move them to different levels of energy and to promote the electromagnetic radiation to be detected at ultraviolet-visible region. UV/Visible spectroscopy is performed by preparing the required detecting material in a solvent and measured with in a cuvette which exposed to the source of radiation with suitable wave length then getting to the monochromator to be passed toward the detector and measuring light intensity. Each detected materials has different spectrum according to the possession of the electron according to the nucleus (Deeney and Sinclair, 1997).

The calibration curve should be made for each sample by preparing standard serial dilution and the unknown measured samples are calculated by linear regression. This technique is used for detecting the proper coating processes in the hybrid nanoparticles formulation in each steps starting with iron oxide core, gold seeding till the final steps of polymer coating which determined different UV absorbance for each one.

2.1.6. Aims and objectives

The main aims of work in this chapter are;

-Synthesize iron oxide- gold hybrid nanoparticles and characterise each fabrication steps to ensure the proper synthesis processes.

-Use ICP-OES, UV/Visible spectroscopy and photon correlation spectroscopy to describe the physical and chemical properties including metal concentration, size, shape and surface charge of the NPs to confirm the proper coating steps in each process .

- Use AFM and TEM to help to determine the size and the shape of the particles.

These types of nanoparticles are binding with cytochrome C by thiol –Au covalent bond which serves as active platform for further biological studies in the next chapter and targeting the apoptosis pathway of liver cancer cell lines.

2.2. Materials and methods

2.2.1. Synthesis of iron oxide nanoparticles

In this work the synthesis of the iron oxide particles follows the (Goon *et al*., 2009) method. Sodium hydroxide (Fisher Scientific Co, UK), Potassium nitrate (Sigma-Aldrich Co, UK), Iron sulphate (ACROS Organics Co, USA), Sulphuric acid (Sigma-Aldrich Co, UK), Polyethyleneimine (Mw:750 000 D)(Sigma-Aldrich Co, UK) were used in the synthesis of the iron oxide core and polymer coating step.

The magnetic core was prepared by wet chemical co-precipitation method. Firstly, 1.03 g of sodium hydroxide and 1.82 g of potassium nitrate were dissolved in 180ml deionized water. Nitrogen was bubbled over for 1 h at 90 °C. Next, (3.89 g) of iron sulphate is mixed with (20 m L) of 0.01 M sulphuric acid and adding to previous solution under nitrogen gas for 1 h and stirred at 90 °C for the rest 24 h under gas. Next day, the iron oxide NPs was separated by using highly permanent magnet from the outside of the mixing glass vial and the supernatant was removed, the magnetic particles then washed 5 times thoroughly and re-suspended in 25 mL deionised water. The iron oxide concentration was characterised by ICP-OES and the hydrodynamic size and charge of the particles was measured by photon correlation spectroscopy (PCS). Transmission electron microscopy and atomic force microscopy are used in the size and shape discovering of magnetic particles.

2.2.2. Polymer coating of iron oxide nanoparticles

The iron oxide NPs are coated electrostatically with poly(ethyleneimine) polymer between cationic polymer and the negatively charged of magnetic particles (Figure 2.2.). These coating served as protecting layer against the aggregation of the particles and as active platform for gold seeds attaching to the iron oxide particles. In this step, the solution of 5 mL iron oxide and 50 mL of (5 $mgmL^{-1}$) PEI (MW 750 KDa) are sonicated together by a probe sonicator (Soniprep 150 plus, MSE Co, MSS150.CX4.5) for 2 h.

The resulted particles are magnetically separated and washed 5 times with deionized water. The final nanoparticles were re-suspended in 5 mL of deionised water.

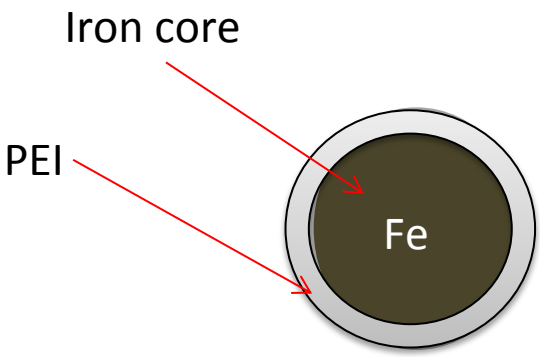

Figure 2.2. Diagram of iron oxide NPS coated with PEI.

In order to confirm the proper coating process, the particles charge was checked by zeta potential measurement which is in this case shift from the negative charge of iron oxide NPs to the positive value of PEI coating.

2.2.3. Gold seeding process

Potassium carbonate (Fisher Scientific Co, UK), Chloroauric acid (Sigma-Aldrich Co, UK),Sodium borohydride (ACROS Organics Co, USA), Hydroxyl amine (Sigma-Aldrich Co, UK),.Polyethyleneimine; Mw:2000 D) (Sigma-Aldrich Co, UK),Sodium hydroxide (Fisher Scientific Co, UK) were used for gold seeding and polymer coating processes.

The mixture of 375 µL chloroauric acid (4% $HAuCl_4$) and 500 µL of potassium carbonate (K_2CO_3, 0.2M) were stirred in 100 mL of icy cold water. After 10 min the 5 mL solution of sodium borohydride (0.5 $mgmL^{-1}$) was added slowly. At this point in time the solution colour change from yellow to deep red.

The electrostatic interaction between the gold (negatively charged) and PEI (positively charged) achieved the Gold seeding formation as illustrated in (Figure 2.3.)

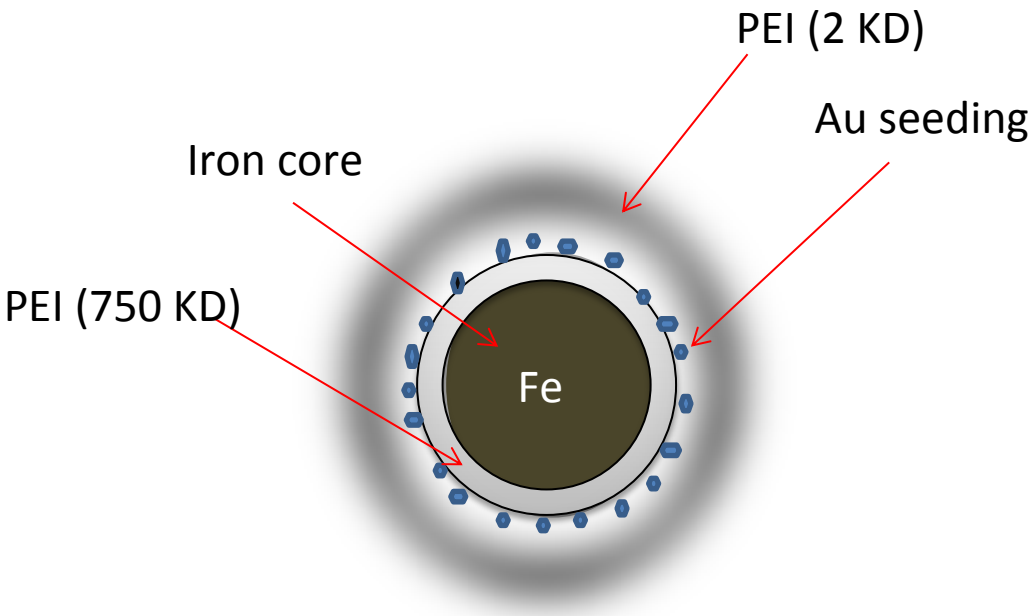

Figure 2.3. Diagram of gold seeding fabrication.

The (2 mL) of the magnetic NPs was mixed with (90 mL) of the previous gold-seed solution and stirrer for (2 h) at room temperature. The resulting particles are separated magnetically and washed 5 times with deionised water. To protect the gold seeds, the particles were stirred with 1 $mgmL^{-1}$ of PEI (2 KD) polymer for 10 min.

The final particles are washed 5 times and re-suspended in 5 mL deionised water, these fabrication steps were characterised by zeta potential measurement by shifting the charge from the negative to positive according to the gold seeding and polymer coating, respectively. Hydrochloric acid (Sigma-Aldrich Co, UK), Nitric acid (Sigma-Aldrich Co, UK), Iron III standard (Sigma-Aldrich Co, UK), Iron oxide standard (Sigma-Aldrich Co, UK), Gold standard (Sigma-Aldrich Co, UK), Chloroform (Sigma-Aldrich Co, UK), Formvar (Agar Scientific Co, UK), Ethanol (Sigma-Aldrich Co, UK), Copper grid (Agar Scientific Co, UK) these materials were used in characterisation of HNPs.

Another method in controlling the synthesis process is UV/Visible spectroscopy through gold SPR affecting the spectrum of magnetic NPs.

2.2.4. Gold coating process

The complete gold shell was achieved by gold reducing in the surface of the prepared particles and this was achieved by stirring with (110 mL, 0.01 M) NaOH at 60°C and (5 mL) of 1% of Chloroauric acid was added with (0.75 mL) of 0.2M hydroxyl amine. The iterative reduction of the two solutions was done by mixing 1% of Chloroauric acid with (0.25 mL) of 0.2M hydroxyl amine for 10 min. After this

stage, the washing process was performed and particles re-suspended in 5 mL deionised water. To examine any surface charge changing of the final coating particles was checked by UV/Visible spectroscopy and zeta potential measurement.

2.2.2.5 Hybrid nanoparticles characterisation

2.2.2.5.1 ICP-OES (Inductively coupled plasma-optical emission spectroscopy)

To determine the metal content of the NPs, the ICP-OES (Inductively coupled plasma-optical emission spectroscopy, Optima 7000V DV, PerkinElmer, Wokingham, UK) was used. The sample preparation for metal detection was achieved by acid digestion (nitric acid: hydrochloric acid, 1:1) of (sample: acid, 1:5) with 100 °C heating. Prior to ICP-OES analysis diluted sample of (1:10) with deionised water was prepared. A calibration curve of Iron and gold standard (R^2: 0.999) was run with (10-0.05) ppm of the both metal respectively (Barnett *et al*. 2013). The calculated ICP-OES iron concentration was determined in all the subsequent HNPs experiments.

2.2.2.5.2. UV/Visible spectroscopy

Aqueous samples of iron oxide, gold seeds and iron oxide –gold NPs were prepared in quartz cuvette to be detected by UV/Visible spectroscopy (UV-2600, UV-Vis, ISR-2600 Plus Integrated sphere, Shimadzu, Germany). Triplicated experiments were run between 300-800 nm at room temperature (Hoskins *et al*. 2012b).

2.2.2.5.3. Photon correlation spectroscopy (PCS)

The particle size and surface charge were measured by Photon correlation spectroscopy (Zetasizer Nano-ZS, Malvern Instruments, UK). Sonicated NPs in deionised water (1 $mgmL^{-1}$) were prepared in screw-top glass vials and analysed at 25°C. Hydrodynamic diameter, zeta potential and polydispersity index (PdI) were measured at each synthesis steps of nanoparticles (Hoskins *et al*. 2012b).

2.2.2.5.4. Transmission Electron Microscopy (TEM)

The imagining of the NPs was performed by Transmission Electron Microscopy (TEM). The supportive film of polyvinyl formal (Formvar) was used in preparing the copper grids (200 mesh, Agar Scientific Co, UK) coated film. Firstly, the copper grids were washed in small beaker with chloroform and then dried by the filter paper. The lint –free cloth was used in polishing of a glass slide which immersed inside (3/4 of height) container of 0.5 $mgmL^{-1}$ formvar. A glass slide removed

quickly and leaves it to dry. By using a sharp the edges of the glass slide were scratched to ensure the complete film removed from it, and then floating on top of fill water container. A film coated copper grids were prepared by laying the grids face down onto the film choosing the proper sit of thickness and wrinkles free. After that, the film was picked up and put it on the clean glass slide and leaves it to dry overnight. (2 µL) of each samples were pipetted onto the grid and dried for 3 h by heat lamp. The prepared sample was visualised under a JEOL JEM-12 microscope (Barnett et al. 2013).

2.2.2.5.5. Protein conjugation and quantification

The conjugation processes was performed by stirring (25 mg) of cytochrome c (Sigma –Aldrich, Gillingham, UK) with (5 mL, 5 $mgmL^{-1}$) of HNPs for 3 h at room temperature. At the same time (12.5 mg) of poly ethylene glycol (PEG) was added in parallel with pro-apoptotic protein (cytochrome c) into the previous solution of HNPs to cover the surfaces of hybrid particles. The final particles were magnetically separated and washed with distilled water five times. The resulted particles were resuspended with 5 mL of distilled water to get 5 $mgmL^{-1}$ of iron which can be detected by ICP-OES instrument. The concentration of cytochrome c binding to HNPs was quantified by UV-VIS spectroscopy (UV-2600 UV-VIS9NIR,Germany) at 410 nm and compared to standard calibration curve (R^2=0.999).

2.3. RESULTS

2.3.1. Photon correlation spectroscopy (PCS)

The HNPs synthesis was checked in each step of formulation by measuring the zeta potential values. As illustrated in (Figure 2.4.)

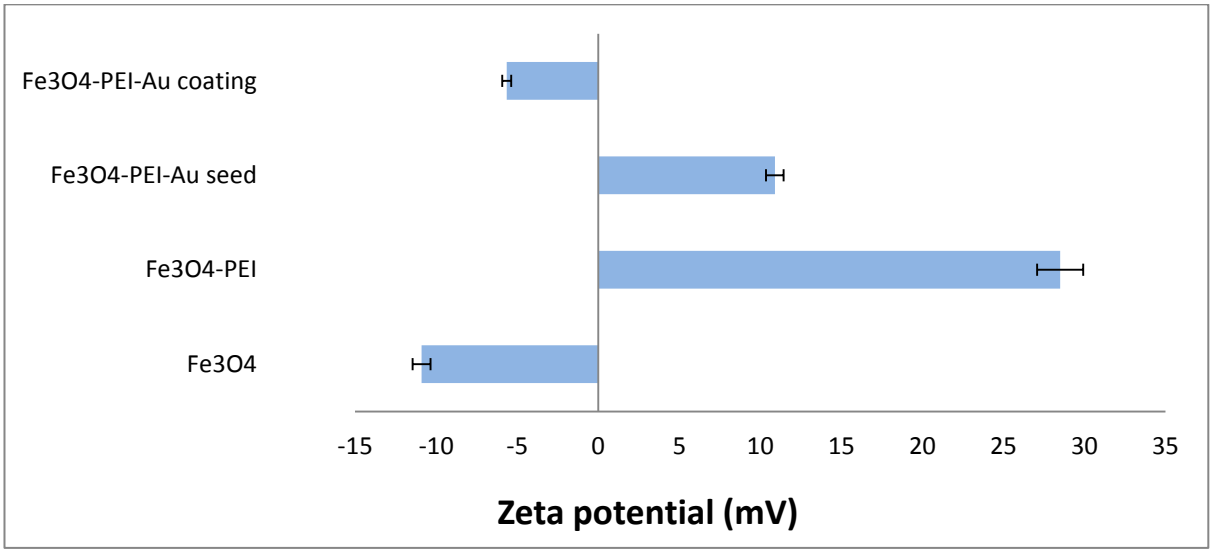

Figure 2.4. Zeta potential measurements of iron oxide-gold hybrid nanoparticles,(n=3,±SD).

The surface negatively charge of iron oxide NPs (-10 mV) was contributed to sulphate surface presence in the synthesis process (Hoskins *et al*. 2012b). The shifting of the zeta potential to the positive charge (+28.5 mV) indicted the successful coating of magnetic NPs with poly(ethyleneimine) polymer. The presence of amine groups in the polymer gives the positively charge in this step of formulation.

The next steps of gold seeding and gold coating of Fe_3O_4-PEI were recorded with remarkable decrease in particles surface charges due to negative gold charge atoms and positive –OH group on polymer coating (+10.9 mV and -5.65 mV) respectively.

The hydrodynamic radius of each NPs synthesis steps were recorded as a large size for magnetic NPs (4160 nm) as a result of inherent magnetic iron particles. Consequently, the particles diameter were remarkably decrease with next formulation steps of polymer and gold coating related to aggregation reducing abilities of magnetic particles (Table 2-1). Polydispersity index (PdI) of HNPs referred to the homogeneity rate of the particles distribution in the formulation, which here showed values near 0.3 that detect a good dispersity index rate of this formulation (Table 2-1).

Table 2-1.Hydrodynamic size and poly dispersity index of HNPs formulation measured by Photon correlation spectroscopy (n: 3, ave±SD)

Formulation	Hydrodynamic Size(nm) ±SD	Poly dispersity index ±SD	UV max
Fe3O4	4160±47.95	0.27±0.33	–
Fe3O4-PEI	830.2±25.05	0.32±0.08	–
Fe3O4-PEI-Au seed	529±6.5	0.28±0.12	560
Fe3O4-PEI-Au coating	392±15.4	0.21±0.11	650

2.3.2. Transmission Electron Microscopy (TEM)

The actual size and shape of the hybrid iron oxide-gold nanoparticles can be recorded by projected area diameter of the grid used in TEM, as in this case it recorded around 40 nm for fully coated HNPs.

First step of hybrid nanoparticle formulation started with TEM imaging of iron core at 150K magnification to verify the proper shape and size which was recorded about 40 nm as shown in (Figure 2.5., A), the PEI coating steps of iron core was imaged at 120K as shown in (Figure 2.5.,B)

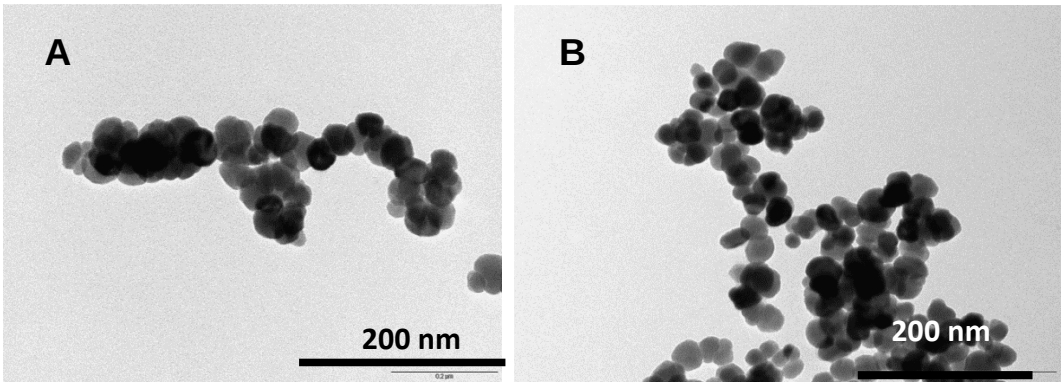

Figure 2.5.TEM images of A) iron oxide core and B) iron core-PEI coating.

The gold seeding processes was confirmed with 2 nm gold nanoparticles surrounding the iron core as shown in (Figure 2.6.) which appeared clearly on the surfaces of NPs at 200K magnification.

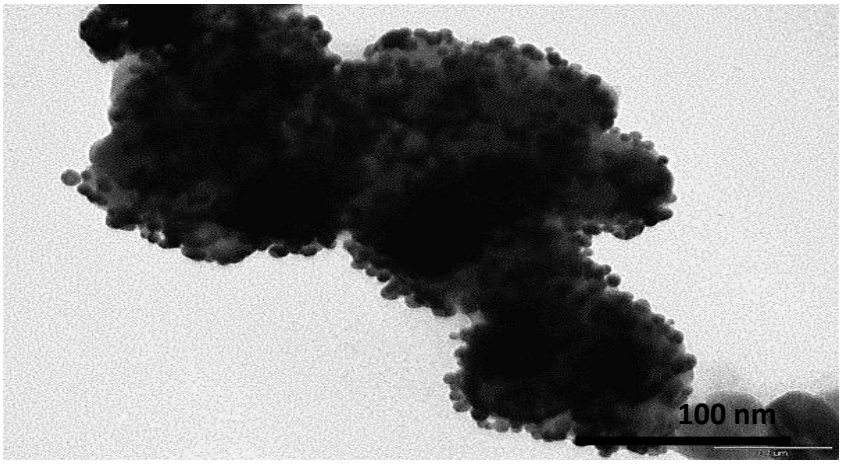

Figure 2.6. TEM image of gold seeded iron NPs.

The final shape of HNPs was imaged at 100K magnification and showed approximately particle size around 40 nm. The image of final particles was showed external smooth shape with fully gold coated layer and no more appearance was observed for the gold seeds (Figure 2.7.)

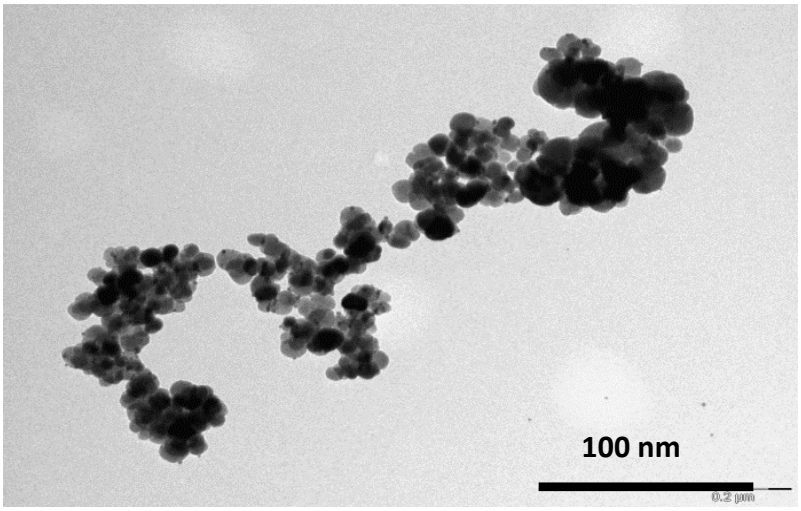

Figure 2.7. TEM image of final HNPs.

2.3.3. Inductively Coupled Plasma-Optical Emission Spectroscopy (ICP-OES)

The metal concentration of the HNPs concerning with (iron and gold) particles content were detected by ICP. In this formulation the iron and gold concentration were 2.09±0.44 $mgmL^{-1}$ (R^2: 0.9997) and 1.16±0.21 $mgmL^{-1}$ (R^2: 0.999), respectively calculated from the standard iron and gold curves. The metal analysis using ICP was repeated for four different patches of iron oxide-gold NPs, presenting the reliable and reproducible synthesis process.

2.3.4. Protein binding

The amount of cytochrome c attached to HNPs was assessed by UV-VIS spectroscopy. The concentration of pro-apoptotic protein was (1.98 $mgmL^{-1}$) attached to HNPs comparing to (1.78 $mgmL^{-1}$) attached to PEG added HNPs (Table 2-2). The changed of CYT-c concentration was contributed to the attachment sites competition between the polymer and protein on the gold surface of the HNPs. The UV-VIS spectra (Figure 2.8.) revealed the absorbance of CYT c in HNPs at 410 nm, while no spectra was detected at previous wave length for HNPs with no protein conjugation.

Table 2-2.Iron, gold and cytochrome C concentration in HNP and HNP-CYT C formulation determined by ICP (Fe and Au) and UV visible (CYT-C).

Samples	Fe	Au	Cytochrome C
	$mgmL^{-1}$	$mgmL^{-1}$	$mgmL^{-1}$
HNP	2.0997	0.7694	–
HNP- C	1.4664	0.2100	1.989
HNP- C-PEG	1.4664	0.2100	1.7866

2.3.5. UV/Visible spectroscopy

The absorption spectra of each formulated part in the HNPs was determined at the maximum absorption wave length in UV/Visible spectroscopy graph (Figure 2.8., A). The Fe_3O_4 alone did not show any absorbance within the wavelengths tested. The colloidal 2 nm gold seeds showed strong absorbance at around 480 nm. Once attached onto the Fe_3O_4-PEI a band shift was observed with a lambda max of approximately 540 nm. After subsequent coating the final HNPs showed a peak absorbance of 600 nm, this indicated that complete coating had formed. The significant signal was observed at 410 nm as successful indicator of pro-apoptotic protein (CYT-C) binding onto the HNPs surfaces (Figure 2.8.,B).

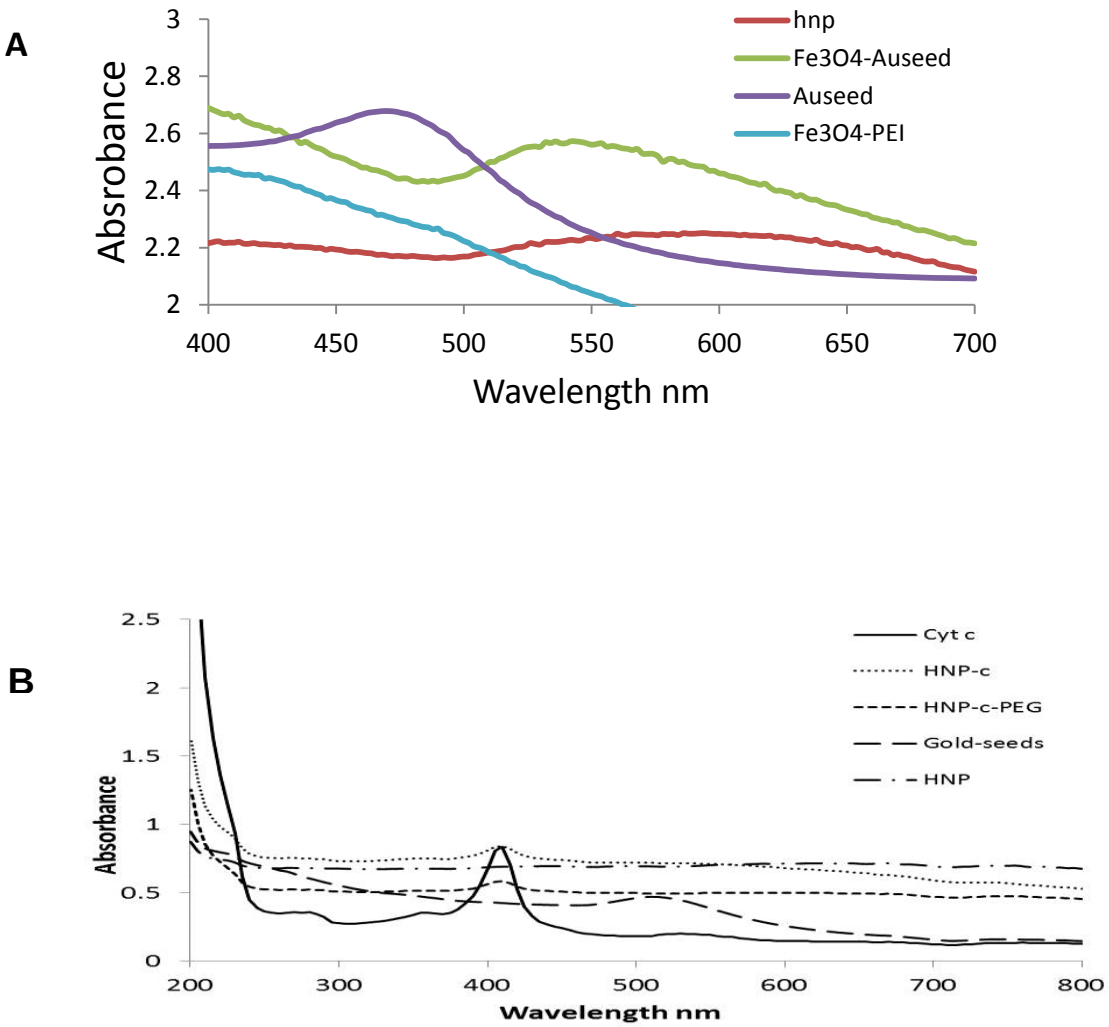

Figure 2.8. UV-Vis absorbance spectra of A) Fe_3O_4, Au seed, Fe_3O_4-PEI and HNPs and B) UV-Vis absorbance spectra detection of CYT-C attachment to the HNPs.

2.4. Discussion

The successful HNPs synthesis were performed and detected by ICP-OES, UV/Visible spectroscopy, TEM and PCS.

Metal content of the HNPs was detected by ICP-OES and calculated the concentration of the gold and iron which is consider as main critical step in the next biological application of the new formulation.

Generally, the gold coating processes of the magnetic nanoparticles was indicated in each step by UV/Visible spectroscopy and zeta potential measurements. Iron oxide core negative charge was shifted to the positive value with successful PEI coating as a functional binding layer to the next gold seeding (around 2 nm) followed by consecutive reduction of the gold onto the particles surfaces in the course of coating process (recording negative charge due to the existence of gold) . The gold coating thickness was studied to determine the ideal physical properties for various applications (Huang *et al*., 2007; Zijlstra and Orrit, 2011). All the previous steps were indicated by the zeta potential measurements (Figure 2.4.) and UV/Visible spectroscopy graph (Figure 2.8.).

Zeta potential values are recorded with lower positive value of Fe_3O_4-PEI-Au seed comparing to second steps of PEI coating formulation. The complete particles coating with gold is showed negative zeta potential value that confirm the proper presence of gold negative charge and confirm the gold seeding and coating processes during the formulation steps. The absorbance measured by the UV/Visible spectroscopy was identified the gold occurrence in these construction.

After the gold seeding and coating processes the remarkable shift in the UV absorbance from 480 nm to 540 nm and 600 nm, respectively. The absorbance signal at 410 nm is confirmed the successful binding of pro-apoptotic protein (CYT-C) onto the HNPs surfaces as no signal was observed at this wave length prior to protein attachment.

The magnetic iron oxide core was observed as aggregated particles when hydrodynamic diameter measured by PCS and this reflected the magnetic inherent properties of magnetic NPs in solution. For that reason, TEM images were recorded with smaller particles diameter comparing to PCS values and these studies were approved with previous researches that confirm the higher hydrodynamic diameter of magnetic NPs with aggregation formulation (Hoskins *et al.* 2012b). The next fabrication steps of iron oxide core coating with PEI polymer showed lower hydrodynamic diameter and recorded as (830 nm) comparing to high diameter measurement observed with iron core which analysed as (4160 nm). These significant decreases in particles diameter were reflected the successful PEI coating that act as stabilising agents by decreasing the undesirable aggregation of magnetic iron core. The electron microscopy images were recorded slight increase in particles size ranging from 30 nm for naked iron core to 40 nm for fully coated NPs and these TEM measurements showed 10 nm thickness of the coated layer. The coating thickness is reflected the gold resonance abilities as well as the heating processes by working as a good heating and magnetic vehicle with thin coated layer formulation (Prodan *et al*. 2003; Barnett *et al*. 2012).

Recently, the binding of nanoparticle with bio- therapeutic protein has been applied in cancer researches. The big challenges of binding of active protein without affecting the proper function of it was achieved by labelling cytochrome C site with negatively charged gold nanoparticles by thiol –Au covalent bind. The binding of gold nanoparticles at different cites of cytochrome C showed the type of electrostatic interaction between the amino acid side with nanoparticle ligand which control the proper behaviour of binding protein. Although, some binding sites of cytochrome C may lead to protein denaturation. In order to preserve the protein structure, the loosely folded motive is prefer in labelling processing as alternative to nucleation centre folding (Marie-Eve Aubin *et al*. 2008)

The possibility of binding between the thiol residue of cytochrome C and the gold is basis on the covalent gold-thiol bonding. This technique used the organic linker between the gold nanoparticles and protein. Moreover, this strategy is offered a highly structurally defined type of bonding (Heaven et al. 2008; Jadzinsky *et al*. 2007). More labelling strategies were used with peptide, oligonuclioside and bioactive molecules (Krpetic *et al*. 2009; Ackerson *et al.* 2010; Bowman *et al.* 2008).

Cytochrome C is categorised as vital targeting protein in many regimens of cancer therapies. However, apoptosis activation with 12.7 KDa CYT C molecular weight is experienced many challenges into cellular delivery mechanism without affecting the physical and chemical stability of bio-therapeutic proteins (Manning *et al.* 2010). Countless efforts were reported to deliver CYT C properly and with sufficient levels inside cell cytoplasm, the electroporation way is one of applied

methods of CYT C intracellular delivery (Sharonov *et al*. 2005). Another technique is concerned with protein nanoparticles formation by nanoprecepitation coated with biocompatible types of polymer such as poly (lactic-co-glycolic) acid to enhance protein circulation time inside the body and to increase the cellular uptake of CYT C by Hela cells to initiate apoptosis (Morales-Cruz *et al*. 2014). Further researches showed the ability of direct binding of CYT C onto the functionalised nanoparticles surfaces such as metal type, gold (Aubin-Tam *et al*. 2009), polymer (Morales-Cruz *et al*. 2014) and silica (Shang *et al*. 2009) . The testing of the apoptotic effects of these combination were reports with remarkable increases in the apoptotic markers and with death of targeting cells. In this study additional advantages are reported with CYT-C binding to the surfaces of HNP which serviced as vital carrier of therapeutic molecules and as imaging agents.

2.5. Conclusion

Hybrid iron oxide-gold NPs have been successfully formulated and characterised by several methods such as PCS, UV–vis absorption and TEM. All the checking steps confirmed the successful formation procedure of hybrid nanoparticles. The magnetic iron core with 30 nm diameter was manufactured and other formulated layers were diagnosed as a polyethylenimine intermediate layer and gold coating. The final size of HNPs was approximately diagnosed as 40 nm by TEM.

The synthesis steps of HNP and protein binding were successful as characterised by UV-Vis spectroscopy, which confirmed that 40% of loaded cytochrome C site are binding with negatively charged gold nanoparticles by thiol –Au covalent bonds. Further biological studies will be carried out on this formulation to detect the cellular uptake, cell viability, apoptotic effect and imaging studies against hepatocellular carcinoma cell lines.

Chapter Three

Biological investigations & Cytotoxicity

3.1. Introduction

Hepatocellular carcinoma (HCC) is the main type of primary liver cancer, which is diagnosed as highly vascular type of cancer and reportedly is the third biggest cause of cancer death in the world. The studies of molecular signaling pathways of this tumor type have been carried out extensively in previous studies, towards the direction of discovering new therapeutic targeting bio-molecules to decrease the high percentage of patient mortality within normal treatment pathways such as chemotherapy and surgery (Sharma *et al*. 2016; Ling Huang *et al*. 2017). The usual methods of cancer treatment often experience poor site specific targeting (Rasmussen *et al*. 2010). One of the new cancer treatment strategies is the use of nanomaterials to make nanomedicines, since 1970 the nanoscales have been used as drug carrier and imaging device in different pharmaceutical applications. The remarkable development in the synthesis of NPs was reported as active drug delivery system and controlled drugs release for trapping different types of the cancer cells (Felice *et al*. 2014; Fernandes *et al*. 2015; Ling Huang *et al*. 2017).

Nanoparticle interaction with proteins has played vital role in the basis of bio-activity of different types of nanoparticles. These give rise to the behavior of therapeutic molecules by affecting cellular uptake, accumulation behavior inside targeting cells and to generate bio-compatible nanoparticles with therapeutic goals in a biological environment.The successful binding of bio-active cytochrome C with hybrid iron –oxide NPs have been studied for HCC treatment (Malekigorji *et al*., 2014; Figueroa CM, *et al*. 2017) and reported with significant synergism between doxorubicin and HNP-C as active cytotoxic device against HepG2 cell line, these

effects were recognized by different cell viability assays and imaging studies (Malekigorji *et al*., 2014). Cytochrome C as illustrated previously has a main role in proper activation of apoptosis pathways which is considered as crucial step in cancer treatment. Previous attempts to introduce cytochrome c have also been studied with lipid–apolipoprotein and mesoporus silica NPs (Kim *et al*., 2012; Park *et al*., 2010).

The effectiveness of the most therapeutic devices should be proven first in different discovery steps of chemical and biological researches before to be proven as acceptable clinical therapies. Therefore, the preclinical screening of novel drug formulation is first done in biological environment by using different types of living cells and tissues to evaluate the pharmacological action of the novel therapeutic formulation (Pathania *et al*. 2014; Megha *et al*. 2015). The biological testing of novel drug formulation is crucial inside biological system which known as complicated chemical and biological system that can be directly or indirectly effects on the bio-therapeutic activities of introduce drug formulation. Most of these factors are related to pH, temperature, digestive enzyme, blood proteins and others factors related to the medium of targeted organs (Wijdeven *et al*. 2014; Lemke 2008).

A variety of tests are used *in vitro* studies to predict the cytotoxicity of novel formulation. However, they cannot fully replace *in vivo* tests but can be considered as optimizing techniques for drugs activities and to avoid highly number of false positive results which start during *in vivo* studies and generate undesirable side effects for animals. By means of this technique we can save time and money for

further improvement in the medical researches and ethical consideration. *In vitro* tests are used to study the stability of the new therapeutic formulation and to evaluate specific criteria of drug mutagenic and cytotoxic effects by using living tissue with already known signaling pathways (Corvi and Madia, 2016).

For novel biomedical and therapeutic applications, the conjugation of therapeutic proteins onto the surfaces of nanoparticles has been of main concern in recent years. Recently, hybrid iron oxide- gold nanoparticles were functionalised with hydrophilic polymer poly (ethylene glycol) to produce long circulating time by hiding HNP from the endoplasmic reticulum system. The presence of a functional gold shell on HNP surface (Au) allows the dative covalent bond to the thiol (-SH) group of cytochrome c (Malekigorji *et al*.,2014).

3.1.1. Aims and Objectives

The main aims of this chapter are:

-To determine the cytotoxicity effect of cytochrome C hybrid formulation against the liver cancer and U937 cell lines and how to improve the potency of doxorubicin, paclitaxel, oxaliplatin, vinblastine and vincristine when co-administer with IC_{10} determine concentration of HNP-C by targeting the main apoptotic mechanism of each drug.

-To investigate the activity of this formulation on liver cancer cell lines by cell viability assays (MTT assay, trypan blue).

- To analyse levels of apoptosis in treated cells by use of apoptosis detection kits and microscopy at different stages (caspase 3, western blot, TUNEL assay, fluorescence microscopy and AFM).

-To measure intracellular concentration quantification of cytochrome c after cellular exposure

3.2. Materials and methods

Doxorubicin, Paclitaxel, Oxaliplatin, Vinblastine and vincristine were purchased from LC Laboratories (Woburn, USA); cytochrome C and other materials were provided from Sigma-Aldrich (Gillingham, UK). Hepatocellular carcinoma cell line (HepG-2) was provided from ATCC [HEPG2] (ATCC® HB8065™), SK-HEP-1 was from ATCC (ATCC® HTB-52™); Huh-7D12 cell line was from ECACC (European Collection of Authenticated Cell Cultures) and U937 cell line was from LGC standard Co., UK. U937 cell line was supplied with phorbol-12-myristate 13-acetate (PMA) (0.02%, 50 μgmL^{-1} in PBS (Phosphate Buffer Saline), Sigma-Aldrich) to prepare differentiated U937 to culture processes. Hybrid iron-oxide gold nanoparticle were synthesised in the lab. The cell lines were grown as monolayer in ATCC- formulated Eagle`s Minimum Essential Medium for (SK-HEP-1);DMEM culture media for (HepG-2 and Huh-7d) and PRMI culture media for (U937) and placed in a humidified incubator with 5% CO_2 at 37 °C. To make efficient growth medium for this cell line were added 10% FBS (fetal bovine serum)

and 1% (penicillin/streptomycin) solution provided from Sigma. The IC_{50} values and cell viability graphs were performed by using Graph Pad Prism 7 software.

3.2.1. Cellular uptake of protein

Liver cell lines and U937 were seeded in 6 well plates and incubated for 24 h at 37 °C with 5% CO_2.Next day the media was replaced by 100 µL (50 and 100 $\mu g mL^{-1}$) of cytochrome C and HNP-C per well and incubated for 1 and 4 h. After each incubation period the media was removed and the treated cells were washed with PBS preparing to detach by trypsin adding to each well. The suspension cells in 1 mL fresh media were counted by automated cell counter (Invitrogen countess, UK) to transfer 100,000 cells of each cell line into Eppendorf tubes and centrifuged for 5 min at (250 g). The resultant supernatant was removed and the precipitated pellets were resuspended with 1ml of sterilised water. The concentration of protein alone and in combination with HNP were measured at 410 nm and analysed per cell by using UV/Vis spectroscopy (UV-VIS with an ISR-2600 Shimadzu, Germany).

3.2.2. Cell viability assays

96 well plates were used to seed 15,000 cells with 100 µL of media per well for each cell lines and allowed to adhere overnight (24 h) in humidified incubator at

37% in 5%CO_2 atmosphere. Serial dilutions of Doxorubicin (5-0.25 µM); Oxaliplatin (128-8 µM); Paclitaxel (100-1 nM); Vincristine and Vinblastine (100-1 nM) alone and in combination with HNP-C (0.012 $mgmL^{-1}$) were added to the 96-wells of HepG2,SK-hep-1,Huh-7d and U937 cell lines and incubated for (24, 48 and 72 h). At these three times vital dye (yellow MTT 3-(4,5-dimethyl-2-thiazolyl)-2,5-diphenyl-2H-tetrazolium bromide) was used to detect the number of live cells which reflected the cytotoxicity effect for anticancer drug alone and with formulation.

3.2.2.1. MTT Assay

The reduction of the MTT by mitochondrial reductase enzyme which is related directly to the number of live cells leads to form insoluble purple formazan crystal; the crystals can be solubilized using DMSO. For each time points (24,48 and 72 h) removed the serial drugs solution from treated cells and add 100 µL of MTT sterilized solution, put in the incubator for 3-4 h to permit the reduction of Tetrazolium dye by oxidoreductase mitochondrial enzyme referring to the metabolic activity of the live cells forming insoluble formazan crystal then removed the MTT solution and replaced by 100 µL of DMSO to form colorimetric solution optical densities were measured in microplate reader(Techan Infinite, Austria) at 570 nm.

3.2.2.2. Exclusion test of cell viability by Trypan blue

The main principle of this technique is the determination of the percentage of viable cells in the suspension cultured media depending on the intact cell membrane that exclude trypan blue staining in the live cells in contrast to blue staining dead cells with a destroyed outer membrane.

HepG2,SK-hep-1,Huh-7d and U937 cell lines were introduced to undergo apoptosis by treating with previous detection serial dilution of (doxorubicin, paclitaxel, oxaliplatin, vincristine and vinblastine) alone and in combination with 10% (0.012 $mgmL^{-1}$) growth inhibition of HNP-cyt C (50,000 cells/well) in 6 well plates for three time points 24 h, 48 h and 72 h and incubated at 37°C with 5% CO_2. At the end of each required time of treatment, the supernatant was removed and put in suitable tube, and 0.5 ml of trypsin added to detach the cells from the bottom of the well and mixed with previous supernatant. The prepared cell suspension (50 µL) was mixed with 50 µL of trypan blue and pipette into automatic counter slide and then read it by (Invitrogen countess, UK) the percentage of viability was detected in relation to control cells.

3.2.3. Apoptosis assays

3.2.3.1. Caspase-3 assay:

Measuring the caspase-3 level as an indicator of apoptosis, this was performed by using caspase substrate (Ac-DEVD-pNA) as a colorimetric assay (Caspase 3 Assay Colorimetric Kit ((ab39401) Abcam). The hydrolysis activity of caspase 3 based on the cleavage pNA part of tetrapeptide chain of DEVD is based on the PARP (Poly (ADP-ribose) polymerase cleavage at (216 –Asp-Gly -217) as a main step in apoptosis execution. The results of this kit are quantified by measuring the light emission from p-NA cleavage part of this moiety and detected at 405 nm using microplate reader (Techan Infinite, Austria). The activity of caspase 3 enzyme is calculated by the comparison between the absorbance of control cell (untreated cells) with the absorbance of treated cells and determined as fold increase from the control, triplicated experiments were performed for each samples.

Liver cancer cells and U937 were induced to undergo apoptosis by treating with 5x IC50 of doxorubicin, paclitaxel, oxaliplatin, vincristine and vinblastine alone and in combination with 10% growth inhibition of HNP-cyt C in specific concentration (1×10^6/well) in 6 well plates. At the end of each required time of treatment, the supernatant were removed and put in suitable tube, and then added 0.5 mL of trypsin to detach the cells from the bottom of the well and mixed with previous

supernatant. The cell suspensions were centrifuged for 10 min at 250g. The supernatant was carefully removed and added 25 µL of cold lysis buffer to the cell pellet. This step allow to release cell protein to be determine by adding 25 µL assay buffer and 25 µL DDT (Dithiothreitol) stoke solution to each hydrolysis samples. To each well that undergo previous reaction were add 5 µL of caspase-3 colorimetric substrate (Ac-DEVD-pNA) which reflect a series of amino acid , then transfer the caspase -3 enzymatic reaction treated cells to 96 well flat bottom plate and incubated at 37°C for 1-2 hours. After incubation the plate was read at 405 nm by micro plate reader (Techan Infinite, Austria). Additional control were prepared by adding assay buffer, lysis buffer and DDT into one well without caspase substrate and assay buffer and DDT plus caspase substrate into other ones.

3.2.3.2. Western blot

Liver cancer cell lines (HepG2, Huh-7D12 and SK-hep-1) with U937 cells underwent apoptosis in the 6 wells plate (1×10^6/well). After 48 h of treatment period, the treated media were removed, and collected in suitable Eppendorf. After that 0.5 mL of trypsin were added to each well to detach the adherent cells and mixed with previous collected supernatant in corresponding pattern. The mixed suspension cells were centrifuged for 3 min at 250 rpm, 4°C.The produced cell pellets were washed with chilled PBS and centrifuged again to keep the final precipitated pellets at -80°C.

The chilled cell pellets were collected and lysed by adding 100 µL of RIPA buffer ("Radio-Immunoprecipitation Assay") constituent from protease and protease inhibitor including, 150 mM sodium chloride (Sigma-Aldrich), 20 mM Hepes (CalbioChem), 2 mM ethylene-diamino-tetraacetic acid (EDTA, Sigma-Aldrich), 1% NP40 (Sigma Aldrich), 120 µM leupeptin (Sigma-Aldrich), 1 mM phenylmethanesulfonyl fluoride (PMSF, Sigma-Aldrich), 10 µM pepstatin (Sigma-Aldrich) and 0.5% sodium deoxycholate (Sigma-Aldrich), for each pellet and centrifuge for 10 min at (14000 rpm, 4°C), the resultant supernatant were collected and kept at -80°C.

(BCA) bicinchoninic assay (Sigma-Aldrich) was used as quantitative method in 96 well plates to detect the protein concentration for each samples by mixing 10 µL of resulted lysate with 100 µL of BCA reagent (Sigma-Aldrich) and incubated for 30 minutes at 37°C to be read it after at 570 nm using plate reader and then compared with BSA standard Bovine serum albumin (Sigma-Aldrich) with concentration range from 0.1-2 $mgmL^{-1}$.

The next step in western blot is the detecting of specific protein which is concern here with (PARP) cleavage as apoptosis indicator, each sample was mixed with 5 µL of prepared buffer of (β-mercaptoethanol ,Sigma-Aldrich), and SDS-Nupage ,1:20, Sigma-Aldrich) and boiled at 80°C then centrifuge gently and applied to gel electrophoresis process using 4-20% Bis Tris gels (Invitrogen) type in an XCell SureLock Mini Cell (Invitrogen) which loaded with hepes running buffer (100 mM hepes, 1% sodium dodecyl sulphate and 100 mM Tris ,SDS, Sigma-Aldrich), the standard protein ladder was used to detect the proper size of gel separated protein

PageRuler Plus Prestained Protein Ladder (Thermo Scientific). After that, the gel proteins were transferred electrically to the PVDF membrane (polyvinylidene difluoride membrane, GE Healthcare Life Sciences) soaked in transfer buffer (200 mM glycine (Sigma-Aldrich), 0.075% SDS, 25 mM Tris and 10% methanol (Sigma-Aldrich)) for 1.5 hours at 25 V. solution. The blocking process was performed to PVDF protein membrane by using milk solution (5 g of semi-skimmed dry milk+100 mL (TBST 1X) Tris buffer saline tween) Tris buffer prepared from 50 mM Tris hydrochloride (pH 7.4, Sigma-Aldrich), 150 mM NaCl, 0.1% Tween 20) and put on a Stuart Scientific Platform Shaker STR6 with gentle shaking for 1 hour and at room temperature to prevent random antibody binding on various banding of separated proteins. The primary detected antibody (PARP, Cell Signalling Technology) in ratio of 1:2000 was prepared to soak PVDF membrane overnight at 4 °C and the membranes were washed after the incubation with TBST 1X , followed by another incubation period with secondary antibody which prepared by mixing anti-rabbit AB (Cell Signalling Technology) with blocking milk solution in dilution ratio equal to 1:2500 (10µl:10ml)respectively. The UptiLight HRP chemiluminescent (Uptima) are used as a substrate to visualise the reactive protein bands on FluorChem M Imager.

3.2.3.3. Terminal deoxynucleotidyl transferase (dUTP) nick end labelling (TUNEL) assay

TUNEL colorimetric method was used to detect DNA damage marker for apoptosis detection in 96 well plate kits which are purchased from (R&D system). Liver cancer cell lines (Hep G2, Huh-7D, SK-hep-1) and U937 cell lines were cultured in 96 well plates with concentration (1×10^5 cells /well) and then treated with(Doxorubicin, Paclitaxel, Oxaliplatin, Vinblastine, Vincristine) alone and in combination with 10% cell viability effect of HNP-C and leave it for 24 h in a humidified incubator with 5% CO_2 at 37 °C. According to the manufacture's kit protocol, the media was removed from each well and then the adherent cells were fixed with 3.7% buffered formaldehyde solution for 7 min, followed by washing with PBS (2 times) and centrifugation between each washing steps. The post-fix step was performed by filling the wells with 100% methanol for 20 min and wash with PBS preparing for the labelling procedure, 96 well plate centrifuge (Sigma Refrigerated centrifuge 4K15) was used for the following steps . Firstly, 50 µL of protein K solution (50 µL of distilled water with 1 µL of protein kinase) was added to each well for 15 min at room temperature and then centrifuged at 1000 X g for 3 min and discard the buffer, Then wash twice with 200 µL of distilled water per well. Positive and negative controls were generated by adding 10 µL of TACS-Nuclease™ (Trevigen Apoptotic Cell System) to the control wells and incubate for 1 h at 37°C to indicate the level of DNA breaks which serves as a substrate for further labelling reaction accompanied with unlabelled control to show the background of labelling processes. After incubation period, 50µl/well of quench endogenous peroxidase (0.5 mL of 30% hydrogen peroxide with 5.5 mL of

methanol (Sigma-Aldrich)) was added to avoid non-specific back ground staining, and then wash twice with distilled water. Labelling reaction is prepared by adding 150 µl/well of 1X TdT (Terminal deoxynucleotidyl Transferase) buffer for 5 min and the 50 µl/well of labelling reaction mix (5ml 1X TdT, 35 µl TdT dNTP mix, 100 µl 50X Mn^{2+} and 35 µl TdT enzyme) were used for more 1 h incubation time at 37°C to facilitate the addition of nucleotide to the 3 terminus of DNA and to detect the number of apoptotic cells. Next to labelling reaction 150µl/well of 1XTdT stop buffer were applied for 5 min to stop the labelling reaction and to prepare the sample to secondary labelling reaction with 50 µl/well Strep-HRP (Streptavidin-horseradish peroxidase) solution for 10min at room temperature to detect biotinylated antibody and to produce colorimetric reaction. At the final steps of the reaction 100 µL/well of 5% phosphoric acid were added to stop the reaction and measure the absorbance at 450 nm by plate reader (Techan Infinite, Austria). Experiments were carried out in triplicate.

3.2.4. Apoptosis detection by imaging studies

3.2.4.1. Fluorescent microscope

Liver cancer cell lines with U937 were seeded on glass cover slip in 6 wells plate (1×10^6/well) and exposed to apoptosis by anticancer drugs alone and in combination with nanoparticle formulation in indicated concentration, after 24 h. treatment period the growth media was removed from each well and washing with

1 mL of (1X Annexin ,Life Technologies Co, UK) binding buffer follows the manufacture instruction and repeated the washing steps to one more time. After that, 5 µL of Annexin V fluorescein probe (life technologies Co, UK) , 5 µL of Hoechst nuclei stain (life technologies Co, UK) and 5 µL of propidium iodide (life technologies Co, UK) are mixed with 100 µL of (1X Annexin) binding buffer was added to each well and incubated at room temperature for 15 min in dark place. Then, repeat the washing process with 1 mL of (1X Annexin) binding buffer. The fluorescence staining cells were fixed with 2% formaldehyde (Sigma-Aldrich) for 10 min to prevent any disruption to cell membrane and then wash with PBS for 3-4 times then put 2-3 drops of mounting media (Sigma-Aldrich) onto the face of each glass cover slip to prevent photo bleaching and to match the refractive index of the sample during the imaging process. The glass slips were fixed on the glass slides and visualise by fluorescence microscopy (Invitrogen^{TM} EVOS^{TM} FL, Thermo Fisher).

3.2.4.2. Nanoparticles internalisation imaging by Transmission electron microscope

Cross section imaging of liver cancer cell lines and U937 were captured by TEM microscope (JEOL, JEM-1230 microscope (Japan)) and all chemicals and materials used are purchased from (Agar Scientific).

Cancer cells were incubated with 25 µgmL^{-1} of HNP-c after cells were seeded into Aclar slides in 6 wells plate for 24 h. next day the treated cells were washed with

PBS followed by fixation steps with 2.5% gluteraldehyde in Na cacodylate buffer: 2 mM calcium chloride for 2 h. Then, cells were washed with previous buffer for 5 min and repeated for 2 times. The post fixation step was performed by using 0.1% Osmium tetroxide in 0.1 M sodium cacodylate buffer: 2 mM Ca chloride for 1 h. Dehydration process with serial percentage (70%, 80%,90%,100% and 100 dry of ethanol for 15 min. to each steps) were used as preparing to next polymerisation and infiltration steps with SPUR resin (13 g of NSA(Nonenyl Succinic Anhydride), 5 g ERL (ERL 4221 RESIN), 3 g of DER(DER 736) and 0.2 g of S-1 DMAE (Dimethyllaminoethanol)) with series of 1:3 dry alcohol/resin,2:3 dry alcohol/resin and 100% resin to get hard film and to be ready to cut and get thinner layer section. The ultra-sectioning process of resin was achieved by diamond knife using (Reichert-Jung Ultracut E Ultra Microtome) and placed the produce ultrathin sections into copper grids to stain by heavy metal (Lead citrate and Uranyl acetate) to increase contrast level of the final imaging of TEM microscope (JEOL, JEM-1230 microscope (Japan)) with specific software.

3.2.4.3. Topographical imaging by atomic force microscopy

Liver cancer cells and U937 were seeded into 6 wells plate containing sterilised glass coverslips and incubated for 24 h at 37% in 5% CO_2. The media was replaced next day with 5x IC50 of (doxorubicin, paclitaxel, oxaliplatin, vincristine and vinblastine) alone and in combination with 10% growth inhibition of HNP-cyt C. After 24 h incubation the treated media was removed and the cells were

washed (3-4 times) with PBS and then fixed with 2.5% gluteraldehyde in PBS and incubated for 10 min. after the fixation process the cells were washed thoroughly with PBS for at least 5 times. The glass cover slips of the fixed cells are mounted on glass slides and leave it overnight to dry. Topographical studies of control and treated cells were imaged by atomic force microscopy (Bruker ,Germany) with Peak Force Tapping mode(ScanAsyst in air cantilever).

3.3. Results

3.3.1. Cell viability assays

The effect of hybrid nanoparticle formulation with cytochrome C (CYT-C) conjugated onto their surface in combination with chemotherapeutic drugs on cell viability of HepG2, SK-hep-1 and Huh-7D was assessed using MTT and trypan blue assays. The cytotoxicity of the drugs alone and in combination was indicated by calculating the dose of the drugs required to decrease 50% of the cell viability which is called IC_{50}.

3.3.1.1. Cell viability assays of CYT-C, HNP and HNP-C

The cytotoxicity of CYT-C, HNP and HNP-C were assessed by MTT and trypan blue assays on hepatocellular carcinoma cell lines HepG2 (epithelial origin), Huh-7D(epithelial origin), SK-hep-1(endothelial origin) and differentiated U937 cell lines. The cell viability results of unloaded HNP and CYT-C did not show any

significant dose response effects against liver cancer cell lines and U937 at three times points of incubation times (P>0.001). The viability assays of HNP-C serial dilution (10-1 µM) were also tested against all liver cancer cell lines. significant decrease in cell viability were noticed around (9.8±1.07µM) as IC_{50} concentration of HNP-C on HepG2 cell line after 72 h incubation time with both viability test (Figure 3.1.).

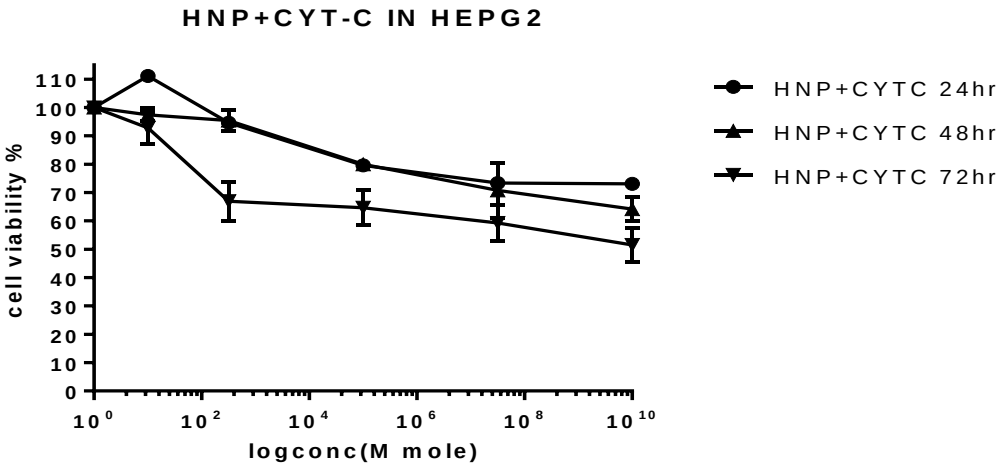

Figure 3.1. Dose response curve of NPs +cytochrome C +HEPG2 cell line of three independent experiments after 24 h,48 h and 72 h incubation time.

In the Huh-7D cell line, a remarkable increase in cytotoxicity of HNP-C was observed after 48 h and 72 h incubation times and recorded as significant IC_{50} (5.9±9.5 µM and 3.4±1.6µM) for each time ,respectively.as showed in (Figure 3.2.).

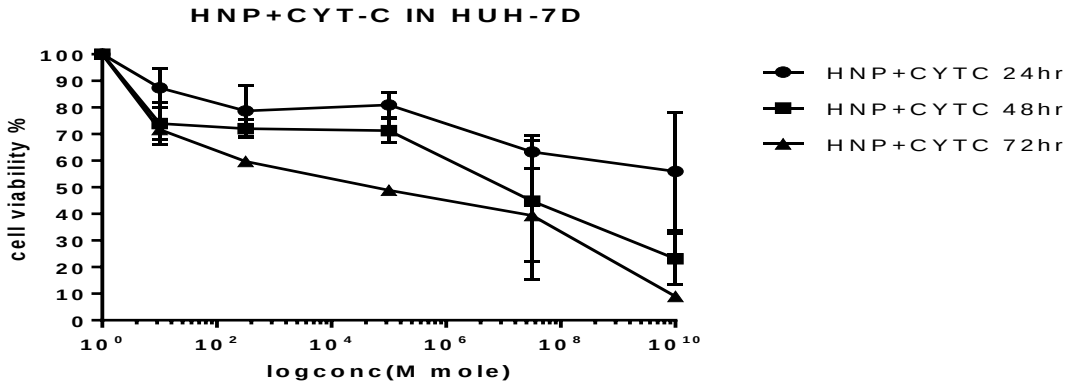

Figure 3.2. Dose response curve of NPs +cytochrome C +Huh-7D cell line of three independent experiments after 24 h,48 h and 72 h incubation time.

The cell viability assays showed a significant reduction in IC_{50} around (4.8±2.18µM) with SK-hep1 after 72 h (figure 3.3.) incubation with the HNP-C.

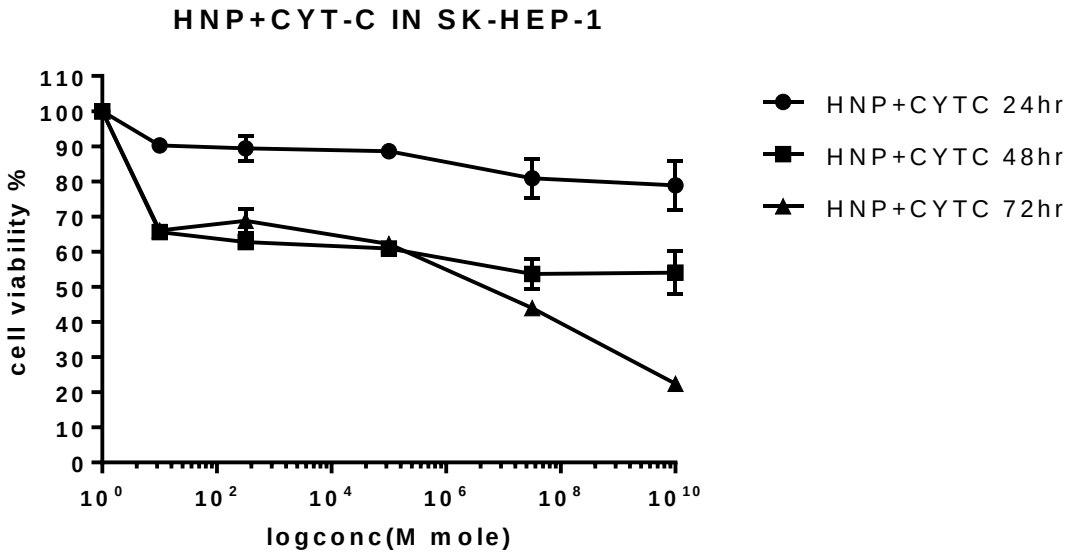

Figure 3.3. Dose response curve of NPs +cytochrome C +SK-hep-1 cell line of three independent experiments after 24 h,48 h and 72 h incubation time.

A dose response curve of HNP loaded with CYT-C are represented with noteable IC_{50} against U937 cell line at all incubated time points (Figure 3.4.) and showed as

9.56±6.01 µM at 24 h; 7.32±5.29 µM at 48 h and 3.87±1.8 µM at 72 h incubation time.

The concentration of HNP-C that correspond to 10% inhibition concentration of cell viability was used in combination therapy and calculated to be approximately 0.012 $mgmL^{-1}$ of hybrid formulation. This percentage was used with serial dilution of chemotherapeutic drugs to evaluate the effect of delivered CYT-C on the cytotoxicity of chemotherapeutic drugs against liver cancer cell lines.

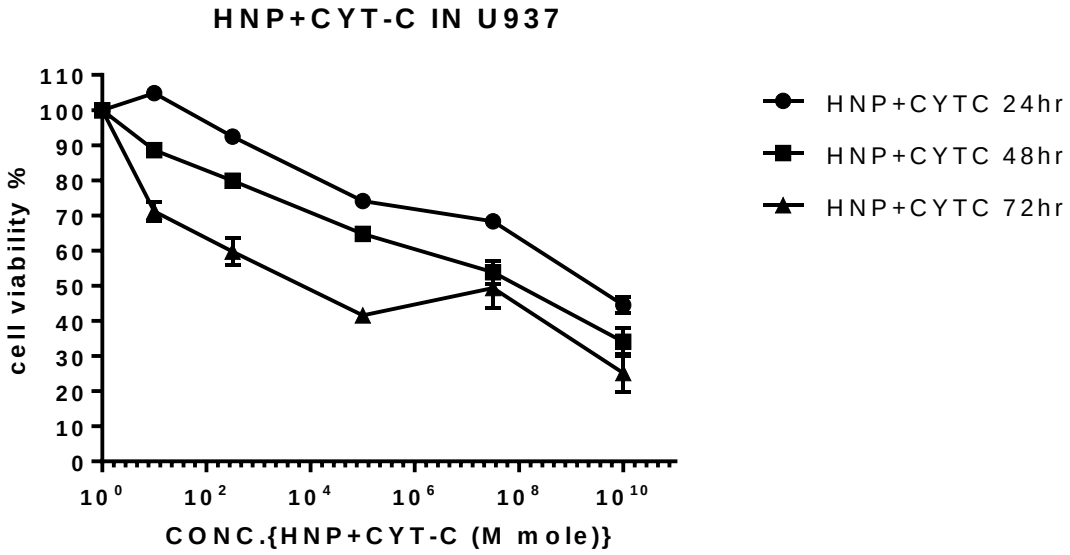

Figure 3.4. Dose response curve of NPs +cytochrome C +U937 cell line of three independent experiments after 24 h,48 h and 72 h incubation time.

3.3.1.2. Cell viability assays of DNA damage drug and anti-microtubule drugs with HNP-C

DNA damaging drugs, doxorubicin and oxaliplatin, showed insignificant results after 24 h incubation in HepG2, Huh-7D and SK-hep-1 cell lines. One exception was observed in Huh-7D cells using MTT and trypan blue assays after doxorubicin exposure (3.79 µM and 4.744 µM, respectively). The combination of doxorubicin with HNP-C (0.012 $mgmL^{-1}$) resulted in a decrease in the IC_{50} of Huh-7D cell line and recorded as 2.16 µM and 3.33 µM for MTT and trypan blue assay, after 24 h respectively. When liver cancer cells were incubated with the doxorubicin combined therapy for 48 h and 72 h a significant reduction in IC_{50} ($p<0.05$) was observed with in all cell lines compared with the drug alone.

Remarkably, insignificant results were evident with either oxaliplatin alone or with HNP-C on SK-hep-1 treated cells at three time points of incubation.

The cytotoxicity of anti-microtubule drugs: paclitaxel, vinblastine and vincristine were also evaluated on HepG2, Huh-7D and SK-hep-1 cell lines both alone and in co-administration with 0.012 $mgmL^{-1}$of HNP-C. After 24 h incubation, no significant IC_{50} ($p>0.05$) was detected in both the MTT and trypan blue assays. Increasing incubation time of treatment to 48 h and 72 h resulted in a significant decrease in IC_{50} ($p<0.05$) in HepG2 and Huh-7D cells exposed to paclitaxel, vinblastine and vincristine. The co-administration of these anti-microtubule drugs with HNP-C

(0.012 $mgmL^{-1}$) resulted in a more potent mix, with a significant increase in cytotoxic effect compared to the single drug treatment. Remarkably, no IC_{50} were noticeable in SK-hep-1(highly resistance cell line) with anti-microtubule drugs alone or when co-administer with HNP-C.

3.3.1.3. Cell viability assays on HepG2 cell line

The cytotoxicity of DNA damaging drugs was evaluated in HepG2 cells (Figure.3.5.) Here, no IC_{50} was observed in those cells treated with either drugs or with the CYT-C nano-formulation after 24 h. However, after 48 h and 72 h, an IC_{50} was observed. After combination therapy, a 15-fold and 10-fold (respectively) decrease in IC_{50} was observed in those cells treated with doxorubicin combination therapy. While, oxaliplatin co-administration showed a 1-3-fold decrease in IC_{50} after 48 h and 72 h incubation points. The anti-microtubule drugs showed no IC_{50} value after 24 h incubation with HepG2 cells. After 72 h a 17.8-fold, 9-fold and 29-fold decrease in IC_{50} was observed in those cells treated with combination therapies of paclitaxel, vinblastine and vincristine, respectively (Figure 3.6. ,3.7.)

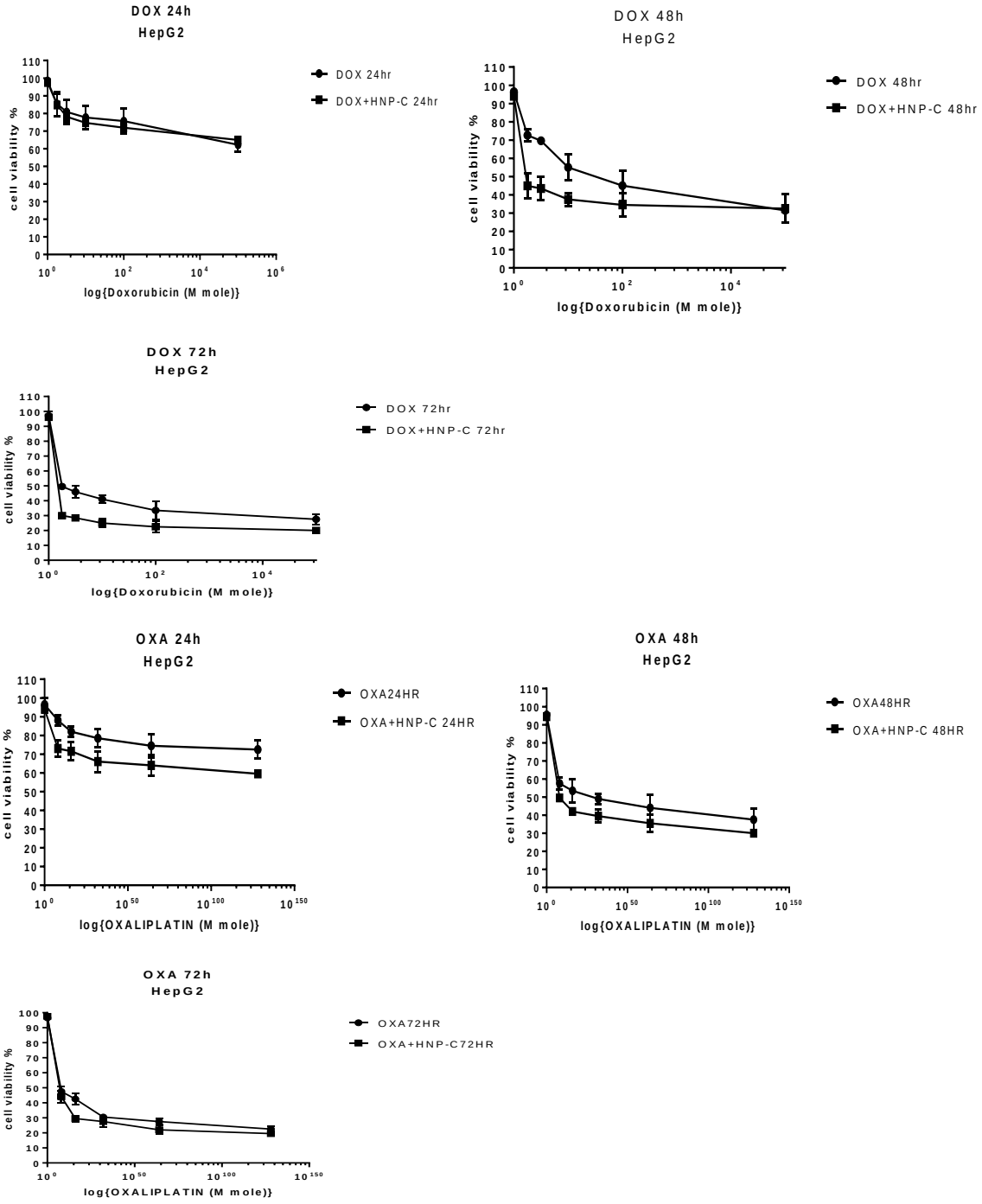

Figure 3.5. Dose response curve of doxorubicin and oxaliplatin on HEPG2 cell line of three independent experiments after 24 h,48 h and 72 h incubation time, the x-axis represent the serial dilutions of the drug and the y-axis represent the absorbance of MTT formazan crystalline which indicate the % of cell viability.

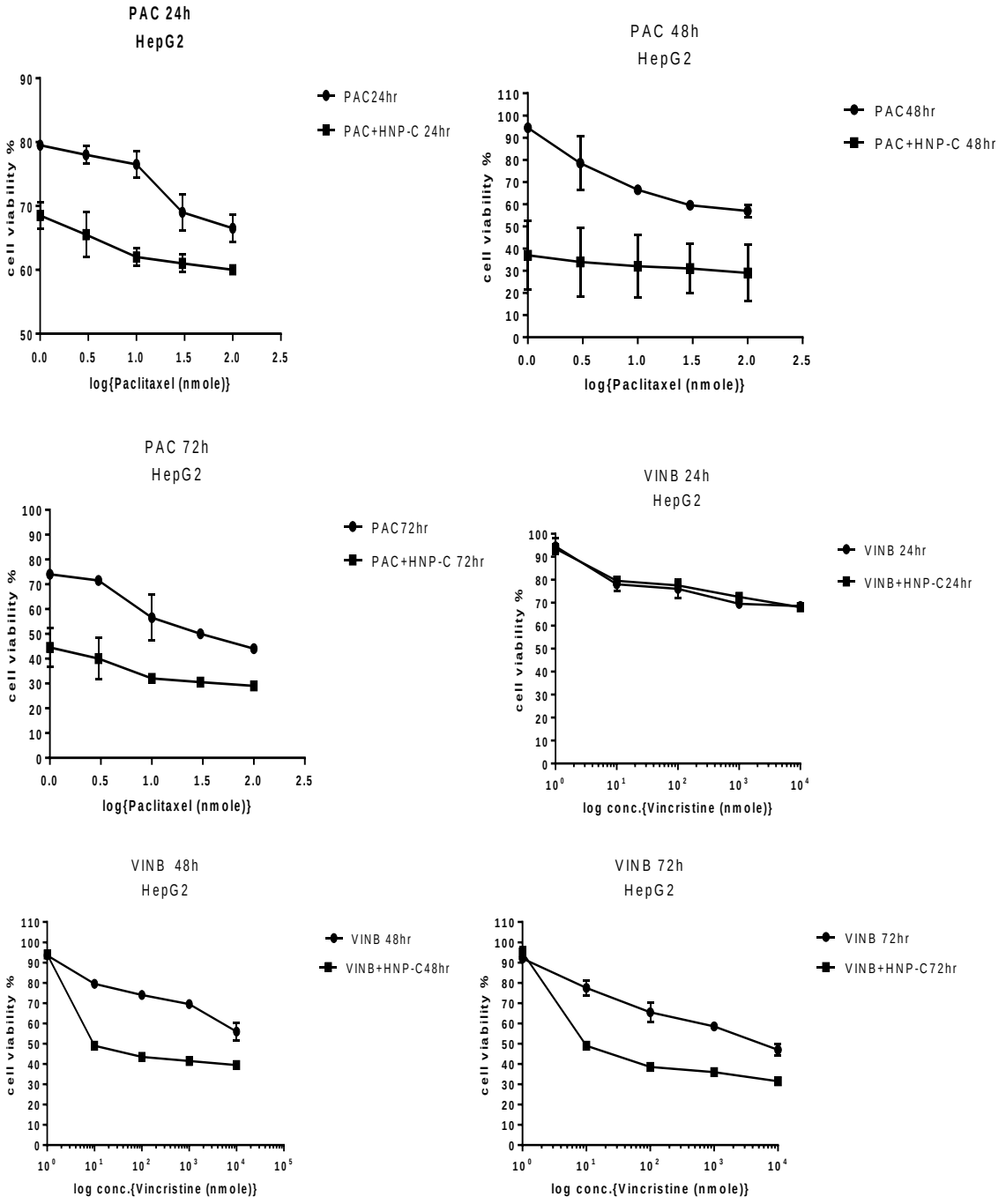

Figure 3.6. Dose response curve of Paclitaxel, vinblastine on HEPG2 cell line of three independent experiments after 24 h,48 h and 72 h incubation time, the x-axis represent the serial dilutions of the drug and the y-axis represent the absorbance of MTT formazan crystalline which indicate the % of cell viability.

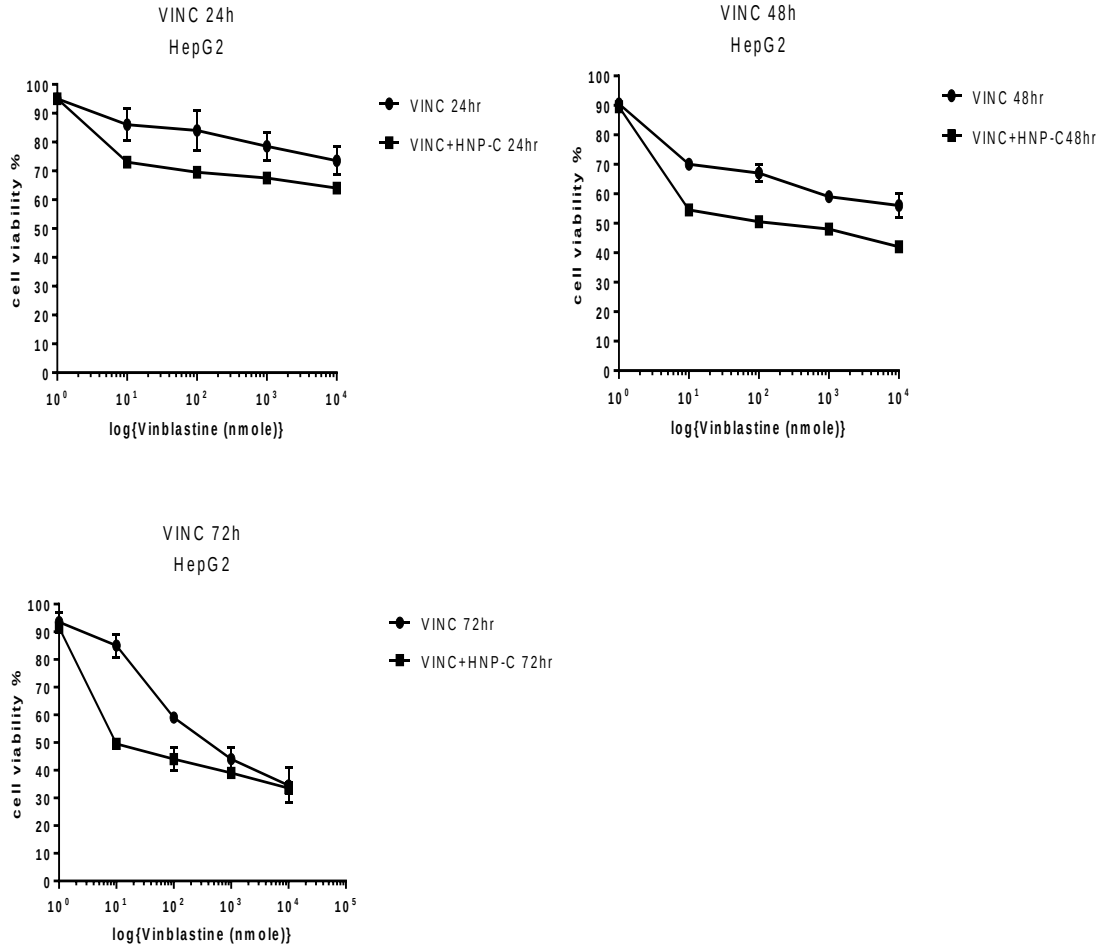

Figure 3.7. Dose response curve of vincristine on HEPG2 cell line of three independent experiments after 24 h,48 h and 72 h incubation time, the x-axis represent the serial dilutions of the drug and the y-axis represent the absorbance of MTT formazan crystalline which indicate the % of cell viability.

Table 3-1. IC_{50} values of DNA damage drugs (Doxorubicin and Oxaliplation) and anti-microtubule drugs (Paclitaxel, vinblastine and vincristine) on HepG2 cell line achieved by MTT and trypan blue assays. Significant increase in the cytotoxicity was calculated by comparing with single drug treatment (n=3, aver ±SD).

HEPG2 Cell line	IC50(drug) MTT	IC50(drug+ HNP-C)(MTT)	IC50(drug) Trypan blue	IC50(drug+ HNP-C) Trypan blue
Doxorubicin				
24 h	NS	NS	NS	NS
Increase in cytotoxicity	-	-		
48 h	1.6±7.5µM	0. 1±2.34 µM	1.46±1.14µM	0.09±1.87µM
Increase in cytotoxicity	-	15-fold		15.2- fold
72 h	0.1±4.69 µM	0.009±0.38 µM	0.27±3.54 µM	0.002±2.82 µM
Increase in cytotoxicity		10.1-fold		12.5-fold
Paclitaxel				
24 h	NS	NS	NS	NS
48 h	NS	2.3±2.09nM	NS	1.60±3.53nM
Increase in cytotoxicity	-	Significant IC_{50}		Significant IC_{50}
72 h	32±4.84 nM	1.7±1.97 nM	35.72±1.41nM	0.18±4.77nM
Increase in cytotoxicity	-	17.8-fold		193-fold
Oxaliplatin				
24 h	NS	NS	NS	NS
Increase in cytotoxicity	-	-		
48 h	17±1.56 µM	8±4.63 µM	25.21±2.82µM	6.510±1.41µM
Increase in cytotoxicity	-	1.1-fold	-	2.8-fold
72 h	7.54±3.06 µM	3±1.03 µM	6.51±2.79µM	3.33±3.72µM
Increase in cytotoxicity	-	1.5-fold	-	1-fold
Vinblastine				
24 h	NS	NS	NS	NS
Increase in cytotoxicity	-	-		
48 h	NS	0.01±4.09 nM	NS	0.01±1.88nM
Increase in cytotoxicity		Significant IC_{50}		Significant IC_{50}
72 h	0.001±2.04 nM	0.0001±1.54 nM	0.02±4.02nM	0.001±2.42nM
Increase in cytotoxicity	-	9-fold		19-fold
Vincristine				
24 h	NS	NS	NS	NS
Increase in cytotoxicity	-	-		
48 h	NS	0.009±3.56 nM	NS	0.001±1.17nM
Increase in cytotoxicity	-	Significant IC_{50}		Significant IC_{50}
72 h	0.003±1.50 nM	0.0001±8.51 nM	0.05±3.39nM	0.0001±1.58nM
Increase in cytotoxicity	-	29-fold		499-fold

3.3.1.4. Cell viability assays on Huh-7D cell line

The cytotoxicity of doxorubicin was tested in Huh-7D cells (Figure 3.8.), after 24 h a 0.75-fold and 0.42-fold decrease in IC_{50} was observed with the combination therapy (MTT and trypan blue respectively). Further increase in cytotoxic effect was observed after 48 h and 72 h incubation. Co-administration with oxaliplatin and HNP-C resulted in a 39-fold and 6.4-fold decrease in IC_{50} after 72 h (MTT and trypan blue, respectively). The anti-microtubule drugs (Figure 3.9., 3.10.) showed no IC_{50} in Huh-7D cells after 24 h. A significant increase in the cytotoxicity was observed in those cells treated with paclitaxel after 48 h and 72 h., Cells incubated with vincristine also showed a significant fold reduction in IC50 value with the combination therapies compared to single drug treatment after 48 h and 72 h.

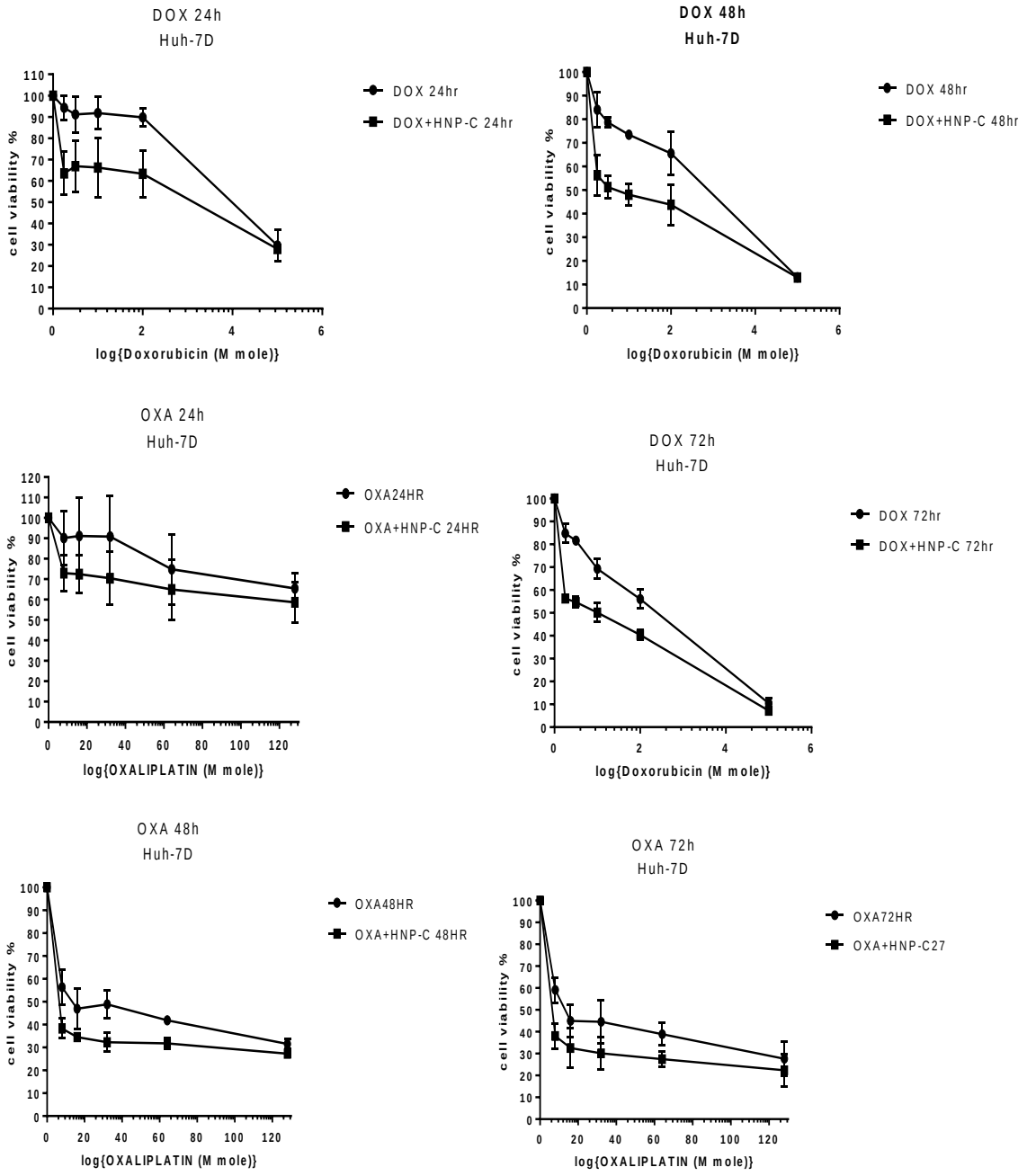

Figure 3.8. Dose response curve of doxorubicin and oxaliplatin on Huh-7D cell line of three independent experiments after 24 h,48 h and 72 h incubation time, the x-axis represent the serial dilutions of the drug and the y-axis represent the absorbance of MTT formazan crystalline which indicate the % of cell viability.

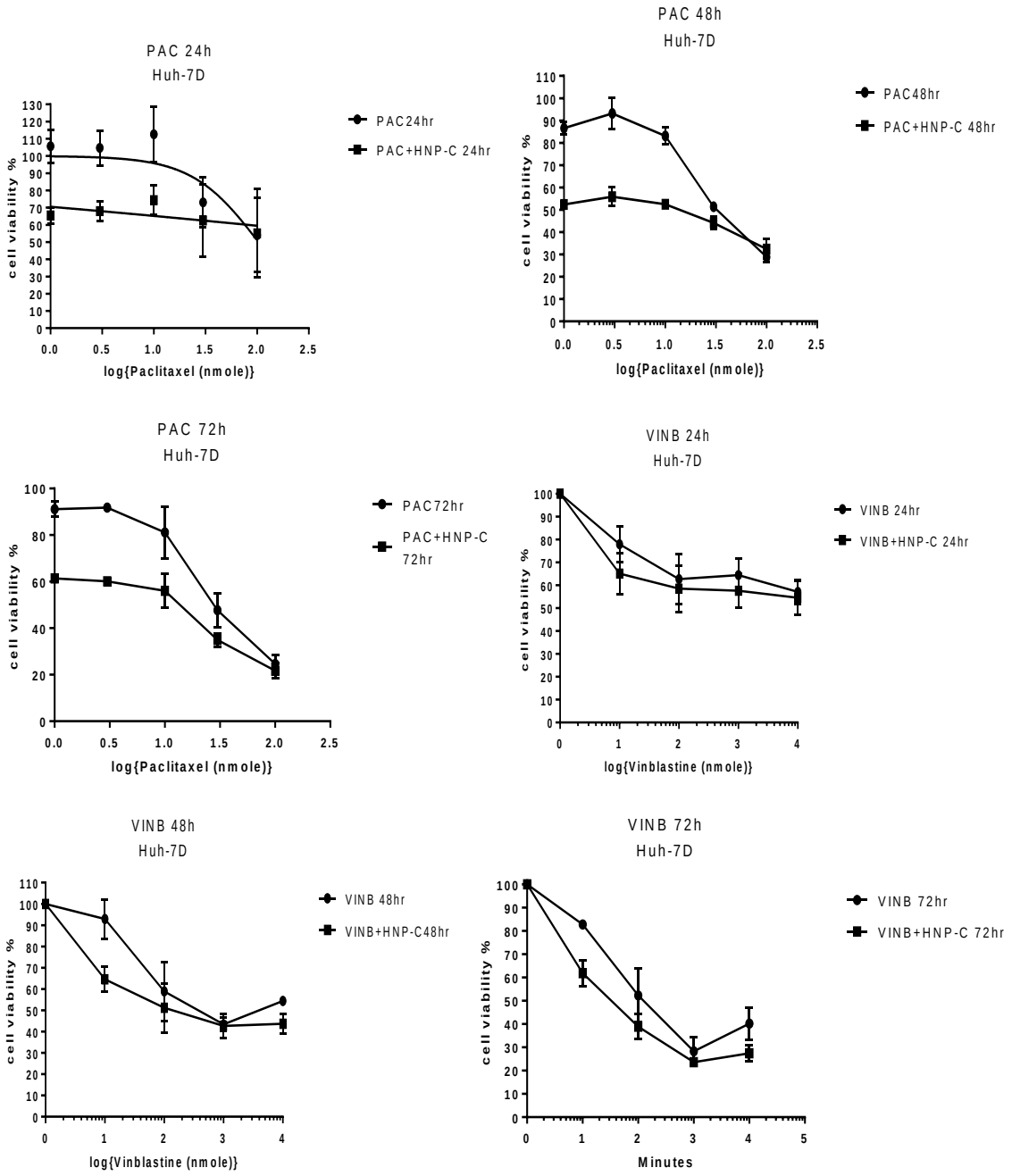

Figure 3.9. Dose response curve of Paclitaxel, vinblastine on Huh-7D cell line of three independent experiments after 24 h,48 h and 72 h incubation time, the x-axis represent the serial dilutions of the drug and the y-axis represent the absorbance of MTT formazan crystalline which indicate the % of cell viability.

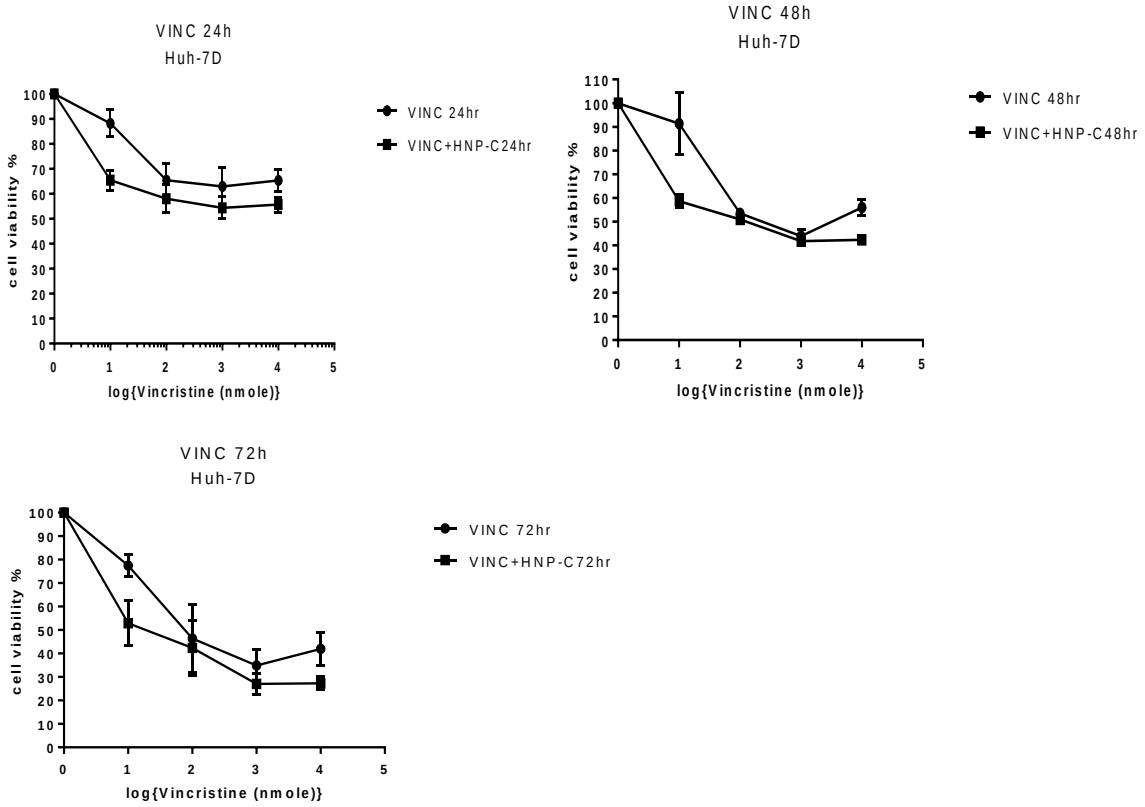

Figure 3.10. Dose response curve of vincristine on Huh-7D cell line of three independent experiments after 24 h,48 h and 72 h incubation time, the x-axis represent the serial dilutions of the drug and the y-axis represent the absorbance of MTT formazan crystalline which indicate the % of cell viability.

Table 3-2 .IC_{50} values of DNA damage drugs (Doxorubicin and Oxaliplation) and anti-microtubule drugs (Paclitaxel, vinblastine and vincristine) on Huh-7D cell line achieved by MTT and trypan blue assays. Significant increase in the cytotoxicity was calculated by comparing with single drug treatment (n=3, aver ±SD).

HUH-7D Cell line	IC50(drug) MTT	IC50(drug+ HNP-C)(MTT)	IC50(drug) Trypan blue	IC50(drug+ HNP-C) Trypan blue
Doxorubicin				
24 h	3.79±7.5 µM	2.16±1.3 µM	4.744±4.16 µM	3.338±2.081 µM
Increase in cytotoxicity	-	0.75-fold	-	0.42- fold
48 h	2.11±1.46 µM	0.58±4.55 µM	2.949± 6.11 µM	1.903± 1.73 µM
Increase in cytotoxicity	-	2.6-fold	-	0.5-fold
72 h	1.7±2.1 µM	0.61±2.2 µM	1.631± 2.51 µM	0.6389± 2.64 µM
Increase in cytotoxicity	-	1.7-fold	-	1.6-fold
Paclitaxel				
24 h	NS	NS	NS	NS
Increase in cytotoxicity	-	-		
48 h	37.04±1.63 nM	5.60±2.88 nM	41.08±1.52 nM	9.945±3.60 nM
Increase in cytotoxicity	-	5.6-fold	-	3.13-fold
72 h	31.48±7.48 nM	7.09±2.80 nM	32.57±3.21 nM	6.204±2.51 nM
Increase in cytotoxicity	-	3.4-fold	-	4.2-fold
Oxaliplatin				
24 h	NS	NS	NS	NS
Increase in cytotoxicity	-	-		
48 h	17±1.57 µM	1.06±4.3 µM	23.58±4.93µM	8.49±1.154µM
Increase in cytotoxicity	-	15-fold	-	1.7-fold
72 h	15±7.48 µM	0.37±5.86 µM	16.83±2.08µM	2.135±1.52µM
Increase in cytotoxicity	-	39-fold	-	6.9-fold
Vinblastine				
24 h	NS	NS	NS	NS
Increase in cytotoxicity	-	-	-	-
48 h	0.029±3.16 nM	0.003±8.53 nM	0.049±2.51nM	0.004±7.63nM
Increase in cytotoxicity	-	8.6-fold	-	9-fold
72 h	0.003±6.30 nM	0.0003±5.39 nM	0.004±3.05nM	0.0003±1.73nM
Increase in cytotoxicity	-	9-fold	-	12-fold
Vincristine				
24 h	NS	NS	NS	NS
Increase in cytotoxicity	-	-	-	-
48 h	0.03±2.92	0.001±1.31	0.012±2.08 nM	0.006±1.53 nM
Increase in cytotoxicity	-	29-fold	-	1-fold
72 h	0.002±6.95	0.0001±9.53	0.003±3.60 nM	0.0002±4.16 nM
Increase in cytotoxicity	-	19-fold	-	14-fold

3.3.1.5. Cell viability assays on SK-hep-1 cell line

The SK-hep-1 cell line exhibited a much greater degree of drug resistance compared to the other cell lines tested (Figures 3.11. and 3.12.) . This may be because they did not possess any mRNA of hepatic-specific proteins (albumin and fibrinogen) or due to a difference in cellular uptake mechanism of drugs compared with the other cell lines (Eun JR. *et al*. 2014). Hence, the highly resistance nature of these cell lines against chemotherapeutics resulted in no IC_{50} values when incubated with all the drug molecules tested with exception of doxorubicin. Doxorubicin has been classified as an intracellular and extracellular affecting chemotherapeutic drug (non-specific cell cycle phase killing drugs) (El-Kareh, A. W., & Secomb, T. W. 2005). Hence, this may render it more effective in drug resistant cells. In this study, an IC_{50} was observed after 48 h in combination therapy of doxorubicin and HNP-C (2.38±2.86 µM and 2.55±3.88 µM) achieved by MTT and trypan blue, respectively. Further, with increasing incubation time to 72 h, a further 0.25-fold and 0.88-fold increase in cytotoxicity was observed (MTT and trypan blue, respectively).

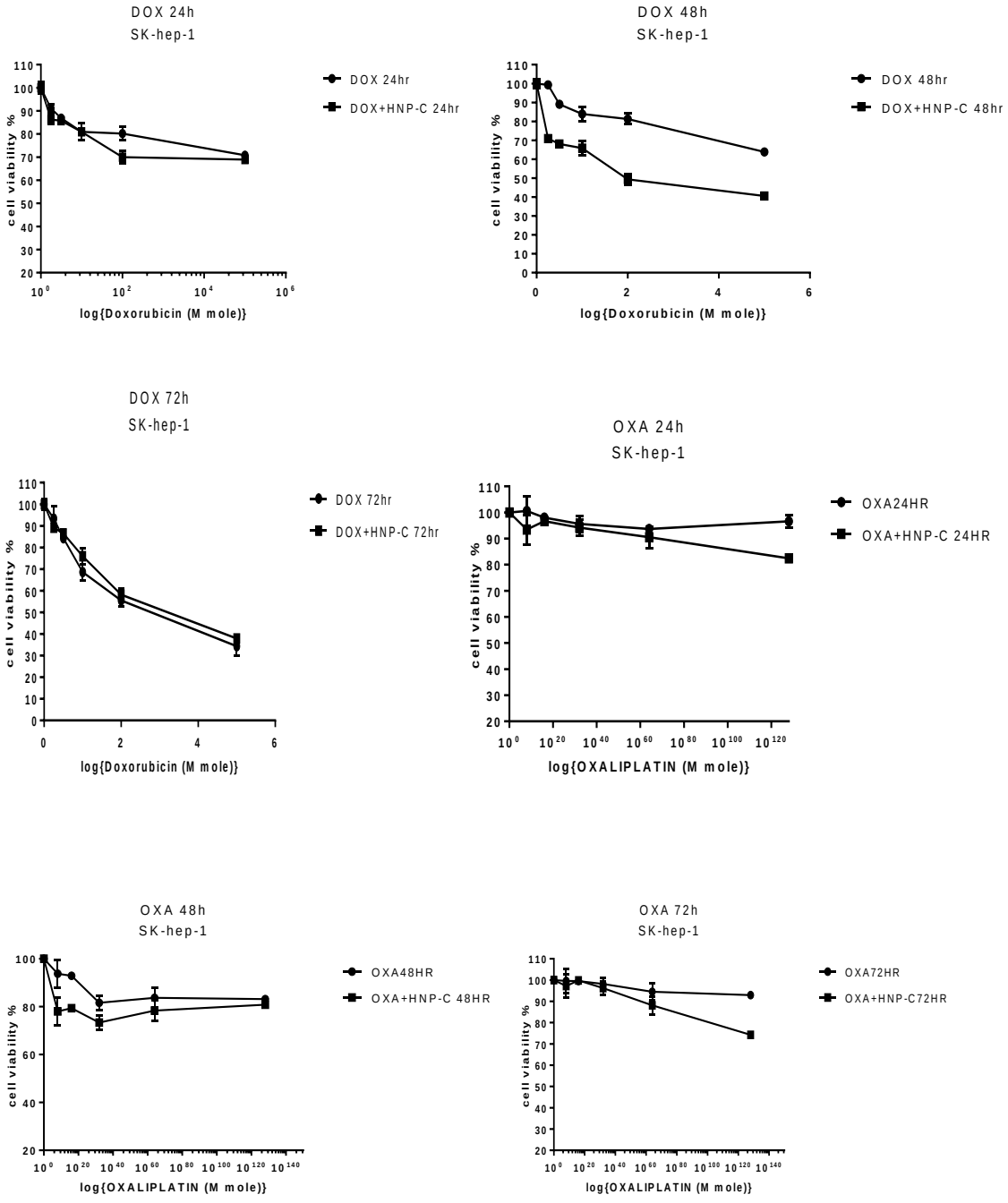

Figure 3.11. Dose response curve of doxorubicin and oxaliplatin on SK-hep-1 cell line of three independent experiments after 24 h,48 h and 72 h incubation time, the x-axis represent the serial dilutions of the drug and the y-axis represent the absorbance of MTT formazan crystalline which indicate the % of cell viability.

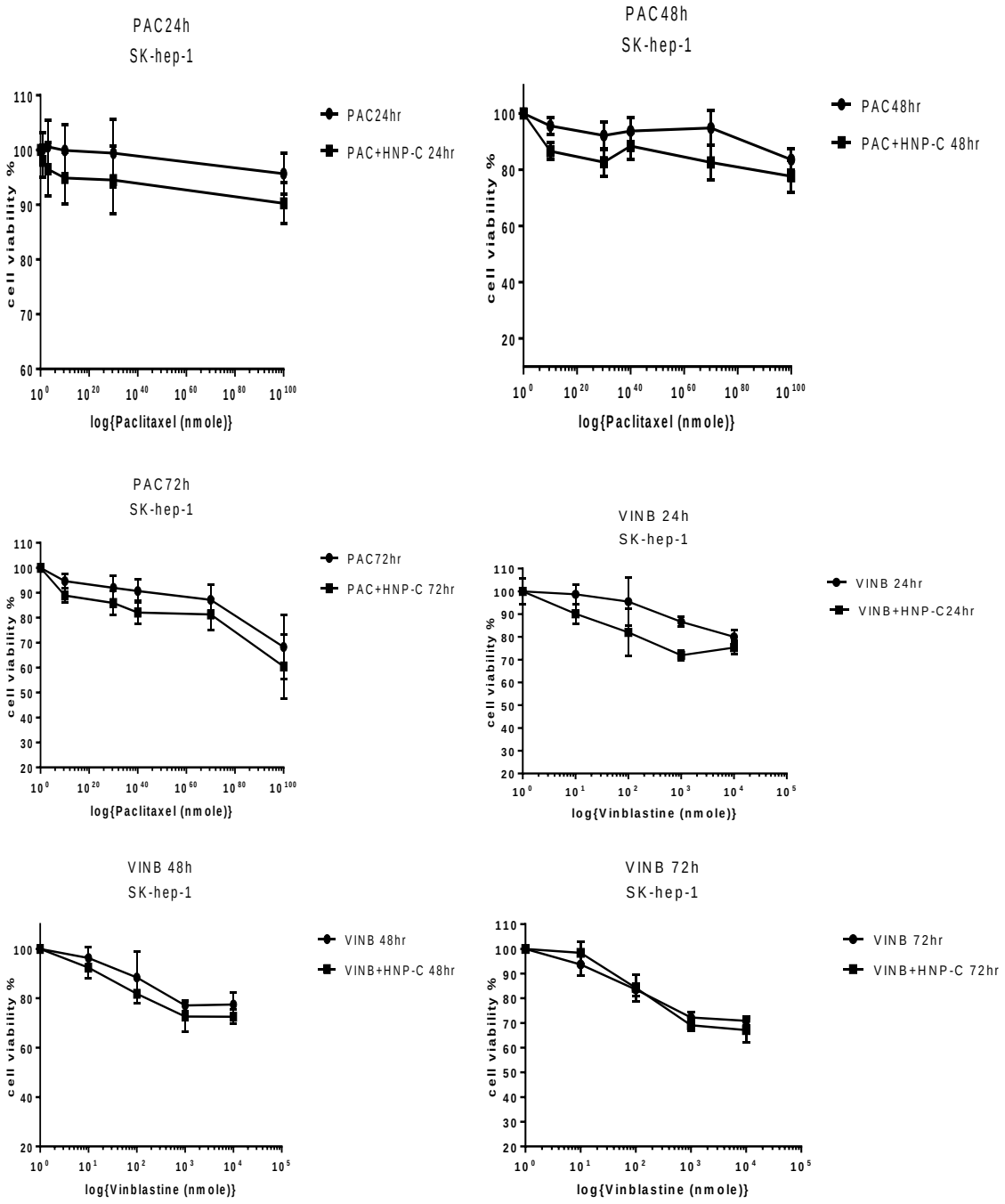

Figure 3.12. Dose response curve of Paclitaxel, vinblastine on SK-hep-1 cell line of three independent experiments after 24 h,48 h and 72 h incubation time, the x-axis represent the serial dilutions of the drug and the y-axis represent the absorbance of MTT formazan crystalline which indicate the % of cell viability.

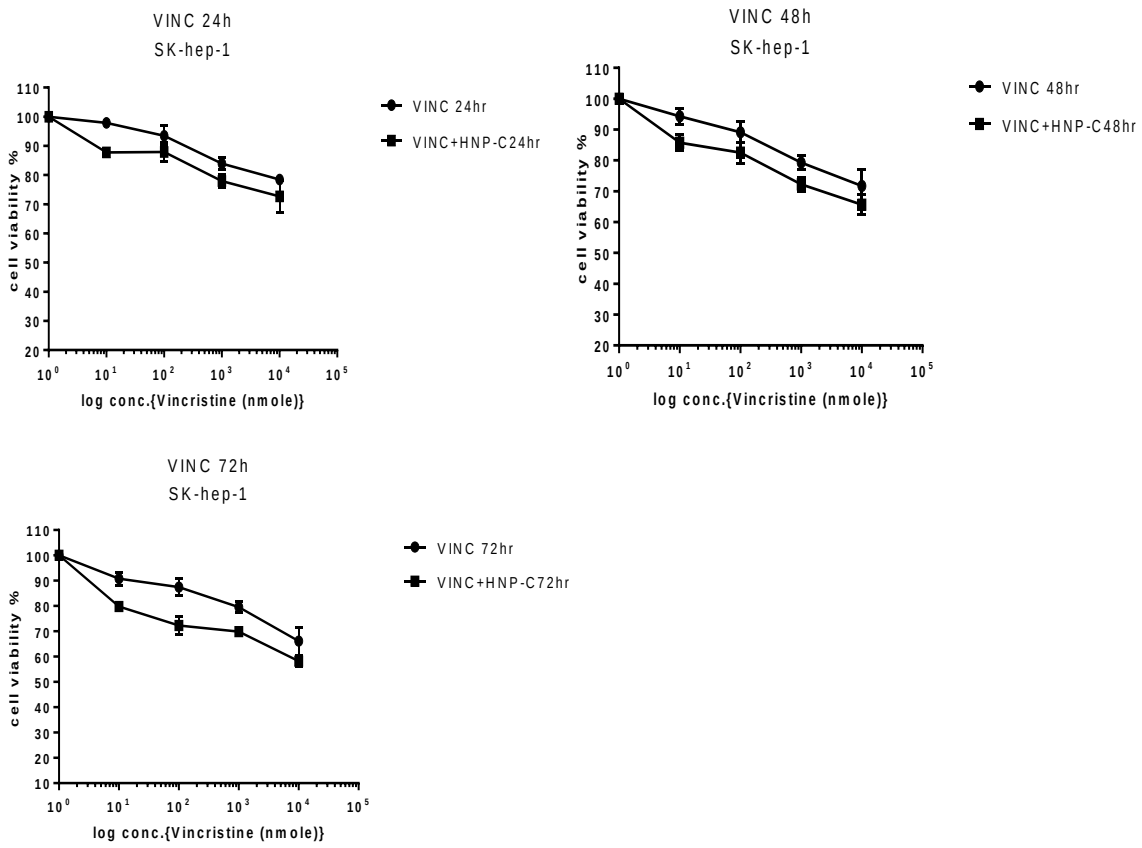

Figure 3.13. Dose response curve of vincristine on SK-hep-1 cell line of three independent experiments after 24 h,48 h and 72 h incubation time, the x-axis represent the serial dilutions of the drug and the y-axis represent the absorbance of MTT formazan crystalline which indicate the % of cell viability.

Table 3-3 .IC_{50} values of DNA damage drugs (Doxorubicin and Oxaliplation) and anti-microtubule drugs (Paclitaxel, vinblastine and vincristine) on SK-hep-1 cell line achieved by MTT and trypan blue assays. Significant increase in the cytotoxicity was calculated by comparing with single drug treatment (n=3, aver ±SD).

SK-HEP-1 Cell line	IC50(drug) MTT	IC50(drug+ HNP-C)(MTT)	IC50(drug) Trypan blue	IC50(drug+ HNP-C) Trypan blue
Doxorubicin				
24 h	NS	NS	NS	NS
	-	-		
48 h	NS	2.38±2.86µM	NS	2.55±3.88 µM
		Significant IC_{50}		Significant IC_{50}
72 h	3±4.34 µM	2.4±1.21 µM	4.034 ± 5.12µM	2.14 ± 3.85µM
	-	0.25-fold	-	0.88-fold
Paclitaxel				
24 h	NS	NS	NS	NS
48 h	NS	NS	NS	NS
72 h	NS	NS	NS	NS
Oxaliplatin				
24 h	NS	NS	NS	NS
48 h	NS	NS	NS	NS
72 h	NS	NS	NS	NS
Vinblastine				
24 h	NS	NS	NS	NS
48 h	NS	NS	NS	NS
72 h	NS	NS	NS	NS
Vincristine				
24 h	NS	NS	NS	NS
48 h	NS	NS	NS	NS
72 h	NS	NS	NS	NS

3.3.1.5. Cell viability assays on U937cell line

The cell viability tests in differentiated U937 cells showed that an IC_{50} was observed with all chemotherapeutic drugs used either alone or in combination with hybrid formulation in the 3 times points tested (Figures 3.14. , 3.15.) . This was with exception of doxorubicin, where no IC_{50} was observed with the single drug treatment, however, combination therapy resulted in IC_{50} values of 3.6 µM and 3.55 µM, after 24 h (MTT and trypan blue assay, respectively). These significant cytotoxic effects may contribute to different cell membrane structures, cell size and the mechanisms of molecules uptake of this cell line, compared to other cultured hepatic cell lines.

For oxaliplatin treated cells the higher toxicity effects were indicated with oxaliplatin combination therapy after 48 h where a 1.03-fold decrease in IC_{50} and 1.73-fold decrease after 72 h was observed. The cytotoxicity of paclitaxel combination treated cells increased after 72 h. However, the most potent formulation observed was using vincristine treated cells after 24 h incubation period where a 52-fold increase in cytotoxicity was observed after combination therapy compared to the single drug treatment.

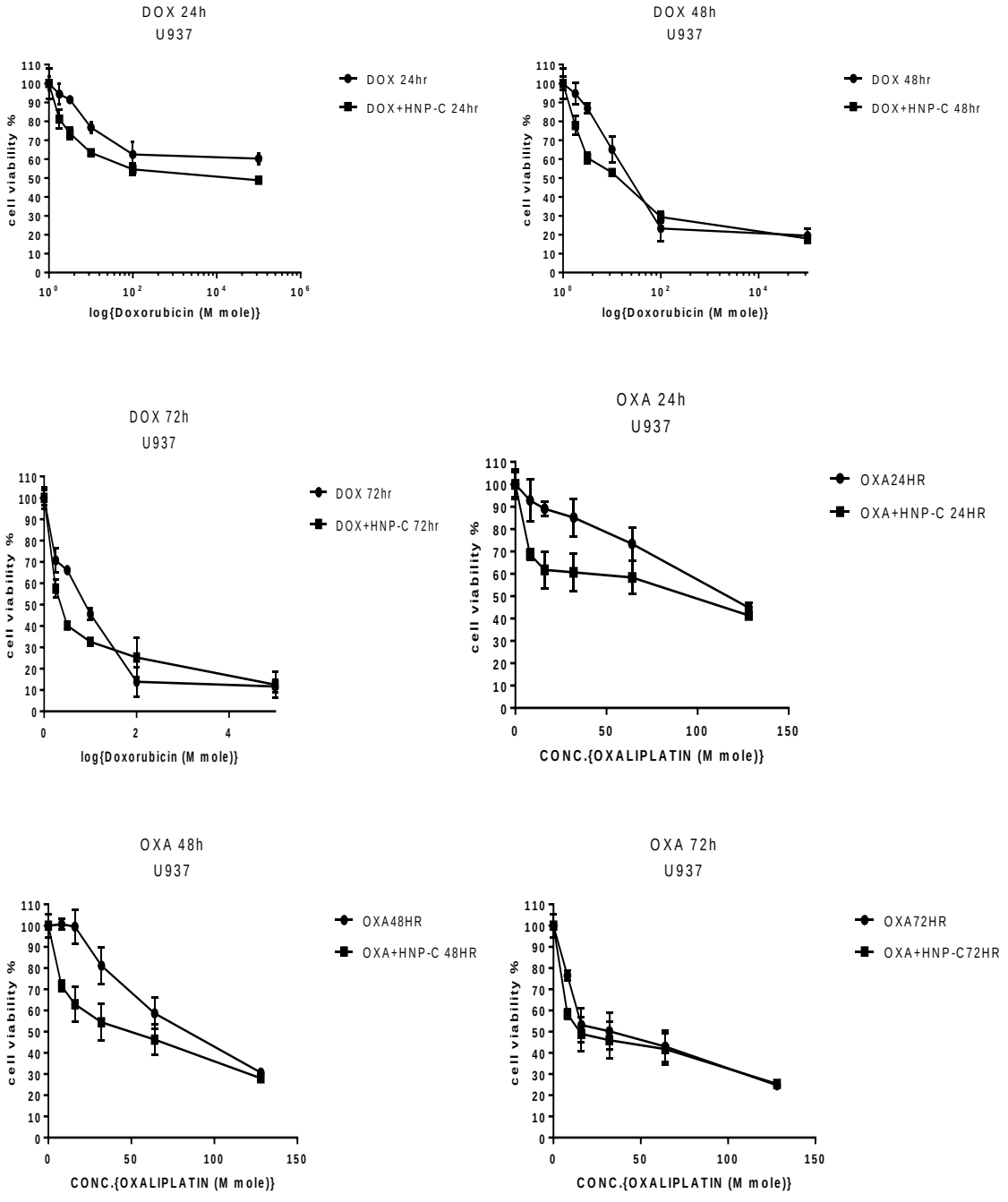

Figure 3.14. Dose response curve of doxorubicin and oxaliplatin on U937 cell line of three independent experiments after 24 h,48 h and 72 h incubation time, the x-axis represent the serial dilutions of the drug and the y-axis represent the absorbance of MTT formazan crystalline which indicate the % of cell viability.

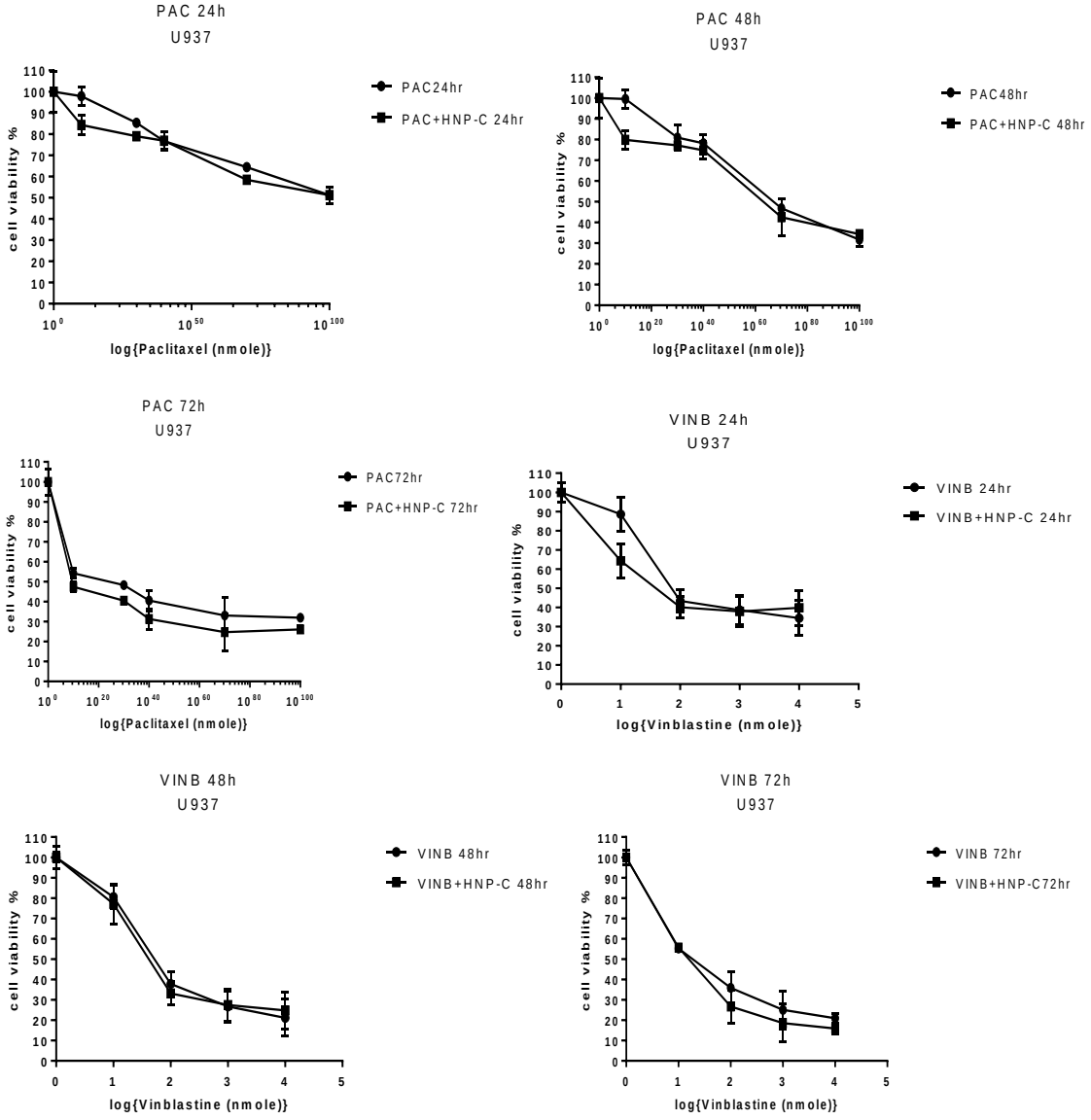

Figure 125. Dose response curve of Paclitaxel, vinblastine on U937 cell line of three independent experiments after 24 h,48 h and 72 h incubation time, the x-axis represent the serial dilutions of the drug and the y-axis represent the absorbance of MTT formazan crystalline which indicate the % of cell viability.

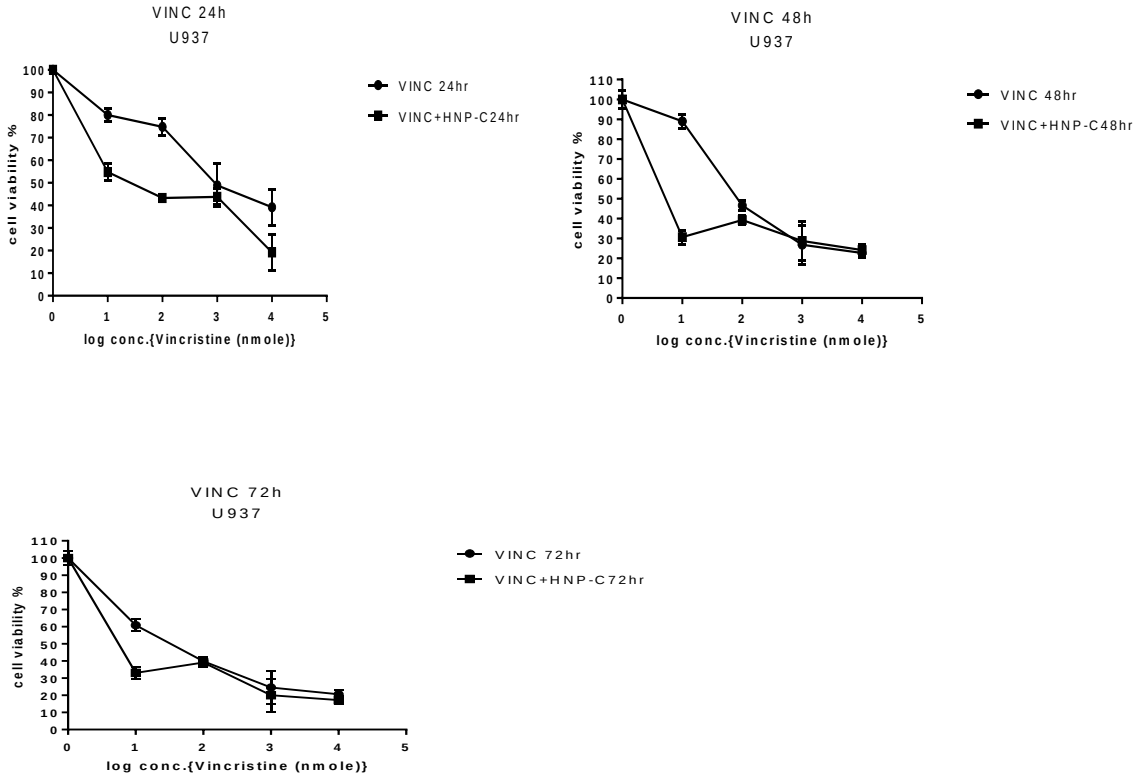

Figure 136. Dose response curve of vincristine on U937 cell line of three independent experiments after 24 h,48 h and 72 h incubation time, the x-axis represent the serial dilutions of the drug and the y-axis represent the absorbance of MTT formazan crystalline which indicate the % of cell viability.

Table 3-4.IC_{50} values of DNA damage drugs (Doxorubicin and Oxaliplation) and anti-microtubule drugs (Paclitaxel, vinblastine and vincristine) on U937 cell line achieved by MTT and trypan blue assays. Significant increase in the cytotoxicity was calculated by comparing with single drug treatment (n=3, aver ±SD).

U937 Cell line	IC50(drug) MTT	IC50(drug+ HNP-C)(MTT)	IC50(drug) Trypan blue	IC50(drug+ HNP-C) Trypan blue
Doxorubicin				
24 h	NS	3.6±1.07 µM	NS	3.55±2.25µM
Increase in cytotoxicity				
48 h	1.3±6.90 µM	0.9±3.02 µM	1.77±8.04µM	1.17±3.6µM
Increase in cytotoxicity		0.4-fold		0.5-fold
72 h	0.7±2.91 µM	0.3±6.07 µM	0.98±4.23µM	0.51±1.762µM
Increase in cytotoxicity		1.3-fold		0.94-fold
Paclitaxel				
24 h	NS	NS	NS	NS
Increase in cytotoxicity				
48 h	67±1.02nM	65.2±4.22 nM	67.67±3.98nM	61.74±7.96nM
Increase in cytotoxicity		0.03-fold		0.09-fold
72 h	17±1.61 nM	8.77±2.62 nM	16.21±1.11nM	7.62±3.6nM
Increase in cytotoxicity		0.93-fold		1.13-fold
Oxaliplatin				
24 h	119.5±2.34 µM	84.30±1.30 µM	102.1±3.48µM	72.04±4.04µM
Increase in cytotoxicity		0.41-fold		0.41-fold
48 h	78.99±7.38 µM	38.76±1.34 µM	100.8±1.91µM	47.37±4.64µM
Increase in cytotoxicity		1.03-fold		1.1-fold
72 h	30.85±2.51 µM	18.09±5.06 µM	77.49±3.75µM	28.3±6.972µM
Increase in cytotoxicity		0.6-fold		1.73-fold
Vinblastine				
24 h	0.003±5.81 nM	0.0007±8.88 nM	0.016±3.51nM	0.006±7.11nM
Increase in cytotoxicity		3.2-fold		1.6-fold
48 h	0.001±2.46 nM	0.0001±5.08 nM	0.002±5.77nM	0.0003±4.219nM
Increase in cytotoxicity		9-fold		5.66-fold
72 h	0.0001±1.75 nM	0.00001±4.39 nM	0.0002±4.26nM	0.00017±3.87nM
Increase in cytotoxicity		9-fold		0.17-fold
Vincristine				
24 h	0.016±3.84	0.0003±2.78 nM	0.015±7.67 nM	0.003±4.97nM
Increase in cytotoxicity		52-fold		4-fold
48 h	0.0016±1.48	0.0001±3.49 nM	0.003±4.55 nM	0.0002±4.50nM
Increase in cytotoxicity		15-fold		14-fold
72 h	0.0003±9.70	0.00001±4.39 nM	0.0004±6.32 nM	0.0001±1.39nM
Increase in cytotoxicity		29-fold		3-fold

3.3.2. Cellular uptake

Most chemotherapies are hindered in their development or use due to major challenges in their ability to be administered or delivered to the correct site of action. Careful formulation into or onto nanoparticles has shown potential in this area for improvement in drug solubilisation, dissolution, circulation times or penetration ability.

The effective targeting strategies of nanoparticles are controlled mainly by physical and chemical means. Physical targeting is achieved by applying specific fabrication technique of nanoparticles size, charge and stiffness process which affects the rate of tissue targeting and cellular uptake of these particles. The chemical site of formulation is the decorating of particle surfaces to receptive the specific environment criteria of delivered device.

The tracking of the nanoparticles traveling way to the cell is the main point in therapeutic process in order to detect the vital site of targeting and also to improve the loading of therapeutic device inside the cells. One of these factors is nano-shape like rod, spherical or disk shape of nanoparticles (Petros and Desimone, 2010). So, the synthesis process and modifying shape of nanoparticles can be considered as a main point in targeting process.

The rigidity of nanoparticles is also reflected the action of targeting processes. Few studies refer to the cellular uptake differences between hard and soft types of nanoparticles. Macrophages engulf the hard type of nanoparticles such as the

metallic ones while the Hela cells prefer the soft particles to be uptake (Jo and Auguste, 2009; Beningio and Wang.2002).

The surface charge of nanoparticles can influence the circulation time of delivered particles and the rate of cellular retention or accumulation. Several studies have concerned with the effect of surface charge on the uptake process. Most researchers are agreed with ability of positively charged particles to be interacting electrostatically better than the negative one in most types of cell lines with some exceptional cases noticed with macrophage and stem cells characterised by different endocytosis or pinocytosis process of stem cells besides macrophage uptake ability rise with increasing surface charge of particles either negative or positive charge (Gratton *et al*., 2008; Chung *et al*., 2007)

The internalisation of nanoparticles into the cells is also dependent on the formulation size that affects the mechanism of the uptake (Zhang, S.*et al*., 2008). The particles size range between 10-500 nm is believed to enter *via* macropinocytosis, while clathrin mediated endocytosis usually required nanoparticles around 100nm in size. The size range of 60-80 nm is more likely to be involved by caveolae pathways of endocytosis (Benmerah, A.,2007). Some reports proposed that the cellular uptake factors may be affected by other formulation design such as charge or surface coating more than the size effect. However, it is obvious that the smaller size of nanoparticle is more helpful to uptake into the cells (Huang *et al*., 2002).

Cellular uptake of cytochrome C coupled to the HNP-C was measured in liver cancer cell lines and macrophage like differentiated U937 by measuring the

concentration per known number of cells and detected in microgram/picogram unit in 1 millilitre of cell suspension (Lison and Huaux, 2011) using UV/VIS spectrometry (Shimaduz,Germany) at 410 nm and calculated the protein concentration per each cell. A calibration curve was calculated by running the serial dilution of cytochrome C from 500-0.75 μgmL^{-1}dissolved in water ($R_{2=}$ 0.996). All the experiments were triplicated and average value was recorded.

Liver cancer cell lines (HepG2, Huh-7D12 and SK-hep-1) and differentiated U937 cells were incubated with 50 μgmL^{-1} or 100 μgmL^{-1} of Cyt-C alone or HNP-C for 1 h and 4 h. The accumulated amount of Cyt-C was calculated by measuring the absorbance at 410 nm using UV/VIS spectrometry. The amount of free cytochrome C inside the HepG2 cell line (Figure 3.17.). was 5 pg and 6.1 pg after 1 h and 4 h respectively at (50 μgmL^{-1} incubation concentration), compared to 12 pg and 13 pg in the HNP-C sample at the same concentration and incubation time.

At 100 μgmL^{-1} incubation concentration, the uptake of free protein did not change significantly from the 50 μgmL^{-1} which detected as (6 pg and 6.5 pg) after 1 and 4 h respectively, this could be to the low stability or the difficulty large proteins often face in order for cellular internalisation to occur. At 100 μgmL^{-1} HNP-C enabled internalisation of 33 pg and 36 pg of Cyt-C per cell which was more than double the intake compared with the lower concentration. This data suggests that cellular uptake level of the Cyt-C conjugated onto the HNP was related to incubation concentration more than the incubation time.

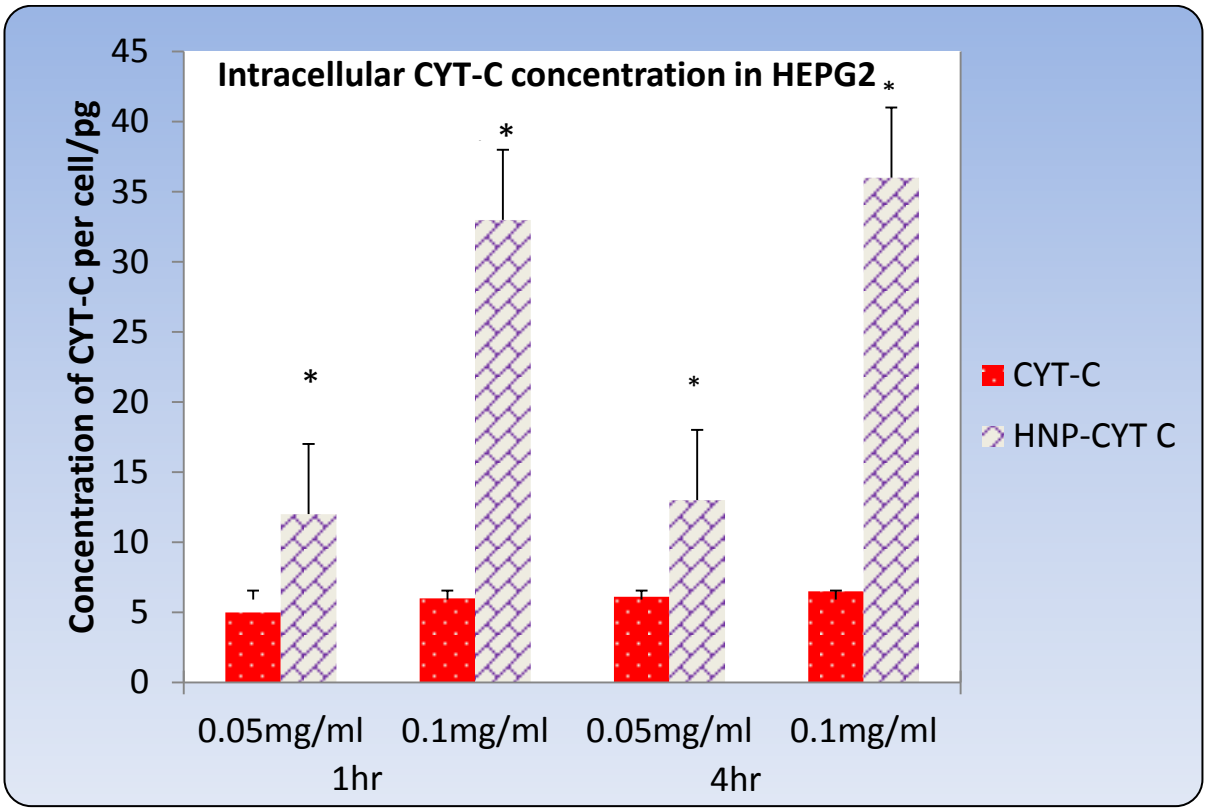

Figure 3.17. Protein uptake study on HepG2 cell line after 1and 4h incubation time with 50 µgmL^{-1} and 100µ µgmL^{-1} concentration of cytochrome C and HNP-C formulation,* indicate the significant differences between hybrid formulation of protein uptake value with the free form of protein uptake at similar time and concentration(n=3 ,average±SD). The t-test analysis is performed by Microsoft Excel software.

The uptake level of HNP-C in Huh-7D12 cells showed a high level of protein inside the cells after 1 h and 4 h with 14 pg and 19 pg being detected respectively at 50 µgmL^{-1}. This was 8-fold and 13-fold higher than for those cells incubated with the free protein (Figure 3.18.). In addition, a 25.5-fold and 28-fold increase in Cyt-C levels was observed in those cells incubated at 100 µgmL^{-1} HNP-C compared with free protein over 1 h and 4 h.

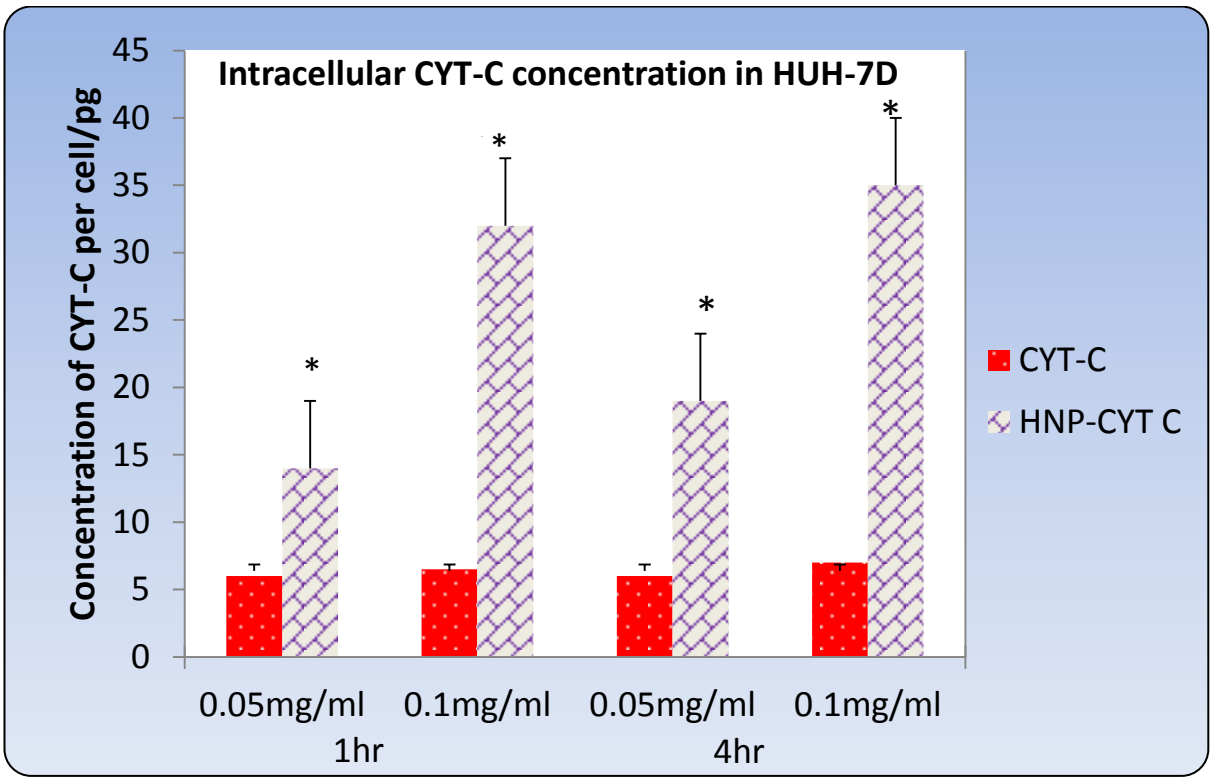

Figure 3.18. Protein uptake study on Huh-7D cell line after 1and 4h incubation time with 50 µgmL^{-1} and 100 µgmL^{-1} concentration of cytochrome C and HNP-C formulation,* indicate the significant differences between hybrid formulation of protein uptake value with the free form of protein uptake at similar time and concentration(n=3 ,average±SD). The t-test analysis is performed by Microsoft Excel software.

For Cyt-C and HNP-C, around 2 pg of free protein was taken up by SK-hep-1 cell line after 1 h and 4 h incubation time at 50 µgmL^{-1} exposure concentration. While, significant uptake levels were recorded by HNP-C 7.5 pg and 9 pg at the same time and incubation concentration. At 100 µgmL^{-1} incubated concentrations, 13 pg and 19 pg of HNP-C were measured, while the uptake level of free protein stayed around 2 pg. These results revealed the higher internalisation ability of hybrid nanoparticles compared to the low free protein uptake (Figure 3.19.).

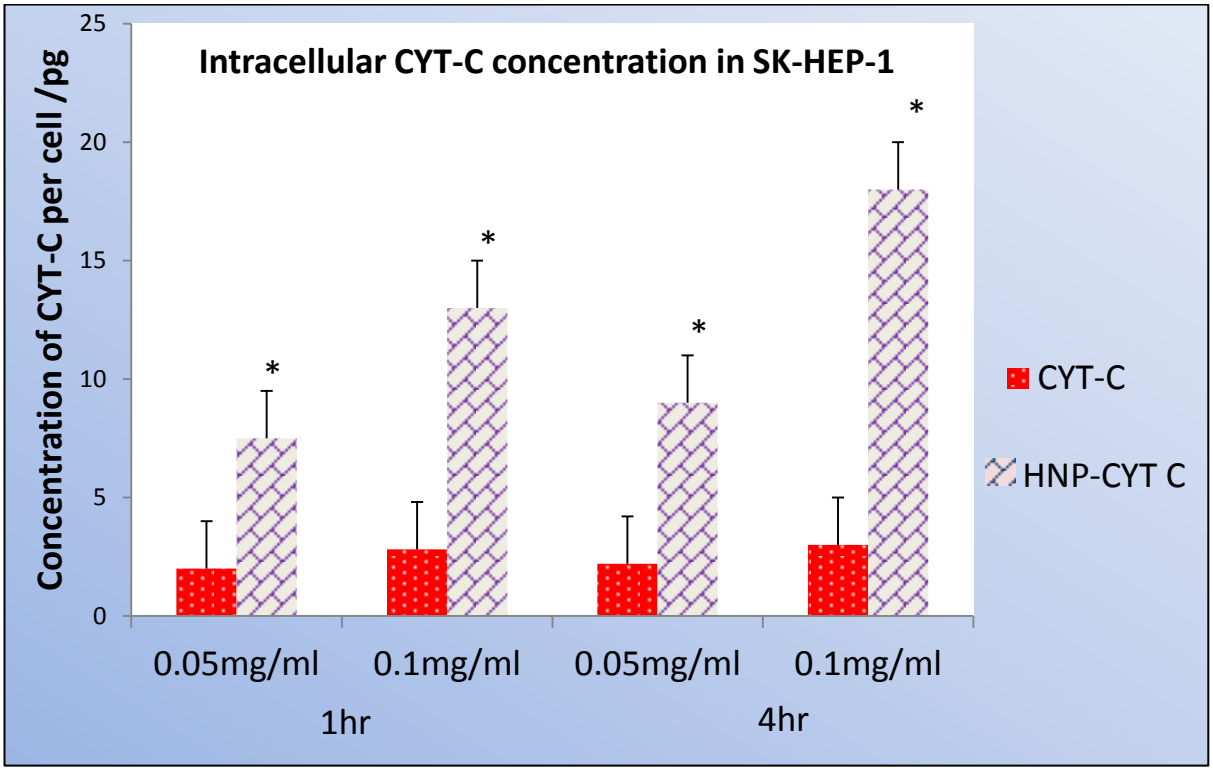

Figure 3.19. Protein uptake study on SK-hep-1 cell line after 1 h and 4h incubation time with 50 µgmL^{-1} and 100 µgmL^{-1}concentration of cytochrome C and HNP-C formulation,* indicate the significant differences between hybrid formulation of protein uptake value with the free form of protein uptake at similar time and concentration(n=3 ,average±SD). The t-test analysis is performed by Microsoft Excel software.

U937 cell line showed low levels of free protein uptake (around 4 pg) after 1 h and 4 h at 50 µgmL^{-1} exposure concentration. However, approximately a 4-fold increase in protein uptake was noticed with HNP-C, which confirms the ability of our formulation for effective passage into the cells. At 100 µgmL^{-1} incubation concentration, the uptake results were recorded as 7-8 fold increase in protein concentration inside the cells comparing to the reduced levels of free protein level inside the cells (4.8 pg and 5 pg) after 1 h and 4 h incubation time (Figure 3.20.).

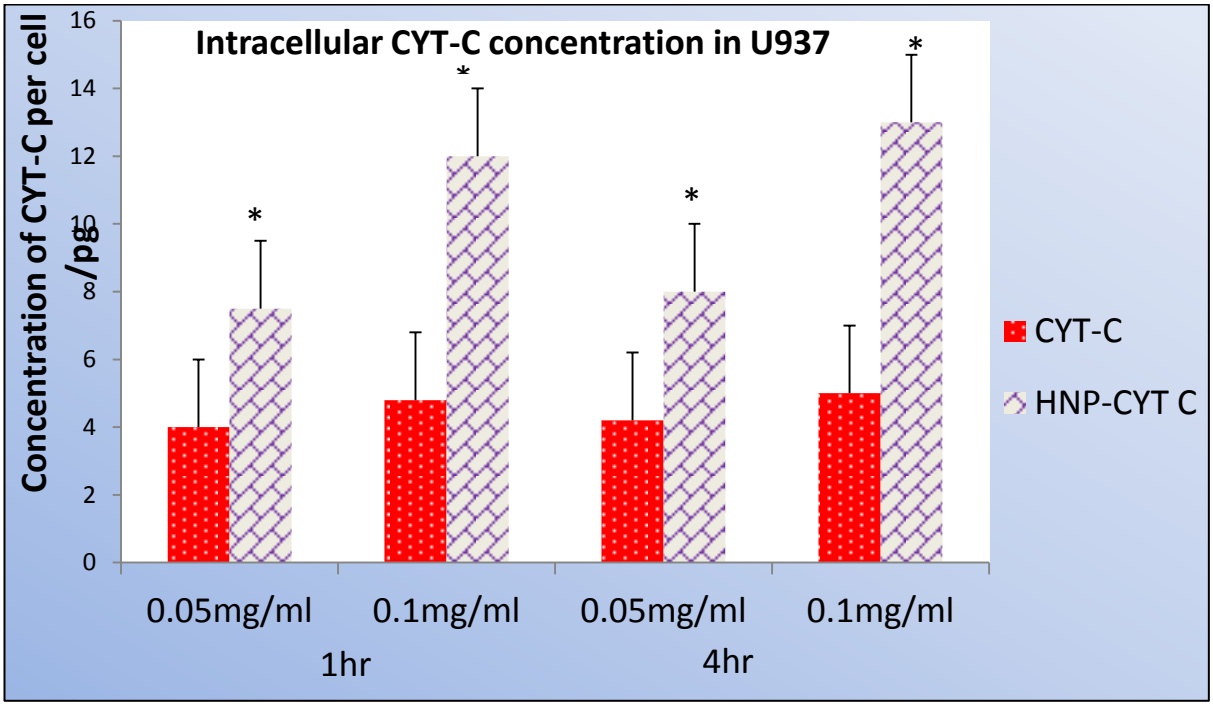

Figure 3.20. Protein uptake study on U937 cell line after 1 h and 4h incubation time with 50 μgmL^{-1} and 100 μgmL^{-1} concentration of cytochrome C and HNP-C formulation,* indicate the significant differences between hybrid formulation of protein uptake value with the free form of protein uptake at similar time and concentration(n=3 ,average±SD). The t-test analysis is performed by Microsoft Excel software.

In all previous uptake experiments of hybrid formulation of protein into cancer cell lines show a concentration dependent pattern of uptake ($p<0.05$), rather than time dependent. The uptake values for HNP- C were maximum 20 pg per cells in U937 and SK-hep-1 cell lines comparing to the higher internalise rate (more than 30pg/cell) of hybrid formulation into HepG2 and Huh-7D cell lines This could be attributed to smaller size of U937 and SK-hep-1 cell lines (12 µm and 15 µm) respectively in parallel to (20 µm and 25 µm) size of HepG2 and Huh-7D cells. The main differences in the cells size may indicate the lower capacity of U937 and SK-hep-1 in uptake value of the protein hybrid formulation (the size measurements

were performed by AFM imaging technique, which will be discussed later). Or perhaps the reduced intake into these two cell lines could be due to differences in proliferation rate between the cell lines. The real reason is unknown, and further investigation into this is required.

3.3.3. Apoptosis Assays

3.3.3.1. Caspase 3 results

The human body has several mechanisms that work as safeguards against tumour progress. The process of apoptosis is considered as one of these vital mechanisms which regulates and recognises any faulty steps in cell proliferation. Caspase enzymes have a crucial role in apoptosis, therefore, any disturbance in there levels can be caused in cell mutation and cancer progression. In the resent years, caspase enzyme detection kits are used as one of the apoptosis markers in cancer research, especially targeting caspase 3 level as one of execution caspase members. In this research caspase 3 colorimetric methods (Abcam) was used as a convenient way in (DEVD) sequence recognition and following the manufacture instruction as mentioned before (materials and methods). The liver cancer cell lines (HepG2, Huh-7D and SK-hep-1) in addition to U937 cell lines are promoted to induce apoptosis by (doxorubicin, oxaliplatin, paclitaxel, vinblastine and vincristine) alone and in combination with hybrid nano-formulation of cytochrome C. The light emission of the P-NA part can be detected by microtiter plate reader at 405 nm. Quantified results can be calculated by comparison between induced

cells (apoptotic cells) absorbance and the absorbance of control (uninduced cells) as folding increase in caspase 3 expression values. In HepG2 cells, the experiments indicated that there was significant levels of Caspase-3 present in those cells treated with combination therapy (Figure 3.21.). Doxorubicin and Oxaliplatin presented a 2-fold and 2.6–fold increase in enzyme levels respectively, in combination form with HNP-C. In the cells treated with drugs alone, no significant increase in caspase-3 was observed compared to the control cells. The combination therapy with resulted in the greatest level of caspase-3 increase compared with the drugs alone in HepG2 cells were those treated with anti-microtubule drugs (paclitaxel, vinblastine and vincristine) (Figure 3.21.). Here we observed a 5.2-fold, 2.8-fold and 3-fold increase in enzyme level respectively..

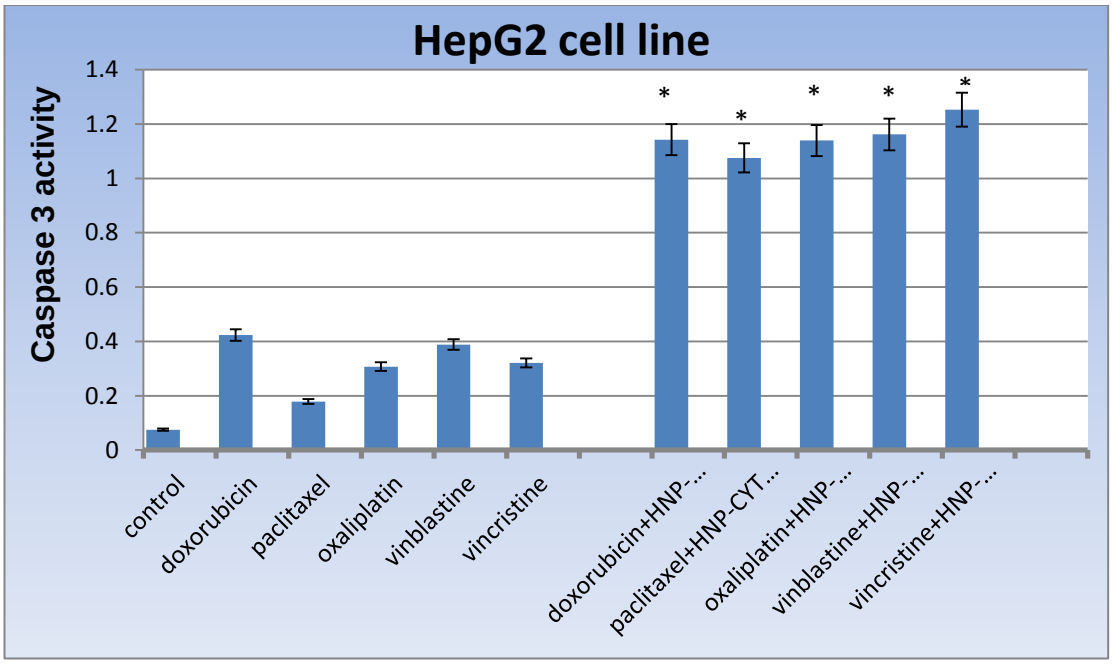

Figure 3.21. Represent the activity of caspase 3 in HEPG2 cells were treated with DNA damage drugs (doxorubicin and oxaliplatin); and antimicrotubule drugs (paclitaxel, vinblastine and vincristine), the results are represented as mean±SD. No. of experiments=3. The results are expressed as a significant difference between drug alone and combination therapy at *P value< 0.05.

In general, in Huh-7D cells, all combination treatments resulted in significant Caspes-3 production inside the cells when compared with the single drug dose and the control cells. The greatest level of caspase-3 enzyme was observed in the combination therapy of HNP-C with doxorubicin or oxaliplatin. These combinations resulted in a 1.8-fold and 2.2-fold increase in caspase 3 level compared to the single drug treatment, respectively. (Figure 3.22.).

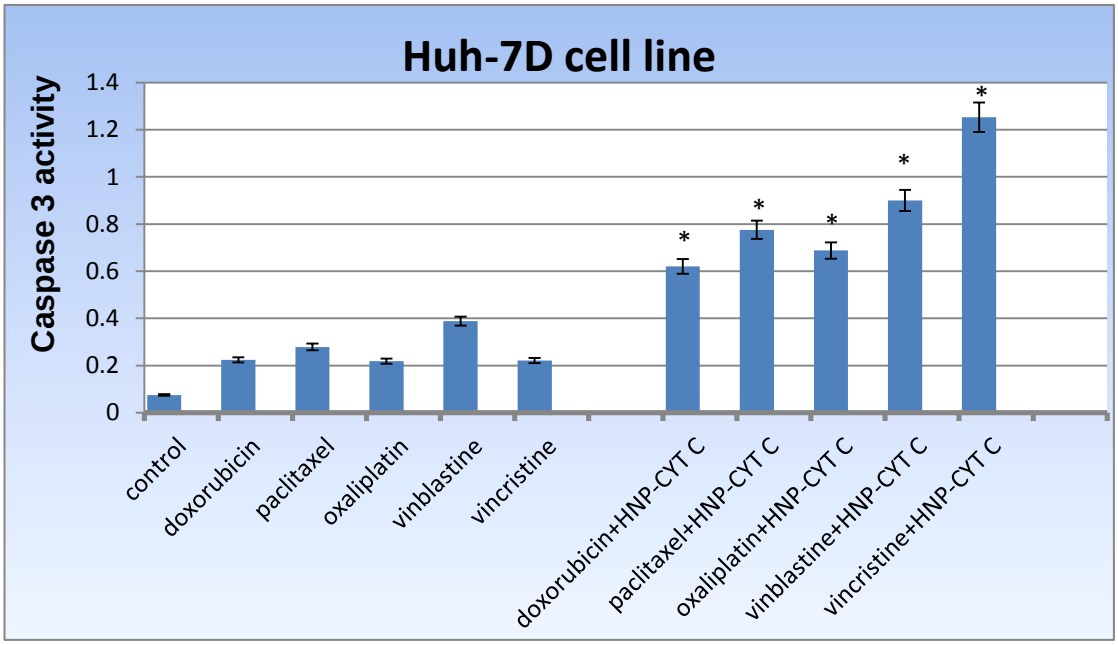

Figure 3.22. Represent the activity of caspase 3 in Huh-7D cells were treated with DNA damage drugs (doxorubicin and oxaliplatin); and antimicrotubule drugs (paclitaxel, vinblastine and vincristine), the results are represented as mean±SD. No. of experiments=3. The results are expressed as a significant difference between drug alone and combination therapy at *P value< 0.05.

For SK-hep-1 cell line, no significant increase in caspase 3 levels was observed in cells treated with either drugs alone or in combination with HNP-C. The exception to this was with combination therapy of HNP-C and doxorubicin. Here, a 3.5-fold

increase in caspase-3 level compared with the single drug treatment occurred (Figure 3.23.).

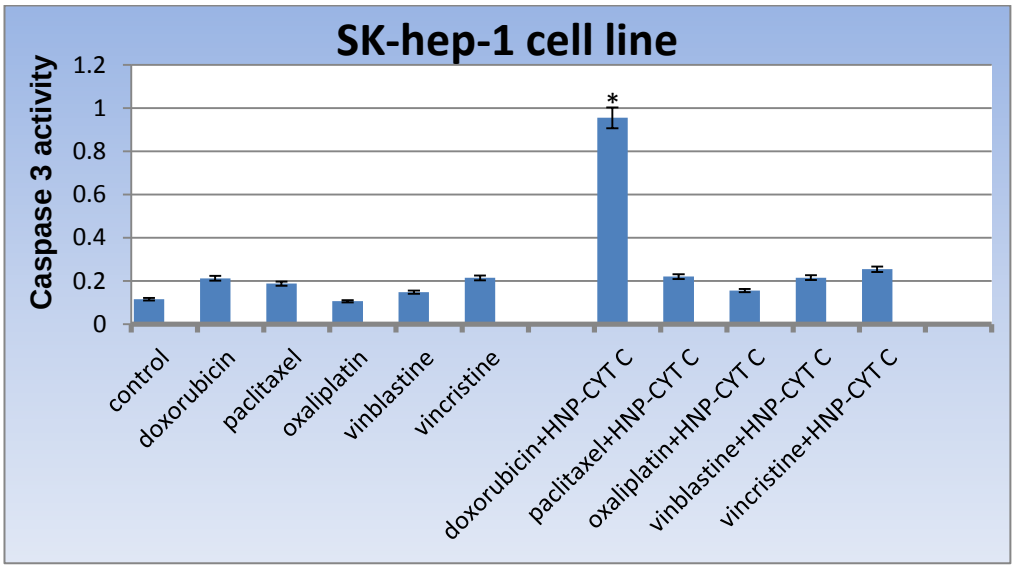

Figure 3.23. Represent the activity of caspase 3 in SK-hep-1 cell line which treated with DNA damage drugs (doxorubicin and oxaliplatin); and antimicrotubule drugs (paclitaxel, vinblastine and vincristine), the results are represented as mean±SD. No. of experiments=3. The results are expressed as a significant difference between drug alone and combination therapy at *P value< 0.05.

Caspase 3 assay in U937 cell line represented as highest levels in both phases of treatment either with chemotherapeutic drugs alone or combined with HNP-C, with no significant differences between these methods of treatment (Figure 3.24.). These results coordinated with other detecting apoptosis methods of protein immunoblotting (western blot) and TUNEL assay results of apoptotic cells which showed the programed killing activities of single drugs alone and in combination therapies. The smallest size of these u937 comparing to other liver cancer cell line used may be considered as main cause of poor proliferative level of U937 cells treated with chemotherapeutic drugs that effect the action of HNP-c combination,

in addition to different mechanism of cellular uptake of these suspension cells comparing to liver cancer cells used in same treatment protocol.

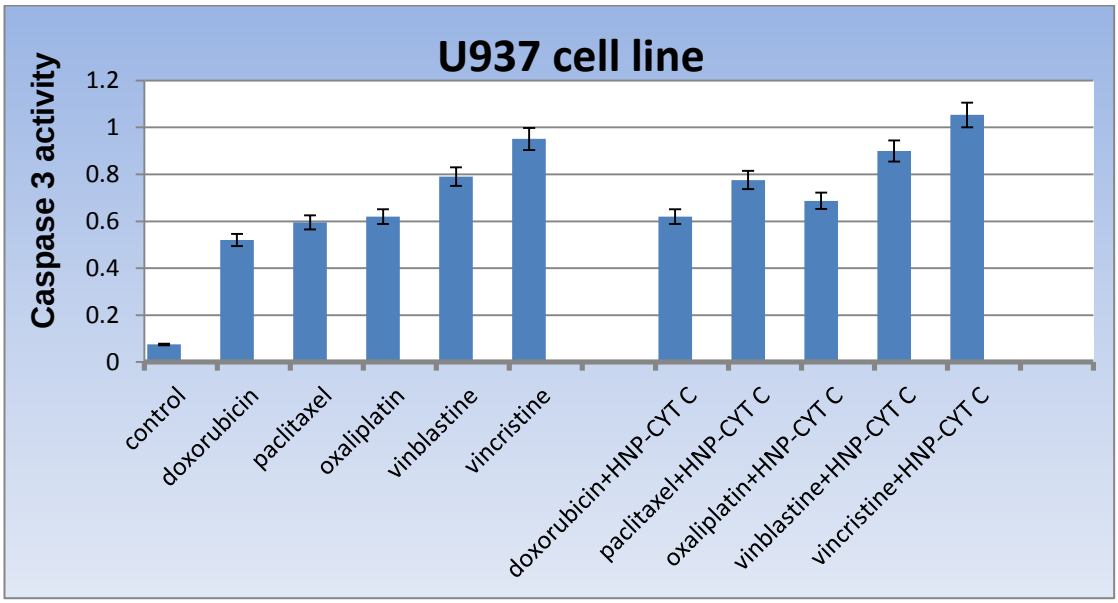

Figure 3.24. Represent the activity of caspase 3 in U937 cell line which treated with DNA damage drugs (doxorubicin and oxaliplatin); and antimicrotubule drugs (paclitaxel, vinblastine and vincristine), the results are represented as mean±SD. No. of experiments=3.

3.3.3.2. Western Blot

Apoptosis follows the regular physiological changes inside the body to control the proper balance between the live and dead cells, controls the morphology of the organ and modeling tissue and eradicates any mutated or injured cells (Galluzzi L. *et al*. 2008).Uncontrolled apoptosis affects the regulated pattern of cell growth and caused hyper-proliferative sickness, cancer and neuro diseases (Cotter TG. 2009).

Cascade signalling pathways are involved in programmed cell death by activation of specialised caspase family. When inactive precursors of these enzymes are

activated by extrinsic and/or intrinsic apoptosis pathways the series of cleaving and stimulating steps are directed to the effector and executioners groups of caspase to initiate apoptosis (Li J and Yuan J., 2008). Apoptosis is mediated by caspase series family by the cleavage of many key proteins used in proper cell growth pathway (Fischer U. *et al.* 2003).

One of the cellular caspase substrates is PARP-1. Cleavage fragments of this protein are considered as the main marker of apoptosis. PARP (Poly (ADP-ribose) polymerase) is a nuclear protein which is responsible to detect and repair any breaks in DNA strand. Once Caspase-3 enzyme cleaved the PARP protein as regular steps in apoptosis process, the repairing DNA step is impaired and cleavage PARP fragments are produced. For that reason, these detecting fragments can be considered as a main mark of apoptosis and can be imaged and analysed by western blot technique (Kaufmann SH. *et al*. 1993).

Cleavage PARP bands in western blot are recognised as the main biomarkers of cells suicide by apoptosis which follows a unique pattern of protease enzymes activity. The detective PARP cleavage bands with combination therapy of anticancer drugs and nanoparticles formulation comparing to unnoticed bands with single drugs treatment are characterized the synergism effects of the combination therapy in contrast to inactivated signal with single drug treatment (Figures 3.25., 3.26. and 3.27.).

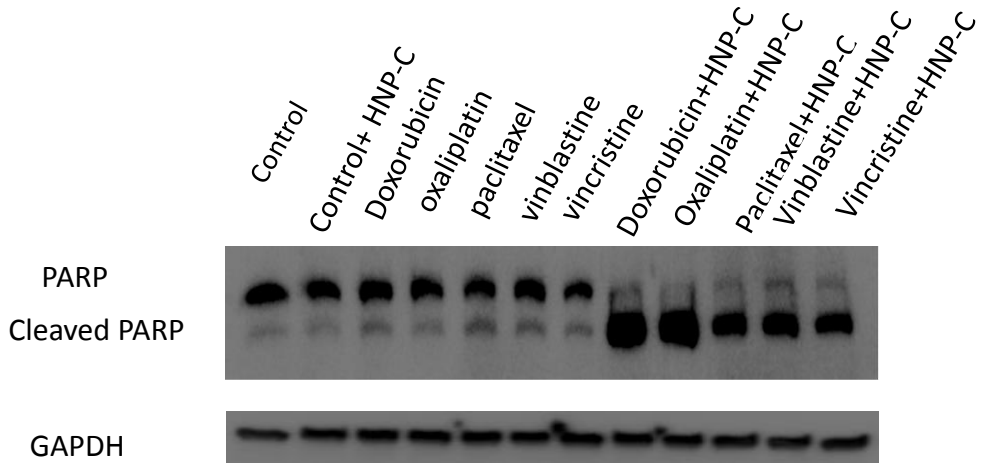

Figure 3.25. illustrates the apoptotic activity of combination therapy in HepG2 which is represented by the detection of the dark PARP cleavage band patterns compared to the faint bands observed in single drug treatment.

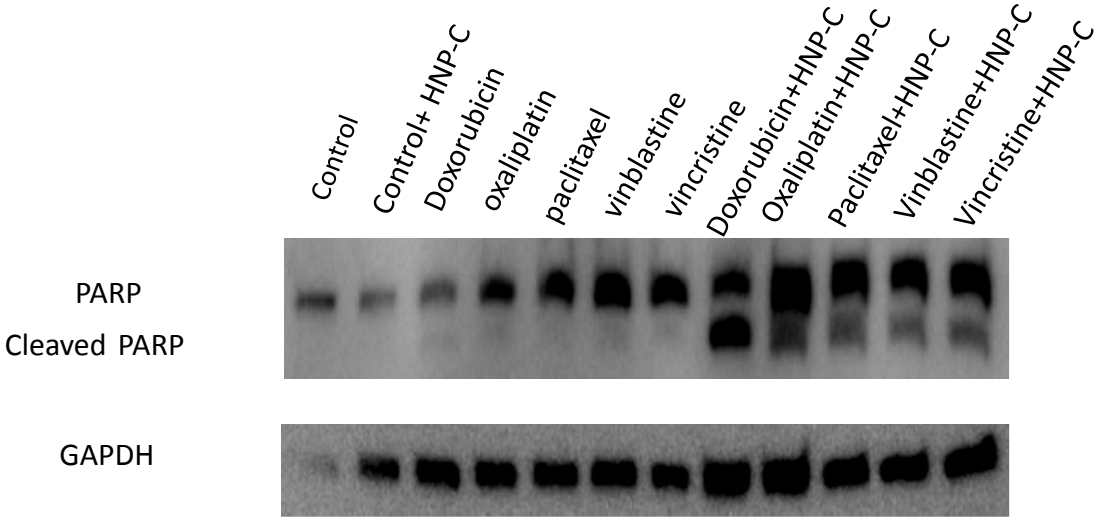

Figure 3.26. Illustrates the apoptotic activity of combination therapy in HUH-7D cell lines which is represented by the detection of the dark PARP cleavage band patterns compared to the faint bands observed in single drug treatment.

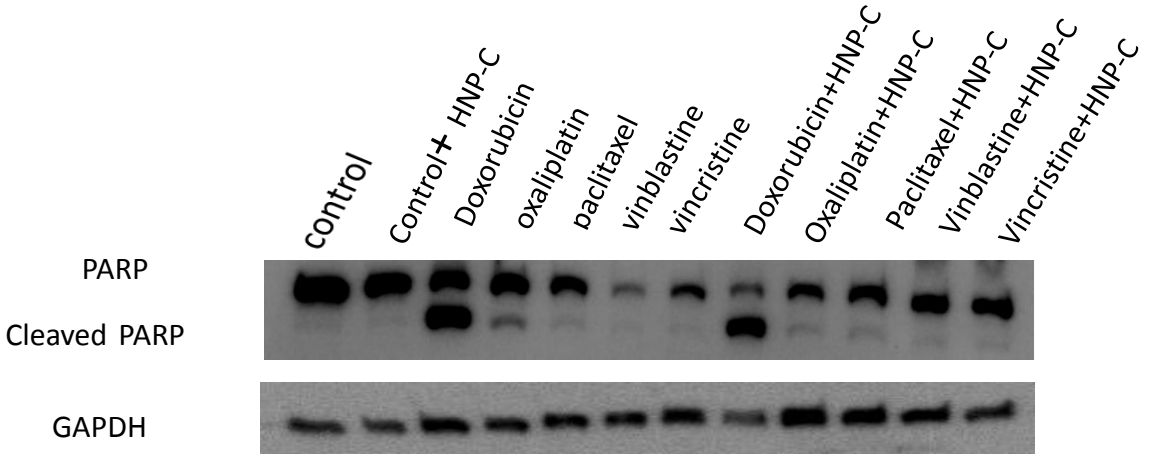

Figure 3.27. Illustrates the apoptotic activity of combination therapy in the SK-hep-1 cell line, dark signature of cleavage PARP is only noticed with doxorubicin with and without combination with HNP-C in these cell line, while unreactive bands being observed with all other combinations and treatments.

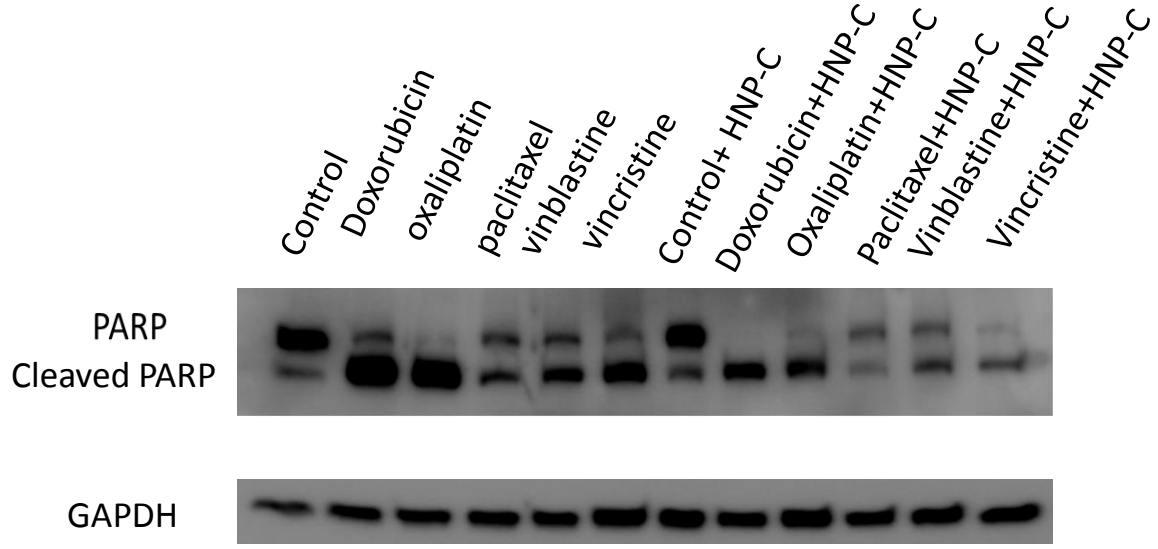

Figure 3.28. Illustrates the apoptotic activity of combination therapy in U937 cell line which is represented by the detection of the dark PARP cleavage band patterns compared to the faint bands observed in single drug treatment.

The PARP bands were present in those cells treated with single drugs in U937 cells, showing a different behaviour compared to the liver cell lines. Strong synergism effects were detected with combination therapies and visualised as robust signalling bands as illustrated in (Figure 3.28.). GAPDH served as loading control.

3.3.3.3. Tunel Assay

The detection of DNA fragmentation as a one of most important features of apoptosis is applied now in many fields of the cancer researches. One of these methods is the labelling nick end of damaged DNA with TDT-mediated dUTP-biotin nick end labelling (Gavrieli *et al*., 1992).

TUNEL assay (HT Titer TACS colorimetric assay, TREVIGEN) was originally used in the quantitative detection of death apoptotic cell at the late stage by dUTP labelling of the free 3-hydroxy termini of DNA breaks and catalyse by the presence of TDT enzyme. The end labelling dUTP was labelled by secondary blue marker (TACS-Sapphire) in the presence of HRP-conjugated streptavidin to be detected at 450nm using plate reader (Lozano, G.M., *et al*., 2009).

In these experiments, the percentage of the DNA fragmentation are illustrated the significant results with the combination therapy comparing to minor level of these fragmentations were observed in single anticancer drug treatment. By means of this labelling process, the results confirm the killing activities of our combination

therapy by apoptosis against the liver cancer cell line except in the case of the Sk-hep-1 cell line only which showed positive results with combination of nanoparticles formulation and DNA damage drugs (Doxorubicin). The experiments are triplicated for each sample and calculated the percentage of apoptotic cells in relative to untreated control cells.

Under conditions of anticancer drugs treatments (doxorubicin, paclitaxel, oxaliplatin, vincristine and vinblastine), negligible apoptosis levels were observed with liver cells treated with each drug, while the highest level of apoptosis signals were noticed with the combined therapies.

In Hep-G2 cells, TUNEL results showed significant levels of apoptosis within cells treated with combination therapy (Figure 3.29.). The DNA damage drugs (doxorubicin and oxaliplatin) presented significant absorbance levels (4-folds and 8 –fold) in DNA damage levels respectively, when combined with hybrid nanoparticle-formulation of cytochrome C. In parallel to non-significant levels of apoptosis was noticed with cells treated with each drugs alone in relative to control (untreated cells). TUNEL assay colorimetric reactions also showed the highest significant level of apoptosis in Hep-G2 cells treated with anti-microtubule drugs (paclitaxel, vinblastine and vincristine) combined with HNP-C (Figure 3.29.) as(3,9 and 6 fold) increase, respectively for each combination in relative to the low absorbance levels on the cells treated with chemicals alone.

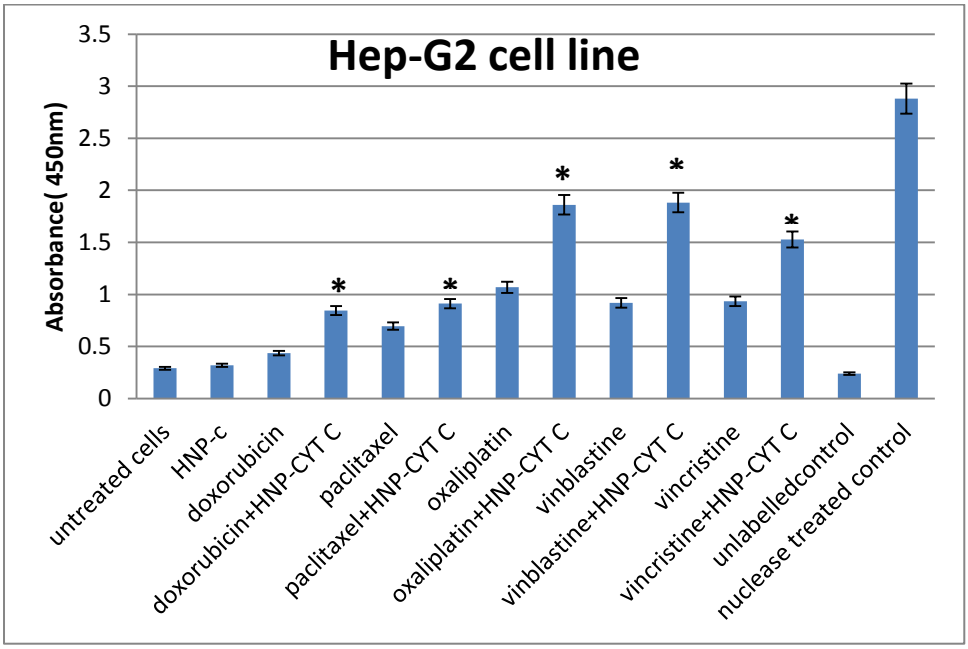

Figure 3.29. Apoptosis percentage from TUNEL assay on Hep-G2 cell line treated with (Doxorubicin, Paclitaxel, Oxaliplatin, Vinblastine and vincristine) alone and in combination with HNP-C for 24 h incubation time.*belong to significant value of combination therapy in relative to free drug ($p<0.05$). All statistical analyses were calculated by t.test using Microsoft Excel software,(n=3,±SD).

TUNEL assay analysis of Huh-7D cell line possessed the higher significant DNA damage levels with chemotherapeutic drugs treatment in combination with HNP-C, the apoptosis absorbance detected levels of cells treated with DNA damage drugs (doxorubicin and oxaliplatin) with hybrid nano-formulation of cytochrome C were showed (4 and 3 fold) increase in apoptosis in comparing to single drugs treatment, respectively. The apoptosis activity also increased in cells treated with combination therapies of HNP-C and anti-microtubule drugs and represent around 4-fold increase in DNA damage levels in parallel with no significant levels were observed with single drugs treatment in relative to control (Figure 3.30.).

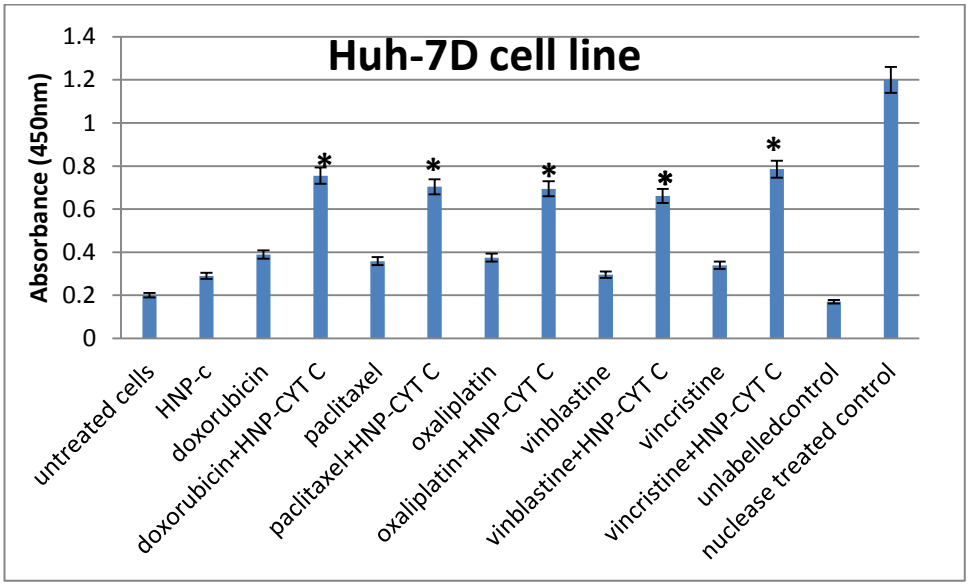

Figure 3.30. Apoptosis percentage from TUNEL assay on Huh-7D cell line treated with (Doxorubicin, Paclitaxel, Oxaliplatin, Vinblastine and vincristine) alone and in combination with HNP-C for 24 h incubation time.*belong to significant value of combination therapy in relative to free drug ($p<0.05$). All statistical analyses were calculated by t.test using Microsoft Excel software,(n=3,±SD).

.

For SK-hep-1 cell line, no significant results were obtained in TUNEL assay with cells treated with drugs alone or with hybrid formulation of cytochrome C, with one exceptional significant level of DNA damage was observed with combination therapy of HNP-C and doxorubicin comparing to negligible value with cells treated with this drug alone and showed 5-fold increase in TUNEL assay response in relative to single drug treatment. The results are calculated as percentage in relative to control as illustrated in (Figure 3.31.).

These results are also confirmed with other apoptotic assays used such as (western blot and fluorescent microscopy) which showed only significant results with combination therapy of doxorubicin and HNP-c comparing to minor responses with other combination drugs formulations.

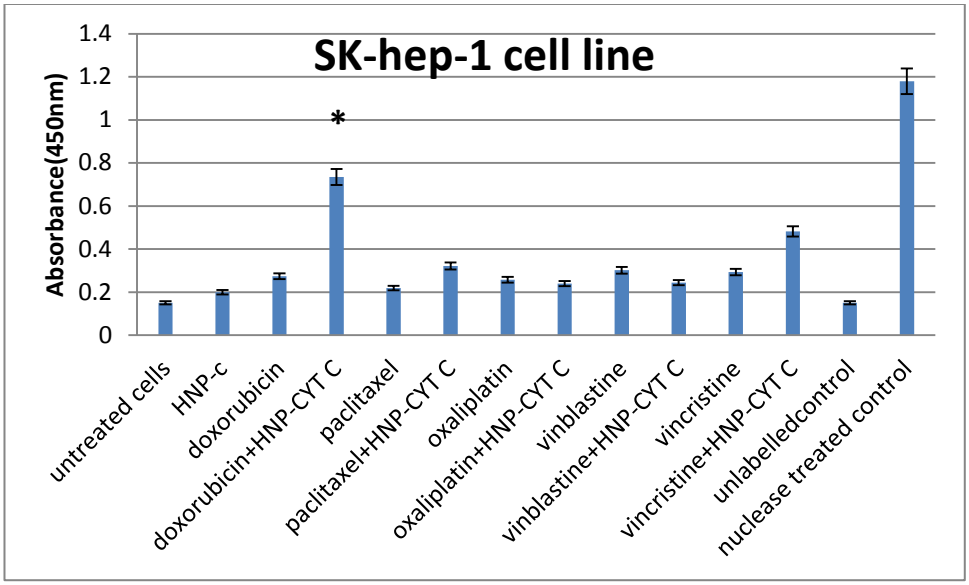

Figure 3.31. Apoptosis percentage from TUNEL assay on SK-hep-1 cell line treated with (Doxorubicin, Paclitaxel, Oxaliplatin, Vinblastine and vincristine) alone and in combination with HNP-C for 24 h incubation time.*belong to significant value of combination therapy in relative to free drug ($p<0.05$). All statistical analyses were calculated by t.test using Microsoft Excel software,(n=3,±SD).

U937 cell line showed the highest DNA damage levels in both phases of treatment either with chemotherapeutic drugs alone or combined with HNP-C, with no significant differences between these methods of treatment (Figure 3.32.). These results matched the other apoptosis methods of protein immunoblotting (western blot) and with fluorescent labelling results of apoptotic cells which showed the

programed killing activities of single drugs alone and in combination therapies. The smallest size of these u937 (as detected by AFM images) comparing to other liver cancer cell line used may be considered as main cause of poor proliferative level of U937 cells treated with chemotherapeutic drugs that effect the action of HNP-c combination, in addition to different mechanism of cellular uptake of these suspension cells comparing to liver cancer cells used in same treatment protocol.

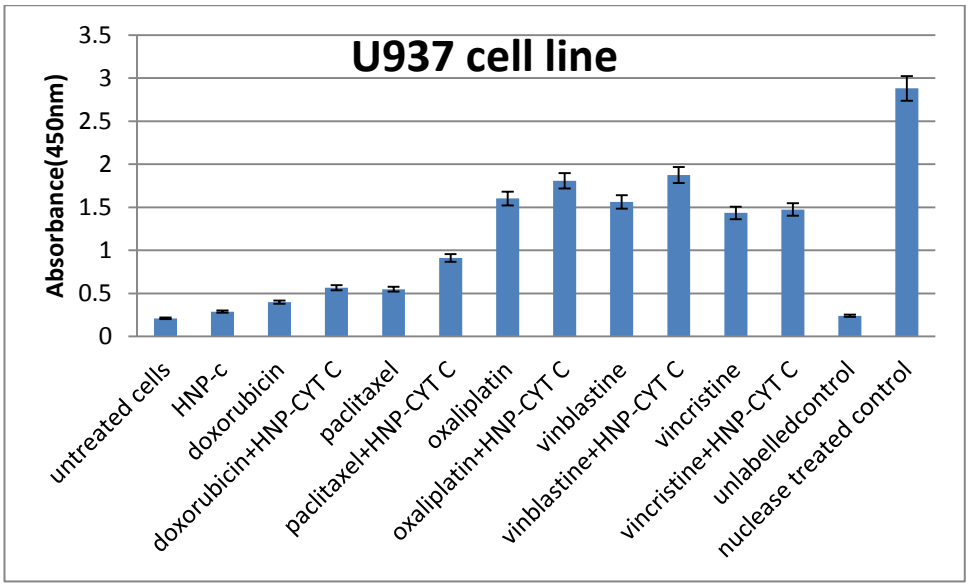

Figure 3.32. Apoptosis percentage from TUNEL assay on U937 cell line treated with (Doxorubicin, Paclitaxel, Oxaliplatin, Vinblastine and vincristine) alone and in combination with HNP-C for 24 h incubation time. All statistical analyses were calculated by t.test using Microsoft Excel software,(n=3,±SD).

3.3.4. Imaging studies

3.3.4.1. Fluorescent microscopy imaging

Apoptosis (programmed cell death) is characterised by several cellular components changes such as condensed nucleus, DNA fragmentation and morphological changes of cell surfaces. During the recent years, detecting of different stages of apoptosis is developed by using different methods concerning with early and late apoptosis level. In the early stage of apoptosis, the phosphotidylserine (PS) is translocated from the inner to outer face of cell membrane which facilitates the early recognition of apoptosis by binding the overlapped PS with fluorescein isothiocyanat labelled- annexin V (annexin V-FITC) that has a strong and natural attraction to PS. The binding fluorescein label is detected by the fluorescence microscopy and considered the most vital indicator of early stage of programmed cell death that caused by a variety of death signals stimuli.

The liver cancer cells were exposed to apoptosis stimuli by anticancer drugs (Doxorubicin, Paclitaxel, Oxaliplatin, Vinblastine and Vincristine) alone and in combination with HNP-C. The early stage of cell death was recognised by binding the annexin- V fluorescence probe to the PS outer membrane of the apoptotic cells. The apoptotic cells were visualised as a green staining of outer membrane under a fluorescence microscope. To recognize cells at the late stage of apoptosis from the earlier one, propidium iodide (PI) was used in fluorescence binding assay that had the ability to penetrate only destructive cell membrane and detecting as a

red colour under the microscope. The condensed nucleus can be further detected as blue staining nuclei with Hoechst fluorescence dye.

Randomly five fields of vision were chosen under the fluorescence microscope (Invitrogen^{TM} EVOS^{TM} FL, Thermo Fisher) for counting the apoptotic cells as a green staining signal by Annexin-V prob.

In HepG2 cell line, the Annexin V assay detected the significant percentage of apoptosis within cells treated with combination therapy in parallel to single treatment models (Figure 3.34.). Doxorubicin and Oxalipltin combined with HNP-C formulation were used to induce apoptosis in HepG2 cell lines which showed an increase in the percentage of early apoptotic cells from single to combination treated cells (28% to 70% Annexin V, respectively) for doxorubicin and (26% to 67% Annexin V, respectively) for oxaliplatin treated cells. Anti-microtubule drugs (Paclitaxel, Vinblastine and Vincristine) also induced highest level of apoptosis stained cells when combined with HNP-C and calculated as (73%, 79% and 78%, respectively). In contrast to slight increase in apoptosis percentage with cells treated with each drugs alone and recorded as (19%, 23% and 18%, respectively).

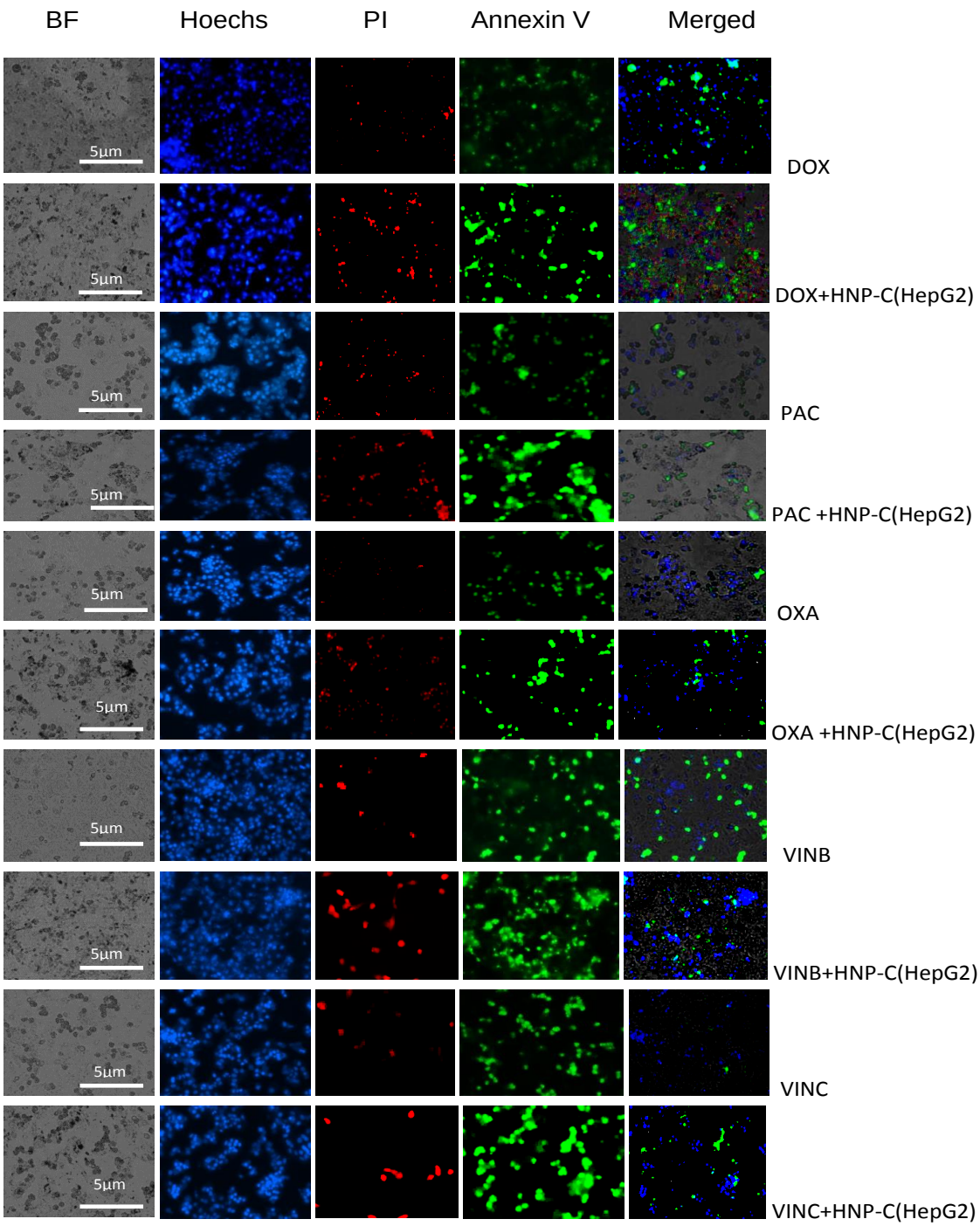

Figure 3.33. Fluorescent microscopy imaging of Doxorubicin (A), Paclitaxel (B), Oxaliplatin (C), Vinblastine (D) and Vincristine(E) and in combination with HNP-C(A+,B+,C+,D+ and E+) for 24 h incubation period in (HepG2**).**

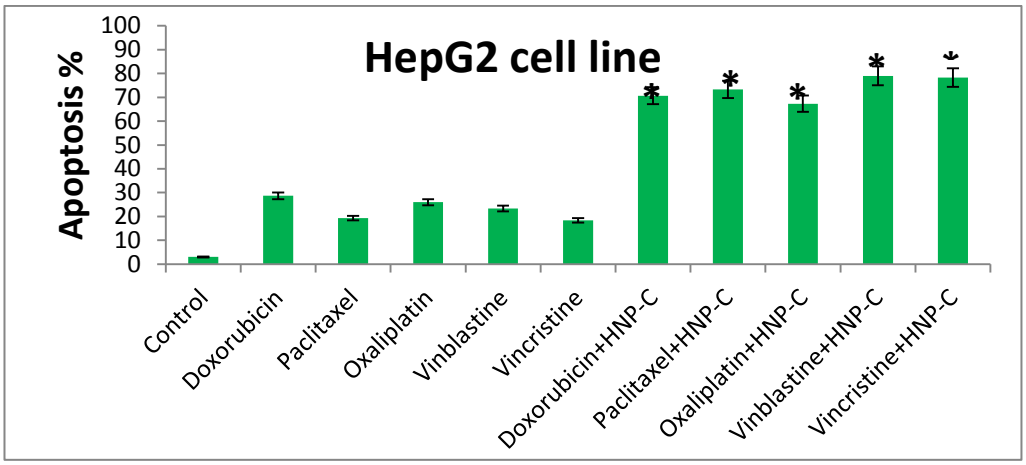

Figure 3.34. Apoptosis detection cells with Annexin V staining probe. HepG2 Cell lines were treated with single drugs Doxorubicin (A), Paclitaxel (B), Oxaliplatin (C), Vinblastine (D) and Vincristine(E) and in combination with HNP-C(A+,B+,C+,D+ and E+) for 24 h incubation period. Data represent as (mean±SD, n=3).*significant difference ($p<0.05$) between combination drugs with HNP-C and single drug treatment by paired t-test.

Huh-7D incubated cells with single chemotherapeutic drugs (Doxorubicin, Paclitaxel, Oxaliplatin, Vinblastine and Vincristine) were analysed under fluorescence microscopy to detect the Annexin V binding probe which showed no noteable increase in apoptotic cells at the early stage (33%, 32%, 35%, 22% and 20%, respectively) comparing to highly significant level of apoptosis cells with combination form of HNP-C with each single drugs (78%, 78%, 66%, 70% and 60%,respectively) (Figure 3.36.) .

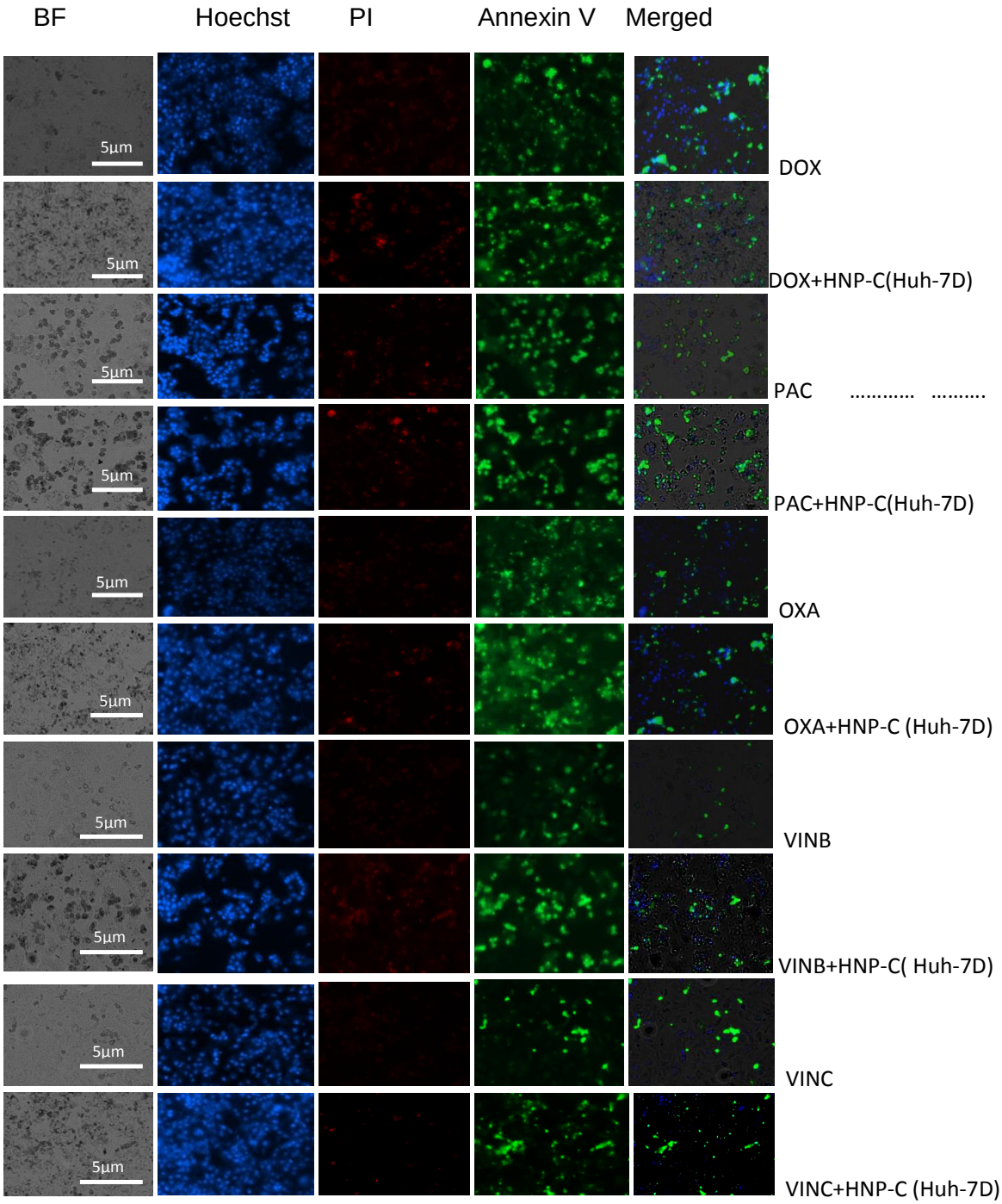

Figure 3.35. Fluorescent microscopy imaging of Doxorubicin (A), Paclitaxel (B), Oxaliplatin (C), Vinblastine (D) and Vincristine(E) and in combination with HNP-C(A+,B+,C+,D+ and E+) for 24 h incubation period in (Huh-7D).

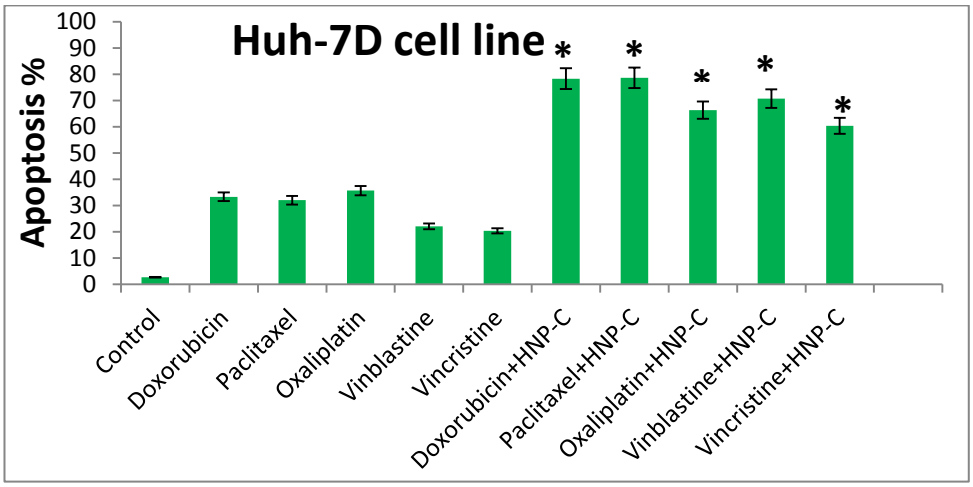

Figure 3.36. Apoptosis detection cells with Annexin V staining probe. Huh-7D Cell lines were treated with single drugs Doxorubicin (A), Paclitaxel (B), Oxaliplatin (C), Vinblastine (D) and Vincristine(E) and in combination with HNP-C(A+,B+,C+,D+ and E+) for 24 h incubation period. Data represent as (mean±SD, n=3).***** significant difference ($p<0.05$) between combination drugs with HNP-C and single drug treatment by paired t-test.

Representative (Figure 3.38.) of SK-hep-1cells treated with combination therapies of HNP-C and each following single chemotherapeutic drugs (Paclitaxel, Oxaliplatin, Vinblastine and Vincristine) for 24 h and then stained with annexin V fluorescent probe as early apoptosis marker shows no major increase in the number of green membrane staining cells of SK-hep-1 with all single and combination therapies with previously mentioned treated drugs. In contrast, to significant apoptotic green signal was observed with doxorubicin and HNP-C combination therapies of SK-hep-1 treated cells comparing to cells treated with doxorubicin alone and calculated as (12% to 49%, single to combination therapy) percentage of apoptosis.

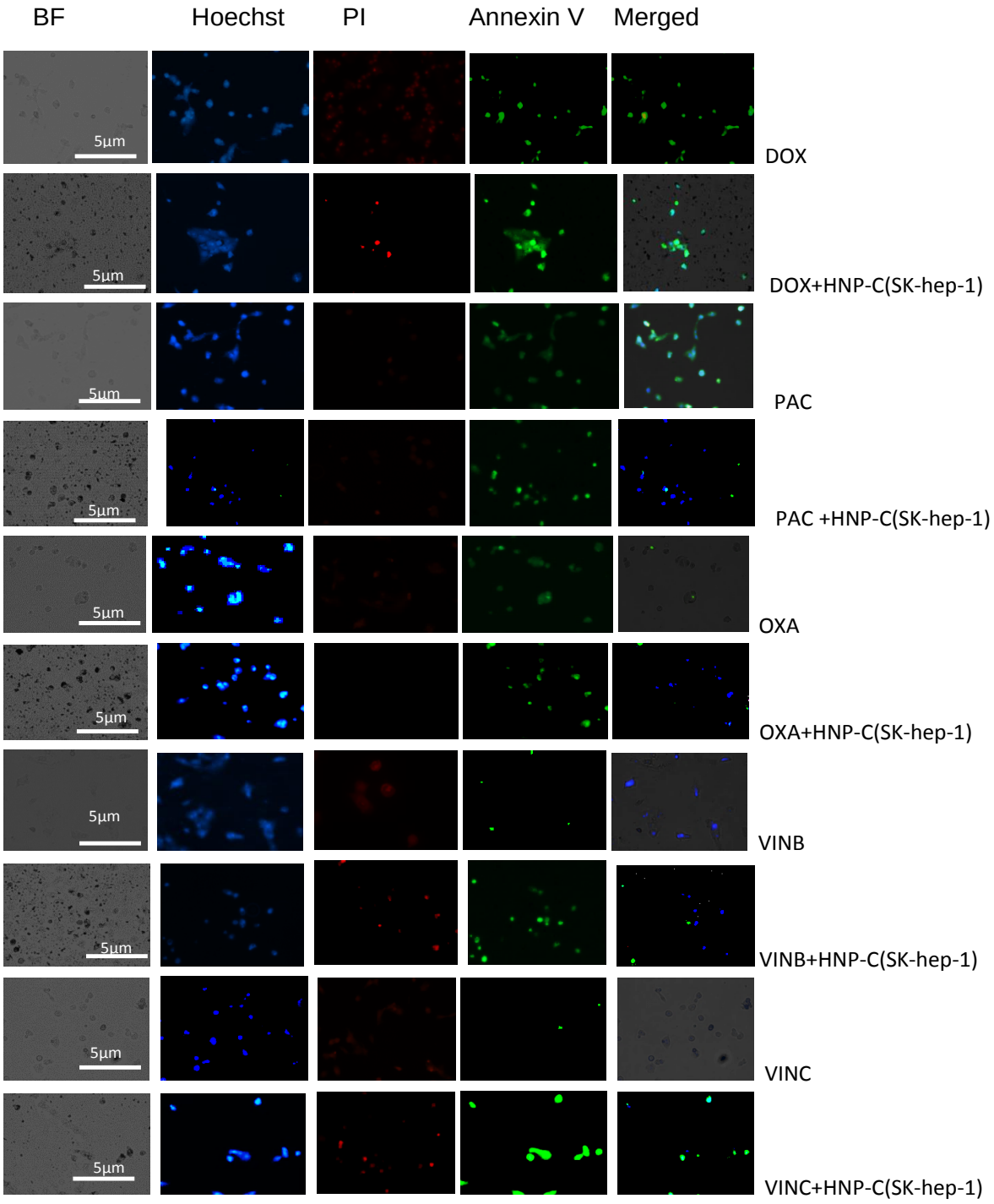

Figure 3.37. Fluorescent microscopy imaging of Doxorubicin (A), Paclitaxel (B), Oxaliplatin (C), Vinblastine (D) and Vincristine(E) and in combination with HNP-C(A+,B+,C+,D+ and E+) for 24 h incubation period in (SK-hep-1).

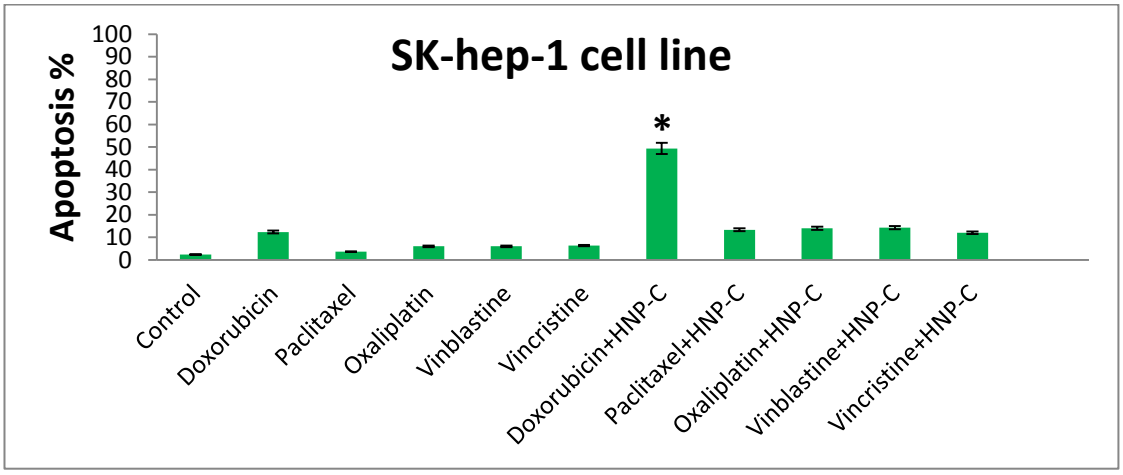

Figure 3.38. Apoptosis detection cells with Annexin V staining probe. SK-hep-1Cell lines were treated with single drugs Doxorubicin (A), Paclitaxel (B), Oxaliplatin (C), Vinblastine (D) and Vincristine(E) and in combination with HNP-C(A+,B+,C+,D+ and E+) for 24 h incubation period. Data represent as (mean±SD, n=3).***** significant difference ($p<0.05$) between combination drugs with HNP-C and single drug treatment by paired t-test.

For U937 cells, (Figure 3.40.) significant positive results were observed with both faces of treatment methods (single and combination therapy), which recorded for (Doxorubicin, Paclitaxel, Oxaliplatin, Vinblastine and Vincristine) as (43%,40%,40%,45% and 44%, respectively) for single drugs treatment, in parallel to combination therapies of each previously mentioned drugs with HNP-C that shows (70%,82%,76%,70% and78%, respectively) for combination therapy. However, this method simplified the weak synergism pattern of combination therapies in U937 in early apoptosis stage comparing to other methods that concern with the detection of more progressive stages of apoptosis process such as DNA damage (TUNEL assay) and cleavage protein (Western blot) which shows more killing pattern but with non-significant qualitative effect between combination of hybrid formulation of cytochrome C and chemotherapeutic drugs paralleling to single treatment.

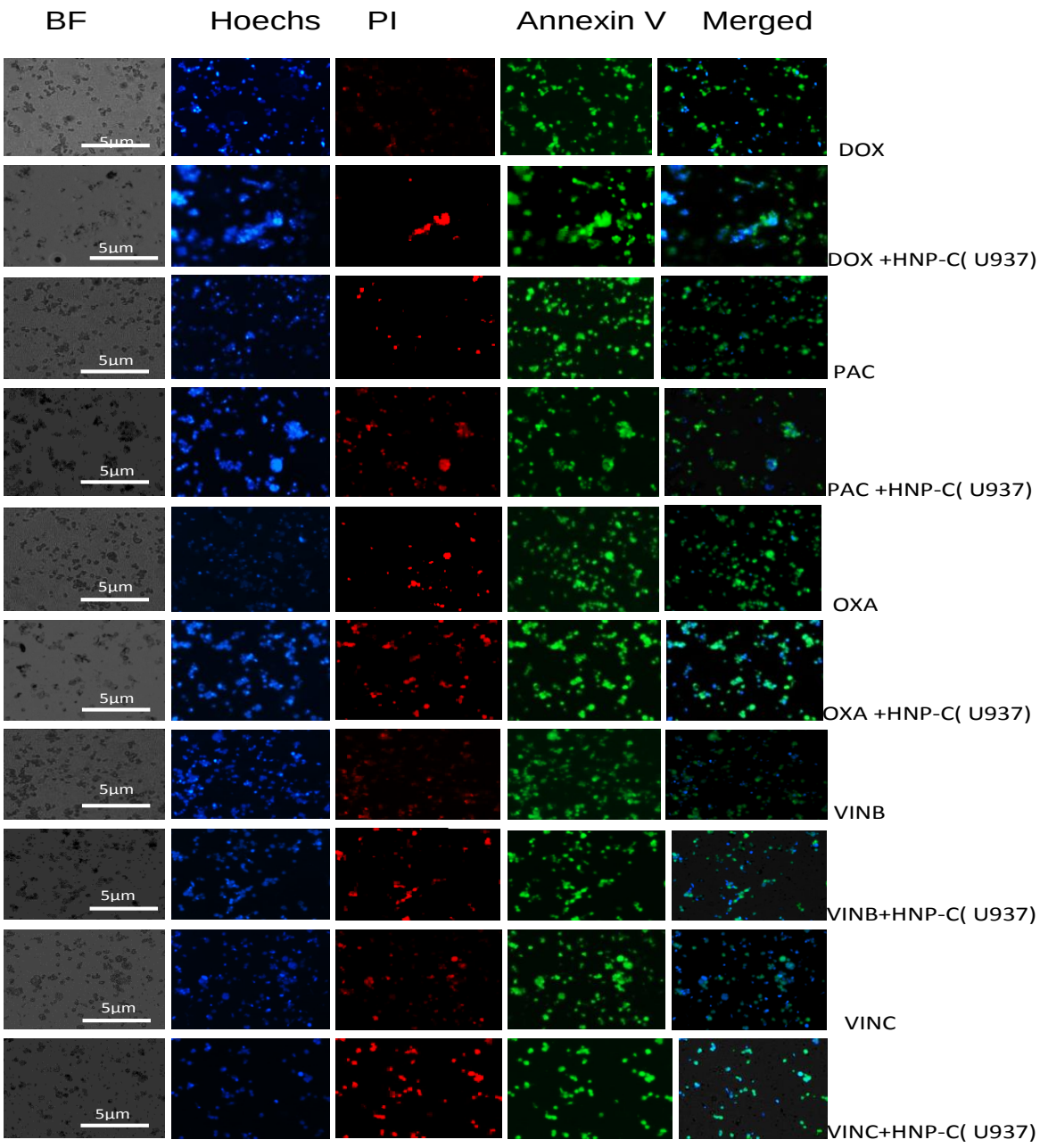

Figure 3.39. Fluorescent microscopy imaging of Doxorubicin (A), Paclitaxel (B), Oxaliplatin (C), Vinblastine (D) and Vincristine(E) and in combination with HNP-C(A+,B+,C+,D+ and E+) for 24 h incubation period in (U937).

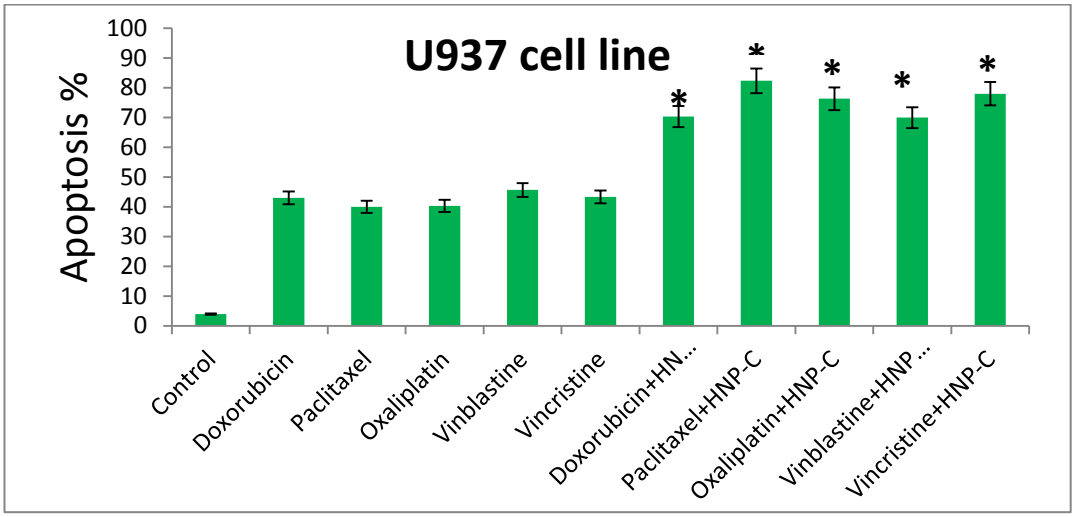

Figure 3.40. Apoptosis detection cells with Annexin V staining probe. U937 Cell lines were treated with single drugs Doxorubicin (A), Paclitaxel (B), Oxaliplatin (C), Vinblastine (D) and Vincristine(E) and in combination with HNP-C(A+,B+,C+,D+ and E+) for 24 h incubation period. Data represent as (mean±SD, n=3).* significant difference ($p<0.05$) between combination drugs with HNP-C and single drug treatment by paired t-test.

3.3.4.2. Nanoparticles internalization inside the cells

Transmission electron microscopy (TEM) was used to verify the internalization of HNP-C formulation inside culture cells. The main pathway of NPs internalisation inside the cells is endocytosis way through several basic mechanisms: caveolae – mediated endocytosis, clathrin-mediated endocytosis and macropinocytosis.

Clathrin-mediated endocytosis is the selective uptake mechanism in internalisation of most types of nutrients, NPs and recycles particles through specific receptors. The HNPs can be visualised in the holes inside the cells (Figure 3.41. A), or be internalised deeper inside the cells by macropinocytosis (Figure 3.41. B and E). Clathrin-mediated endocytosis of HNPs are also observed near the cell nucleus (Figure 3.41. C, D, G and F) as HNPs visualised at cell membrane and near nucleus and mitochondria in Huh-7D cell line (Figure 3.41. F and H) .Higher internalisation levels of HNPs with different mechanisms were observed on HepG2 cell line as illustrated in (Figure 3.41. E).The bioactivity of NPs has been confirmed with successful internalisation of nano-formulation with the living cells. It is important to know their ability to cross the cell membrane and their intracellular concentration to exert the targeting therapeutic goal. TEM can offer unique imaging information of NPs cellular uptake by endocytosis. It is important to discover the ability of the NPs to reach the targeted biological cells and to predict the specific traffic pathways of these therapeutic formulations to select the suitable therapeutic protocol of administration. Moreover TEM images are played additional role in detection of any structural changes of treated cells (Manuela. 2016).

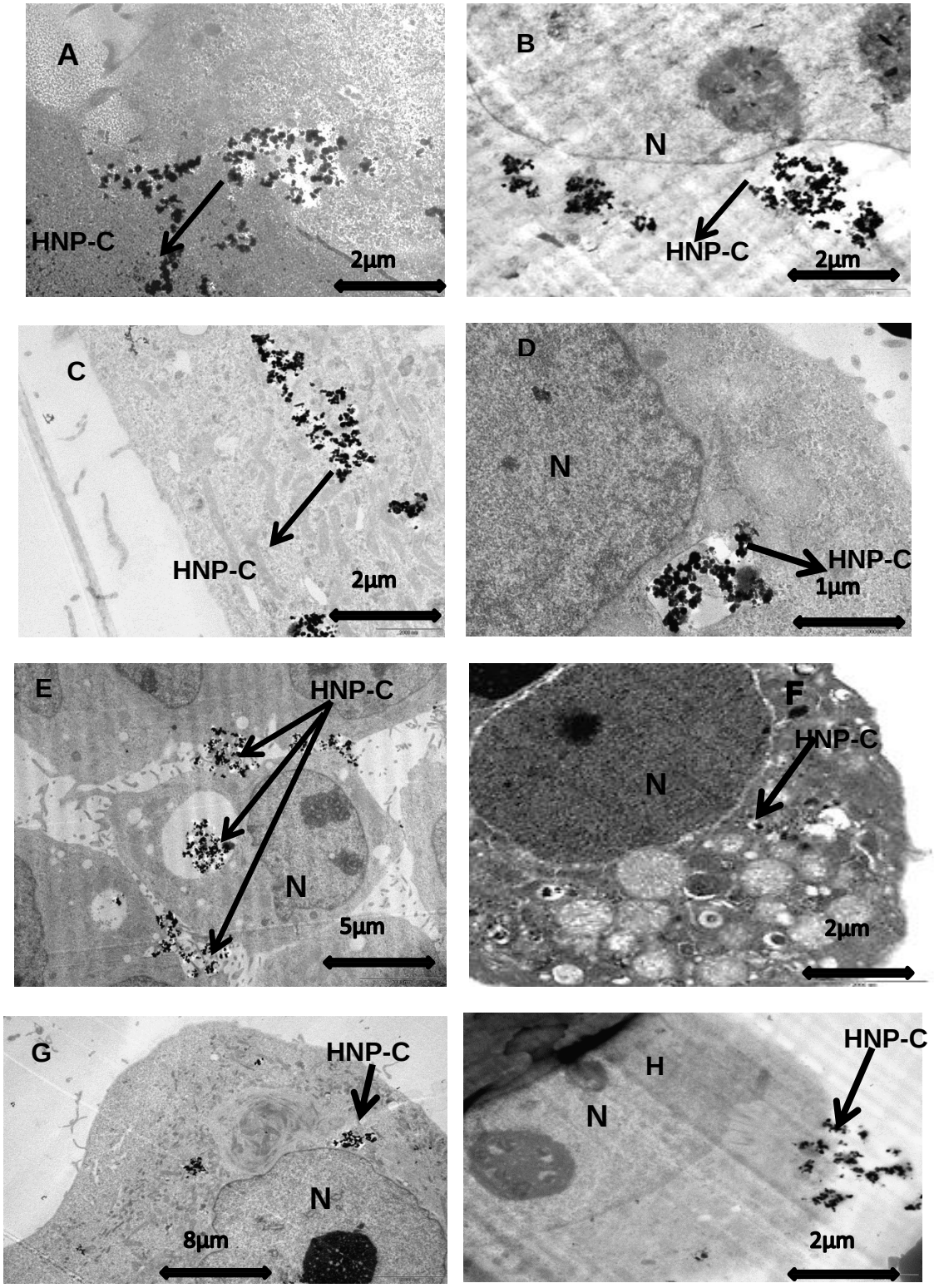

Figure 3.41.*In vitro* cellular uptake studies of HNP-C in(A,E) HepG2 cell line, (B,F,H) Huh-7D cell line, (C,G) SK-hep-1 cell line and (D) U937 cell line after 24 h incubation with 25 µgmL^{-1}of HNP-C using TEM microscope (N) is referred to cell nucleus.

. 3.3.4.3. AFM topography imaging

Atomic force microscopy (AFM) imaging was used in order to visualize the surface morphological of the liver cancer cells treated with combination therapies in parallel to cell treated with single chemotherapeutic drugs. The tapping model of AFM microscope was used to obtain images and in order to visualize the roughness and blebbing of the apoptotic cell surfaces in order to truly evaluate the differences in cellular state between the drug and combination treatment. The treated cells are compared to control (no treatment) cells and cells treated with IC_{10} of HNP-C used as percentage of combination therapy.

AFM images of HepG2, Huh-7D, Sk-hep-1 and U937 cell lines (Figures 3.42., 3.43., 3.44. and 3.45.), show that there was no obvious morphological changes between the control cells and the cells incubated with HNP-C. This confirms the previous tests of the safety usage of HNP-C against liver cancer cell lines. The AFM images of single drugs treated cells (Figures 3.42., 3.43. and 3.44., A1-F1) showed only slight surface modification of treated cells compared to the control. These results are confirmed the previous cytotoxicity assays of not detected any significant IC_{50} values after 24 h of single drugs treated cells. In contrast, obvious morphological changes were observed in the cells treated with combination therapies of CYT-C nanoformulation and chemotherapeutic drugs in all cell lines as illustrated in (Figures 3.42., 3.43. and 3.44.,B2-F2). Here, it can be observed that cellular rearrangement is occurring with surface bobbling and roughness obvious. This can only be due to the synergy between the drugs and HNP-C in combination and their enhanced cytotoxic effect. The only exception to this trend

were observed in the SK-hep-1 cell lines that pictured with non-obvious morphological changes on the surfaces of combination therapies treated cells with all chemotherapeutic treated cells with unique changes was observed (Figure 3.40.,B2) by remarkable changes with blebbing cells surfaces with doxorubicin and CYT-C treated cells and again these are confirmed previously with different cell cytotoxicity assays and apoptosis detecting kits of the negative detecting results with highly resistance SK-hep-1 cell lines in parallel to other cultured liver cancer cell lines.

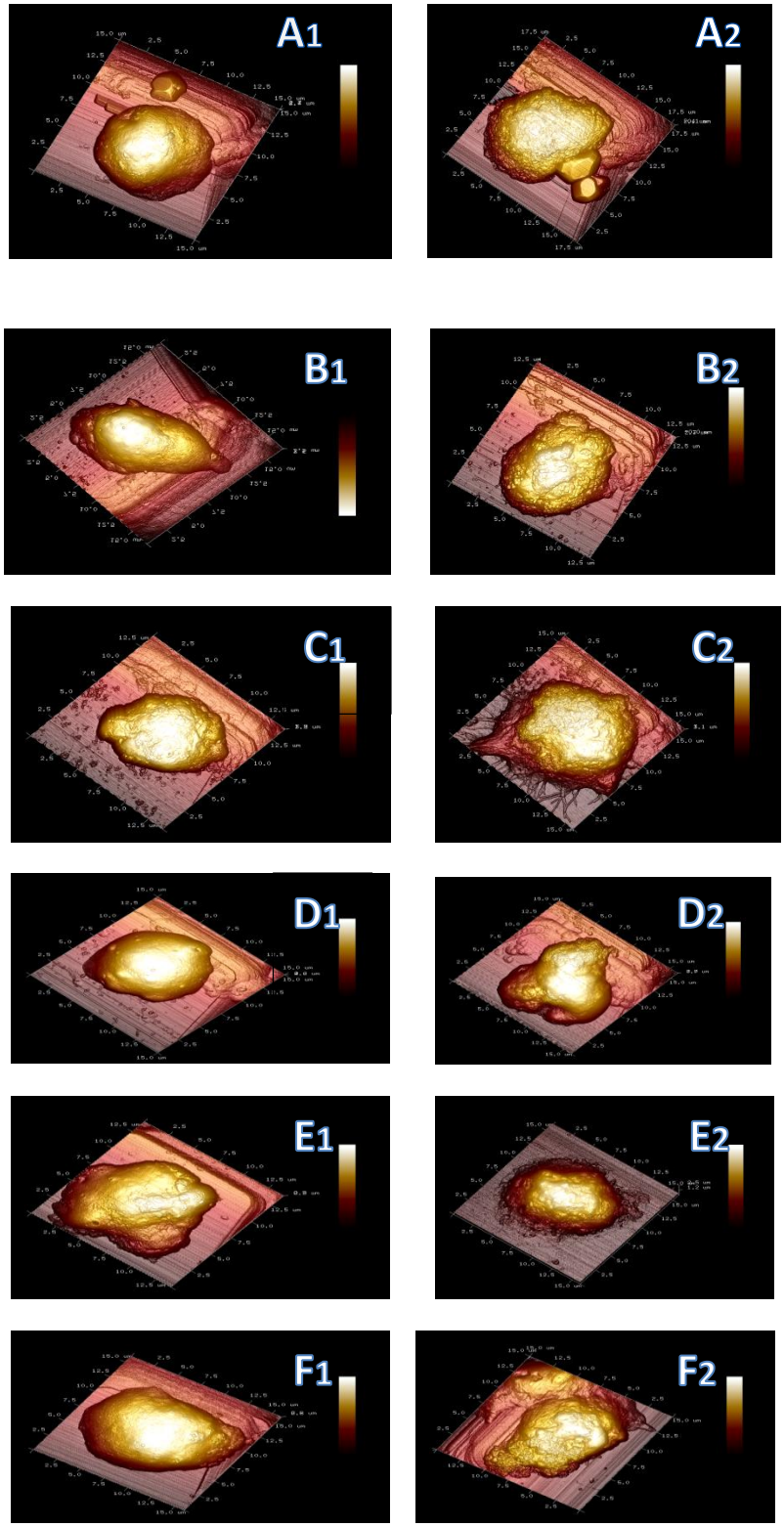

Figure 3.42. AFM image of Hep G2 cells: A1) Control cells, A2) Cells with HNP-C, B)Cells with DOX,C)Cells with OXA,D)Cells with PAC,E)Cells with VINB,F)Cells with VINC. Cells incubated with drug alone (1) and with drug combination (2) for 24 h.

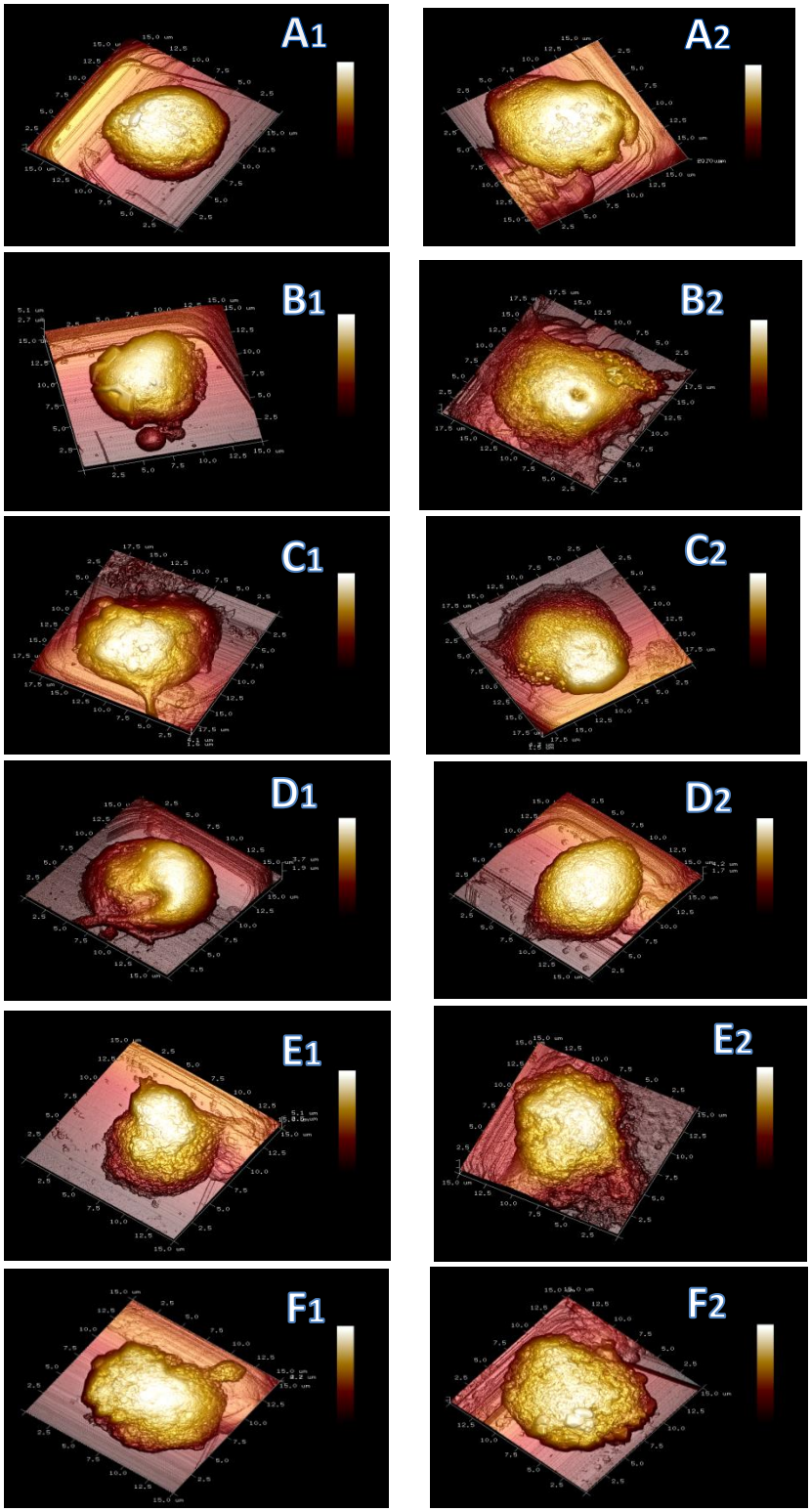

Figure 3.43. AFM image of Huh-7D cells: A1) Control cells, A2) Cells with HNP-C, B)Cells with DOX,C)Cells with OXA,D)Cells with PAC,E)Cells with VINB,F)Cells with VINC. Cells incubated with drug alone (1) and with drug combination (2) for 24 h.

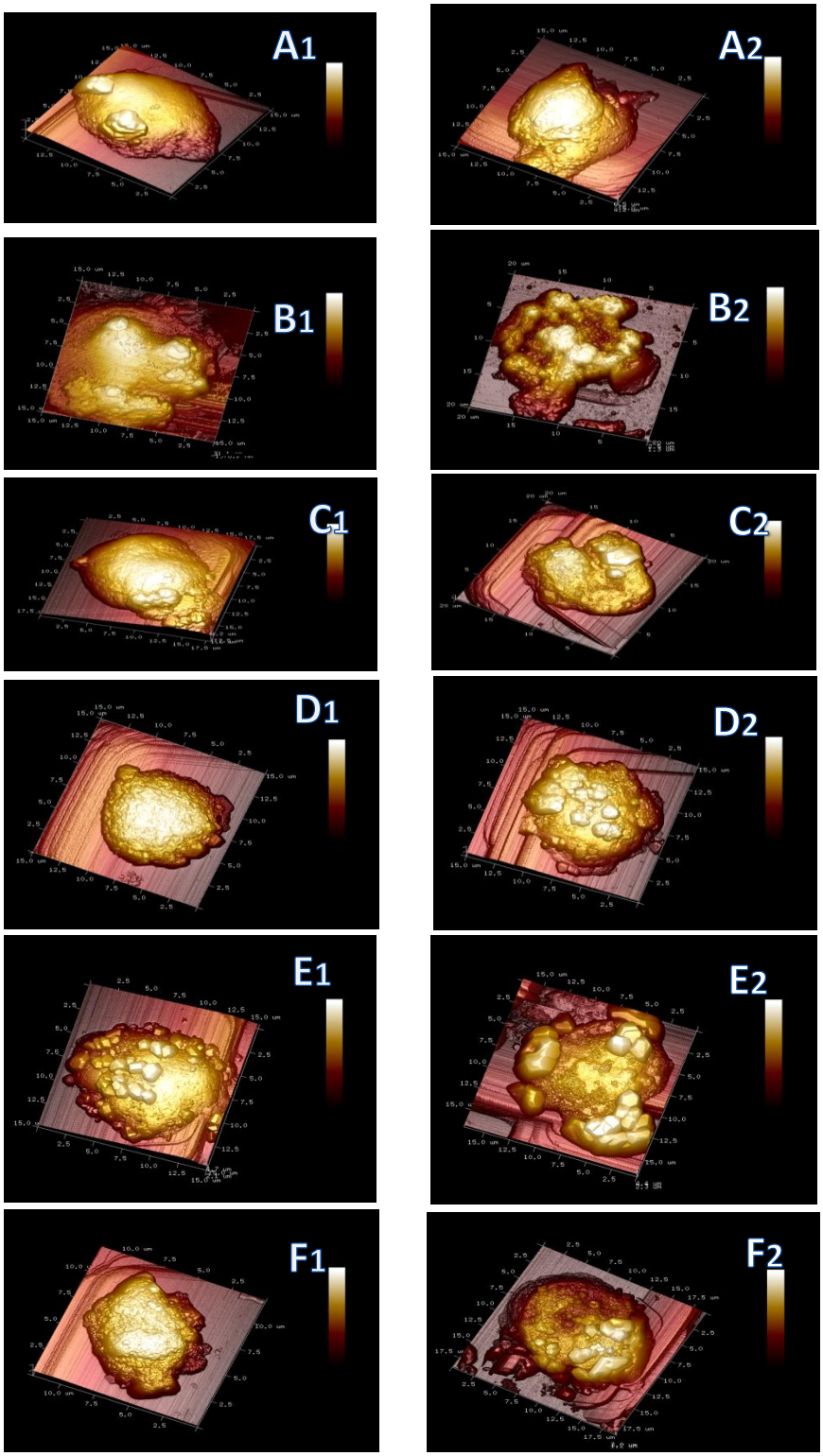

Figure 3.44. AFM image of SK-HEP-1 cells: A1) Control cells, A2) Cells with HNP-C, B)Cells with DOX,C)Cells with OXA,D)Cells with PAC,E)Cells with VINB,F)Cells with VINC. Cells incubated with drug alone (1) and with drug combination (2) for 24 h.

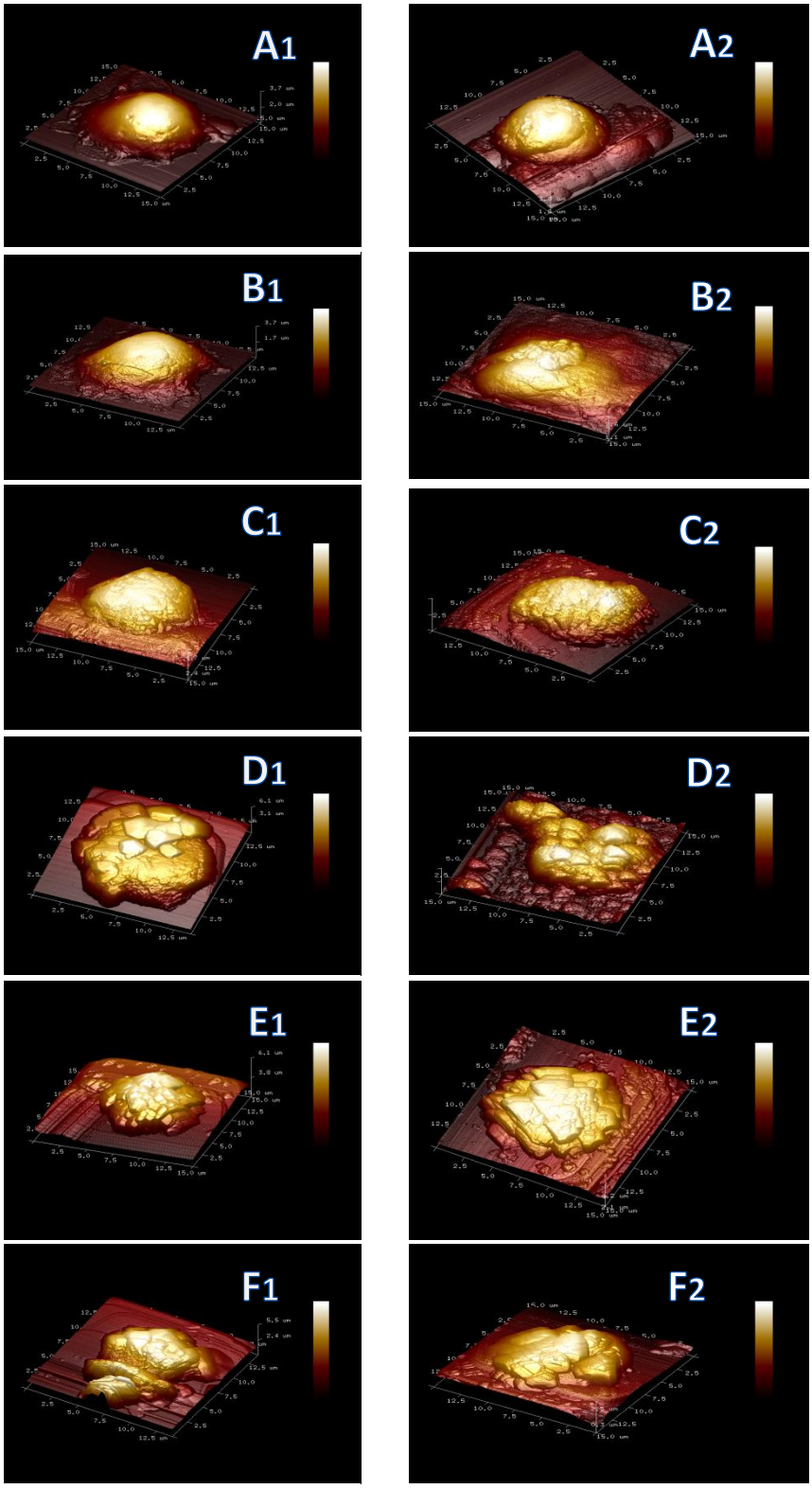

Figure 3.45. AFM image of U937 cells: A1) Control cells, A2) Cells with HNP-C, B)Cells with DOX,C)Cells with OXA,D)Cells with PAC,E)Cells with VINB,F)Cells with VINC. Cells incubated with drug alone (1) and with drug combination (2) for 24 h.

3.4. Discussion

The production of novel drug is crucial to develop with the remarkable increase in mortality rate among liver cancer suffering patients. One of these methods is concerned with targeting of pro-apoptotic protein (Cytochrome-C) towards affected cells and stimulating apoptosis. This could offer a significant increase in the efficacy of chemotherapeutic drugs by working in synergism pattern with main killing pathway of chemo drug. This successful combination can be done by understanding the mechanism of action of each component (Yamada Y. and Harashima H., 2008; Delgado *et al*. 2014).

Actually, many cancers are associated with a mutant P53 tumour suppressor pathway that is responsible for a short and inadequate chemotherapeutic drug response against cancer. Consequently, many efforts have motivated to use (Cyt-C) a vital mediator of death program with direct stimulating of intrinsic apoptosis pathway and avoiding mutant extrinsic pathway that is responsible to release Cyt-C from the mitochondrial intermembrane space (Lanni J. S. *et al*., 1997; Ryan K.M. *et al.,* 2001; Santra S.*et al.,* 2010).

The most usable method in the cancer treatment is the systemic administration of chemotherapeutic agent; with unspecific directing goal inside the body this type of treatment will experience undesirable side effects towards healthy cells. Liver cancer is usual treatment with few reported drugs such as doxorubicin, paclitaxel and sorafenibe, with effective results in only 20-25% of treated patients which unmet medical requirements. This however needs to be formulated with effective

drug delivery vehicle to overcome unspecific targeting problem of the cancer therapy (Gish RG, et al, 2007).

Targeting apoptosis is the main goal of most anticancer therapy that is participated in proper cell growth, so any disturbance in apoptosis pathways has been considered a main cause of cancer. Cancer cells are recognized to be ATP-consuming cells -which fuel by mitochondria - to nourish the highly proliferation rate of tumour cells (Dias N. and Bailly C., 2005). Therefore, this part of the cell is considered as a main goal of cancer research to understand the molecular targeting pathways of apoptosis mechanisms inside the cells. Most chemotherapeutic agents commonly activate apoptosis by releasing pro-apoptotic protein (cytochrome C) from inter mitochondrial membrane space and initiate cell death. Therefore, many efforts were made to develop mitochondrial targeting therapy to initiate the killing process (Hail N. Jr., 2005; Sharma *et al*. 2016; Ling Huang *et al*. 2017).

The delayed response to chemotherapy regime or to any inducer of cytochrome c release alone comparing to rapid response of the combination therapy has been approved to be the main activating way of apoptosis inside the mitochondria (Rajendran L. *et al*., 2010; D'Souza G.G. and Weissig V., 2009). So, the successful delivering of cytochrome C with anticancer drug to increase the potency of the active drug part in starting apoptosis is the main goal of this research.

Numerous chemotherapeutic agents have been participated in activation of apoptotic pathways upstream of the mitochondria and then joined by the intrinsic

apoptotic route. However, the mutation of many key death proteins such as P53 creates resistance to the action of the most anti-cancer drugs. So, the delivery of the effective modulator that acts directly on the downstream of apoptosis and stimulate effector caspase to produce irreversible cell death even in the presence of improper upstream function is the main reason to evade any resistance of extrinsic pathway (Amaral JD., *et al*., 2010). Activation of the caspase cascade is considered as a key step to initiate apoptosis. In this study, it proved that apoptosis stimulated through mitochondrial pathway (intrinsic apoptosis pathway) downstream of effector caspase 3 by successful targeting of cytochrome-c with iron oxide-gold hybrid nanoparticles (Malekigorji *et al.* 2014).

Pro-apoptotic protein (cyt c) is faced restricted factors to be effectively transported across cell membrane. Generally, proteins are experienced a lot of difficulties inside the body such as degradation and unstable physical and chemical features making it challenging to be used alone without developing proper delivery system to support a required dose of the drug into the cell cytoplasm and to utilize a desired healing effect (Torchilin, V., 2008).

The delivery of the cytochrome c binding to the iron oxide-gold hybrid nanoparticles are offered many features of applied the gold as the shell of the nanoparticles which can simply be decorated with different types of ligand such as cyt c. In addition, the magnetic properties of the iron oxide nanoparticles core which could be directed to the specific site in the body by applying external source of magnetic field, by this application we can get highly aggregation of the bio-

activated magnetic nanoparticles inside tumour cells (Yallapu MM *et al*. 2011; Pissuwan D. *et al*. 2006).

The biological tests of the new formulation were investigated by applying different assays such as MTT and trypan blue. These two methods are applied to detect the cytotoxicity effect of either the nano-formulation or chemotherapeutic drugs and supported with apoptotic examined methods to evaluate the effectiveness of the new formulation and to prepare the formulation to future *in vivo* studies.

The effect of HNP, CYT C and HNP-C on the viability of the hepatoma cell lines and differentiated U937 were tested by MTT and trypan blue methods with serial dilution ranged from (10 -1 μM) for both formulation respectively. A dose response curves were recorded with no noteable cytotoxicity effect of HNP and CYT-C on the cultured cell line at all incubation time points (24 h, 48 h and 72 h), which detected the biocompatibility of the applied formulation to be safely used for further *in vitro* studies. Moreover, no cytotoxic effects of HNP against pancreatic cancer (Bxpc3 cell line) (Hoskins *et al*. 2012a) and cytochrome C on liver cancer (HepG2cell line) (Malekigorji *et al.* 2014; Ling Huang *et al*. 2017) were also verified in previous studies.

The dose response studies of CYT-C hybrid formulation were constructed to investigate the apoptotic activity of this protein against liver cancer and differentiated U937 cell lines. Generally, significant IC_{50} were noticed after 72 h incubation time with cultured cancer cell lines as illustrated in the results section. In order to prove the effect of co-administration of CYT-C with experimental chemotherapeutic used in this study, the effective IC_{10} concentration of CYT-C

hybrid formulation were used with detectable serial dilutions of anti-cancer drugs which noticed to be 0.012 $mgmL^{-1}$ of loaded CYT-C and dosed the cultured cancer cells with these combination. This chosen amount of CYT-C is corresponding to 10% inhibition effect on the cell viability that represented the perfect percent to be used together with varying concentration of chemotherapeutic drugs. Previous studies were recorded the effective concentration of internalised CYCT-C and to investigate the required dose – which itself does not trigger apoptosis- which can improve the apoptotic action of a conventional chemotherapeutic drugs. In this study, the recorded IC_{10} value of loaded CYT-C was considered to be 10-100% lower than that previous reported studies (Malekigorji *et al.* 2014). By means of this combination, significant IC_{50} were verified with the most combination therapies in comparing to single drug treatment against the cultured hepatoma and U937 cell lines (as mentioned previously in results section). By this way, the efficacies of the used anti-cancer drugs are remarkably increased and the required treated dose will be decreased lower than the usual experience one with single drug treatment, confirming the synergism effect between the pro-apoptotic protein and anti-cancer drugs by targeting the main mechanism pathway of each drug and enhance its apoptotic activity.

These results were considered as a smart way for hepatocellular carcinoma treatment, since no effective chemotherapy regime was recorded with exceptional concern with surgical inoperable liver cancer types.

The apoptotic effects of delivered CYT-C were checked by several studies that concerned with enzymatic and morphological changes related to different

apoptotic stages. The relative caspase 3 activity was measured as a result of CYT-C binding to Apaf-1 and pro-caspase 9 to form apoptosome and consequently start the apoptotic signal of caspase cascade pathway (McIlwain *et al*. 2013). As illustrated previously, the combination of chemotherapeutic and hybrid formulation of CYT-C were activated 3-4 fold levels of caspase 3 in relative to single drug treatment in liver cancer cell lines. This activation is confirmed the affordable apoptotic effect of CYT-C hybrid formulation towards liver cancer cell lines. Moreover, the activation of initiator caspase (Caspase 9) and execution caspase 3 were also confirmed by targeting the CYT-C binding to hyaluronic acid against human lung adenocarcinoma (A549) cell line which results in the induction of downstream apoptosis pathway (Figueroa *et al*. 2017).

The apoptosis induction is also confirmed by protein binding visualization protocol which is known as western blot (immunoblotting technique), with concern that the most detectable cleavage nuclear protein poly (ADP-ribose) polymerase-1 (PARP) is used as a main apoptotic marker of bio-therapeutic treatment. In previous study, they examined the covalently binding of cytochrome C to antennapedia (Antp) peptide and used Hela cervical cell line as *in vitro* cultural model. Significant apoptosis marker results of immunoblotting assay were listed with cells exposed to CYT-C binding ANTP and recorded with remarkable cleavage of 116 KDa PARP-1 precursor into 89 KDa PARP-1 fragments in parallel to unaffected response against PARP-1 protein in cancer cell treated with either CYT-C or Antp alone (Imesch *et al*. 2013; Delgado *et al*. 2014; Weon Sup Shin *et al*. 2016). In this

study, remarkable bands were clearly imaged under the combination therapies channels comparing to fairly detected protein bands with single drugs treatments.

Subsequently, this confirms the previous apoptotic effect of CYT-C hybrid formulation combined with anti-cancer drugs against caspase 3 levels.

Further laboratory investigations were performed to detect the apoptotic effects of CYT-C nano-formulation and they concerned with DNA 3-OH labeling kits (TUNEL assay) which considered as one of apoptosis indicating methods. As illustrated in results section, the quantification methods of TUNEL assay were expressed as significant fold increase in the absorbance levels of combination therapy against liver cancer and U937 cell lines in parallel to the reduced spectro-absorbance of anti-cancer treated cells. Moreover, the fluorescent binding (Annexin) probes were used to detect the early stages of apoptosis by labeling the external cell membrane folding protein in apoptotic cells phosphotidylserine (PS) and to be differentiated from late apoptosis and necrotic cells that permit to fluorescent propidium iodide (PI) probes to penetrate the cell membrane. The apoptosis induction were confirmed previously in (A549) cell line when incubated with CYT-C loaded nano-formulation comparing to native loading cytochrome C and imaged under confocal microscope to visualise green fluorescent Annexin-V signal in cells underwent apoptosis and red fluorescent signal for late apoptotic cells (Figueroa *et al*. 2017). Another fluorescent study is also reported with HepG2 incubated with doxorubicin alone and binding to hollow mesoporous silica nanoparticles (HMSNs) as active drug delivery system, the last formulation is grafted with CYT-C and studied the apoptotic effect of each formulation against HepG2 cell line. The

HMSNs nanoparticles grafted with doxorubicin and CYT-C were showed significant apoptosis levels of this formulation comparing to negligible apoptotic effects with nanoparticle alone or with doxorubicin. These results are confirmed our investigation in potentiate the apoptotic killing activity of DOX- nano-formulation when binding to CYT-C in dose dependent manner (Ling Huang *et al*. 2017).

3.5. Conclusion

The results of this chapter were reflected the increasing killing abilities of chemotherapeutic therapies when co-administered with cytochrome C hybrid formulation by targeting the natural killing mechanism inside the cells and activated its pathways. Subsequent to this work further lab work were done in chapter 4 to formulate one platform therapeutic device and to check its chemical and biological effects against hepatic cancer cells.

Chapter Four

Polymer Formulation &

Characterisation

4.1. Introduction

Polymeric amphiphiles have been used as an excellent vehicle to improve the drug solubilisation in aqueous environment (Bromberg L. 2008; Branco MC. *et al.* 2009). These types of polymers have the spontaneous ability to form micelle like aggregates through hydrophobic-hydrophobic interaction once they interact with aqueous environment (Qui L. *et al*. 2007). The agricultural nature of polymeric nano-aggregate may be formed as different shaped such as copolymer (Letchford K and Burt H. 2007), star polymer (Lapienis G. 2009), dendrimers (Duncan R. and Izzo L. 2005) and graft polymer (Thompson C. *et al.* 2008). The grafting polymer is performed by water soluble backbone and then grafted with hydrophobic groups to form a comb like structure. Generally, the most usage types of hydrophilic polymer as a backbone are polyethylenimine (Cheng *et al*. 2006) and polyallylamine (Hoskins *et al.* 2011). Previous research has concerned with promising drug solubilizer agents by grafting poly (allylamine) polymer with cholesterol and dansyl moiety (Hoskins *et al.* 2012d). The hydrophobic model drugs used with this macromolecule are prednisolone, propofol and griseofulvin (Hoskins *et al.* 2012d).

The formation of single platform of polymeric amphiphiles and HNPs is served as dual function vehicle for imaging and active delivery of pharmaceutical products. Previous study is concerned with grafting of hydrophilic poly (allylamine) polymer (PAA) with 5-(4-chlorophenyl)-1,3,4-oxadiazole-2-thiol(oxadiazole, Ox) in ratio of 5% (PAA-OX) (Barnett *et al*. 2013a). The polymer grafting with oxadiazole is presented as the hydrophobic site of the micelles *via* its aromatic nature. Moreover, it offers an active binding site to HNP by possessing thiol group (SH) in

its structure and forming dative covalent bond between (SH) functional group and gold surface of HNP (Barnett *et al*. 2013b).

Paclitaxel (PTX) will be used in this chapter as hydrophobic drug model to check its water solubility behaviour after loading into PAA-HNP-C platform. This chemical compound is poor water soluble (less than 1 μgmL^{-1}) with lacking ionisable functional groups (Singla *et al*. 2002; Beijnen *et al*. 1994). The bioavailability of this compound is indicated as (< 2%) and low penetration abilities through cell membrane (increase level of P-glycoprotein) that makes the most common administration route of this drug by intravenous. The higher metabolism level of this drug is also recorded inside the body by P450 enzymes. The current trade formulation of PTX is named Taxol® and dissolved in mixture of 50 % Cremophor® EL with 50 % dehydrated ethanol (*v/v*), this solvent mixture is responsible to produce serious side effects affecting nervous and cardiac system which limits its use (Fu-Heng Yang *et al.* 2015). Moreover, Cremophor® EL is responsible to produce serious systemic haematological toxicity *via* stress based oxidative damage mechanism. For that reason, it is urgent to improve a new way to administer PTX without affecting its efficacy and to direct its action towards specific cancerous site with lower undesirable side effects (Fu-Heng Yang *et al.* 2015). In this study, PTX is encapsulated into PAA-OX5 alone and into PAA-OX5-HNP platform to check the loading percentage of hydrophobic drugs and to check its solubility improvement comparing to drug alone. *In vitro* studies in hepatocellular carcinoma (HepG2, Huh-7D and SK-hep-1) cell lines were

performed to check the cytotoxicity effect and cellular uptake of PTX alone and incorporated with PAA amphiphiles.

4.1.1 Aims and objectives

The aims of this chapter are:

- To perform synthesis and grafting of hydrophilic poly (allylamine) polymer (PAA) with 5-(4-chlorophenyl)-1,3,4-oxadiazole-2-thiol(oxadiazole, Ox).

-To increase efficacy of paclitaxel against HepG2, SK-hep-1 and Huh-7d cell lines by combining the HNP-CYT-C and paclitaxel into polymer formulation as a single platform for treatment.

-To detect the cytotoxicity effect of these new formulations using the MTT assay and to determine the cellular uptake level of paclitaxel alone and after the polymer loading formulation by HPLC.

4.2. Materials and Methods

4.2.1. Polymer preparation

PAA (2 g)(Sigma-Aldrich, UK) was dissolved in (1:1) methanol: chloroform with stirring at 37C° accompanied by the addition of (2 mL) of triethylamine drop by drop and left the reaction for 30 min. 5-(4-chlorophenyl)-1,3,4-oxadiazole-2-thiol (Oxadiazole, Ox) (0.375 g) was dissolved in 20 mL (1:1) methanol: chloroform and added drop by drop over 30 min to the previous polymer solution and left for 18 h

at 37 ° C. Next day, the solution was evaporated by reduced pressure rotary evaporating; the resultant polymer residue was washed with diethyl ether for 3 times and dried thoroughly. Then, the residue was dissolved in deionised water and dialysed by 12-14 KDa visking membrane (Medical international Ltd, UK) for 24h against deionised water. The dialysed solution was freeze-dried and further polymer structure characterisation was performed by using proton nuclear magnetic spectroscopy (^{1}H NMR, 400 MHz) at 25 °C in deuterated water (D_2O)(Bruker, UK) and functional groups spectra on a diamond tipped was obtained by attenuated total reflectance- fourier transform infrared spectroscopy (ATR-FTIR) (Nicolette IS50, Thermo-Fisher, UK).All the rest chemicals used in preparation were purchased from (Sigma-Aldrich, UK). HNP synthesis was performed as illustrated in chapter 2.

4.2.2. PAA-Ox5-HNP Conjugation and characterisation

PAA (10 mL, 5 $mgmL^{-1}$) was prepared in deionised water with probe sonication for 10min. HNPs-C (500 µl) (previously prepared in chapter 2) were added into polymer solution and sonicated for further 10 min. Nano-aggregates were formed in aqueous solution *via* probe sonication. The resultant solution was filtered using 0.22 µm syringe filters preparing to additional analysis. The critical aggregation concentration (CAC) was calculated by using a hydrophobic methyl orange UV probe following adaptation of Uchegbu's method. The stock solution of methyl orange was prepared with sodium tetraborate buffer as (25 µM, 0.02 M, pH 9.4, respectively) in deionised water. Polymer serial solutions of (0.0195 - 5 $mgmL^{-1}$)

were prepared with methyl orange solution as the diluent. After that, each prepared sample was sonicated for 5min and left to cool for another 5 min to reach room temperature. The prepared polymer solutions were measured in a UV-2600 UV-VIS(NIR) spectrometer (Shimadzu, Germany) and recorded the maximum absorbance at (350-600 nm) and the control was the stoke solution of methyl orange. The hypsochromic shift upon aggregate formation of the polymer solution wavelength maxima was determined comparing with the λ_{max} of methyl orange stock solution (463 nm).

The other method was used to detect the CAC by measuring the surface tension of the polymers which made up in aqueous solution (nine solutions, 0.0195 - 5 $mgmL^{-1}$) were prepared and sonicated for 5 min before cooling to room temperature. The surface tension of polymer solutions was measured at 25 °C using a torsion balance (OS, White Electrical Instrument Co, London). The platinum ring and platform were cleaned with ethanol and doubly distilled water prior to analysis of each sample. The measurement was conducted in triplicate for each polymer solution to obtain an average value. The surface tension of deionised water was determined between each concentration to ensure no cross contamination of samples had occurred.

TEM imaging, Photon correlation spectroscopy and Zeta potential were carried out as previously illustrated in (Chapter 2).

4.2.3. Drug Loading of Nano-aggregates

The PTX was loaded into aqueous polymer solution alone and into nano-aggregate using prob sonication with (25 mg) drug: polymer feed ratio (1:1) for 10 min. the resultant solution was filtered to remove unsolubilised PTX molecules using 0.22 µm syringe filter for further study of optimal loading concentration of PTX with both formulations. PTX concentrations standard curve were determined by preparing (10mg) serial dilution of PTX with mobile phase consisting of 55:45 (v:v) water: acetonitrile and measuring with HPLC (Perkin Elmer Flexar LC Auto sampler) the mobile phase was run at 1 mL/min and sample analysis performed at 227 nm absorbance measurements. All measurements are performed at room temperature and PTX encapsulation concentration calculated in respect to PTX standard curve. The PTX optimal formulation was analysed using Photon correlation spectroscopy, Zeta potential and TEM imaging. The formulation was also freeze-dried for NMR and ATR-FTIR spectra measurements.

4.2.4. Biological characterisation of nano-aggregates and formulation

4.2.4.1. Cell viability assay (MTT)

96 well plates were used to seed 15,000 cells with 100µL of media per well for each cell lines and allowed to adhere overnight (24 h) in humidified incubator at 37% in 5% CO_2 atmosphere. Serial dilutions of Paclitaxel (100-1nanomole) alone and in combination with active IC_{10} value of CYT-C combination in PAA-Ox5-HNP-C formulation (0.012 $mgmL^{-1}$) (as illustrated in Chapter 3) was added to the 96-

wells of HepG2,SK-hep-1 and Huh-7d cell lines and incubated for (24 h, 48 h and 72 h). At these three times vital dye (yellow MTT 3-(4,5-dimethyl-2-thiazolyl)-2,5-diphenyl-2H-tetrazolium bromide) was used to detect the number of live cells which reflecting the cytotoxicity effect for anticancer drug alone and with formulation.

For each time points (24 h,48 h and 72 h) removed the serial drugs solution from treated cells and add 100 µL of MTT sterilized solution, put in the incubator for 3-4 h to permit the reduction of Tetrazolium dye by oxido-reductase mitochondrial enzyme referring to the metabolic activity of the live cells forming insoluble formazan crystal then removed the MTT solution and replaced by 100 µL of DMSO to form colorimetric solution optical densities were measured in microplate reader(Tecan Infinite, Austria) at 570 nm. The percentage of cell viability was calculated relative to the absorbance of untreated cells and PBS as (positive and negative control, respectively).

4.2.4.2. Cellular uptake of PTX

Liver cell lines were seeded in 6 well plates (50,000 cells /well) and incubated for 24 h at 37 °C with 5% CO_2.Next day the media was replaced by100 µL (50 $\mu g mL^{-1}$) of PTX concentration (in PAA-Ox5-HNP-C formulation comparing to free drug) per well and incubated for 4 h. After incubation period the media was removed and the treated cells were washed with PBS preparing to detach by trypsin adding to each well. The suspension cells in 1 mL fresh media were counted by automated

cell counter (Invitrogen countess, UK) to transfer 100,000 cells of each cell line into Eppendorf tubes and centrifuged for 5 min at (250 g). The resultant supernatant was removed and the precipitated pellets were resuspended with 1 mL of sterilised water and vortex for 30 seconds. The concentration of PTX alone and in combination PAA-Ox5-HNP-C were measured at 227 nm using HPLC (Perkin Elmer Flexar LC Autosampler) and analysed per cell by T-Test analysis within the Microsoft Excel® software package.

4.3. Results

4.3.1. Synthesis and Characterisation of PAA-Ox5

The fabrication of PAA-Ox5 polymers were performed by simple substitution of the primary amines in the parent PAA structure and the chloride functional group of the oxadiazole compound. The spectra of ^{1}H NMR spectroscopy was detected the successful steps of polymer synthesis (Figure 4.1.). The showed peaks at δ0.75, δ 2.50, δ 3.00, δ1.40 and δ 1.50 can be attributed to the CH_2 and CH groups in the homopolymer backbone, respectively.

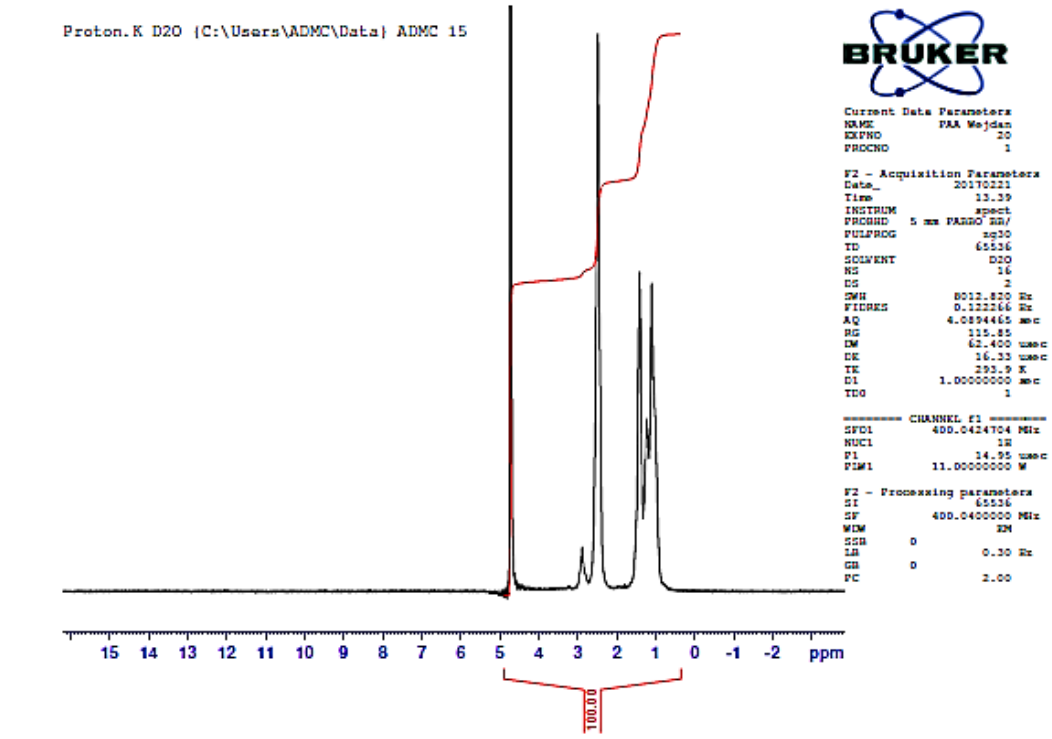

Figure 4.1. The spectra of ^{1}H NMR spectroscopy of PAA polymer structure carried out on 400MHz NMR at 25 °C.

More peaks were observed at δ7.25-7.75 when fabricated PAA-Ox5 polymers were analysed and it detected the aromatic CH groups present in the oxadiazole pendant group (Figure 4.2.). The proton on the –SH group of the oxadiazole pendant was not detected on this spectra; this is likely to be due to rapid exchange between the thiol and D_2O solvent.

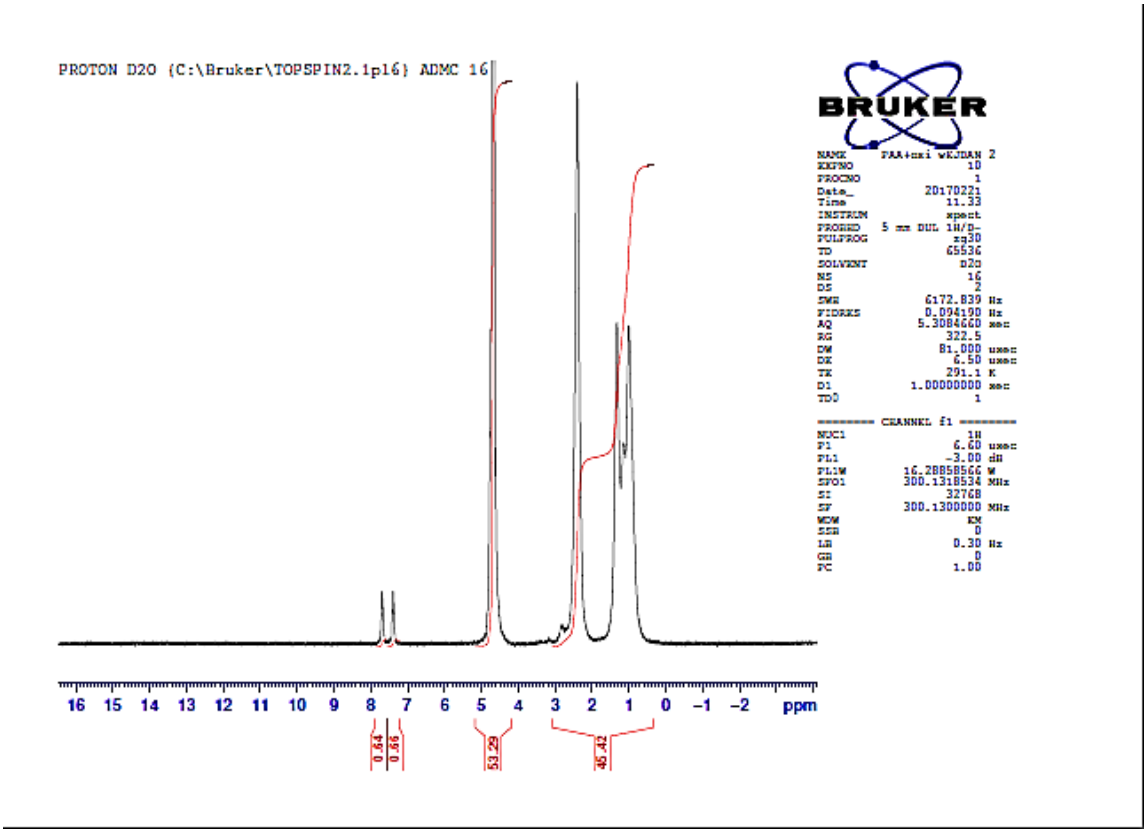

Figure 4.2. The spectra of ^{1}H NMR spectroscopy of fabricated PAA-Ox_5 polymer structure carried out on 400MHz NMR at 25 °C.

4.3.1.1. FTIR

FTIR analysis of the PAA-Ox_5 amphiphile was run between 4000 – 650 cm^{-1} to detect the specific functional groups existing (Figure 4.3.). Here, characteristic peaks were observed at 3273 cm^{-1} and 2846 cm^{-1} which result from the N-H stretching and C-H stretching in the PAA backbone, respectively. An additional peak at 1597 cm^{-1} was observed and indicated that hydrophobic pendant group attachment had been successful as a result of this peak the bending and stretching vibrations of the aromatic ring C=C present in the oxadiazole structure.

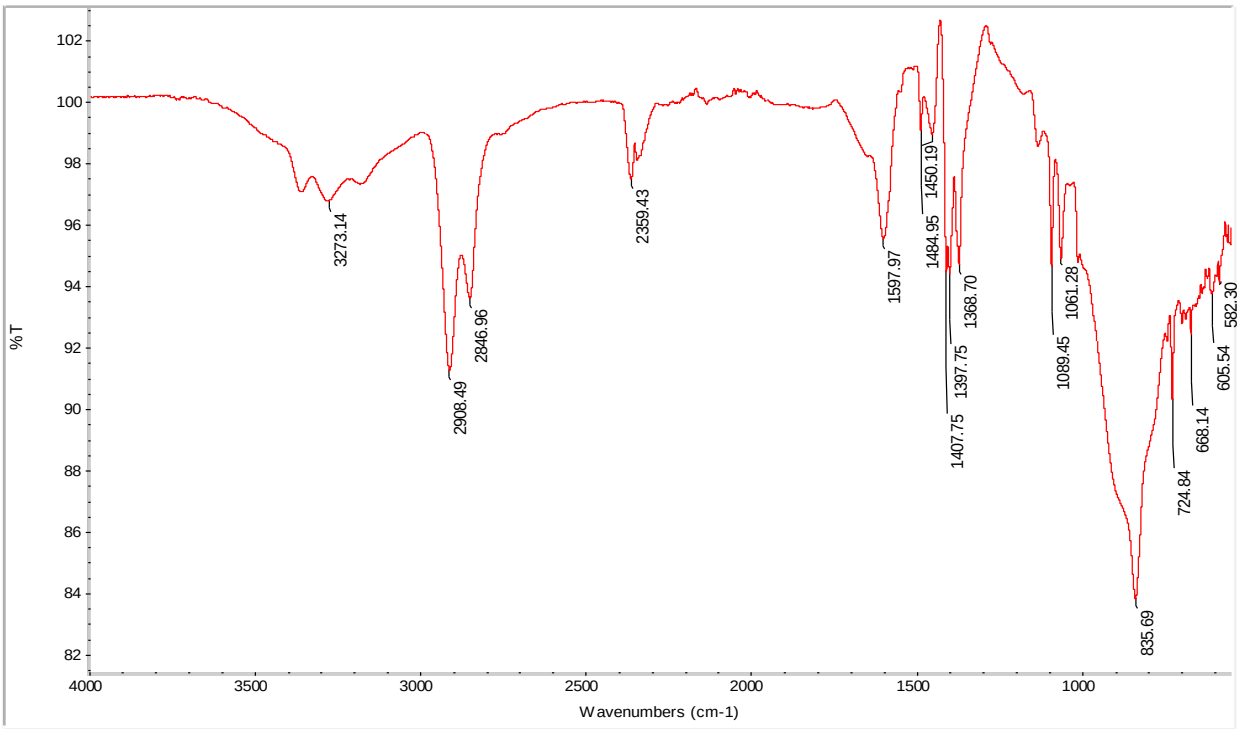

Figure 4.3.FTIR spectra of PAA-Ox5 using diamond tripped ATR-FTIR (64scan).

4.3.1.2. Methyl orange

The CAC was determined for the amphiphiles using a hydrophobic methyl orange UV probe. Here, a hypsochromic shift was not observed in the λ_{max} values for absorbance in the UV spectra (Figure 4.4.). At higher concentrations an increase in λ_{max} was observed but this is likely to be due to the translucent nature of the concentrated sample interfering with absorbance measurement. As such the CAC was determined using a different measurement via surface tension.

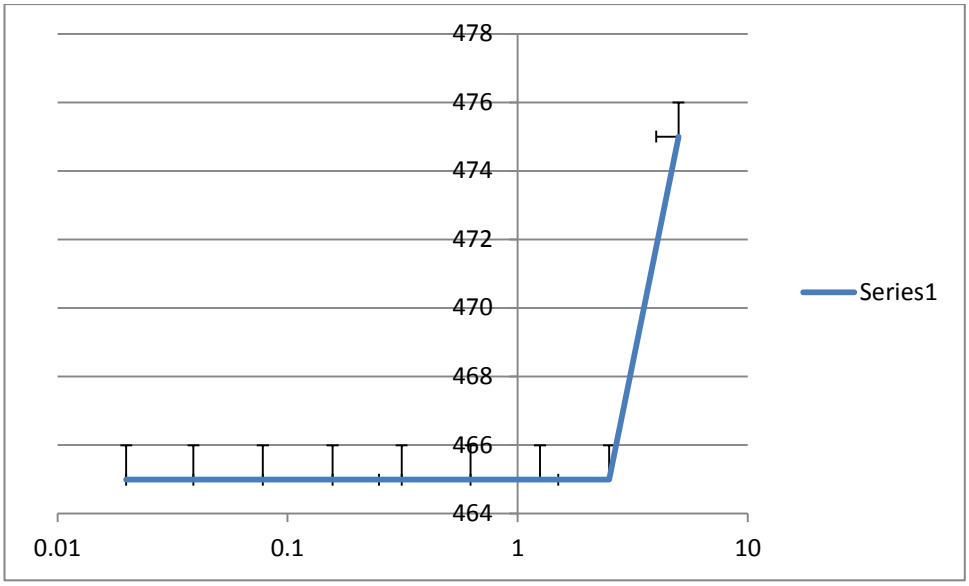

Figure 4.4. Methyl orange CMC measurement

4.3.1.3. Surface tension (N/M)

The surface tension for the PAA amphiphiles both with and without incorporation of HNPs was determined. The surface tension of water is 0.072 N/m. As the nano-aggregates form, they cause a change in surface tension of the aqueous media due to the surface layer becoming saturated forcing the amphiphiles into the bulk and hence aggregation occurs. The CAC is a measure of how stable the aggregates are in solution and give an indication of whether they will undergo breakdown after dilution. The data from this test (Figure 4.5.) shows that the CAC for the PAA-Ox5 was 0.313 $mgmL^{-1}$ whereas; the HNP containing amphiphile was 0.039 $mgmL^{-1}$. This suggested that the aggregates formed at lower concentration

when the magnetic HNPs were incorporated in the structure. The reason for this is not known, however, it may be possible that the magnetic attractive forces being stronger than the intermolecular forces and hence drive forward aggregation.

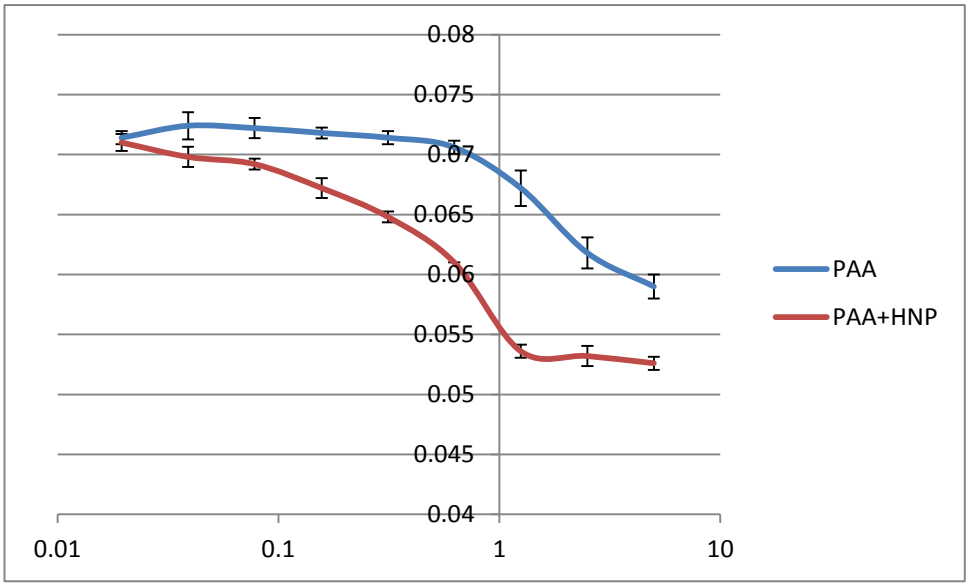

Figure 4.5. Surface tension (N/M) of PAA-Ox5 and PAA-Ox5-HNP.

4.3.2. Characterisation of PAA-Ox5 and PAA-Ox5-HNP Nano-aggregates

The formations of nano-aggregates were achieved by probe sonication of the PAA in deionised water. Variable techniques were used to characterise the formulation synthesis steps which concern with size and zeta potential measuring by PCS and TEM. TEM imaging were showed the PAA-Ox5 micelles structure with approximately (50 nm) diameter which smaller value comparing to PCS value that showed (88 nm). These differences are due to the different measurement techniques between the TEM and PCS as illustrated before in HNPs synthesis

chapter (Chapter 2). The poly dispersity index of the PAA-Ox5 was (0.55) indicating that the mono-dispersity of nano-aggregates were not exist for long time. PAA-Ox5 zeta potential was also measured and showed (+ 38 mV), this high value is due to the presence of function amine groups to PAA backbone.

HNP was conjugated with PAA-Ox5 through dative covalent linkage between the gold surfaces of HNP and the thiol functional group of oxadiazole pendant group in PAA-Ox5. It is supposed that only one thiol group was attached to one HNP contributing to low concentration of HNP used in conjugation and to the steric hindrance effect. HNP attachment to PAA-Ox5 was confirmed by TEM images which observed as dark condense parts within nano-aggregate (Figure 4.6.B) owing to randomly attachment of HNP onto oxadiazole pendant to form PAA-Ox5-HNP.

The zeta potential value of PAA-Ox5-HNP (17 mV) was showed a sharp decrease value comparing to nano-aggregate surface charge. This change is possibly contributing to HNPs incorporation detecting to the PCS during aggregate formation and to dynamic equilibrium effect.

Remarkable increases in PAA-Ox5-HNP particles size were recorded as PCS measurements (186nm) and with TEM instrument as (100 nm). These big variations are contributing to HNPs conjugation that inhibits the compact aggregate due to steric hindrance. Moreover, significant decrease in PDI values from 0.55 to 0.137 for PAA-Ox5 and PAA-Ox5-HNP, respectively were also observed during measurements and may contribute to the steric hindrance effect of conjugated HNPs that increase the intramolecular aggregate formation in

parallel to low levels of larger intermolecular aggregate which results in less compact PAA-Ox 5-HNP aggregates formation.

TEM images showed clear structure of PAA-Ox5 (Figure 4.6.A) comparing to condensed unclear ones with PAA-Ox5-HNP TEM (Figure 4.6.B). Probably due to the cluster formation of the PAA-Ox5-HNP by inherent magnetic effects of HNP during the TEM grid drying time before the complete water droplet drying, this phenomenon is familiar with variety of magnetic nano-material organising to be imaged by TEM.

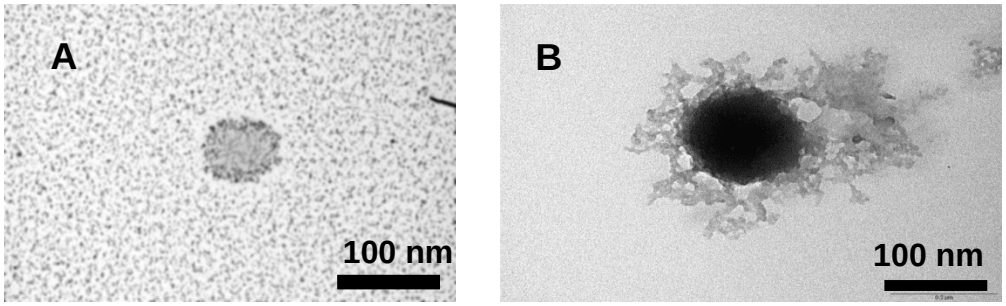

Figure 4.6.TEM images A) PAA-Ox5 and B) PAA-Ox5-HNP nano-aggregates.

4.3.3. PTX loading into nano-aggregates

The PTX was incorporated into PAA nano-aggregate *via* hydrophobic-hydrophobic interaction. Polymer concentration to drug ratio was used is (1:1) by loaded 25 mg of PTX into 5 mg (5 $mgmL^{-1}$) of aqueous PAA nano-aggregate solution. Interestingly, the PAA-Ox5-HNP nanoparticles presented with higher encapsulation ability of PTX (0.684 $mgmL^{-1}$) into their hydrophobic core comparing to (0.598 $mgmL^{-1}$) of PTX into PAA-OX5 nano-aggregate; this may possibly happen due to the nature of PAA-Ox5-HNP which characterised as less compact aggregate that accommodate a larger amount of PTX molecules The aqueous solubility of PTX was increased 700-fold and 600-fold with the PAA-Ox5 and PAA-Ox5-HNP aggregates, respectively.

4.3.4. Biological characterisation of drug nano-aggregates

The cytotoxicity of the PTX-PAA amphiphiles on liver cancer cell lines was detected *via* MTT assay (Figure 4.7.). Serial dilutions of Paclitaxel (100-1 nM) alone and in combination with active IC_{10} value of CYT-C combination in PAA-Ox5-HNP-C formulation (0.012 $mgmL^{-1}$) (as illustrated in Chapter 3) was added to the 96-wells of HepG2,SK-hep-1,Huh-7d and U937 cell lines and incubated for (24 h, 48 h and 72 h). At these three times vital dye (yellow MTT 3-(4,5-dimethyl-2-thiazolyl)-2,5-diphenyl-2H-tetrazolium bromide) was used to detect the number of live cells which reflecting the cytotoxicity effect (IC_{50}) for anticancer drug alone and with formulation. After 24 h incubation time with PTX-PAA amphiphiles significant

IC_{50} was determined on HepG2 at (50 nM and 40 nM) of PAA-Ox5 and PAA-Ox5-HNP-C formulation comparing to the IC_{50} of PTX alone, respectively.

Through increasing incubation time to 48 h also significant IC_{50} of PAA-Ox5 and PAA-Ox5-HNP-C formulation was detected as 1.99 nM and 0.8 nM in parallel to the cytotoxic concentration of PTX alone, respectively. Moreover, 72 h incubation period was showed 31-fold and 43-fold decreased in IC_{50} of PAA-Ox5 and PAA-Ox5-HNP-C formulation compared to free drug cytotoxicity.

The cytotoxicity results of PTX against Huh-7D cell line (Figure 4.7.) were showed significant IC_{50} (53nM and 11nM) of PAA-Ox_5 and PAA-Ox_5-HNP-C formulation after 24 h comparing to the IC_{50} with PTX alone. Both 48 h and 72 h incubation times were determined with 8-fold and 10-fold increase in cytotoxicity with PAA-Ox5 formulation comparing to PTX alone at each time, respectively. Besides to remarkable increase in PAA-Ox5-HNP-C formulation cytotoxicity which determined as 15.7-fold and 33-fold decrease in IC_{50} after 48 h and 72 h comparing to PTX alone at each time, respectively.

SK-hep-1 cell line was showed no significant response to PTX alone and to PAA-Ox5-HNP-C formulation after 24 h and 48 h incubation time with one significant exception result was recorded with PAA-Ox5-HNP-C formulation after 48 h incubation time and determined as (84.27 nM). However, significant IC_{50} of both PAA-Ox5 and PAA-Ox5 polymer formulation was determine after 72 h incubation time and recorded as (73.32 nM and 57.39 nM) corresponding to undetected IC_{50} value with PTX alone, respectively.

Table 4-1.IC_{50} values of (Paclitaxel ,PTX+ PAA-Ox5 and PTX+ PAA-Ox5 –HNP-C) on HepG2 ,Huh-7D and SK-hep-1 cell lines achieved by MTT assay. Significant increase in the cytotoxicity was calculated by comparing with single drug treatment (n=3, aver ±SD).

HepG2 cell line	**Drug alone**	**PTX+PAA-Ox5**	**PTX+PAA-Ox5-HNP-C**
Paclitaxel			
24 h	NS	50±3.05 nM	40±1.5nM
Increase in cytotoxicity		Significant IC_{50}	Significant IC_{50}
48 h	NS	1.99±0.7 nM	0.98±1.3 nM
Increase in cytotoxicity	-	Significant IC_{50}	Significant IC_{50}
72 h	32±4.84 nM	1 nM	0.7 nM
Increase in cytotoxicity	-	31-fold	43-fold
Huh-7D cell line			
24 h	NS	53 ±1.52 nM	11±2.5 nM
Increase in cytotoxicity	-	Significant IC_{50}	Significant IC_{50}
48 h	37±1.05 µM	4±2.61 nM	2.21±1.82 nM
Increase in cytotoxicity	-	8-fold	15.7-fold
72 h	31±1.12 µM	3±2.5 nM	0.9±2.1 nM
Increase in cytotoxicity	-	10-fold	33-fold
SK-hep-1 cell line			
24 h	NS	NS	NS
Increase in cytotoxicity	-	-	
48 h	NS	NS	84.27±3.1nM
Increase in cytotoxicity		-	Significant IC_{50}
72 h	NS	73.32±1.54 nM	57.39±4.02nM
Increase in cytotoxicity		Significant IC_{50}	Significant IC_{50}

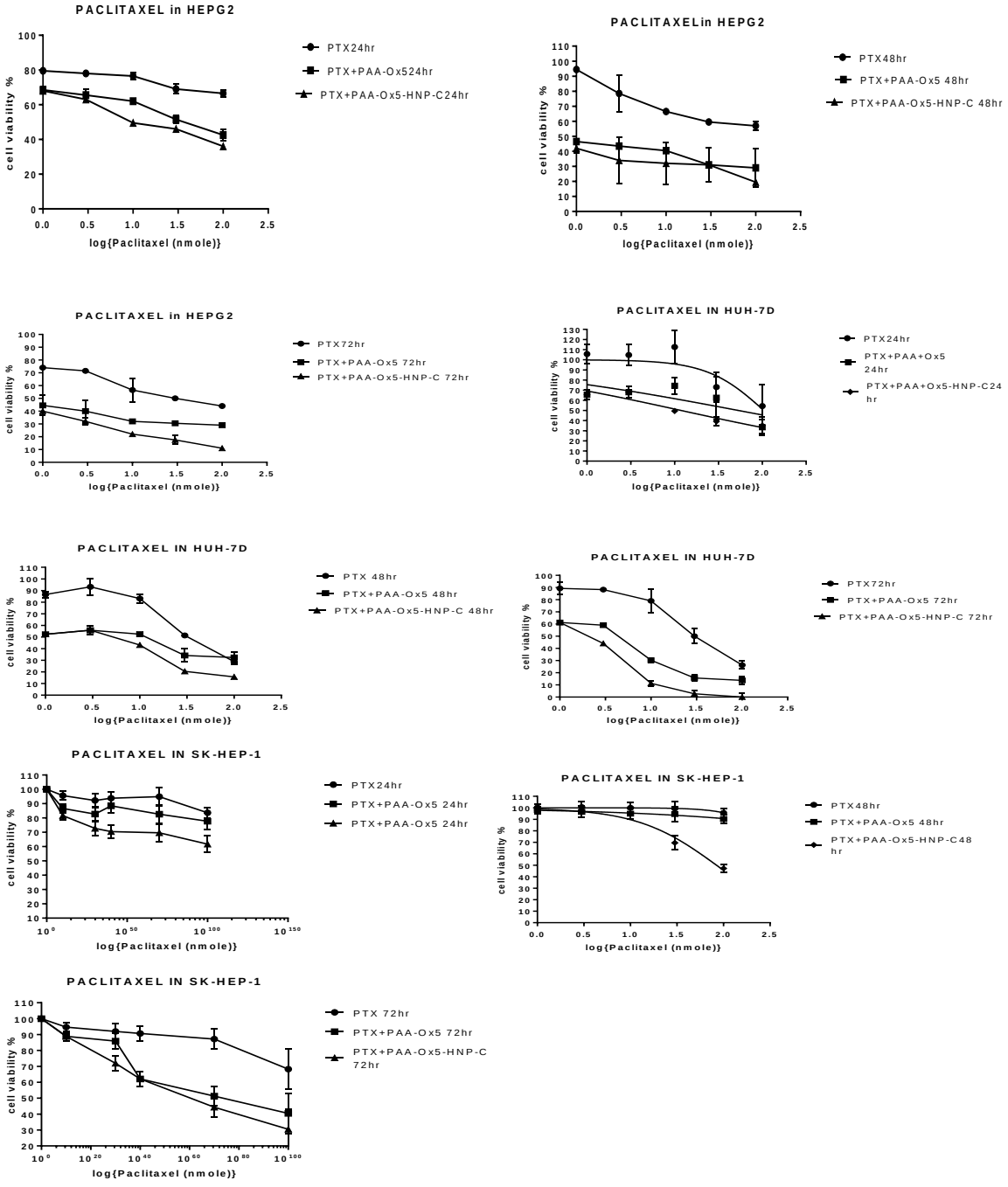

Figure 4.7. Dose response curve of (Paclitaxel ,PTX+ PAA-Ox5 and PTX+ PAA-Ox5 –HNP-C)on HepG2 ,Huh-7D and SK-hep-1 cell lines of three independent experiments after 24 h,48 h and 72 h incubation time, the x-axis represent the serial dilutions of the drug and the y-axis represent the absorbance of MTT formazan crystalline which indicate the % of cell viability.

PTX uptake studies were carried out with liver cancer cell lines (Fig.8) and the drug concentration was quantified per cell. After 4 h incubation time with 50 µgmL^{-1}of PTX alone and with PAA-Ox5 formulation, 145-fold more drug uptake by the HepG2 cell comparing to free drug. Moreover, 174-fold more PTX concentration was founded inside the cancerous cell incubated with PAA-Ox5-HNP-C formulation. Huh-7D uptake studies are also showed significant PTX uptake level inside the cell with both formulation and determined as (134-fold and 156-fold) with PAA-Ox5 and PAA-Ox5-HNP-C formulations, respectively. Interestingly, remarkable increase in PTX level were also observed when incubated with SK-hep-1 cells and resulted in significant (99-fold and 124-fold) increase in cellular uptake level comparing to free drug with both PAA-Ox5 and PAA-Ox5-HNP-C formulations

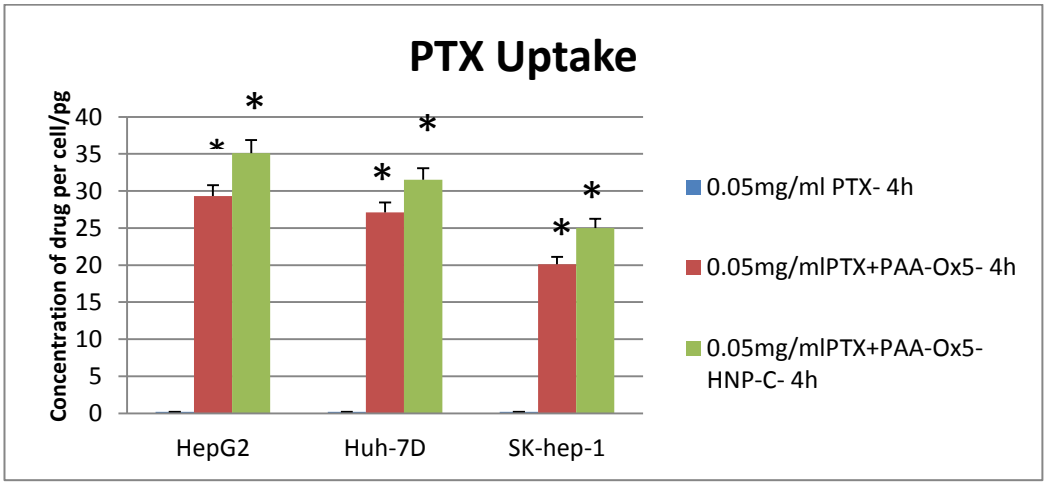

Figure 4.8.PTX uptake study on A)HepG2 ,B)Huh-7D and C)SK-hep-1 cell lines after 4h incubation time with 50 µgmL^{-1} concentration of PTX and PAA-OX5 and PAA-OX5-HNP-C formulations,* indicate the significant increase in drug uptake between free drug and formulation (n=3 ,average±SD). The t-test analysis is performed by Microsoft Excel software.

4.4. Discussion

Over the past decade the study of emerging bi-functional platform as active drug delivery vehicles has been extensively studied (Barnett *et al*. 2013a). One of the interesting emerging designs is Incorporation of HNPs with PAA-OX5 amphiphilic polymer that serves as active way in therapeutic imaging and drug delivery(Barnett *et al*. 2013a). In this chapter the potential of metallic amphiphilic polymer function was used as drug carrier with ability of incorporation of specific bio-particle to the surfaces of HNP. As studied previously with the binding of CYT-C as dative covalent bond to gold surfaces (Malekigorji *et al*., 2014).

The HNPs were incorporated into PAA-OX5 polymer *via* dative covalent bonding between the gold surfaces and thiol function group of the oxadiazole pendant group. Several techniques were used to characterise the synthesis steps of polymer and HNP binding by ^{1}H NMR, FTIR, TEM and Zeta potential measurements as illustrated in results section. PTX incorporation mechanism with PAA-OX5-HNP-C was carried out by exploiting hydrophobic drug encapsulated into hydrophobic core of amphiphilic polymer. Here, PTX molecule was used to investigate the optimal improvement of hydrophobic drug hydro-solubilisation by preparing drug: polymer feed ratio (1:1). The encapsulation concentration results were showed (0.684 $mgmL^{-1}$) of PTX into PAA-Ox5-HNP-C hydrophobic core comparing to (0.598 $mgmL^{-1}$) of PTX into PAA-OX5 nano-aggregate; this may be due to the nature of PAA-Ox5-HNP which characterised as less compact aggregate that accommodate a larger amount of PTX molecules (Table 4-1). The aqueous solubility of PTX was increased 700-fold and 600-fold with the PAA-Ox5

and PAA-Ox5-HNP aggregates, respectively. These results are agreements with previous studies of the propofol and griseofulvin loading drugs into PAA-Ox5 alone and with nano-aggregate, these loading procedure were improved the aqueous solubility of propofol and griseofulvin by 137-fold and 53-fold increase for both drugs, respectively. Moreover, the loading capacities of nano-aggregates were presented with higher solubility levels of propofol and griseofulvin by 250-fold and 56-fold increase, respectively (Barnett *et al*. 2013a)

The cytotoxicity of paclitaxel was evaluated on HepG2, Huh-7D and SK-hep-1 cell lines alone and in co-corporation with PAA-Ox5 and nano-aggregates. After 24 h and 48 h incubation on HepG2, no significant IC_{50} ($p>0.05$) was detected in the MTT assay with PTX alone, while significant IC_{50} ($p<0.05$) were detected as (50±3.05 nM ; 40±1.5nM ,at 24 h) and (1.99±0.7 nM; 0.98±1.3 nM, at 48 h) with both PTX- PAA-Ox5 and nano-aggregates, respectively. Increasing incubation time of treatment to 72 h resulted in a 31-fold and 43-fold decrease in IC_{50} was observed in those cells treated with PTX-PAA-Ox5 and nano-aggregates respectively (Figure 4.7.) comparing to PTX treated cells. These significant increases in PTX amphiphilic polymer and nano-aggregate cytotoxicity are approved with increasing the potency of this hydrophobic drug by increasing the uptake levels through the cell membrane and enhancing the aqueous solubility of PTX. These results are in agreement with previous results of improving the cytotoxicity of propofol and griseofulvin on BXPC-3 pancreatic cell line after their incorporation with PAA-Ox5 and nano-aggregates (Barnett *et al*. 2013a).

The cytotoxicity of PTX was tested in Huh-7D cells, after 24 h a significant decrease in IC_{50} was observed with (PTX+ PAA-Ox5 and PTX+ PAA-Ox5 –HNP-C). Further increase in cytotoxic effect was observed after 48 h and 72 h incubation. PTX encapsulation resulted in a 8-fold and 15.7-fold decrease in IC_{50} after 48 h (PAA-Ox5 and PAA-Ox5 –HNP-C, respectively). A significant increase in the cytotoxicity was observed in those cells treated with PTX after 72 h., and showed a significant (10-fold and 33-fold) reduction in IC50 value with (PTX-PAA-Ox5 and PTX-PAA-Ox5 –HNP-C, respectively) compared to single drug treatment after 48 h and 72 h.

As illustrated in (Chapter 3) The SK-hep-1 cell line showed a different behaviour against chemotherapeutic drugs compared to the other cell lines tested. Hence, the highly resistance nature of these cell lines against PTX resulted in no IC_{50} values when incubated at all-time points incubation tested. However, remarkable changes were observed with PTX+ PAA-Ox5 and PTX+ PAA-Ox5 –HNP-C formulation which showed significant increase in cytotoxicity of these formulation after 48 h and 72 h incubation period. These results are confirmed the activity of a PTX-PAA amphiphiles polymer in increasing the aqueous solubility of PTX and increasing the uptake level by the highly resistance SK-hep-1 cell line. The cytotoxicity results are showed highly increasing levels of the nano-aggregate cytotoxicity comparing to PTX-PAA amphiphiles polymer as shown in all incubated liver cancer cell line which confirmed the potential activity of CYT-C protein in PTX+ PAA-Ox5 –HNP-C formulation to increase the potency of PTX and increasing its cytotoxicity against liver cancer cell line.

PTX uptake studies were also showed significant increase in drug uptake level when encapsulated with 50 μgmL^{-1} of PTX-PAA amphiphiles polymer and nano-aggregate after 4 h incubation comparing to cell incubated with free drug. This investigation is in agreement with previous studies of 6-TG conjugate to the surfaces of HNP (Barnett *et al*. 2013b) which showed 10-fold decrease in IC_{50} when compared with free drug cytotoxicity. Moreover, the increasing uptake level of CYT-C protein levels inside liver cancer cell lines (Chapter 2) when conjugated to gold surfaces of HNP in parallel to negligible level of free protein inside the cancer cells.

4.5 Conclusion

The work in this chapter highlights the potential benefit from formulating the HNP-CYT-C and PTX into one single platform for co-administration. These exciting findings require further investigation but hold great potential as a future therapy for liver cancer patients.

Chapter Five

General Conclusions &Future Work

5.1. General Conclusions

This research focused on testing five different chemotherapeutic agents in combination with HNP-c for liver cancer treatment. The data consistently showed that on HepG2, Huh-7D and U937 cells, there was a synergistic effect with combined therapy resulting in greater apoptosis and increase in cytotoxicity compared to the drug alone. The cytotoxicity assays showed that the lower IC_{50} values were obtained using the anti-microtubule drugs (paclitaxel, vinblastine and vincristine) compared to the DNA damaging drugs (doxorubicin and oxaliplatin). The third cell line tested (SK-hep-1 cells) demonstrated resistant behavior against treatment with exceptionally significant results observed with DNA damage drugs, doxorubicin in both treatment regimes. The data offered the hypothesis that, by introducing the cytochrome C into the liver cancer cells and co-administering with anticancer agents, a synergistic effect will occur, resulting in increased apoptotic levels and cellular death. These findings indicate that clinical use of cytochrome C in parallel with clinically used anticancer agents may result in more positive patient outcome and novel low cost therapy.

In order to push this formulation forward, it is important to combine HNP-C and chemotherapeutic agents in single supramolecular device to be used clinically as single therapeutic agent with multifunctional components. Unfortunately, most anticancer drugs are hydrophobic with impossible binding ability to HNP-C. Therefore, a new formulation has been designed to improve the cytochrome –c nano-formulation.

A single device treatment was designed by combining HNP-C and PTX together with PAA polymer. Here I fabricated an amphiphilic poly(allylamine) derivative grafted with oxadiazole groups (PAA-Ox5). The thiol functionality in the oxadiazole groups allowed for irreversible conjugation of the HNP-CYT-C constructs into the integral polymer structure, whilst the PTX was encapsulated into core-shell polymeric aggregate formed *via* hybrophobic-hydrophobic interactions. The PAA-Ox5-HNP nanoparticles offered higher encapsulation ability of PTX (0.684 $mgmL^{-1}$) comparing to (0.598 $mgmL^{-1}$) of PTX into PAA-OX5 nano-aggregate; this may contribute to the less compact aggregate nature of PAA-Ox5-HNP that capsulate larger amount of PTX molecules. In addition to remarkable aqueous solubility of PTX was increasing to 700-fold and 600-fold with the PAA-Ox5 and PAA-Ox5-HNP aggregates, respectively.

Cell viability studies were performed in order to check whether this supramolecular formulation was useful in the fight against liver cancer. Here, measuring PTX cellular uptake levels and cytotoxicity effect of PTX against (HepG2, Huh-7D and SK-hep-1) and differentiated U937 cell lines. After 24 h and 48 h incubation in HepG2, no significant IC50 ($p>0.05$) was detected in the MTT assay with PTX alone, while significant IC50 ($p<0.05$) were detected as (50±3.05 nM ; 40±1.5nM ,at 24 h) and (1.99±0.7 nM; 0.98±1.3 nM, at 48 h) with both PTX- PAA-Ox5 and nano-aggregates, respectively. Increasing incubation time to 72 h resulted in a 31-fold and 43-fold decrease in IC_{50} was observed in those cells treated with PTX-PAA-Ox5 and nano-aggregates, respectively. These results showed the remarkable cytotoxicity effect of PTX increasing against HepG2 cell line at 24 h

incubation time compared to non-significant IC_{50} recorded when co-administered with HNP-C. Moreover, Huh-7D12 cell line responded significantly to PTX-PAA-Ox5 and nano-aggregates with decreasing IC_{50} values (increasing cytotoxicity) of PTX treated cells starting from 24hr treated time and recorded as (53 nM ,11nM) for PTX-PAA-Ox5 and nano-aggregates, respectively. The PTX combination therapy with HNP-C that was used in Chapter 3 showed no IC_{50} values after 24 h treatment; these results confirmed the increasing potency of PTX after its encapsulation with PAA-Ox5 and nano-aggregates with increasing the uptake and solubility levels of PTX.

Other reported studies also confirmed the activities of other types of nano-formulation in targeting and killing the hepatocellular carcinoma such as PEGylated liposomes composed of distearoylphosphatidylcholine(WU *et al.* 2018) against SK-hep-1 cell line and hollow mesoporous silica nanoparticles (HMSNs) hosted with CYT-C against Hep-G2cell line (Ling Huang *et al*. 2017)

5.2. Future work

Regardless of all the advantages of nanoparticles, there is always a chance for additional improvements in this field. For example, polymer formulation was only tested with selected cytotoxicity assays and it would be useful to investigate this novel formulation further using flow cytometry, western blot and apoptotic assays to track the different stages of apoptosis. Furthermore, this formulation needs to be applied to primary cell lines with highly differentiated types of cells in

preparation for this formulation to be used in vivo studies, and to check its cytotoxic effect against animal models such as mice. The work in this thesis has shown that a nano-formulation using a combined strategy for treatment of liver cancer has resulted in optimal therapeutic effects. Following on from these studies, *in vivo* trials are required. These will be carried out in xenograft mouse models in order to determine whether the *in vitro* effect being observed translates into *in vivo* success. Other reported *in vivo* studies also confirmed the activities of other types of nanoparticles such as Silica nanoparticles (SiNPs) (Wai-Tao *et al.* 2017), Silicon dioxide (silica) nanoparticles (SDNPs) against hepatic cancer (Almansour *et al*. 2018) and Hybrid iron oxide–gold against pancreatic cancer (Oluwasamni *et al.* 2016).Nanoparticles (HNPs) are tested via intravenous and subcutaneous administration in mice and tracked the pharmacokinetic and pharmacodynamics behaviour of these nanoparticles. The rate of accumulation and clearance of the particles are also tested and the size of each treated cancer checked before and after nano-therapy.

It is postulated that in fact, greater tumour retardation will be experienced *in vivo* compared with only drug treatment, however, the ability to either eradicate tumour regrowth or indeed totally eliminate liver cancer requires full investigation.

References

References

Ackerson CJ, *et al*. (2010). Synthesis and bioconjugation of 2 and 3 nm-diameter gold nanoparticles. Bioconjug Chem.;21:214–218.

Adams, J.M., Cory, S. (2007). The Bcl-2 apoptotic switch in cancer development and therapy. *Oncogene* 26 (9):1324–1337.

Agarwal, M. L., Taylor, W. R., Chernov, M. V., Chernova, O. B., and Stark, G. R. (1998). Stabilization and activation of p53 are regulated independently by different phosphorylation events. *J Biol Chem.* 273, 1–4.

Albanese A, Chan WCW. (2011). Effect of Gold Nanoparticle Aggregation on Cell Uptake and Toxicity. ACS Nano.;5:5478–5489.

Alison, M.R. (2005). Liver stem cells: implications for hepatocarcinogenesis. *Stem Cell Rev*. 1(3):253-260.

Amaral JD, Xavier JM, Steer CJ, Rodrigues CM. (2010). the role of p53 in apoptosis, Discov Med.;9(45):145-52.

Ambudkar, S.V., Dey, S., Hrycyna, C.A. (1999).Biochemical, cellular and pharmacologicalaspects of the multidrug transporter.*Annu. Rev. Pharmacol. Toxicol.* 39:361-398.

Antonsson, B., Conti, F., Ciavatta, A., Montessuit, S.,Lewis, S., Martinou, I., Bernasconi, L., Bernard, A., Mermod, J.J. , Mazzei, G. K., Maundrell, Gambale, F. , Sadoul, R. , Martinou, J.C. (1997). Inhibition of Bax channel-forming activity by Bcl-2, Science 277 ,370–372.

Antonsson, B., Montessuit, S., Lauper, S., Eskes, R., Martinou, J. C. (2000). Bax oligomerization is required for channel-forming activity in liposomes and to trigger cytochrome c release from mitochondria. Biochem J; 345 Pt 2:271.

Arango D, Wilson AJ, Shi Q, *et al*. (2004). Molecular mechanisms of action and prediction of response to oxaliplatin in colorectal cancer cells. Br J Cancer. 91:1931–46.

Arruebo,M., Fernández-Pacheco, R., Ibarra, MR., Santamaría, J. (2007). Magnetic nanoparticles for drug delivery. *Nanotoday*, 2(3):22-32.

Aubin-Tam ME, Hwang W, Hamad-Schifferli K. (2009). Site-directed nanoparticle labeling of Cytochrome c. Proc Natl Acad Sci USA 106(11): 4095-4100.

Aubin-Tam, ME. (2013). Conjugation of nanoparticles to proteins. *Methods Mol Biol*, 1025:19-27.

Auffan, M., Rose, J., R. Wiesner, M., Bottero, J. (2009). Chemical stability of metallic nanoparticles: A parameter controlling their potential cellular toxicity in vitro. *Environmental Pollution*, 157:1127-1133.

Bai RL, Pettit GR, Hamel E.(1990). Binding of dolastatin 10 to tubulin at a distinct site for peptide antimitotic agents near the exchangeable nucleotide and vinca alkaloid sites. J Biol Chem.

Baptista, P. (2009). Cancer nanotechnology - prospects for cancer diagnostics and therapy. *Curr. Cancer Ther. Rev*. 5, 80–88.

Baptista, P., Pereira, E., Eaton, P., Doria, G., Miranda, A., Gomes, I., *et al.* (2008). Gold nanoparticles for the development of clinical diagnosis methods. *Anal. Bioanal. Chem*. 391, 943–950.

Barnett C, Gueorguieva M, Lees MR, Darton R, McGarvey D, *et al*. (2012). The effect of the hybrid composition on the physicochemical properties and morphology of iron oxide-gold nanoparticles. J Nano Res 14: 1170.

Barnett, C. M., Lees, M. R., Curtis, A. D. M., Kong Thoo Lin, P., Cheng, W. P. and Hoskins, C. (2013a). Poly (allylamine) magneto micelles for image guided drug delivery. Pharmaceutical Nanotechnology, 1 (3), pp. 224-238.

Barnett C, Gueorguieva M, Lees MR, Darton R, McGarvey D, *et al*.(2013b). Physical stability, biocompatibility and potential use of hybridiron oxide-gold nanoparticles as drug carriers. J Nano Res 15: 1076.

Beijnen, J.H.; Huizing, M.T.; Ten, B.H.W.; Veenhof, C.H.; Vermorken, J.B.; Giaccone, G.;Pinedo, H.M.(1994). Bioanalysis, pharmacokinetics, and pharmacodynamics of the novel anticancer drug paclitaxel (Taxol). *Semin Oncol*, *21* (Suppl. S8), 53–62.

Bekyarova, E., Ni, Y., Malarkey, EB. *et al*. (2005). Applications of carbon nanotubes in biotechnology and biomedicine. *J. Biomed Nanotechnol*, 1(1):3-17.

Beningo KA, Wang YL. (2002). Fc-receptor-mediated phagocytosis is regulated by mechanical properties of the target. J Cell Sci 115:849–856.

Benmerah A., C. Lamaze .(2007).Clathrin-coated Pits: Vive La Différence?Traffic, 8, pp. 970–982.

Berne, B.J.; Pecora, R. (2000).Dynamic Light Scattering. Courier Dover Publications ISBN 0-486-41155-9.

Bhattacharjee, S., (2016). DLS and zeta potential – What they are and what they are not? *Journal of Controlled Release*, 235, pp.337–351.

Bianco, A., Kostarelos, K., Partidos, DC., Prato, M. (2005). Biomedical applications of functionalized carbon nanotubes. *Chem. Commun*, 5:571-577.

Bleicken, S., Classen, M., Padmavathi, P.V.L., Ishikawa, T., Zeth, K., Steinhoff, H. J.,Bordignon, E.,(2010). Molecular details of Bax activation, oligomerization, and membrane insertion. J. Biol. Chem. 285 (9), 6636–6647.

Borst, P., Evers, R., Kool, M., Wijnholds, J. (2000).A family of drug transporters: the multidrugresistance-associated proteins. *J.Natl. Cancer Inst.* 92:1295–301.

Bosch, F.X., Ribes, J., Diaz, M., Cleries, R. (2004). Primary liver cancer: worldwide incidence and trends. *Gastroenterology*. Nov; 127(5 Suppl 1):S5-S16.

Bouguer P.(1729) . Essai d'optique sur la gradation de la lumière (Paris, France: Claude Jombert,) pp. 16–22.

Bowman MC, *et al*. (2008). Inhibition of HIV fusion with multivalent gold nanoparticles. J Am Chem Soc.;130:6896–6897.

Branco MC, Schneider JP. (2009). Self-assembling materials for therapeutic delivery. Acta Biomater; 5: 817-3.

Bras M. B. Queenan, and S. A. Susin. (2004). "REVIEW: Programmed Cell Death via Mitochondria: Different Modes of Dying."protein.bio.msu.ru/biokhimiya/contents

Brigger, Dubernet, C., Couvreur, P. (2002). Nanoparticles in cancer therapy and diagnosis, Advanced drug delivery reviews., 54, 631–651.

Bromberg L.(2008). Polymeric micelles in oral chemotherapy. J Control Release; 128: 99-112.

Bruix, J; Sherman, M. American Association for the Study of Liver Diseases. (2011). "Management of hepatocellular carcinoma: an update." *Hepatology (Baltimore, Md.)* 53 (3): 1020–1022.

Bulte, J., Douglas,T., Witwer,B. *et al.*(2007). Magnetodendrimers allow endosomal magnetic labeling and *in vivo* tracking of stem cells. *Nature Biotechnol.* 19:1141

Busdar, A. U., Marcus, C., Smith, TL., Blumenschein, GR.(1985). Early and delayed clinical cardiotoxicity of doxorubicin. Cancer; 55:2761-2765.

Cai, W., Chen, X. (2007). Nanoplatforms for targeted molecular imaging in living subjects. *Small*, 3(11): 1840-1854.

Cai, W., Gao, T., Hong, H., Sun, J. (2008). Applications of gold nanoparticles in cancer nanotechnology. *Nanotechnology, Science and Applications*, 1:17-32.

Carthy, Mc., JR., Perez, JM., Bruckner, C., Weissleder, R.(2005). Polymeric nanoparticle preparation that eradicates tumors. Nano. Lett., 5(12):2552–2556.

Cartron, P. F., Gallenne, T., Bougras, G. , Gautier, F. , Manero, F. , Vusio, P. , *et al.* (2004).The first alpha helix of Bax plays a necessary role in its ligand-induced activation by the BH3- only proteins Bid and PUMA. Mol Cell; 16:807–818.

Cedervall T, Lynch I, Foy M, Berggad T, Donnelly S, Cagney G, Linse S, Dawson K.(2007). Detailed identification of plasma proteins adsorbed on copolymer nanoparticles. Angew Chem Int Ed. 46:5754–5756.

Chan, WCW. (2007). Bio-applications of nanoparticles. *Advances in experimental medicine and biology*, 620.

Chan, WCW., Nie, S. (1998). Quantum dot bioconjugates for ultrasensitive nonisotopic detection. *Science*, 281 (5385):2016-2018.

Cheng WP, Gray AI, Tetley L, *et al.* (2006). Polyelectrolyte nanoparticles with high drug loading enhances the oral uptake of hydrophobic compounds. Biomacromol; 7: 1509-20.

Chiarugi, A., Moskowitz, M. A. (2002). "PARP-1—a perpetrator of apoptotic cell death?" *Science* 297 (5579): 259–263.

Chithrani BD, Ghazani AA, Chan WCW. (2006). Determining the size and shape dependence of gold nanoparticle uptake into mammalian cells. Nano Lett. ;6(4):662–668.

Cho, SJ., Idrobo, JC., Olamit, J., Liu, K., Browning, ND., Kauzlarich, SM. (2005). Growth Mechanisms and Oxidation Resistance of Gold-Coated Iron Nanoparticles. *Chem. Mater*,17: 3181.

Chu, K.S., Hasan, W., Rawal, S., Walsh, M.D. , Enlow, E.M. , Luft JC, Bridges AS, Kuijer JL, Napier ME, Zamboni WC, Desimone JM. (2013). "Plasma, tumor and tissue pharmacokinetics of Docetaxel delivered via nanoparticles of different sizes and shapes in mice bearing SKOV-3 human ovarian carcinoma xenograft". *Nanomedicine* 9 (5): 686–693.

Chuang, S.C., La Vecchia, C; Boffetta, P. (2009). "Liver cancer: descriptive epidemiology and risk factors other than HBV and HCV infection.". *Cancer letters* 286 (1): 9–14.

Chung TH, Wu SH, Yao M, Lu CW, Lin YS, Hung Y, Mou CY, Chen YC, Huang DM. (2007). The effect of surface charge on the uptake and biological function of mesoporous silica nanoparticles in 3T3–L1 cells and human mesenchymal stem *cells. Biomaterials* 28:2959–2966.

Ciobanu, CS., Iconaru, SL., Gyorgy, E., Radu, M., Costache, M., Dinischiotu, A., Coustumer, PL., Lafdi, K., Predoi, D. (2012). Biomedical properties and preparation of ironoxide-dextran nanostructures by MAPLE technique. Chemistry Central Journal, 6:17.

Colombini, M., (1979). A candidate for the permeability pathway of the outer mitochondrial membrane. Nature 279 (5714), 643–645.

Comoucka, J., Drbohlavova, J., Huska, D., Adam, V., Kizek, R., Hubalek, J. (2010). Magnetic Nanoparticles and Targeted Drug Delivering. *Pharmacol Res*, 62:144-149.

Conde, J., Doria, G., and Baptista, P. (2012). Noble metal nanoparticles applications in cancer. *Journal of drug delivery*. 2012:751-775.

Corvi, R., Madia, F. (2016). In vitro genotoxicity testingeCan the performance be enhanced?, Food and ChemicalToxicology. http://dx.doi.org/10.1016/j.fct.2016.08.024

Costantini, P., Jacotot, E., Decaudin, D., Kroemer, G. (2000). Mitochondria as novel target of anticancer chemotherapy. J Natl Cancer Inst 92: 1042-1053.

Cotter TG.(2009). Apoptosis and cancer: the genesis of a research field. Nat Rev Cancer.;9:501–507 .

Danhier F.; Feron O.; Preat V. (2010). To Exploit the Tumor Microenvironment: Passive and Active Tumor Targeting of Nanocarriers for Anti-Cancer Drug Delivery. J. Controlled Release, 148,135−146.

David J. Smith .(2015). Characterization of Nanomaterials Using Transmission Electron Microscopy, in *Nanocharacterisation RSC Nanoscience & Nanotechnology (2)*, pp. 1-29

Davis, M. E., Chen, Z. G, Shin, D.M. (2008). Nanoparticletherapeutics: an emerging treatment modalityfor cancer. Nat. Rev. Drug Discov. 7(9), 771–782.

De Lope, C.R., Tremosini, S., Forner, A., Reig, M; Bruix, J. (2012). Management of HCC. *Journal of hepatology*. 56 Suppl 1: S75–87.

De Miguel D, Lemke J, Anel A, Walczak H and Martinez-Lostao L. (2016). Onto better TRAILs for cancer treatment. *Cell Death and Differentiation* 23, 733–747.

Debatin, K.M. (1999). Activation of apoptosis pathways by anticancer drugs. Adv Exp Med Biol .547: 237-244.

DeBaun, M.R; Tucker, M. A., (1998). "Risk of cancer during the first four years of life in children from The Beckwith-Wiedemann Syndrome Registry.". *The Journal of pediatrics* 132 (3 Pt 1): 398–400.

Deeney, RC., Sinclair, R. (1997). Ultraviolet and Visible Spectroscopy, 2nd Edition, Thomas.M UK, John Wiley and Sons.

Delgado *et al*. (2014). Chemical glycosylation of cytochrome c improves physical and chemical protein stability. BMC Biochemistry, 15:16.

DeLong, RK., Reynolds, CM., Malcolm, Y., Schaeffer, A., Severs, T., Wanekaya, Ad. (2010). Functionalized gold nanoparticles for the binding, stabilization, and delivery of therapeutic DNA, RNA, and other biological macromolecules. *Nanotechnology, Science and Applications*, 3:56-63.

Denkhaus, E., Salnikow K. (2002). Nickel essentiality, toxicity, and carcinogenicity. *Crit Rev Oncol Hematol*, 42(1):35-56.

Di Francesco A, Ruggiero A, Riccardi R.(2002). Cellular and molecular aspects for drugs of the future: oxaliplatin. Cell Mol Life Sci.;59:1914–27.

Dias N., Bailly C. (2005). Drugs targeting mitochondrial functions to control tumor cell growth, Biochem. Pharmacol. 70 (1) 1–12.

Dolder, M., Zeth, K., Tittmann, P., Gross, H., Welte, W., Wallimann, T. (1999). Crys-tallization of the human, mitochondrial voltage-dependent anion-selectivechannel in the presence of phospholipids. J. Struct. Biol. 127 (1), 64–71.

Doroshow, J.H. (1986). Role of hydrogen peroxide and hydroxyl radical formation in the killing of Ehrlich tumor cells by anticancer quinones. Proc Natl Acad Sci U S A.; 83:4514–4518.

Dos Santos T, Varela J, Lynch I, Salvati A, Dawson KA. (2011). Quantitative Assessment of the Comparative Nanoparticle-Uptake Efficiency of a Range of Cell Lines. Small.;7:3341–3349..

Dreaden EC, Mwakwari SC, Sodji QH, Oyelere AK, El-Sayed MA. (2009). Tamoxifen-poly(ethylene glycol)-thiol gold nanoparticle conjugates: enhanced potency and selective delivery for breast cancer treatment. Bioconjug. Chem.;20(12):2247–2253.

Drummond DC, Meyer O, Hong K and Kirpotin DB (1999). Papahadjopoulos. Optimizing liposomes for delivery of chemotherapeutic agents to solid tumors, Pharmacol Rev., 51: 691-743.

D'Souza G.G., Weissig V. (2009). Subcellular targeting: a new frontier for drug-loaded pharmaceutical nanocarriers and the concept of the magic bullet, Expert Opin.Drug Deliv. 6 (11) 1135–1148.

Dubrez, Daloz, L., Dupoux, A., Cartier, J. (2008). IAPs more than just inhibitors of apoptosis proteins. Cell Cycle. 7(8):1036–1046.

Duncan R, Izzo L.(2005). Dendrimer biocompatability and toxicity. Adv Drug Deliver Rev; 57: 2215-37.

Dutta, D. , Sundaram, S. K. , Teeguarden, J. G. , Riley, B. J. , Fifield, L. S. , Jacobs, J. M. , Addleman, S. R. , Kaysen, G. A. , Moudgil, B. M. , Weber, T.J.(2007). Adsorbed proteins influence the biological activity and molecular targeting of nanomaterials. Toxicol Sci. Nov; 100(1):303-315.

Eiman Mukhtar, Vaqar Mustafa Adhami and Hasan Mukhtar .(2014). Targeting Microtubules by Natural Agents for Cancer Therapy, *Mol Cancer Ther; 13(2); 275–84.*

El-Kareh, A. W., & Secomb, T. W. (2005). Two-Mechanism Peak Concentration Model for Cellular Pharmacodynamics of Doxorubicin. *Neoplasia (New York, N.Y.)*, *7*(7), 705–713.

Emre, S; McKenna, G.J. (2004). "Liver tumors in children.". *Pediatric transplantation* 8 (6): 632–638.

Erlacher, M., Labi, V., Manzl, C., Böck, G. , Tzankov, A. , Häcker, G. , Michalak, E., Strasser, A. , Villunger, A. (2006). "Puma cooperates with Bim, the rate-limiting BH3-only protein in cell death during lymphocyte development, in apoptosis induction" . The journal of exprimental medicine, vol. 203 no. 13 2939-2951

Erster, S., Moll, U. M. (2005). Stress-induced p53 runs a transcriptionindependent death program. Biochem Biophys Res Commun 331:843–850.

Eskes, R., Desagher, S. , Antonsson, B. , Martinou, J. C. (2000). Bid induces the oligomerization and insertion of Bax into the outer mitochondrial membrane. Mol Cell Biol; 20:929–935.

Eun JR, Jung YJ, Zhang Y, Zhang Y, Tschudy-Seney B, *et al.* (2014). Hepatoma SK Hep-1 Cells Exhibit Characteristics of Oncogenic Mesenchymal Stem Cells with Highly Metastatic Capacity. PLOS ONE 9(10)

Faivre S, Chan D, Salinas R, Woynarowska B, Woynarowski JM.(2003). DNA strand breaks and apoptosis induced by oxaliplatin in cancer cells. Biochem Pharmacol.;66:225–37. doi: 10.1016/S0006-2952(03)00260-0.

Farokhzad, OC., Langer, R. (2006). Developing smarter therapeutic and diagnostic modalities. *Adv. Drug Deliv*. Rev. 58:1456-1459.

Fattovich, G., Stroffolini, T., Zagni, I., Donato, F. (2004). "Hepatocellular carcinoma in cirrhosis: incidence and risk factors.". *Gastroenterology* 127 (5 Suppl 1): S35–50.

Felice, B.; Prabhakaran, M.P.; Rodríguez, A.P.; Ramakrishna, S.(2014). Drug delivery vehicles on a nano-engineering perspective. *Mater. Sci. Eng. C*, *41*, 178–195.

Fernandes, E.; Ferreira, J.A.; Peixoto, A.; Lima, L.; Barroso, S.; Sarmento, B.; Santos, L.L. (2015). New trends in guided nanotherapies for digestive cancers: A systemic review. *J. Control Release*, *209*, 288–307.

Feynman, R. (1959). Engineering and Science. *California Institute of Technology*.

Figueroa CM, Suárez BN, Molina AM, Fernández JC, Torres Z, *et al*. (2017). Smart Release Nano-formulation of Cytochrome C and Hyaluronic Acid Induces Apoptosis in Cancer Cells. J Nanomed Nanotechnol 8: 427.

Finsterer, J., and Segall, L. (2010). Drugs interfering with mitochondrial disorders.Drug Chem. Toxicol. 33, 138–151.

Fischer U, Janicke RU, Schulze-Osthoff K.(2003). Many cuts to ruin: a comprehensive update of caspase substrates. Cell Death Differ.

Fu-Heng Yang, Qing Zhang, Qian-Ying Liang, Sheng-Qi Wang, Bo-Xin Zhao, Ya-Tian Wang,Yun Cai and Guo-Feng Li .(2015). Bioavailability Enhancement of Paclitaxel via a Novel Oral Drug Delivery System: Paclitaxel-Loaded Glycyrrhizic Acid Micelles; *Molecules*, *20*, 4337-4356

Gabrielli B1, Brooks K, Pavey S. (2012). Defective cell cycle checkpoints as targets for anti-cancer therapies, Front Pharmacol. doi: 10.3389/fphar

Galluzzi L, Joza N, Tasdemir E, Maiuri MC, Hengartner M, Abrams JM. *et al*. (2008). No death without life: vital functions of apoptotic effectors. Cell Death Differ.;15:1113–1123

Gao, W., Xu, K., Ji, L., Tang, B. (2011). Effect of gold nanoparticles on glutathione depletion-induced hydrogen peroxide generation and apoptosis in HL7702 cells. *Toxicol Lett*, 205:86-95.

Gareth A. Hughes. (2005). Nanostructuremediateddrug delivery. Nanomedicine: Nanotechnology, Biology, and Medicine. 1:22–30.

Gasser M, Rothen-Rutishauser B, Krug HF, Gehr P, Nelle M, Yan B, Wick P.(2010).The adsorption of biomolecules to multi-walled carbon nanotubes is influenced by both pulmonary surfactant lipids and surface chemistry. J Nanobiotechnology.

Gavrieli, Y., Sherman, Y., and Ben-Sasson, S. A. (1992). Identification of programmed cell death *in situ* via specific labeling of nuclear DNA fragmentation. *J. Cell Biol.*

Gewirtz, D. A. (1999) .A critical evaluation of the mechanisms of action proposed for the antitumor effects of the anthracycline antibiotics adriamycin and daunorubicin. Biochem Pharmacol.; 57:727–741.

Giannakakou P, Sackett D, Fojo T. (2000). Tubulin/microtubules: still a promising target for new chemotherapeutic agents. J Natl Cancer Inst.;92:182–3.

Gielen, M., Tiekink, ERT. (2005). Metallotherapeutic Drugs and Metal-Based Diagnostic Agents: The Use of Metals in Medicine. Hoboken, NJ: John Wiley and Sons.

Gil, P. R., and Parak, W. J. (2008). Composite nanoparticles take aim at cancer. *ACS Nano* 2: 2200–2205.

Gish RG, Porta C, Lazar L, Ruff P, Feld R, Croitoru A, Feun L, Jeziorski K, Leighton J, Gallo J, Kennealey GT. (2007). Phase III randomized controlled trial comparing the survival of patients with unresectable hepatocellular carcinoma treated with nolatrexed or doxorubicin. *J Clin Oncol*; 25: 3069-3075

Gonzales, D.H., W. Neupert, J. (1990). Bioenerg. Biomembranes Institut fur Physiologische Chemie, Physikalische Biochemie und Zellbiologie der Universitat Munchen, D-8000 Munchen 2, Germany, 22:753-768.

Goon, IY., Lai, LMH., Lim, M., Munroe, P., Gooding, JJ., Amal, R. (2009). Fabrication of gold-shell-protected magnetite nanoparticles: systematic control using polyethyleneimine. *Chem Mater*, 21:673-681.

Gouaze, V., Mirault, M. E., Carpentier, S., Salvayre, R., Levade, T., and Andrieu-Abadie, N. (2001). Glutathione Peroxidase-1 Overexpression Prevents Ceramide Production and Partially Inhibits Apoptosis in Doxorubicin-Treated Human Breast Carcinoma Cells *Mol. Pharmacol.* 60: 488–496

Gratton SE, Napier ME, Ropp PA, Tian S, DeSimone JM.(2008). *Microfabricated particles for engineered drug therapies: elucidation into the mechanisms of cellular internalization of PRINT particles. Pharm Res 25:2845–2852.*

Green, D. R. (2005). Apoptotic pathways: ten minutes to dead. Cell 121:671-674

Green, S.K., Frankel, A., Kerbel, R.S. (1999).Adhesion-dependent multicellular drug resistance. *Anticancer-Drug Designs* 14:153–168.

Gregoria, G., Wills, EJ., Swain, CP., Tavill, AS. (1974). Drug-Carrier Potential of Liposomes in Cancer Chemotherapy. *Lancet*, 1: 1313-1316.

Gross, A., Jockel, J., Wei, M.C., Korsmeyer, S.J. (1998). Enforced dimerization of BAX results in its translocation, mitochondrial dysfunctionand apoptosis, EMBO J. 17:3878–3885.

Gupta, A.K., Gupta, M. (2005).Synthesis and surface engineering of iron oxide nanoparticles for biomedical applications. *Biomaterials* 26:3995–4021.

Gyrd-Hansen, M.and Meier, P. (2010). IAPs: from caspase inhibitors to modulators of NF-κB, inflammation and cancer. Nat Rev Cancer. 10:561-574.

Hail N. Jr. (2005). Mitochondria: a novel target for the chemoprevention of cancer, 6504–6510.

Hanahan, D., Weinberg, R.A. (2000). the hallmarks of cancer. *Cell*, 100:57-70.

Hayden JH, Bowser SS, Rieder CL.(1990). Kinetochores capture astral microtubules during chromosome attachment to the mitotic spindle: direct visualization in live newt lung cells. J Cell Biol.;111:1039–45.

Heath, J. R., and Davis, M. E. (2008). Nanotechnology and cancer. *Annu. Rev. Med*. 59, 251–265.

Heaven M, *et al*.(2008). Crystal structure of the gold nanoparticle [N(C(8)H(17))(4)][Au (25)(SCH(2)CH(2)Ph)(18)] J Am Chem Soc.;130:3754–3755.

Hellstrand E, Lynch I, Andersson A, Drakenberg T, Dahlbäck B, Dawson KA, Linse S, Cedervall T.(2009). Complete high-density lipoproteins in nanoparticle corona. FEBS J.;276:3372–3381.

Hill, M. M., C. Adrain, P. J. Duriez, E. M. Creagh, and S. J. Martin. (2004). Analysis of the composition, assembly kinetics and activity of native Apaf-1 apoptosomes. EMBO J. 23:2134-2145.

Hoque, M.O., Begum, S., Sommer, M., Lee, T., Trink, B., Ratovitski, E., Sidransky, D. (2003). PUMA in head and neck cancer . *Cancer Lett.* 199 (1): 75–81.

Hoskins C, Kong Thoo Lin P, Tetley L, *et al*. (2011). Novel fluorescent amphiphilic poly(allylamine) and their supramolecular selfassemblies in aqueous media. Polym Advan Technol: 23:710-9.

Hoskins, C., Cuschieri, A., Wang, L. (2012a). Cytotoxicity of polycationic iron oxide nanoparticles: Common endpoint assays and alternative approaches for improved understanding of cellular response mechanism. *J Nanobiotechnol*, 10:15.

Hoskins, C., Min, Y., Gueorguieva, M., McDougall, C., Volovick, A., Prentice, P., Wang, Z., Melzer, A., Cuschieri, A., Wang, L. (2012b). Hybrid gold-iron oxide nanoparticles as a multifunctional platform for biomedical application. *Journal of Nanobiotechnology*, 10:27.

Hoskins, C., Wang, L., Cheng, WP., Cuschieri, A. (2012c). Dilemmas in the reliable estimation of the in-vitro cell viability in magnetic nanoparticle engineering: which tests and what protocols? *Nanoscale Res Letts*, 7:77.

Hoskins C, Kong Thoo Lin P, Tetley L, *et al*. (2012 d).The use of nano polymeric self-assemblies based on novel amphiphilic polymers for oral hydrophobic drug delivery. Pharm Res; 3: 59-79.

Hou, X., T. Jones, B. (2000). Inductively Coupled Plasma/Optical Emission Spectrometry. *Encyclopedia of Analytical Chemistry*, 9468-9485.

Hsu, Y.T., Wolter, K.G. , Youle, R.J. (1997). Cytosol-to-membrane redistribution of Bax and Bcl-X(L) during apoptosis, Proc. Natl. Acad. Sci. U. S. A. 94 3668–3672.

Hu, Che-Ming J.; Zhang, Liangfang. (2009). Therapeutic Nanoparticles to Combat Cancer Drug Resistance Current Drug Metabolism, Vol. 10, No. 8.

Huaizhi, Z., Yuantao, N. (2001). China's ancient gold drugs. *Gold Bull*, 34:24–29.

Huang M., Z. Ma, E. Khor, *et al.* (2002).Uptake of FITC-chitosan nanoparticles by A549 cells Pharm Res, 19, pp. 1488–1494

Huang X., Jain, PK., El-Sayed, IH. *et al*. (2007). Gold nanoparticles: interesting optical properties and recent applications in cancer diagnostics and therapy. *Nanomed*, 2: 681–693.

Imesch, P., Scheiner, D., Szabo, E., Fink, D., & Fedier, A. (2013). Conjugates of cytochrome c and antennapedia peptide activate apoptosis and inhibit proliferation of HeLa cancer cells. Experimental and Therapeutic Medicine, 6, 786-790.

Jadzinsky PD, *et al*.(2007). Structure of a thiol monolayer-protected gold nanoparticle at 1.1 angstrom resolution. Science. 318:430–433.

Jain, S., Hirst, DG., O'Sullivan, JM. (2012). Gold nanoparticles as novel agents for cancer therapy. *Br J Radiol*, 85(1010):101-113.

Jeong, S.W., Jang, J.Y., Chung, R.T. (2012). "Hepatitis C virus and hepatocarcinogenesis.". *Clinical and molecular hepatology* 18 (4): 347–356.

Jiang, W., Kim, BYS., Rutka, JT., Chan, WCW. (2008). Nanoparticle-mediated cellular response is size-dependent. *Nat. Nanotechnol*, 3(3):145-150.

JO, Auguste DT.(2009). Nanocarrier cross-linking density and pH sensitivity regulate intracellular gene transfer. Nano Lett 9:4467–4473

Jordan MA, Wilson L. (2004). Microtubules as a target for anticancer drugs. Nat Rev Cancer.;4:253–65

Jordan MA.(2002). Mechanism of action of antitumor drugs that interact with microtubules and tubulin. Curr Med Chem Anticancer Agents.;2:1–17.

Jordan, *A.*, Martinou, J. C. (2009). Mitochondrial outer-membrane permeabilization and remodelling in Apoptosis *The International Journal of Biochemistry & Cell Biology* 41:1884–1889.

Joubert, JC., Quim, An. (1997). Magnetic Microcomposites as Vectors for Bioactive. Agents: The State of Art. *Anales de Quimica*, Int. Ed: 93 S70.

Kaparissides, C., Alexandridou, S., Kotti, K., Chaitidou, S. (2006). Recent advances in novel drug delivery systems, *Journal of nanotechnology online*. 2:4-11.

Karajanagi SS, Vertegel AA, Kane RS, Dordick JS. (2004) .Structure and Function of Enzymes Adsorbed onto Single-Walled Carbon Nanotubes. Langmuir;20:11594–11599.

Kaufmann SH, Desnoyers S, Ottaviano Y, Davidson NE, Poirier GG.(1993).Specific proteolytic cleavage of poly(ADP-ribose) polymerase: an early marker of chemotherapy-induced apoptosis. Cancer Res.;53:3976–3985.

Kaufmann, S.H., Earnshaw, W.C. (2000). Induction of apoptosis by cancer chemotherapy. *Exp Cell Res* 256: 42-49

Kawamura, G., Nogami, M., Matsuda, A. (2013). Shape-Controlled Metal Nanoparticles and Their Assemblies with Optical Functionalities. *Journal of Nanomaterials*, 2013:1-17.

Kelling J, Sullivan K, Wilson L, Jordan MA. (2003). suppression of centromere dynamics by Taxol in living osteosarcoma cells. Cancer Res. 2003;63:2794–801

kerman, M.E., Chan, WC. ,Laakkonen , P., Bhatia, S.N. , Ruoslahti, E., Chan, Laakkonen, Bhatia, Ruoslahti .(2002) ."Nanocrystal targeting in vivo". *Proceedings of the National Academy of Sciences of* the *United States of America* 99 (20): 12617–21.

Kew, M.C. (2013). "Hepatitis viruses (other than hepatitis B and C viruses) as causes of hepatocellular carcinoma: an update". *Journal of viral hepatitis* 20 (3): 149–157.

Khan, S.A., Davidson, B.R., Goldin, R.D., Heaton, N., Karani, J., Pereira, SP., Rosenberg, W.M., Tait, P., Taylor-Robinson, S.D., Thillainayagam, A.V., Thomas, H.C., Wasan, H. (2012). "Guidelines for the diagnosis and treatment of cholangiocarcinoma: an update". British Society of, Gastroenterology, *Gut* 61 (12): 1657–1669

Khlebtsov N.G., Dykman L.A.. J. Quant. (2010). Spectrosc. Radiat. Transfer.;111:1–35.)

Kim SK, Foote MB, Huang L. (2012). The targeted intracellular delivery of Cytochrome C protein to tumors using lipid-apolipoprotein nanoparticles. Biomaterials 33(15): 3959-3966.

Kim, K. Y. (2007). Nanotechnology platforms and physiological challenges for cancer therapeutics. *Nanomedicine* 3, 103–110.

Kim, M.R., Jeong, E.G., Chae, B., Lee, J.W., Soung, Y.H., Nam, S.W., Lee, J.Y., Yoo, N.J., Lee, S.H. (2007). "Pro-apoptotic PUMA and anti-apoptotic phospho-BAD are highly expressed in colorectal carcinomas". *Dig. Dis. Sci.* 52 (10): 2751–2756.

Kim, S. K.; Foote, M. B.; Huang, L. (2012). The Targeted Intracellular Delivery of Cytochrome c Protein to Tumors Using Lipid apolipoprotein Nanoparticles. Biomaterials, 33, 3959−3966

Kivisto, K.T., Kroemer, H.K., and Eichelbaum, M. (1995). The role of human cytochrome P450 enzymes in the metabolism of anticancer agents: implications for drug interactions. *Br J Clin Pharmacol* 40: 523-530.

Ko, J. L., and Prives, C. (1996). Changes in p53 expression in mouse fibroblasts can modify motility and extracellular matrix organization .*Genes Dev.* 10, 1054–1072

Kogan, MJ., Olmedo, I., Hosta, L., Guerrero, AR., Cruz, LJ., Albericio, F. (2007). Peptides and metallic nanoparticles for biomedical applications. *Nanomedicine (Lond)*, 2(3):287-306.

Koppolu, B., Bhavsar, Z., Wadajkar, A., Nattama, S., Rahimi, M., Nwariaku, F., Nguyen, K. (2012). Temperature-Sensitive Polymer-Coated Magnetic Nanoparticles as a Potential Drug Delivery System for Targeted Therapy of Thyroid Cancer. *Journal of Biomedical Nanotechnology*, 8(6):983-990.

Korsmeyer, S.J., Yin, X.M., Oltvai, Z.N., Veis-Novack D.J., Linette, G.P. (1995).Reactive oxygen species and the regulation of cell death by theBcl-2 gene family. *Biochim Biophys Acta*; 1271: 63-6.

Kroemer, G., Galluzzi, L., Brenner, C. (2007). Mitochondrial membrane permeabilization in cell death. Physiol Rev; 87:99–163.

Krpetic Z, *et al.* (2009). A multidentate peptide for stabilization and facile bioconjugation of gold nanoparticles. Bioconjug Chem.;20:619–624.

Kuida, K., Haydar, T.F., Kuan, C.Y., Gu, Y., Taya, C., Karasuyama, H., Su, M.S., Rakic, P., Flavell, R.A. (1998). Reduced apoptosis and cytochrome c-mediated caspase activation in mice lacking caspase 9. *Cell*, 94(3):325-337

Lake, J.R. (1993). Benign and malignant neoplasms of the gallbladder, bile ducts and ampulla. In: Sleisinger MH, Fordtran JS, eds. Gastrointestinal Disease. 5th ed. Vol 2. *Philadelphia, Pa: WB Saunders*.:1891-1902.

Lammers, T., Aime, S., Hennink, W. E., Storm, G., and Kiessling, F. (2011). Theranostic nanomedicine. *Acc. Chem. Res*. 44, 1029–1038.

Lanni JS, Lowe SW, Licitra EJ, Liu JO, Jacks T. (1997). p53-independent apoptosis induced by paclitaxel through an indirect mechanism. Proc Natl Acad Sci U S A, 94:9679-9683.

Lapienis G. (2009).Star-shaped polymers having PEO arms. Prog Polym Sci; 34: 852- 92.

Lee, K., Lee, H., Bae, KH., Park, TG. (2010). Heparin immobilized gold nanoparticles for targeted detection and apoptotic death of metastatic cancer cells. *Biomater*, 31: 6530-6536.

Lee, KH., Galloway, JF., Park, J., Dvoracek, CM., Dallas, M., *et al*. (2012). Quantitative molecular profiling of biomarkers for pancreatic cancer with functionalized quantum dots. *Nanomedicine*, 8(7):1043-1051.

Lee, SK., Han, MS., Asokan, S., Tung, CH. (2011). Effective gene silencing by multilayered siRNA-coated gold nanoparticles. *Small*, 7(3):364–370.

Lemke, T., (2008). *Medicinal Chemistry* 6th Edition.

Letchford K, Burt H. (2007). A Review of the formation and classification of amphiphilic block copolymer nanoparticulate structures: Micelles, nanospheres, nanocapsules and polymersomes. Eur J Pharm Biopharm; 65: 259-69.

Li J, Yuan J.(2008). Caspases in apoptosis and beyond. Oncogene.;27:6194–6206.

Lin, Z., Monteiro-Riviere, N., Riviere, J. (2014). Pharmacokinetics of metallic nanoparticles. *Wiley Interdisciplinary Reviews: Nanomedicine and Nanobiotechnology*, 7(2):189-217.

Lind, M.J. (2008). "Principles of cytotoxic chemotherapy". *Medicine* 36 (1): 19–23

Ling Huang, Qingfeng Zhang, Liangliang Dai, Xinkun Shen, Weizhen Chen, Kaiyong Cai.(2017). Phenylboronic acid-modified hollow silica nanoparticles for dual-responsive delivery of doxorubicin for targeted tumor therapy. *Regen Biomater*; 4 (2)

Lison, D., Huaux, F. (2011). *In vitro* studies: Ups and downs of cellular uptake. *Nature Nanotechnology,* 6:332-333.

Liu, H.-C., Shan, E.-B., Zhou, L., Jin, H., Cui, P.-Y., Tan, Y., & Lu, Y.-M. (2014). Combination of percutaneous radiofrequency ablation with transarterial chemoembolization for hepatocellular carcinoma: observation of clinical effects. *Chinese Journal of Cancer Research*, *26*(4), 471–477.

Lobert S, Correia JJ.(2000). Energetics of vinca alkaloid interactions with tubulin. Methods Enzymol.;323:77–103.

Loo, C., Lin, A., Hirsch, L., Lee, M.H., Barton, J., Halas, N., West, J., Drezek, R. (2004). "Nanoshell-enabled photonics-based imaging and therapy of cancer". *Technol Cancer Res Treat.* 3 (1): 33–40.

Lotem, J., Peled-Kamar, M., Groner, Y., and Sachs, L. (1996) .Cellular oxidative stress and the control of apoptosis by wild type p53 .*Proc. Natl. Acad. Sci. U. S. A.* 93, 9166–9171

Lowe, S. W., Bodis, S., McClatchey, A., Remington, L., Ruley, H. E., Fisher, D. E., Housman, D. E., and Jacks, T. (1994).P53 status and the efficacy of cancer therapy in vivo. *Science journal* 266, 807–810

Lozano G.M., Bejarano, I., Espino, J., González, D., Ortiz, A., García, J.F., Rodríguez, A.B., Pariente, J.A. (2009). "Relationship between Caspase Activity and Apoptotic Markers in Human Sperm in Response to Hydrogem Peroxide and Progesterone". Journal of Reproduction and Development 55(6).

Lozano, R. (2012). "Global and regional mortality from 235 causes of death for 20 age groups in 1990 and 2010: a systematic analysis for the Global Burden of Disease Study 2010". *Lancet* 380 (9859): 2095–2128.

Lu, W., Zhang, G., Zhang, R., *et al*. (2010). Tumour site–specific silencing of NF-κB p65 by targeted hollow gold nanosphere–mediated photothermal transfection. *Cancer Res*, 70(8):3177-3188.

Lundqvist M, Stigler J, Cedervall T, Berggård T, Flanagan MB, Lynch I, Elia G, Dawson K.(2011). The Evolution of the Protein Corona around Nanoparticles: A Test Study. ACS Nano.;5:7503–7509.

Lyon, JL., Fleming, DA., Stone, MB., Schiffer, P., Williams, ME. (2004). Synthesis of Fe Oxide Core/Au Shell Nanoparticles by Iterative Hydroxylamine Seeding. *Nano Lett*, 4(403):719-723.

Maeda, H. (2001). The enhanced permeability and retention (EPR) effect in tumor vasculature: The key role of tumor selective macromolecular drug targeting, Adv. Enzyme Regul., 41,189–207.

Magnelli, L., Cinelli, M., and Chiarugi, V. (1995). Phorbol esters attenuate the expression of p53 in cells treated with doxorubicin and protect TS-P53/K562 from apoptosis.*Biochem. Biophys. Res. Commun.* 215, 641–645

Mak, SY., Chen, DH. (2005). Binding and sulfonation of poly(acrylic acid) on iron oxide nanoparticles: a novel, magnetic, strong acid cationnano-adsorbent. *Macromol Rapid Comm*, 26:1567-1571.

Makin, G., Kickman, J.A. (2000). Apoptosis and cancer chemotherapy. Cell Tissue Res 301: 143-152 -Malignant tumours of the liver". *Surgery (Oxford)* 27 (1): 30–37.

Malekigorji M, Hoskins C, Curtis T, Varbiro G. (2014). Enhancement of the Cytotoxic Effect of Anticancer Agent by Cytochrome c Functionalised Hybrid Nanoparticles in Hepatocellular Cancer Cells. J Nanomed Res 1(2)): 00010.

Mansour Almansour, Saud Alarifi, Bashir Jarrar (2018).In vivo investigation on the chronic hepatotoxicity induced by intraperitoneal administration of 10-nm silicon dioxide nanoparticlesInt J Nanomedicine; 13: 2685–2696. Published online. doi: 10.2147/IJN.S162847.

Manning MC, Chou DK, Murphy BM, Payne RW, Katayama DS. (2010). Stability of protein pharmaceuticals: an update. Pharm Res 27(4):544-575.

Manning, M., Chou, D., Murphy, B., Payne, R., Katayam, D. (2010). Stability of protein pharmaceuticals: anupdate. Pharmaceutical Research. 27:544–575.

Manuela Malatesta. (2016). Transmission electron microscopy for nanomedicine: novel applications for long-established techniques. *European Journal of Histochemistry 2016; 60:2751 doi:10.4081/ejh.2016.2751*

Marani, M., Tenev, T., Hancock, D., Downward, J., Lemoine, N.R. (2002). Identification of novel isoforms of the BH3 domain protein Bim which directly activate Bax to trigger apoptosis. Mol Cell Biol; 22:3577–3589.

Marie-Eve Aubin-Tama,Wonmuk Hwangb and Kimberly Hamad-Schifferli .(2008). Site-directed nanoparticle labeling of cytochrome c PNAS vol. 106 no. 11 Marie-Eve Aubin-Tam, 4095–4100, doi: 10.1073/pnas.0807299106

MARINO, G., NISO-SANTANO, M., BAEHRECKE, E.H., and KROEMER, G. (2014). Self-Consumption: the interplay of autophagy and apoptosis. *Nature Reviews. Molecular cell biology*, 15(2), pp. 81-94.

Martinou JC, Youle RJ. (2011). Mitochondria in apoptosis: Bcl-2 family members and mitochondrial dynamics. Dev Cell 21(1): 92-101.

Mathurin, P., Raynard, B., Dharancy, S. (2003). Meta-analysis: evaluation of adjuvant therapy after curative liver resection for hepatocellular carcinoma. *Aliment Pharmacol Ther*.;17(10):1247-1261.

Mavridou DA, Ferguson SJ, Stevens JM. (2013). "Cytochrome c assembly". IUBMB Life. 65 (3): 209–16.

McCarthy, J.R., Weissleder, R. (2008). Multifunctional magnetic nanoparticles for targeted imaging and therapy. *Adv. Drug Deliver. Rev*. 60:1241–1251.

McIlwain DR, Berger T, Mak TW. (2013). Caspase functions in cell death and disease. Cold Spring Harb Perspec Biol 5: a008656.

Megha, K. *et al*. (2015). Low intensity microwave radiation induced oxidative stress, inflammatory response and DNA damage in rat brain. *NeuroToxicology*, 51, pp.158–165.

Merkle, C.J. (2009). Cellular adaptation, injury, and death. In Pathophysiology:concepts of altered health states. 8 edition. Edited by: Porth CM, Matfin G.Philadelphia: Wolters Kluwer/Lippincott Williams and Wilkins; 94-111.

Mermet, JM. (2005). "Is it still possible, necessary and beneficial to perform research in ICP-atomic emission spectrometry?". *J. Anal. At. Spectrom*. 20:11-16.

Michael M Gottesman, Joseph Ludwig, Di Xia, Gergely Szakacs. (2009). Defeating drug resistance in cancer, Discovery medicine.

Michaelis, K., Hoffmann, M. M., Dreis, S., Herbert, E., Alyautdin, R. N., Michaelis, M., Kreuter, J. and Langer, K., Institute. Germany (M.M.H.); and Department of Pharmacology, Sechenov Medical . jection (Kreuter et al., 1995; Kreuter, 2002; Steiniger et al., 97139/3116950. JPET 317:1246–1253, 2006. - KASIBHATLA, S., and TSENG, B., 2006. Why Target Apoptosis in Cancer Treatment? *Molecular Cancer Therapeutics,* 2, pp. 573-580.

Michalak, E.M., Villunger, A., Adams, J.M., Strasser, A. (2008). In several cell types tumour suppressor p53 induces apoptosis largely via Puma but Noxa can contribute. *Cell Death Differ*; 15:1019–1029.

Mikami, Y., Dhakshinamoorthy, A., Alvaroa, M., García, H. (2013). Catalytic activity of unsupported gold nanoparticles. *Catal. Sci. Technol*, 3:58-69.

Minelli, C., Lowe, S. B., and Stevens, M. M. (2010). Engineering nanocomposite materials for cancer therapy. *Small* 6, 2336–2357.

Minn, A.J., Velez, P., Schendel, S.L. , Liang, H., Muchmore, S.W. , Fesik, S.W. , Fill, M., Thompson, C.B. (1997). Bcl-x(L) forms an ion channel in synthetic lipid membranes, Nature 385 353–357.

Mitchison TJ.(1988). Microtubule dynamics and kinetochore function in mitosis. Annu Rev Cell Biol.;4:527–49.

Mohan, H. (2010). Textbook of pathology. New Delhi: Jaypee BrothersMedical Publishers;, 5 edition 21-60.

Monopoli MP, Walczyk D, Campbell A, Elia G, Lynch I, Baldelli Bombelli F, Dawson KA. (2011). Physical − Chemical Aspects of Protein Corona: Relevance to in Vitro and in Vivo Biological Impacts of Nanoparticles. J Am Chem Soc.;133:2525–2534.

Montes Ruiz-Cabello, F.J. *et al*. (2014). Electric double-layer potentials and surface regulation properties measured by colloidal-probe atomic force microscopy. *Physical Review E*, 90(1), p.12301.

Morales-Cruz M, Figueroa CM, Gonzalez-Robles T, Delgado Y,Molina A, *et al*. (2014). Activation of caspase-dependent apoptosisby intracellular delivery of Cytochrome c-based nanoparticles. JNanobiotechnology 12: 33.

Morgan, M.T., Nakanishi, Y., Kroll, D.J., Griset, A.P., Carnahan, M.A., Wathier, M., Oberlies, N.H., Manikumar, G., Wani, M.C., Grinstaff, M.W. (2006). Dendrimer-encapsulated camptothecins: increased solubility, cellular uptake, and cellular retention affords enhanced anticancer activity in vitro. *Cancer Res.*; 66:11913–11921.

Moselhy J, Wu XY, Nicholov R and Kodaria K (2000). In vitro studies of the interaction of poly (NIPAm/MAA) nanoparticles with protein and cells. J. Biomat. Sci. Polymer Ed., 11: 123-147.

Moses, MA., Brem, H., Langer, R. (2003). Advancing the field of drug delivery: taking aim at cancer. *Cancer Cell*, 4:337-341.

Murthy. N., Xu, M.C., Schuck, S., Kunisawa, J., Shastri, N., Frechet, J.M.J. (2003). In vivo targeting of dendritic cells for activation of cellular immunity using vaccine carriers based on pH-responsive microparticles.*J. Proc. Natl. Acad. Sci. U.S.A.*; 100: 4995–5000.

Nakamura, T., Ueda, Y., Juan, Y., Katsuda, S., Takahashi, H., and Koh, E. (2000). Fas-mediated apoptosis in adriamycin-induced cardiomyopathy in rats: In vivo study. *Circulation* 102, 572–578.

Nakano, K., Vousden, K.H. (2001). "PUMA, a novel proapoptotic gene, is induced by p53". *Mol. Cell* 7 (3): 683–694.

National Cancer Institute: Metastatic Cancer: Questions and Answers. Retrieved on 2008-11-01

Nie, Shuming, Yun Xing, Gloria J. Kim, and Jonathan W. Simmons. (2007). "Nanotechnology Applications in Cancer" *Annual Review of Biomedical Engineering* 9: 257–288

Nijhawan, Li, P., D. I. Budihardjo, S. M. Srinivasula, M. Ahmad, E. S. Alnemri, and X. Wang. (1997). Cytochrome c and dATP-dependent formation of Apaf-1/caspase-9 complex initiates an apoptotic protease cascade. Cell 91:479-489.

Noack, A., Noack, S., Hoffman, A., Maalouf, K., Buettnr, M., Couraud, P.O., Romero, I.A., Weksler, B., Alms, D., Romermannn, K., Naim, H.Y., and Loscher, W. (2014). Drug-Induced Trafficking of P-Glycoprotein in Human Brain Capillary Endothelial Cells as Demonstrated by Exposure to Mitomycin C. *PLOS ONE,* 9(2), 88-154.

Nogales E, Wolf SG, Khan IA, Luduena RF, Downing KH. (1995). Structure of tubulin at 6. 5 A and location of the taxol-binding site. Nature.;375:424–7.

Oluwasamni , A, Malekigorji, M, Jones, S, Curtis, ADM & Hoskins, C 2016, 'Potential Of Hybrid Iron Oxide-Gold Nanoparticles As Thermal Triggers For Pancreatic Cancer Therapy' RSC Advances. DOI: 10.1039/C6RA20552F

Panyam, J., Labhasetwar, V. (2004). Sustained cytoplasmic delivery of drugs with intracellular receptors using biodegradable nanoparticles. Mol. Pharm.; 1(1):77–84.

Paraskevi A. Farazi & Ronald A. DePinho. (2006). *Nature Reviews Cancer* 6, 674-687.

Park HS, Kim CW, Lee HJ, Choi JH, Lee SG, *et al*. (2010). A mesoporous silica nanoparticle with charge-convertible pore walls for efficient intracellular protein delivery. Nanotechnology 21(22): 225101.

Park, J.H., Von Maltzahn, G., Xu, M.J, Fogal, V., Kotamraju, V.R., Ruoslahti, E., Bhatia, S.N., Sailor, M.J. (2010). Cooperative nanomaterial system to sensitize, target, and treat tumors. Proc. Natl. Acad. Sci. U S A.; 107(3):981–986.

Patel, V.R. & Agrawal, Y.K. (2011). Nanosuspension: An approach to enhance solubility of drugs. *Journal of advanced pharmaceutical technology & research*, 2(2), pp.81–7.

Pathania, D. *et al.* (2014). Design and discovery of novel quinazolinedione-based redox modulators as therapies for pancreatic cancer. Biochimica et Biophysica Acta (BBA) - General Subjects, 1840(1), pp.332–343.

Pattekari, P., Zheng, Z., Zhang, X., Levchenko, T., Torchilinb, V., Lvov, Y. (2011). Top-down and bottom-up approaches in production of aqueous nanocolloids of low solubility drug paclitaxel. *Phys Chem Chem Phys*, 13:9014-9019.

Petros RA, DeSimone JM. (2010). Strategies in the design of nanoparticles for therapeutic applications. Nat Rev Drug Discov 9:615–627.

Pilkington, G.J., Parker, K., Murray, S.A. (2008). Approaches to mitochondrially mediated cancer therapy. Semin. Cancer Biol.; 18(3):226–235.

Pissuwan D, Valenzueka SM, Cortie MB. (2006).Therapeutic possibilities of plasmonically heated gold nanoparticles. *Trends Biotechnol*, 24:62-67.

Pluen,A., Boucher, Y., Ramanujan, S., Tevor, D.,Takeshi, G.,Emmanuelledi, T.,Edward, B.,Yotaro, I.(2001). Role of tumor-host interactions ininterstitial diffusion of macromolecules:cranial vs. subcutaneous tumors. *Proc.Natl. Acad. Sci. USA* 98:4628–4633.

Pradelli, L.A., Bénéteau, M., Ricci, J.E. (2010). Mitochondrial control of caspase-dependent and -independent cell death. *Cell. Mol. Life Sci.* 67(10), 1589–1597.

Prodan, E., Radloff, C., Halas, NJ., Nordlander, P. (2003). A hybridization model for the plasmon response of complex nanostructures. *Science*, 302(5644):419-422.

Pylaev T.E., Khanadeev V.A., Khlebtsov B.N. (2011). Colloid J.; 73(2):1–12.

Pyrpassopoulos, S., Niarchos, D., Nouneis, G., *et al.* (2007). Synthesis and selforganizationof Au nanoparticles. *Nanotechnology*, 18:485-604.

Qian, X., Peng, XH., Ansari, DO., Yin-Goen, Q., Chen, GZ., Shin, DM., Yang, LA., Young, N., Wang MD., Nie, S. (2008). *In vivo* tumour targeting and spectroscopic detection with surface-enhanced Raman nanoparticle tags. *Nat. Biotechnol*, 26:83-90.

Qui L, Zheng C, Jin Y, *et al*. (2007). Polymeric micelles as nano carriers for drug delivery. Expert Opin Ther Pat; 17: 819-30.

Racila, E., Euhus, D., Weiss, A. J., Rao, C., McConnell, J., Terstappen, L. W., and Uhr, J. W. (1998). Detection and characterization of carcinoma cells in the blood. Proc. Natl.Acad. Sci. USA, *95:* 4589–4594.

Rajendran L., Knolker H.J., Simons K. (2010). Subcellular targeting strategies for drug design and delivery, Nat. Rev. Drug Discov. 9 (1) 29–42.

Ralphs, S; Khan, SA. (2013). "The role of the hepatitis viruses in cholangiocarcinoma.". *Journal of viral hepatitis* 20 (5): 297–305.

Ramon Roset, Laura Ortet, Gabriel Gil-Gomez. (2007). Frontiers in Bioscience 12, 4722-4730.

Rasmussen, J.W.; Martinez, E.; Louka, P.; Wingett, D.G.(2010). Zinc oxide nanoparticles for selective destruction of tumor cells and potential for drug delivery applications. *Exp. Opin. Drug Deliv.*, *7*, 1063–1077.

Rawat, M., Singh, D., Saraf, S., Saraf, S. (2006). Nanocarriers: promising vehicle for bioactive drugs. Biol Pharm Bull, 29, 1790–1798.

Ray, S., Almasan, A. (2003). Apoptosis induction in prostate cancer cells and xenografts by combined treatment with Apo2 ligand/tumor necrosis factor-related apoptosis-inducing ligand and CPT-11. Cancer Res; 63: 4713–4723.

Razumilava, N; Gores, GJ. (2013). "Classification, diagnosis, and management of cholangiocarcinoma.". *Clinical gastroenterology and hepatology : the official clinical practice journal of the American Gastroenterological Association* 11 (1): 13–21.

Rezwan K, Meier LP, Rezwan M, Vörös J, Textor M, Gauckler LJ.(2004).Bovine Serum Albumin Adsorption onto Colloidal Al2O3 Particles: A New Model Based on Zeta Potential and UV–vis Measurements. Langmuir.;20:10055–10061.

Richards, D.G., McMIllin, D.L., Mein, E.A., *et al*. (2002). Gold and its relationship to neurological/glandular conditions. *Int J Neurosci*, 112:31–53.

Robinson, I., Tung, LD., Maenosono, S., Walti, C., Thanh, NTK. (2010). Synthesis of core-shell gold coated magnetic nanoparticles and their interaction with thiolated DNA, *Nanoscale*, 2:2624-2630.

Ruge CA, Kirch J, Canadas O, Schneider M, Perez-Gil J, Schaefer UF, Casals C, Lehr C-M. (2011) .Uptake of nanoparticles by alveolar macrophages is triggered by surfactant protein A. Nanomedicine-Nanotechnology Biology and Medicine.;7:690–693.

Rusan NM, Fagerstrom CJ, Yvon AM, Wadsworth P.(2001). Cell cycle-dependent changes in microtubule dynamics in living cells expressing green fluorescent protein-alpha tubulin. Mol Biol Cell.;12:971–80.

Ryan KM, Phillips AC, Vousden KH.(2001).Regulation and function of the p53 tumor suppressor protein. Curr Opin Cell Biol, 13:332-337.

Saelens, X., N. Festjens, L. Vande Walle, M. van Gurp, G. van Loo, and P. Vandenabeele. (2004). Toxic proteins released from mitochondria in cell death. Oncogene 23:2861-2874.

Sahoo, S.K., Labhasetwar V. (2003). Nanotech approaches to drug delivery and imaging .Drug Discov Today.; 8(24):1112-1120.

Saikumar, P., Dong, Z., Mikhailov, V., Denton, M., Weinberg, J.M.,Venkatachalam, M.A.(1999). Apoptosis: definition, mechanisms, and relevance to disease. Am J Med; 107: 489-506.

Saito, M., Korsmeyer, S.J., Schlesinger, P.H. (2000). BAX-dependenttransport of cytochrome c reconstituted in pure liposomes.Nat Cell Biol, 2:553-555.

Santra S, Kaittanis C, Perez JM.(2010). Cytochrome C encapsulating theranostic nanoparticles: a novel bifunctional system for targeted delivery of therapeutic membrane-impermeable proteins to tumors and imaging of cancer therapy. Mol Pharm, 7:1209-1222 .

SASI, N., HWANG, M., JABOIN, J., CSIKI, I., and LU, B. (2009). Regulated cell death pathways: new twists in modulation of BCL2 family function. *Molecular Cancer Therapeutics,* 8(6), pp. 1421-1429.

Seied Sajadi, M., Fathi, F., Farhadyar, N. (2014). Synthesis and Surface modification of Iron Oxide Nanoparticles for Drug Delivery. *IJCPS*, 2(4):760-764.

Schadt, W., Cheung, J., Luo, C., J. Zhong *et al*. (2006). Molecularly Tuned Size Selectivity in Thermal Pro cessing of Gold Nanoparticles. *Chem. Mater*, 18(22):5147-5149.

Schafer, B., Quispe, J., Choudhary, V., Chipuk, J.E., Ajero, T.G., Du, H., Schneiter,R., Kuwana, T. (2009). Mitochondrial outer membrane proteins assist Bid inBax-mediated lipidic pore formation. Mol. Biol. Cell 20 (8), 2276–2285.

Schendel, S.L. , Azimov, R., Pawlowski, K., Godzik, A., Kagan, B.L., Reed, J.C. (1999). Ion channel activity of the BH3 only Bcl-2 family member,BID, J. Biol. Chem. 274 ,21932–21936.

Schendel, S.L., Xie, Z., Montal, M.O., Matsuyama, S., Montal, M., Reed, J.C. (1997). Channel formation by antiapoptotic protein Bcl-2, Proc. Natl.Acad. Sci. U. S. A. 94, 5113–5118.

Schlesinger, P.H., Gross, A., Yin, X.M. , Yamamoto, K., Saito, M., Waksman, G., Korsmeyer, S.J. (1997). Comparison of the ion channel characteristics of proapoptotic BAX and antiapoptotic BCL-2, Proc. Natl. Acad. Sci. U. S. A. 94 ,11357– 11362.

Schuler, M., Green, D.R. (2005). Transcription, apoptosis and p53: catch-22.Trends Genet 21:182–187.

Scorrano, L., Ashiya, M., Buttle, K., Weiler, S., Oakes, S.A., Mannella, C.A., Korsmeyer, S.J. (2002). Adistinct pathway remodels mitochondrial cristae and mobilizes cytochrome c during apoptosis. Dev Cell, 2:55-67

Seeff, L.B. (2004) .The burden of hepatocellular carcinoma. *Gastroenterology*.; 127(5 Suppl 1):S1-4.

Shang W, Nuffer JH, Muniz-Papandrea VA, Colon W, Siegel RW, *et al*. (2009) .Cytochrome C on silica nanoparticles: influence of nanoparticle size on protein structure, stability and activity. Small 5(4): 470-476.

Sharma S, Tanwar A, Gupta DK. Curcumin .(2016). an adjuvant therapeutic remedy for liver cancer. Hepatoma Res;2:62-70.

Sharonov GV, Feofanov AV, Bocharova OV, Astapova MV, Dedukhova VI, *et al.* (2005). Comparative analysis of proapoptotic activity of Cytochrome c mutants in living cells. Apoptosis 10(4): 797-808.

Shi, Y. (2002). Mechanisms of caspase inhibition and activation during apoptosis. Mol Cell 9: 459–470.

Shruti R Saptarshi, Albert Duschl, and Andreas L Lopatacorresponding .(2013). Interaction of nanoparticles with proteins: relation to bio-reactivity of the nanoparticle. J Nanobiotechnology.;11: 26.

Shukla, R., Bansal, V., Chaudhary, M., Basu, A., Bhonde, RR., Sastry M. (2005). Biocompatibility of gold nanoparticles and their endocytotic fate inside the cellular compartment: a microscopic overview. *Langmuir*, 21:10644-10654.

Shvedova, A. A., Kagan, V. E., and Fadeel, B. (2010). Close encounters of the small kind: adverse effects of man-made materials interfacing with the nano-cosmos of biological systems. *Annu. Rev. Pharmacol. Toxicol*. 50, 63–88.

Simone Göschl , Ekaterina Schreiber-Brynzak , Verena Pichler , Klaudia Cseh , Petra Heffeter , Ute Jungwirth , Michael A. Jakupec , Walter Berger and Bernhard

K. Keppler .(2017). Comparative studies of oxaliplatin-based platinum(IV) complexes in different in vitro and in vivo tumor models,University of Vienna, Institute of Inorganic Chemistry, Waehringer Strasse 42, 1090 Vienna, Austria.

Singal, P. K., and Iliskovic, N. (1998) .Doxorubicin-induced cardiomyopathy.*N. Engl. J. Med.* 339, 900–905

Singla, A.K.; Garg, A.; Aggarwal, D. (2002).Paclitaxel and its formulations. *Int. J. Pharm. 235*, 179–192.

Slowing II, Trewyn, B. G., Lin, VSY. (2007). Mesoporous silica nanoparticles for intracellular delivery of membrane-impermeable proteins. J. Am. Chem. Soc.; 129(28):8845–8849.

Smolensky, ED., Neary, MC., Zhou, Y., Berquo, TS., Pierre, VC. (2011). Fe3O4@organic@Au: core-shell nanocomposites with high saturation magnetisation as magnetoplasmonic MRI contrast agents. *Chem Commun*, 47:2149-2151.

Štarha, P., Smola, D., Tuček, J., and Trávníček, Z. (2015). Efficient Synthesis of a Maghemite/Gold Hybrid Nanoparticle System as a Magnetic Carrier for the Transport of Platinum-Based Metallotherapeutics. *Int. J. Mol. Sci*, 16:2034-2051.

Stroh, A., Zimmer, C., Gutzeit, C., Jakstadt, M., Marschinke, F., Jung, T, *et al*. (2004). Iron oxide particles for molecular magnetic resonance imaging cause transient oxidative stress in rat macrophages. *Free Radic Biol Med*, 36:976-84.

Suh H, Jeong B, Rathi R, Kim SW. Stuart R.A., W. Neupert .(1998) . Regulation of smooth muscle cell proliferation using - Biochimie 72 ,115-121.

Suresh, A., Guedez, L., Moreb, J., and Zukali, J. (2003). Overexpression of manganese superoxide dismutase promotes survival in cell lines after doxorubicin treatment. *Br. J. Haematol.* 120(3):457-463.

Susin, S. A., Lorenzo, H. K., Zamzami, N., Marzo, I., Snow, B. E., Brothers,G. M., Mangion, J., Jacotot, E., Costantini, P., Loeffler, M., *et al*. (1999).Molecular characterization of mitochondrial apoptosis-inducing factor.Nature 397, 441–446.

Suzuki, Y., Imai, Y., Nakayama, H., Takahashi, K., Takio, K., Takahashi, R. (2001). A serine protease, HtrA2, is released from the mitochondria and interacts with XIAP, inducing cell deathMol Cell. Sep; 8(3):613-621.

Tabata, Y., Ikada, Y. (1998). Protein release from gelatin matrices. Adv Drug Deliv Rev.; 31:287–301.

Tartaj, P., Morales, M.D., Veintemillas-Verdaguer, S., Gonzalez-Carreno, T., Serna, C.J. (2003). The Preparation of Magnetic Nanoparticles for Applications in Biomedicine. *J. Phys. D Appl. Phys*. 36(13):182-197.

Tewey, K.M., Rowe, T.C., Yang, L., Halligan, B.D., Liu, L.F. (1984). Adriamycin-induced DNA damage mediated by mammalian DNA topoisomerase-II. Science.; 226:466–468.

Thompson C, Ding C, Qu X, *et al*. (2008).The effect of polymer architecture on the nano self-assemblies based on novel comb-shaped amphiphilic poly(allylamine). Colloid Polym Sci: 286: 1511-26.

Thompson, C.B. (1995). Apoptosis in the treatment and treatment of disease. *Science* 267, 1456-1462.

Tommaso, D. i., Sangiovanni, L., Borzio, A., Park, M., Farinati, Y. N., Roncalli, F. (2013). "Advanced precancerous lesions in the liver". *Best practice & research. Clinical gastroenterology* 27 (2): 269–284.

Torchilin, V.(2008). Intracellular Delivery of Protein and Peptide Therapeutics. Drug Discovery Today: Technol., 5, e95−e103.

Torchilin, VP., Rammohan, R., Weissig, V., Levchenko, TS. (2001). TAT peptide on the surface of liposomes affords their efficient intracellular delivery even at low temperature and in the presence of metabolic inhibitors. *Proc. Natl Acad. Sci*. USA, 98(15):8786-8791.

Tsujimoto, Y. (2003). 14-3-3 Interacts directly with and negatively regulatespro-apoptotic Bax, J. Biol. Chem. 278, 2058– 2065.

Vaux, D.L. (1993). Toward an understanding of the molecular mechanisms of physiological cell death, Proc. Natl. Acad. Sci. USA, 90 (1993), pp. 786–789

Vogelstein, B., Kinzler, K.W. (2004). "Cancer genes and the pathways they control". *Nat. Med.* 10 (8): 789–799.

Von Maltzahn G, Centrone A, Park JH, *et al*. (2009). SERS-coded gold nanorods as a multifunctional platform for densely multiplexed near-infrared imaging and photothermal heating. Adv. Mater. ;21:1–6.

Vousden, K.H., Lu, X. (2002). Live or let die: the cell's response to p53. *Nat Rev* Cancer*;* 2:594–*604.*

Vroman L. (1962). Effect of Adsorbed Proteins on the Wettability of Hydrophilic and Hydrophobic Solids. Nature.;196:476–477.

Wai-Tao Chan, Cheng-Che Liu, Jen-Shiu Chiang Chiau, Shang-Ting Tsai, Chih-Kai Liang, Mei-Lien Cheng, Hung-Chang Lee, Chun-Yun Yeung, Shao-Yi Hou (2017). Int J Nanomedicine.; 12: 3421–3432. Published online 2017 Apr 28. doi: 10.2147/IJN.S126823

Walsh, M.D., Hanna, S.K., Sen, J., Rawal, S., Cabral, C.B., Yurkovetskiy, A.V., Fram, R.J., Lowinger, T.B., Zamboni, W.C. (2012). "Pharmacokinetics and antitumor efficacy of XMT-1001, a novel, polymeric topoisomerase I inhibitor, in mice bearing HT-29 human colon carcinoma xenografts". *Clin. Cancer Res.* 18 (9): 2591–2602.

Wang H, Huff TB, Zweifel DA, *et al*.(2005). *In vitro* and *in vivo* two-photon luminescence imaging of single gold nanorods. Proc. Natl Acad. Sci. USA. ;102(44):15752–15756.

Wang Z, Tiruppathi C, Minshall RD, Malik AB. (2009). Size and Dynamics of Caveolae Studied Using Nanoparticles in Living Endothelial Cells. ACS Nano. ;3:4110–4116.

Wang, L., Ma, W., Markovich, R., Chen, J. W., and Wang, P. H. *Circ.*Wang, ZG; Zhang, GF; Wu, JC; Jia, MK. (2013). "Adjuvant therapy for hepatocellular

carcinoma: Current situation and prospect.". *Drug discoveries & therapeutics* 7 (4): 137–143.

Wang, X., Zhou, L., Ma, Y., Li, X., Gu H. (2009). Control of aggregation size of polyethyleneimine-coated magnetic nanoparticles for magnetofection. *Nano Res*, 2:365-372.

Waterman-Storer CM, Salmon ED.(1997). Microtubule dynamics: treadmilling comes around again. Curr Biol.;7:R369–72.

Weon Sup Shin, Min-Goo Lee, Peter Verwilst,,, Joung Hae Lee,, Sung-Gil Chi and Jong Seung Kim.(2016). Mitochondria-targeted aggregation induced emission theranostics: crucial importance of in situ activation. *Chem. Sci*., , 7, 6050-6059.

Wijdeven, R.H., Neefjes, J. & Ovaa, H. (2014). How chemistry supports cell biology: the chemical toolbox at your service. Trends in Cell Biology, 24(12), pp.751–760.

World Health Organization. February .(2014). Retrieved 10 June 2014.

Wu, C.-H., Lan, C.-H., Wu, K.-L., Wu, Y.-M., Jane, W.-N., Hsiao, M., & Wu, H.-C. (2018). Hepatocellular carcinoma-targeted nanoparticles for cancer therapy. *International Journal of Oncology*, *52*(2), 389–401. http://doi.org/10.3892/ijo.2017.4205

Xiang C, Zou Y, Qiu S, Sun L, Xu F, *et al*. (2013). Bienzymatic glucose biosensor based on direct electrochemistry of Cytochrome c on gold nanoparticles/polyaniline nanospheres composite. Talanta 110: 96-100.

Yallapu MM, Othman SF, Curtis ET, Gupta BK, Jaggi M, Chauhan SC. (2011). Multi-functional magnetic nanoparticles for magnetic resonance imaging and cancer therapy. *Biomaterials*, 32:1890-1905.

Yamada Y, Harashima H. (2008). mitochondrial drug delivery systems for macromolecule and their therapeutic application to mitochondrial diseases. Adv Drug Deliv Rev, 60:1439-1462.

Yoo, N.J., Lee, J.W., Jeong, E.G., Lee, S.H. (2007). "Immunohistochemical analysis of pro-apoptotic PUMA protein and mutational analysis of PUMA gene in gastric carcinomas". *Dig Liver Dis* 39 (3): 222–227.

Youle, R.J., Strasser, A. (2008). The BCL-2 protein family: opposing activities that mediate cell death. Nat Rev Mol Cell Biol; 9:47–59

Yu, J., Zhang, L. (2005). The transcriptional targets of p53 in apoptosis control.*Biochem. Biophys. Res. Commun.* 331 (3): 851–858

Yu, J., Zhang, L. (2008). PUMA, a potent killer with or without p53. *Oncogene*. 27 Suppl 1: S71–83.

Yuan, F., Dellian, M., Fukumura, D. (1995).Vascular permeability in a human tumor xenograft: molecular size dependence and cutoff size. Cancer Res; 55: 3752-3756.

Yvon AM, Wadsworth P, Jordan MA. (1999). Taxol suppresses dynamics of individual microtubules in living human tumor cells. Mol Biol Cell. 10:947–59.

Zhang L, Zhou F, ten Dijke P. (2013). Signaling interplay between transforming growth factor-β receptor and PI3K/AKT pathways in cancer. Trends Biochem Sci 38(12): 612-620.

Zhang S., J. Li, G. Lykotrafitis, *et al.* (2008). Size-dependent endocytosis of nanoparticles Adv Mater, 21, pp. 419–424.

Zhang, Q., Ge, J., Goebl, J., Hu, Y., Sun, Y., Yin, Y. (2010). Tailored synthesis of superparamagnetic gold nanoshells with tunable optical properties. *Adv Mater*, 22:1905-1909.

Zhang, XQ., Xu, X., Lam, R., Giljohann, D., Ho, D., Mirkin, CA. (2011). Strategy for increasing drug solubility and efficacy through covalent attachment to polyvalent DNA–nanoparticle conjugates. *ACS Nano*, 5(9):6962-6970.

Zhao, Ma, X., Y., and Liang, X. J. (2011). Theranostic nanoparticles engineered for clinic and pharmaceutics. *Acc. Chem. Res*. 44, 1114–1122.

Zijlstra, P., Orrit, M. (2011). Single metal nanoparticles: optical detection, spectroscopy and applications. *Rep Prog Phys*, 74:106401-106456.

Zou, H., Li, Y., Liu, X., Wang, X. (1999). An APAF-1. cytochrome c multimeric complex is a functional apoptosome that activates procaspase-9. *J Biol Chem*, 274(17):11549-11556.